

UNCLASSIFIED

AD NUMBER
AD059622
NEW LIMITATION CHANGE
TO Approved for public release, distribution unlimited
FROM Distribution authorized to U.S. Gov't. agencies and their contractors; Administrative/Operational Use; 1949. Other requests shall be referred to Bureau of Ordnance, Department of the Navy, Washington, DC.
AUTHORITY
BUWEPS ltr dtd 5 Aug 1965

THIS PAGE IS UNCLASSIFIED

AD

59622

Armed Services Technical Information Agency

Reproduced by
DOCUMENT SERVICE CENTER
KNOTT BUILDING, DAYTON, 2, OHIO

Because of our limited supply, you are requested to
RETURN THIS COPY WHEN IT HAS SERVED YOUR PURPOSE
so that it may be made available to other requesters.
Your cooperation will be appreciated.

NOTICE: WHEN GOVERNMENT OR OTHER DRAWINGS, SPECIFICATIONS OR OTHER DATA ARE USED FOR ANY PURPOSE OTHER THAN IN CONNECTION WITH A DEFINITELY RELATED GOVERNMENT PROCUREMENT OPERATION, THE U. S. GOVERNMENT THEREBY INCURS NO RESPONSIBILITY, NOR ANY OBLIGATION WHATSOEVER; AND THE FACT THAT THE GOVERNMENT MAY HAVE FORMULATED, FURNISHED, OR IN ANY WAY SUPPLIED THE SAID DRAWINGS, SPECIFICATIONS, OR OTHER DATA IS NOT TO BE REGARDED BY IMPLICATION OR OTHERWISE AS IN ANY MANNER LICENSING THE HOLDER OR ANY OTHER PERSON OR CORPORATION, OR CONVEYING ANY RIGHTS OR PERMISSION TO MANUFACTURE, USE OR SELL ANY PATENTED INVENTION THAT MAY IN ANY WAY BE RELATED THERETO.

UNCLASSIFIED

AD059622

An Abridged Translation of
M. E. Serebryakov's "Interior Ballistics"
Originally published in Moscow, 1949

Translated by
V. A. Nekrassoff, Dr. Eng.

The Catholic University of America
Contract NOrd 10,260

ERRATA

(An Abridged Translation)

Page

- 5 The effective caliber d , instead of printed d' .
- 12 Unite pressure, instead of printed "unit, pressure".
- 47 Omit--"Fig. 9.-unburned grains of powder".
- 144 Kisanemsky instead of printed "Kiszemsky".
- 265 Fig. 103 is missing.
- 278 χ is missing at the beginning of the 5th line.
- 302 ρ' -density of gas instead of ρ .
- 353 $v_k = \frac{2}{\varphi} \cdot \frac{I_k}{(\frac{2}{3})} (1-Z_0)$ instead of $v_k = \frac{2}{\varphi} \cdot \frac{I_k}{(\frac{2}{3})} (1-Z_0)$ in
Formula (12).
- 355 In the last line: his instead of printed "this".
- 359-362 Tables of Logs instead of printed "Lugs".
- 375 Name of table should be: Table for h .
- 448 Third line from the bottom: t_r instead of printed t_n . n .
- 465 Table 18, insert Δ before 1 -instantaneous burning;
and Δ_{ma} before -the most advantageous density of
loading; also insert Δ on last two lines of column 1
of Table 18.
- 491 Chapter 4 instead of printed Chapter IV.
- 598 In title of Chapter 3 (Section II): - Evaluation instead ead
of printed "Evolution".

Table of Contents

(An Abridged Translation of Prof. M. E. Serebryakov's
Russian Course in Interior Ballistics - 1950)

Foreword.....	1
Translator's Preface.....	3
List of Terms, Symbols, Definitions.....	4
Introduction.....	15
 <u>PART I - PHYSICAL FUNDAMENTALS OF INTERIOR BALLISTICS</u>	
Section I - Powder as the Source of Energy.....	41
Section II - General Pyrostatics	
1. Burning of Powders.....	45
2. The Characteristic Equation - Relation- ship between the Pressure and Loading Conditions.....	62
3. Evaluation of the Amount of Heat Trans- mitted through the Walls of the Mano- metric Bomb.....	70
4. The Law of Gas Formation.....	82
5. The Rate of Burning.....	116
6. Variation of the Gas Pressure as a Function of Time.....	128
Section III - Ballistic Analysis of Powders Based On the Physical Law of Burning	
1. Development of Method for the Ballistic Analysis of Powders.....	133
2. Ballistic Analysis of the Actual Burning.....	149
3. Special Features of Burning of Multiper- forated Powders.....	179
4. The Application of the Integral Diagram.....	206
Section IV - Physical Principles of Pyrodynamics	
1. The Firing Process and Its Principal Relationships.....	237

2. Energy Balance During the Firing.....	240
3. The Study of the Principal Relationships.....	245
4. Forces Acting during the Travel of a Projectile in a Rifled Bore.....	262
5. Formulae for Evaluation of the Secondary Works.....	273
6. Additional Questions.....	282
Section V - The Outflow of Gases from the Gun	
General Remarks.....	296
1. General Informations of the Gas Dynamics.....	299
2. The Application of the Principal Formulas Concerning the Discharge of Gases.....	313
3. Burning of Powder in Partially Closed Volume.....	321
4. Outline of the Theory of Muzzlebrakes.....	339
 <u>PART II - THEORETICAL AND APPLIED PYRODYNAMICS</u>	
Introduction.....	346
Section VI - Analytical Methods of Solution of the Direct Problem of Interior Ballistics	
Basic Assumptions.....	348
1. The Solution of the Basic Problem Using the Geometric Law of Burning and Con- sidering the Engraving Pressure.....	349
2. Prof. N. Drosdov's Rigorous Integration of the Basic Equation.....	371
3. Solutions for the Simpler Cases.....	377
4. A Detailed Analysis of the Basic Relation- ships for the Simpler Case: $\chi = 1; \psi_0 = 0; \alpha = \frac{1}{2}$	386
5. Other Methods of Solution of the Basic Problem.....	395
6. Prof. M. E. Serebryakov's Method, Based on the Physical Law of Burning.....	398

	111
Section VII - Numerical Methods	
1. Numerical Integration in Finite Differences..	416
2. Solution by Development in Taylor's Series...	417
Section VIII - Empirical Methods	
1. Monomial and Differential Formulas.....	418
2. Empirical Formulas and Tables.....	423
Section IX - Tabular Methods of Solution for the Problems of Interior Ballistics	
1. The Importance of Tabular Methods for the Artillery Practice.....	427
2. Tables for the Principal Elements of Firing ($P_m; C_m; C_k; U_0$)	430
3. Detailed Tables for the Curves of Pressures and Velocities.....	432
4. Tables Based on the Generalized Formulas with the Reduced Number of Parameters or with the Relative Variables.....	434
5. General Information on the Theory of Similarity.....	438
Section X - Ballistic Design of Guns	
General Remarks.....	443
1. Initial Data.....	447
2. Theoretical Fundamentals of Ballistic Design.....	460
3. Applications of the Obtained Relationships to the Design of Guns.....	484
4. Additional Information.....	491
 <u>PART III - SOLUTIONS OF THE MORE INVOLVED PROBLEMS OF INTERIOR BALLISTICS</u>	
Section XI - Solution for Composite Powder Charges	
1. General Information, Characteristics and Theoretical Solution given by Professor G. Oppokov.....	509
2. Solution Taking into Account the Gradual Engraving of the Driving Band.....	522
3. Solution for the Minethrowers.....	524

Section XII - Guns with Tapered Bores (Conic Guns)	
Introduction.....	540
1. Specific Features and Ballistic Properties of the Tapered Guns.....	544
2. Solution of the Problem of Interior Ballis- tics for the Conic Bore.....	581
3. The Ballistic Design of the Conic Gun.....	588
Bibliography: for the Part I.....	593
for the Part II.....	594
for the Part III.....	596
Table of Contents for the Complete Translation of the Russian Course in Interior Ballistics....	598

Foreword

Professor M. E. Serebryakov's book, "Interior Ballistics" was published in Moscow in 1949, and comprises a course of lectures presented at the Artillery Academy of the U. S. S. R.. Professor Serebryakov is a Member of the Russian Academy of Artillery Sciences, and his book is used as a textbook in the engineering and technological institutes and the physics and mathematics departments of the universities of the U. S. S. R.

The Russian book is an imposing volume of 670 pages of large size, and it is not a scientific treatise but a textbook, intended for students of the subject. Accordingly it has not been thought worth while to issue a translation of the entire book, but to include only such material that is not readily available in English. A full translation has, however, been prepared and the manuscript copy is being retained in the Department of Chemistry of The Catholic University of America.

The task of making the complete translation was carried out by Dr. Nez of under contract with the

Department of the Army, while the condensation was done by him at Catholic University. In preparing the condensation the procedure has been to include the titles of every section in the complete book, but to omit such parts of the text as appeared unnecessary. In this way it is hoped that the continuity of the original text will be preserved, while at the same time there will be all possible economy of space and reading time.

Dr. Nekrassoff is at present engaged in preparing a report which will compare and contrast the Russian interior ballistic system with various other methods.

K. J. Laidler

Translator's Preface

A translator may decide to produce a smooth "literary" version, as a more or less free interpretation of the original book, or he may attempt to give in the new language as nearly "literal" reproduction as is compatible with the necessity of getting a readable and understandable text. The latter course has been chosen for this translation. The present version represents an abbreviation of my original translation, which was a complete one. Perhaps the present translator may be permitted to mention the following partly historical, partly personal detail.

In 1902 Professor A.F. Brynk, of the Russian Artillery Academy in St. Petersburg, translated at the request of the U.S. Navy Department his course in Interior Ballistics into English. This book was published in the U.S.A. in 1904. It was my unlooked-for good fortune that I, a former student and assistant of Prof. Brynk (1906-1914) at the Russian Artillery Academy, was employed on a contract with the General Adjutant's Office of the U.S. Army Department to translate into English the present course in Interior Ballistics of the Russian Artillery Academy in Moscow.

V.N.

List of terms, symbols and definitions.

a. The following subscripts are used in this book:

t_0 = the time of the beginning of the projectile motion.

t_m = the time of the maximum pressure.

t_s = the time of the beginning of fragmentation of the powder grains.

t_k = the time of "all-burnt" (the end of burning).

t_{exit} = the moment when the projectile leaves the muzzle.

b. The metric system of units: decimeter (dm) -

kilogram (kg) - second (sec.) - is used here.

c. The term "powder grain" means a separate element of the powder charge, e.g., strip, tube, plate, cord.

d. Initial dimensions of the grain are those measured before the beginning of the burning.

Characteristics of the gun, projectile and powder charge.

1. (a) Caliber of a cylindrical bore-diameter, d , measured between the opposite lands of rifling; d' is a diameter measured between the opposite bottoms.

(b) Caliber of tapered (conic) bore: d_0 (breech caliber); d_m (muzzle caliber).

2. (a) Cross sectional area of a rifled bore:

$$S = \frac{\pi}{4} \cdot d^2 \left[\frac{a + b \left(\frac{d'}{d} \right)^2}{a + b} \right]^2$$

Here, a = width of a land; b = width of a bottom.

(b) The effective caliber,

$$d_e = \sqrt{\frac{2ad^2 + b^2d^2}{a+b}}; \quad S = \frac{\pi}{4} \cdot d_e^2 \approx (0.80-0.83)d^2$$

3. Total length of the canal (bore) measured from the breech to the muzzle = L_{on}
4. Length of the rifled part of the bore = L_r
5. Chamber = the space behind the base of a projectile in its initial position.
6. Chamber capacity = the volume of chamber, W_0 .
7. Weight of projectile = q .
8. (a) Weight of powder charge ω ; ρ = density of powder.
(b) Volume of powder charge = $\frac{\omega}{\rho}$

Characteristics of powder and powder gases.

9. Total heat of the explosive process Q_w = the amount of heat derived from 1 kg. of powder burned in the closed vessel and cooled down to 15° C. (water vapor).
Potential energy of powder: $\Pi = 4270 Q_w$ kg. dm.
10. Specific volume of powder gases = w_1 = the volume occupied by gases delivered by 1 kg. of powder at 0° C. and pressure of 760 mm (water vapor).
11. Temperature of the powder burning = T_1 = temperature

of the explosive process of powder read on K°
(absolute scale).

12. The "force" of powder = $f = \frac{R \cdot W \cdot T}{273}$. (10, 11), here
 $p_a = 1 \text{ atm} = 1.033 \text{ kg/cm}^2$.

13. Covolume of the powder gases = ϕ = a volume proportional to the total volume of gas molecules derived from 1 kg. of powder (dm^3/kg).

14. Rate of powder burning, u = the linear velocity of the burning process normal to the surface of the grain (in mm/sec.).

15. (a) Rate of powder burning at the pressure equal to
 $p_a = 1 \text{ atm}$: $u \left(\frac{\text{mm}}{\text{sec}} / \frac{\text{kg}}{\text{cm}^2} \right)$

(b) Gas constant, $R = \frac{R \cdot W}{273}$ is the work produced by 1 kg. of gas at its heating on 1° at the pressure
 $p_a = 1.033 \text{ kg/cm}^2$ (1 atmosphere).

(c) Specific heat of the gas at constant pressure
 C_p . Specific heat of the gas at constant volume C_v

$$\frac{C_p}{C_v} = K ; C_p - C_v = AR$$

A = thermal equivalent of work.

(d) $K - 1 = \theta$

Dimensions of powder grain.

16. Thickness of a burned layer = variable e .
17. Initial thickness (web) = $2 e_1$
18. Surface of the grain = variable S .
19. Initial surface of the grain = S_1 .
20. Volume of the grain = variable Λ
21. Initial volume of the grain = Λ_1
22. Relative thickness of the burned layer = variable Z
 here: $Z = \frac{e}{e_1} = \frac{I}{I_1}$ (16; 17; 32; 33; 14; 15).
23. Relative surface of the grain: $\sigma = \frac{S}{S_1}$ (18; 19).
24. (a) Rel. Vol. of the burned grain = variable: $\psi = \frac{\Lambda - \Lambda_1}{\Lambda_1}$
 (b) Volume of the burned part of charge: $\psi \left(\frac{\Lambda}{\Lambda_1} \right)$
 $(1 - \psi) \frac{\Lambda}{\Lambda_1}$ of the unburned part.
 (c) Value of the covolume of burned part = $\alpha \cdot \psi \cdot \omega$

Travels, velocities and pressures.

25. Time of departure of a projectile - the moment the base of projectile leaves the muzzle.
26. Relative travel of projectile = variable l , measured from the initial position of the base of projectile.
27. Total travel along the bore l_2 (26; 25).
28. Relative velocity of projectile = variable $v(v) = a$ translatory velocity of a projectile in its travel relative to the barrel. (26).

29. Muzzle velocity = a relative velocity of a projectile (28) at the moment of departure from muzzle (25) = \vec{v}

30. Powder pressure (variable) p = mean value of all local pressures behind the projectile in the bore at any moment.

31. Mean powder pressure $p_{av} = \frac{p p v^2}{2 g s l}$
(37; 7; 28; 2; 26)

Here g = acceleration of gravity.

32. Impulse of powder gas pressure (variable)

$$I = \int p dt. \text{ Here } t = \text{time.}$$

33. Impulse at the end of powder burning $I_k = \int_0^{t_k} p dt$

Special quantities and coefficients.

34. Density of loading $\Delta = \frac{\omega}{W_0}$ (8; 6); $\omega \text{ kg.}; W_0 \text{ dm.}^3$

35. Gravimetric density is the ratio of the weight of freely poured powder in a vessel of a definite form and a definite volume to the weight of water at 4°C. filling the same vessel to the same volume. Note: It is essential to specify precisely what form and volume of a vessel must be used and in what particular manner the powder must be poured in the vessel. Any change in these specifications will affect the numerical value of the obtained gravimetric density.

36. (a) Effective length of the chamber l_0 is the length of a cylinder having its volume equal to the chamber capacity (6) and its circular base equal to the cross sectional area of the bore (s): $sl_0 = W_0$.
- (b) Actual length of a chamber l_0 is the distance between the bases of the barrel and the projectile;

$$\frac{l_0}{l} = \gamma > 1.$$

37. (a) Coefficient accounting for the secondary energy losses = φ

(b) Theoretical formula: $\varphi = a + b\left(\frac{w}{d}\right)$

Here: $a \approx (1.03-1.06)$; $b = 1/3$.

(c) Empirical formula: $\varphi = 1.05\left(1 + \frac{1}{4} \cdot \frac{w}{d}\right)$

38. Coefficient of the weight of projectile $C_p = \frac{q}{d^3}$
 q in kg.; d in dm.

39. Coefficient of the utilization of the powder charge:

$$\eta_w = \frac{2.25^3}{2g} \cdot \frac{1}{w} \quad (7; 29; 8).$$

40. Coefficient of projectile's location at the time of "burnt".

$$\eta_k = \frac{L_k}{L_0} \quad (27).$$

41. Relative weight of powder charge: $\frac{w}{d^3} \quad (2; 1).$

42. Coefficient of the gun potency:

$$C_g = \frac{L_0}{d^3} = C_g \cdot \frac{2.25^3}{d^3}$$

43. Total efficiency of the powder charge:

$$\eta = \frac{L_0}{d^3} = \eta \cdot \frac{2.25^3}{d^3}$$

44. Professor Drosdov's parameter of loading:

$$B = \frac{S^2 I_k^2 g}{f \omega \varphi q}$$

45. Coefficient of chamber's widening
- $\gamma = \frac{\ell}{\ell_0}$
- (33 a; b).

46. Mean diameter of the chamber
- $D = d \sqrt{\gamma}$

47. At
- n
- rifles with their depth
- t_r
- and caliber
- d
- , the total length of the cross sectional perimeter of the bore will be:
- $\pi(d + t_r) + 2nt_r = \pi d''$

here d'' is the effective diameter of a circumference having the same length as the perimeter of the bore.

Since $t_r = (0.01 \dots 0.02)d$, we will have: $d'' = d(1.19 \dots 1.38)$ at $n = 28$ or: $d'' = (1 + \alpha_1)d$.

48. Initial working surface of the bore
- Σ_0
- , at the beginning
- $t = t_0$
- :

$$\Sigma_0 = \pi D \ell_0 + 2 \cdot \frac{\pi}{4} (d'')^2 = \pi d \ell_0 \left[\sqrt{\gamma} + \frac{1}{2} \cdot \frac{d''^2}{\ell_0^2} (1 + \alpha_1) \right] \sim \pi d \ell_0 (1 + \alpha_1)$$

49. Final working surface of the bore at
- $t = t_2$
- :

$$\Sigma_{en} = \pi d (1 + \alpha_1) (\ell_0 + \ell_2)$$

50. Working surface of the bore
- Σ
- at any
- t
- :

$$\Sigma = \pi d (1 + \alpha_1) (\ell_0 + \ell)$$

Thus we have:

$$\frac{\Sigma}{\Sigma_0} = \frac{\ell_0 + \ell}{\ell_0} = 1 + \frac{\ell}{\ell_0}; \quad \frac{\Sigma}{\Sigma_{en}} = \frac{\ell_0 + \ell}{\ell_0 + \ell_2}$$

51. Total length of the gun canal:

$$L_{cn} = l_0 + l_2 = \frac{W_0}{S} + l_2 + l_0 - l_0 = l_0 + l_2 - l_0 \left(1 - \frac{1}{\lambda}\right) = L'_{cn} - l_0 n'$$

Here L'_{cn} is the "effective" total length of the gun canal and $n' = 1 - \frac{1}{\lambda} = 1 - \frac{l_2}{l_0} = \frac{l_0 - l_2}{l_0} = \frac{\partial(l_0)}{l_0}$

i.e., n' is the relative increment of l_0 .

52. Total volume of the gun canal: $W_{cn} = S L'_{cn}$

53. Working volume of the canal: $W_0 = S l_0$

54. Total volume behind the projectile:

$$W = W_0 + S l = S(l_0 + l)$$

55. Volume W corrected for the volume of unburned powder

$$\text{and for the covolume of powder gases: } W - \frac{W}{\lambda}(1 - \psi) - \alpha \omega \psi = \\ = W_0 - \frac{W}{\lambda}(1 - \psi) - \alpha \omega \psi + S l = W_0 + S l = S l_0 + S l = S(l_0 + l)$$

$$\text{Here: } l_0 = \frac{W_0}{S} = \frac{W_0 - \frac{W}{\lambda}(1 - \psi) - \alpha \omega \psi}{S} = l_0 \left[1 - \frac{\Delta}{\lambda} - \Delta \left(1 - \frac{1}{\lambda}\right) \psi\right]$$

l_0 is the effective length of the free volume of chamber at a given moment of time when a fraction ψ of the powder charge is burned. At the beginning:

$$(\psi = 0): l_0 = l_0 \left(1 - \frac{\Delta}{\lambda}\right) = \frac{W_0}{S} = \frac{W_0 - \frac{W}{\lambda}}{S}$$

At the end: ($\psi = 1$)

$$l_1 = l_0 (1 - \alpha \Delta) = \frac{W_1}{S} = \frac{W_0 - \alpha \omega}{S}$$

56. The function $\Gamma = \frac{1}{p} \cdot \frac{d\psi}{dt}$ is a specific rate of gasification per unit, pressure, or the intensiveness of the process of gasification.

$$\Gamma = \frac{1}{p} \cdot \frac{S_1}{\lambda_1} \cdot \frac{S}{S_1} \cdot u = \frac{1}{p} \cdot \frac{S_1}{\lambda_1} \cdot \frac{S}{S_1} \cdot u \cdot \rho = \frac{S_1}{\lambda_1} \cdot \frac{S}{S_1} \cdot u,$$

57. Specific surface of grain: $\frac{S_1}{\lambda_1} = \frac{\gamma}{e}$

58. Relative surface of grain: $\frac{S}{S_1} = \sigma$;

59. $2e_1$ is a thickness of strip

$$\frac{2e_1}{2e} = \alpha; \quad 1 + \alpha + \beta = \gamma$$

$2e$ is a length of strip

$$\frac{\alpha + \beta + \alpha\beta}{1 + \alpha + \beta} = \lambda$$

$$\frac{2e_1}{2e} = \beta; \quad \frac{\alpha\beta}{1 + \alpha + \beta} = \mu$$

$2b$ is the width of strip.

60. $\psi = \gamma z (1 + \lambda z + \mu z^2)$

or: $\psi = \gamma_1 z (1 + \lambda_1 z)$

61. $\sigma = 1 + 2\lambda z + 3\mu z^2$

or: $\sigma = 1 + 2\lambda_1 z$; $\sigma = \sqrt{1 + 4\frac{\gamma_1 \mu}{\gamma_1^2}}$

where: $\gamma_1 = \gamma (1 - \frac{\mu}{2})$, $\lambda_1 = \frac{\lambda + \frac{\gamma_1 \mu}{2}}{1 - \frac{\mu}{2}}$.

62. Volume in which gases are emitted from the powder surface:

$$V = W_0 - \frac{W}{\gamma}$$

63. $\frac{S}{V} = \gamma$ ratio of a burning surface to volume V.

For the inner surface of perforation:

$$\gamma'' = \frac{S_K}{W_K} = \frac{\pi d l_K}{\frac{\pi d^2}{4} l_K} = \frac{4}{d}$$

Here S_K = inner surface of channel in grain.

W_K = volume of channel in grain. For the outer surface of a grain:

$$\gamma' = \frac{S'}{W_0 - \frac{W}{\gamma} - N_K W_K} = \frac{S'}{\lambda_1} \cdot \frac{S'}{\delta_1} \cdot \frac{1}{\frac{S'}{\delta_1} - 1 - \frac{N n W_K}{\lambda_1}}$$

S' = outer surface of all grains. For 7 perfora-

tion powder: $\frac{\gamma''}{\gamma'} \approx 70$

N = number of grains; n = number of perforations in a grain.

- 64.

$$u_1 = - \frac{(e_1)_{av.}}{\int_0^{t_K} p dt} ; \int_0^{t_K} p dt = I_K$$

65. Various forms of the law of burning:

$u = u_1 p$, when I_k is not affected by the value of Δ
(u_1 may be a variable).

$u = A p^\gamma$ when $\gamma < 1$ I_k is increased with the in-
creased Δ .

$u = ap + b$ when I_k is increased with the in-
creased Δ .

66. If ω' , f' , I_k' , Δ' are values of characteristics
of the powder adopted in service and ω'' is a de-
sired value of a charge of the experimental powder
which is expected to produce the same p_m and v_s
obtainable in service. Then

$$\frac{\omega''}{\omega'} = \frac{\frac{f'}{f''} \cdot \frac{I_k'}{I_k''}}{1 + \frac{\Delta'}{\Delta''} \left(\frac{f'}{f''} \cdot \frac{I_k'}{I_k''} - 1 \right)}.$$

f'' and I_k'' are determined by the experiment.

INTRODUCTION.

General Description of the Contents.

The present book is essentially different from its first edition of 1939 and contains several chapters which were written anew. An extensive editorial and methodological work has been done by the chair of Interior Ballistics of the Artillery Academy during the years of the Great War II and afterwards and the entire course has been completed as a collective work of Soviet scientists and teaching staff of the chair of Interior Ballistics of the Artillery Academy. Necessary references to the works of foreign authors are made only for historical elucidations of certain questions (prior to 1925) especially in discussions of the burning process of powders.

This course is intended as a textbook for students of the Engineering faculties of the Artillery Academy and for other higher technical institutions; it may also serve as a manual for the technicians of manufacturing plants, (~~Артиллерийских~~) construction bureaus, laboratories working for the Ordnance Engineering Department; this book can be used by scientific workers and engineers as

well as by graduate university students of physico-mathematical sciences.

The course begins with an Introduction and has 3 parts. A large part of the introduction has been rewritten and special attention is paid to the adequate presentation of the importance of a direct connection between Interior Ballistics and the Ordnance Engineering designs of artillery systems and their ammunition.

A new chapter - "Historical outline of the development of Interior Ballistics" has been added, in which due acknowledgement is paid to the leading role played by Russian scientists of both periods - before the October Revolution of 1917 and after it.

Part I. "Physical fundamentals of Interior Ballistics" - presents the physical aspect of the entire firing process of the firing from the moment when the powder begins to burn until the end of the after effect of powder gases acting on the projectile as well as on the barrel of the gun. Part I consists of the following 5 Sections:

Section I. "Powder as a source of Energy" - contains general information about various types of powders and their principal characteristics.

Even though not a few current authorities have rejected the use of the terms "Pyrostatics" and "Pyrodynamics" these terms, nevertheless, are being used in this textbook merely for the sake of their simplicity and clarity.

Section II. "General Pyrostatics" has been considerably enlarged in this volume and its material is redistributed in a different order as compared with the 1st edition.

Section III. "Ballistic analysis of propellants based on the physical law of the burning process" has been enlarged and in accordance with current theories of burning propellants, deals with finding a sound and secure criterion for determining the various laws controlling the rate of burning.

Section IV. "Physical bases of Pyrodynamics" - has a new material in it and a new treatment of some old questions of the importance of variations in powder chamber capacity or of the relationships between the three powder pressures: 1) acting at the base of the projectile. 2) at the breech of the gun and 3) the average pressure acting behind the moving projectile.

Section V. "Phenomena produced by the flow of powder gases" deals with the after-effect of powder gases continuing their action of increasing velocities - of the projectile as well as of the recoiling system and also working on the muzzle brake (if such is present).

Part II. "Theory and practice of the solution of the basic problems of Interior Ballistics" - represents a general exposition of theoretical and applied Pyrodynamics. Here are given various methods (analytical, numerical, empirical, tabular) of solutions of basic problems.

A special introduction to Part II presents a general outline of the approaches to the basic problems when using one or another method among the four mentioned above.

Section VI. "Analytical methods of solution of the direct problem of Interior Ballistics". A basic analytical method is presented in the form of the famous rigorous solution, published for the first time in world literature on the subject by Prof. N. F. Drosdov in 1910. We also have here some other simplified solutions due to Prof. Grave and Prof. Oppokov. A separate chapter contains a new solution proposed by Prof. Serebryakov based on his own research on the physical law of burning ("The physical law of burning in Interior Ballistics", 1949).

Section VII. "Numerical Methods" has been reprinted from the 1st Edition.

Section VIII. "Empirical Methods" has been considerably abridged because these methods and their tables became obsolete in comparison with present usage of new tables, based on analytical solutions; special auxiliary tables of necessary corrections calculated by Prof. Slukhotzky are nevertheless also given.

Section IX. "Tabular methods of solution of problems of Interior Ballistics" - contains special revised instructions for making tables and additional material collected from the new tables issued in 1942 by the Chief Artillery Board. Here is also presented a revised theory of similarity, based on formulae which were used in the construction of the ballistic tables. For the first time a new method is given, which is based on the use of *relative* variables and reduced number of parameters. This method is due to Profs. Drosdov and Okunev and Messrs. Gorokhov and Sviridov and is included in the text of this course.

Section X. "Ballistic methods of gun design" - is entirely new and leads to practical results regarding the characteristics of a gun whose design is to be determined with respect to the specific techniko-tactical performance

desired. A special "Directive Diagram" affords a substantial reduction in the number of variants considered, and a method of evaluation of durability of gun, proposed by Prof. Slukhotzky is presented.

Part III. "Solutions of special more involved problems of Interior Ballistics". Here, in Section XI, we have:

1. Solutions obtained analytically and by means of tables for the problem of composite powder charges.
2. The case of a trench-mortar (mine thrower) when leakage of gases is taken into consideration.
3. Solution of the basic problem when the process of the gradual engraving of the band is accounted for (by Prof. G. Oppokov).

The last Section XII contains a special case of design of tapered-bore guns (coned bore).

Thus the present course deals with the major part of current problems of Interior Ballistics.

A Brief Historical Survey of the Development of Interior Ballistics in Russia

The history of the development of Interior Ballistics is naturally related to the general development of artillery. During the period between the end of the XVIIth century and the beginning of XVIIIth the artillery was

definitely incorporated into all armies. It had already lost all its old medieval traits and traditions and thus became capable of a normal progressive development. As a result - an almost immediate improvement began. A disorderly confusion of numerous calibers and models, an absence of firmly established general principles and the uncontrollable arbitrariness of empirical rules of thumb - all these defects became obviously objectionable and were disposed of.

In all countries there were organized special artillery experiments, and scientific attempts were originated for systematical investigations within the province of fire arms.

The meaning of gun-caliber, its relation to the length and weight of a gun, and the weight of powder charge; the distribution of metal over the gun body, the effective distance of a firing, recoil action on a gun mount - all these riddles and questions were investigated with gratifying results among which must be mentioned a marked cutting down of powder charge to $1/3$ or $1/2$ of the cannon balls.

In Russia, the czar, Peter the Great (1672-1725) was personally interested in the artillery art and he even wrote "A manual for the use of Artillery". Since those remote times the Russian Artillery became one of the best artilleries in Europe.

The organization and tactical progress of the artillery moved ahead together with the progress of a new Artillery Science which concentrated its studies mainly on the air resistance affecting the trajectory of a projectile.

Daniel Bernoulli (1700-1782) in his classic "Hydrodynamics" laid the foundation of gas mechanics, introduced a concept of elastic gas expansion and showed how, by taking into account this expansion to calculate the shot travel in the gun barrel. The great Euler (1707-1783) spent much of his creative efforts in studying the processes taking place in the gun barrel but the complete lack of experimental data precluded a further development of his work. (Euler as a member of the Russian Academy of Science lived in St. Petersburg in 1727-1741 and 1766-1783).

Benj. Robins (1707-1751) invented and constructed a ballistic pendulum which was used in ballistic experiments for more than 100 years.

Robins in 1742 wrote "New Principles of Artillery Science" in which he subdivided this science into Exterior Ballistics and Interior Ballistics. He formulated the basic problem of Interior Ballistics in the following words: "Knowing the length and caliber of a gun, weights of the powder charge and of the shot, and the elastic force of powder gases at the first moment of their ignition - to calculate the velocity at which the shot will be propelled out of a gun".

Together with the theoretical and experimental development of the Artillery Science, technical reorganization of Artillery also continued its progress in the Artillery practice: new mechanisms were constructed, the loading procedure was improved and the general level of the fighting qualities of the Artillery was markedly raised.

Considerable progress in the Russian Artillery was achieved during the period from 1750 to 1760, when Count P. I. Shouvalov introduced his own artillery system which became very popular and serviceable under the name "Shouvalov's Unicorns". These unicorns turned out to be very successful during the Great Patriotic War of 1812, as well as during the Seven Year War (1756-1763).

This system was continually in the army service till the rifled guns took their place. It is of interest to note here, that in all textbooks of artillery in all countries (Russia included) we read that the rifled guns came into artillery practice almost at the same time, namely in the middle of the XIXth century (1855-1865). And yet the irrefutable fact is that in the Museum of the Russian Artillery Academy there are several rifled guns dated as far back as 1615 and several guns dated 1645 and 1680 having very primitive but effective enough breech mechanisms. And there is another well known fact, that no other person but A. Krupp himself, when visiting St. Petersburg in 1885, had offered a fabulous sum of money for all these models which still remain in the same ~~museum~~ at present. It would be however not very reasonable to proclaim that the Russian artillery used the rifled guns with breech mechanisms as early as in the XVIIIth century. Besides this we have a documentary evidence in form of a comprehensive description of experiments with rifled guns in 1547 made in England. No such guns however were preserved as relics of those remote days.

The first scientifically established principles of the theoretical and experimental ballistics begin only in the second half of the XIXth century, being founded on the solid basis of a general scientific development of technics and technology of that period.

The first theory of the powder burning process has been published in 1857 in Russia by a chemist Shiskov and in Germany by Bunzen.

In 1860, Captain of the Russian Artillery A. P. Gorlov published an article on the motion of a projectile along the rifled bore of a gun; this article was republished in the Comptes Rendue of the French Academy of Sciences (1862)

In 1868, Colonel of the Russian Artillery . . .

N. P. Fedoroff, by means of experimental firings from a pistol and 4 lb. gun, found how the products of the burnt powder were affected by the conditions of the burning process within the gun barrel.

These works laid the foundation for further research on the burning process during firing conducted by the future investigators.

In the middle of the XIXth century there were introduced the two most important and successful devices of Experimental Ballistics - the chronograph by Le Bulange

and the crusher by Noble. Then as a natural next step the manometric bomb was constructed and a new branch of the Experimental Ballistics - Manometry-began. In 1868-1875 Nobel and Abel conducted important experimentations on the qualitative and quantitative analysis of the products of the burning powder, together with measurements of maximum pressures, temperatures, specific heats and the amounts of heat derived from the combustion of powder in the closed volume of a manometric bomb. Hence the maximum pressure was determined as a function of the "force" of powder and "density of loading". All of this work was largely based on the results of the above mentioned researches of Shishkov, Bunzen and Fedorov.

During the second half of the XIXth century new developments in the Kinetic Theories of Heat and Gases, of Thermodynamics and General Chemistry naturally enough furnished sufficient material for a solid scientific foundation for the studies of the burning process of powder as well as of the conversion of the energy of powder gases into kinetic energy of these gases and of the moving projectile in the bore of a gun.

In 1864 Resal gave a differential equation for the balance of the energy derived from the combustion of a

powder and the energy absorbed by the whole mechanical system affected by the firing.

This equation was utilized by Sarreau in 1876 for a derivation of his popular and useful formulae used in the artillery practice of almost all countries. In Russia in 1898-1901 Prof. A. F. Brynk of the Artillery Academy and Prof. N. F. Drosdov of the same Academy have introduced their own formulae in place of Sarreau's formulae.

A very important contribution to the progress of Artillery in general and Artillery Science in particular has been made by the invention of smokeless powder: pyroxylin powder in France by Vieille (1884), nitroglycerine powder in England by Noble and Able (1888), and pyrocolloidal powder in Russia by Mendeleev (1890).

Having perfected a manometric bomb by the mechanism registering the pressure as a function of time, Vieille has definitely established a fundamental difference between the instantaneous explosion of the black powder and the rapid but gradual and regular burning of the smokeless colloidal powders. Thus has been found the very important technical possibility of the control of the process of gasification by the use of "grains" of

propellant prepared in the form of tubes or strips with definite sizes of their geometrical patterns.

Finally after a long series of theoretical and laboratory work a new type of a smokeless colloidal powder with pyroxylin base was found. Vielle personally designed and prepared such a powder for 65 m/m gun and all experimental results perfectly verified theoretical calculations and expectations.

This new powder turned out to be 3 times more powerful than ordinary black powder, and produced a much higher muzzle velocity at a lower maximum pressure.

The introduction of smokeless powder considerably increased the effective distance of firing and at the same time disposed of smoke and brought in many marked innovations in tactics on the battlefields.

In Russia the experimental preparation and testing of the French pyroxylin powder began in 1887 and this powder was finally admitted into artillery service, disregarding the fact that Mendeleev's pyrocolloidal powder was markedly better. But personal reasons during that period were as a rule more powerful than scientific ones. All the merits of Mendeleev's powder were appreciated afterwards by the U.S.A. government and this powder was

taken into American artillery service. During the Great war I in 1914-18 this powder was sold in great quantities to the Russian Government.

Even though the technics and industry in czarist Russia were on a lower level than in the Western countries nevertheless the Russian theoretical ballisticians not infrequently were far in advance of their foreign colleagues and played leading roles in the progress of many scientific achievements. After the abovementioned names of Shishkov, Gorlov and Fedorov it will not be amiss to note a few more.

In 1870 Professor P. M. Albitzky published the first course of Interior Ballistics in Russia, which he taught in the Russian Artillery Academy.

In 1879 a graduate of the Artillery Academy, Colonel Kalakutsky, published his experimental and theoretical investigation of the abnormal pressures in small rifled firearms. In this work he took into account the propagation of the wave motion of gases. Only several years afterwards Vielle also published a similar work in France.

A direct successor of Professor Albitzky, Professor V. A. Pashkevich, published in 1885 - 1891 two books - "Theoretical Ballistics" and "Experimental Ballistics".

These books were translated in England and in the U.S.A. The two most outstanding Russian ballisticians of the second half of the Nineteenth Century and of the very beginning of the Twentieth Century were professors of the Russian Artillery Academy - N. V. Mayevsky (1823-1858-1898) and his pupil and successor N. A. Zabudsky (1853-1890-1917). N. V. Mayevsky is of world wide fame as the originator of the scientific Exterior Ballistics but his works in the field of Interior Ballistics were no less famous.

In 1856 long before Noble's experiments, Mayevsky found a very original method of measuring the powder pressures at various sections of the gun barrel and his design of the 60 lb. smooth bore gun was so perfect that this gun, in competition with many others, showed the best results.

In 1867 Mayevsky organized special experiments determining the shot travel as a function of time and then curves of powder pressure as functions of shot travel and time were calculated. This work became of great importance for Interior Ballistics as well as for the design of guns. In 1878 Mayevsky was elected a correspondent-member of the Russian Academy of Sciences.

H. A. Zabudsky was a worthy and prolific successor of his teacher in both branches of Ballistics.

In 1911 the French Academy of Science elected Zabudsky as a correspondent-member in the chair of Mechanics.

In 1904 Zabudsky finished a preliminary investigation of the powder pressures in various guns and proposed a series of empirical formulae for muzzle velocities and maximum pressures.

In 1914 he published a monumental experimental work on the determination of pressures and velocities as functions of projectile travel for the 3rd field artillery gun. Here he adopted the original method of a gradually shortened gun barrel. From these results he obtained empirical formulae for muzzle velocities and maximum pressures in terms of loading conditions (powder charge, weight of projectile, chamber capacity, web size of a powder). This work with its extensive experimental material is not infrequently of practical value even at present.

In 1902 Professor of the Russian Artillery Academy, A. F. Brynk began his course of Interior Ballistics which in 1900 was published in its final form. Professor Brynk

extended Sarreau's formulae into the new province of smokeless pyroxylin powders, having accordingly changed all the coefficients and exponents. For the pressure curve Professor Brynk proposed his own empirical formula.

At that time this course was the most complete, and practicable one among all existing course of Interior Ballistics in other countries.

In 1901 Professor Brynk's course was translated into German and by the request of the U. S. Navy Dept. in 1902 into English.

In 1903 N. F. Drosdov then the adjunct of the Russian Artillery Academy gave for the first time in the world literature of the subject a complete rigorous integration of the equations of the basic problem of Interior Ballistics without any simplifying assumptions, facilitating the integration of differential equations in this case. This memoir was published in the Russian Artillery Journal. In 1910 the same memoir in a more complete and developed form was presented by N. F. Drosdov as his dissertation for the professorship of the Artillery Academy.

In 1920 Professor Drosdov published special ballistic tables for practical solutions of numerous ballistic problems and especially of problems in the ballistic design of guns.

I. P. Grave, adjunct of the Artillery Academy in 1904, presented his dissertation on experimental and theoretical investigations of the rates of burning of powders and of observed pressures in a closed vessel. This work was received with great interest and was published in France.

In 1908 Charbonnier published in France his Interior Ballistics in two parts - "Pyrostatics and Pyrodynamics"; he disagreed with Vieille's geometrical law of burning and proposed his own method for finding the laws of the process powder burning in the manometric bomb; besides this he gave a more refined treatment of the problem of secondary losses of gas energy during the firing process, and presented a more detailed analysis of the building up of the "shot-start-pressure" corresponding to the moment of a complete engraving of the driving band at the beginning of the projectile motion.

Among Charbonnier's followers of his rather theoretical trend we must mention another French ballisticians, Sugot, with his course of Interior Ballistics published in 1926. As a parallel trend but of a more experimental nature we have works of Gossot and Liouville who in 1920-1922 presented solutions of Interior Ballistics problems based exclusively on experimental firings.

In Germany Granz was the outstanding ballisticians of the beginning of the Twentieth Century; he published his 3 volumes of the Course in Ballistics (Exterior-Interior-Experimental) in 1920-1926. Granz also organized a special Ballistic Laboratory at the Military Technical Academy in Berlin; he was also a well known inventor of many special apparatuses and instruments for ballistic research.

Among the Italian authors we need to mention Bianchi whose solutions of Interior Ballistics problems (1917) were used (with certain alterations and improvements) by Professor Grave in his course of lectures in the Artillery Academy.

Fully appreciating the value of the work of foreign scientists, the Russian ballisticians cannot disregard the fact of the systematical silence about their work on the part of their foreign colleagues. For example - in the course on Interior Ballistics published in 1938 by the French ballistician Winter he says that the French school of ballisticians naturally enough occupies the first place with the Italian school occupying second place; many other British, German and American ballisticians and their works are mentioned and there is not a single word about the work of the ballisticians of the Russian School of Interior Ballistics.

During the czarist regime Russian Artillery Scientists have been well known abroad for their successful activities in the Artillery Science in general and in Interior Ballistics in particular. The works of N. V. Mayevsky, N. A. Zabudsky, A. W. Gadolin, 1828-1892, V. M. Trofimov, N. F. Drosdov, I. P. Grave were the outstanding contributions to the Artillery Science and they are still important and valued among the experts at present. All these works usually were published in the Russian oldest, widely known "Artillery Journal" (founded in 1808 and continually existing until present time). And a still wider development of the Russian Artillery and Interior Ballistics has been attained immediately after the Great War I under the leadership of the famous Russian Artillery scientist V. M. Trofimov (1864-1892-1926). Among other outstanding Trofimov's works (most published also in France) his reports on the "extra distant firing" are particularly important. Having received (1918) information concerning the artillery bombardment of Paris by Germans at the distance of 120 km. Trofimov immediately set up his problem - "to get still better results" and in 1919 he had a detailed ballistic solution of his problem of a complete control of firing at a distance of 140 km. The next stage of the problem was to find the most efficient system of the gun

and its ammunition including the sort and dimensions of the most progressive suitable powder. Thus a Commission of Special Artillery Experiments (COSARTEX or in Russian KOCAPTOEK) was organized under the chairmanship of Trofimov. Not only this problem of the "extra distant firing" but many other important problems of gas dynamics, of tactico-technical compromises, of the automotive artillery, of mine throwers have been successfully solved under the guidance of the COSARTEX and a solid foundation was laid for the complete modernization of the Red Army Artillery.

Trofimov succeeded in bringing into the Commission COSARTEX not only most prominent members of the Chief Artillery Committee but also professors of the Artillery Academy and a great number of the outstanding Russian Civilian Scientists.

During the last 30 years a new generation of Soviet artillery scientists came to life. Thus it can be stated positively that in the U.S.S.R. there is a solid advanced scientific school of artillery constructors, ballisticians and technologists pursuing their own independent ways in the domain of artillery sciences.

In 1945 the Academy of the Artillery Sciences (AAS) was organized as the highest scientific institution wholly dedicated to dealing exclusively with principal artillery problems.

Thus in summing up the facts of the above outline of the activities of the present Russian School of Interior Ballistics it must be admitted that its continually increased personnel have quite successfully handled and solved all the current problems and have blazed many new trails in the progressive development of interior ballistics.

This School has been gradually built up by V. M. Trofimov and by the two other prominent scientists, real creators of many future generations of the Russian ballisticians and constructors: one among them is the Scientist Emeritus of the U. S. S. R., the laureate of the Stalin Premium, member of the presidium of the AAS, General colonel of the Artillery, N. F. Drosdov; another one - is the Laureate of the Stalin Premium, member of the AAS, the professor of the Artillery Academy, major-general of the Ordnance Engineering Corps, I. P. Grave.

As it was stated above Professor N. F. Drosdov was the first ballistician in the world who gave a rigorous mathematical solution of the basic problem of the Interior Ballistics without recourse to any simplifying assumptions. Since 1911 Drosdov has been the professor of the Interior Ballistics in the Navy Academy.

Professor Drosdov is the author of many works among which are of a particular interest his numerous tables prepared for handy manipulations with his theoretical results in the practice of the Gun Design calculations. In 1947-1948 Drosdov published two important works - one on the characteristics of the "Optimum Gun" and another presents a new solution of the problems of the Interior Ballistics in terms of the relative variables for both - ordinary and composite charges; here also are given tables greatly simplifying all the calculation.

Thus Professor Drosdov is the true founder of the Russian School of the ballistic design of guns, having already to its credit many excellent artillery systems.

Professor I.P. Grave, since 1911 the Professor of Interior Ballistics of the Artillery Academy, is the author of one of the most extensive and complete treatments of the subject in the world literature, course of the Interior Ballistics in 4 volumes - "Pyrodynamics" (1932-1937) and "Pyrostatics" (1938); here an exceptional bibliographical material is presented in references to Russian and foreign sources in five languages.

In 1926 Professor Grave organized a Ballistic Laboratory at the Artillery Academy. Since 1938 and especially during the years of the Great Patriotic War Professor Grave

was continually engaged in series of the most important successful researches on the current problems of the Interior Ballistics. We will mention here only several among the outstanding original results achieved by Russian ballisticians belonging to this new Russian School of Interior Ballistics. Problems of the composite charges had their solutions given by N. F. Drosdov, V. E. Slukhot-sky, I. P. Grave analytically as well as by means of tables in 1940-1942.

The first analytical solution of the problem of "leaking guns" (trench mortar, mine thrower) was given in 1940 by M. E. Serebryakov and K. K. Greten and with more details by G. V. Oppokov.

All the methods of the ballistic design of guns are presented in Russian works in the most complete and rational form.

Specific problems of the "optimum gun" and "minimum volume gun" are solved by the Russian ballisticians using their own methods with results which are more perfect economically as well as constructively, than the results of the French ballisticians. A new method of the ballistic analysis of powders, experimentally determining the actual burning process with additional corrections, which were entirely omitted in the earlier investigations, has been

developed in 1923-1937 by M. E. Serebryakov.

For the first time in 1916 V. M. Trofimov has applied the method of the numerical integration of differential equation of the Exterior Ballistics.

Particularly valuable methods of the numerical solutions of the Ballistic problems were applied by the Professor G. V. Oppokov. Even this incomplete list of achievements of our Russian scientists shows convincingly that the Russian Interior Ballistics School always has been and is at present on the solid theoretical basis being developed by its own ways and means.

Chapter 1-

- 1.1 General Information.
- 1.2 Types of Smokeless Powders.
- 1.3 Forms, sizes, brands of powder.

2.1 Chemical Characteristics - Nitrogen contents - Percentage of volatiles

- 2.2 Physico-Chemical Characteristics. Amount of heat ($\frac{\text{cal.}}{\text{kg.}}$) delivered by 1 kg. of burning powder when cooled to 15°C:

$$Q_{\text{(water vapor)}} = Q_{\text{(water liquid)}} + 620 \left(\frac{n}{100} \right) \text{ where } n \text{ is the percentage of water in the products of burning.}$$

Volume of gases W_{gas} after burning of 1 kg. of powder: $W_1(\text{vapor}) = W_1(\text{liquid}) + 1240 \left(\frac{n}{100} \right)$ where n is the percentage of water vapor in gases.

Temperature T_1 , of powder gases at the absolute scale (determined from Q_w)

The specific heats C_p and C_v :

$$C_p - C_v = AR$$

hence: $C_w = a + bT$ (Mallard and LeChatelier) $\sqrt{a^2 + 250}$
 $dQ = C_w dT = (a + bT) dT$; $Q = aT + \frac{b}{2} T^2$; $T = \frac{-a + \sqrt{a^2 + 250}}{b}$

Table 1
Average Molecular Specific Heats

tC°	$N_2; O_2$ CO	H_2	H_2O	CO_2
100	6.96	6.95	8.04	9.08
500	7.07	7.02	8.32	10.34
1000	7.30	7.15	8.83	11.33
1500	7.52	7.38	9.46	11.92
2000	7.70	7.56	10.27	12.29
2500	7.84	7.70	11.38	12.55
3000	7.96	7.83	12.98	12.74

Density of powder δ

Table 2

<u>Characteristics</u>	<u>Pyroxylin Powder</u>	<u>Nitroglycerine Powder</u>
Amount of heat $Q_w \frac{\text{cal.}}{\text{kg.}}$	900-800	1100-1200
Volume of gases $W_1 \frac{\text{dm}^3}{\text{kg.}}$	900-970	860-800
Temperature T_1 (K°)	2800-2500	3000-3500
Percentage of volatiles	2.0 - 7.0	0.5
Powder density δ	1.62- 1.56	1.62 - 1.56

Table 5

Kisnensky's formulae

N%	11	12	13	14
W_1	979	931	882	833
T_1	2165	2456	2750	3096

$$W_1 = 1515 - 48.72N; \quad T^* = 273 + 34.7 N^{5/3}$$

Prof. V. Shekleyne's empirical formulae for Q_w , W_1 and T_1 as functions of the chemical components (in %) of the Russian powders taking as basic values $Q_w = 730$; $W_1 = 944$ and $T_1 = 2790$ for the pyroxylin powder containing $N = 11.8\%$, and using the following notations for the percentages of various components: Nitrogen - N ; Nitroglycerine - n ; Centralite - C ; Dibutylphthalate - D ; Vaseline - V ; Removable volatiles - h ; unremovable volatiles - h^1 ; Diphenylamine - P ; Camphore - K ; graphite - G then we will have these formulae as follows:

$$Q_w = 730 + 148.5 (N-11.8) + 9.41 n - 28.5C - 24.3 D - 37.5V - 13.6h - 26.7h^1 - 31.0P - 32.5K$$

$$W_1 = 944 - 47.3(N-11.8) - 2.45n + 14.0C + 12.0D + 23.0V + 3.4h + 16.9h^1 + 14.6P + 17.4K + 10.0G$$

$$T_1 K^* = 2790 + 375(N-11.8) + 22.0n - 71.0C - 59.0D - 100.0V - 54.0h - 82.0h^1 - 88.0P - 92.0K - 125.0G$$

2.3. Ballistic Characteristics of Powder:

"Force" of powder $f \frac{\text{kg} \cdot \text{dm}}{\text{kg}} = RT_1 = \frac{R W_1}{\lambda T_1} T_1$; $R = 1/\lambda m = 1.033 \text{ kg/cm}^2$
 $R = \frac{R W_1}{\lambda T_1}$

Corovolume $\propto \left(\frac{\text{dm}^3}{\text{kg}}\right) \sim 0.001/W_1$; Kisnemy's: $\alpha = \frac{5.7}{N^{0.7}}$

The rate of burning u_1 at the pressure $p = 1$

Table 4

Powders	f	α	$u_1, \frac{\frac{\text{dm}}{\text{sec.}}}{\text{kg/dm}^2}$
Pyroxylin	770000-950000	0.95-1.10	0.0000060- 0.0000090
Nitroglycerine	900000-1200000	0.75-0.85	0.0000070- 0.0000150
Smokey	280000-300000	0.5	---

Dimensions and forms of grains and "specific surface" = $\frac{\text{initial surface of grain}}{\text{volume}} = \frac{S_1}{V}$

Density of loading: $\Delta = \frac{W}{W_0} \frac{\text{kg}}{\text{dm}^3}$, its value when the powder fills up the entire volume is called "gravimetric density" which is a measure of "compactness" of powder.

Section II - General Pyrostatics. General relationships and laws of gas formation during combustion in a closed volume. (p.43-p.118)

Chapter 1. - Burning of Powders.

- 1.1 Manometric Bomb (conic crusher of Prof. M. Serebryakov)
- 1.2 Principal phases of burning (ignition, inflammation, burning in the interior of the grains)
- 1.3 Burning of powder under atmospheric pressure.
- 1.4 Burning at a pressure lower than atmospheric.
- 1.5 Burning in a vacuum.

1.6 Powder burning at the higher pressures. The rate of burning is greatly affected by pressure. This fact has long been known but only Vielle experimentally investigated the relationship between the pressure and the rate of burning. It is also interesting to note that these experiments have verified and firmly established Vielle's hypothesis of burning by parallel layers.

Kastan found from his observations of incompletely burnt grains of black powder thrown out of the gun after firing, that at a density of $\delta = 1.64$ the powder burned without any fragmentary residues; at $\delta = 1.72$ the fragments were of quite irregular shapes and only at $\delta = 1.81$ did the remaining grains display a marked similarity between their final form and their initial form before burning.

Vielle arranged special experiments with similar grains in the form of tablets and cylinders of different sizes a_1 and a_2 ; powder having these grains was burned at the same density of loading and maximum pressures, and their times of the complete burning t_1 and t_2 were recorded. At a density of powder of 1.64 or lower t_1 and t_2 were practically equal even when a_1 and a_2 were markedly different. (see Fig. 9 where shaded areas represent the unburned part of the initial grain).

At a density of 1.72 the times of burning were increased but not in proportion to the increase in sizes - this result corresponds to the result observed by Kastan in the unburned grains thrown out of the gun.

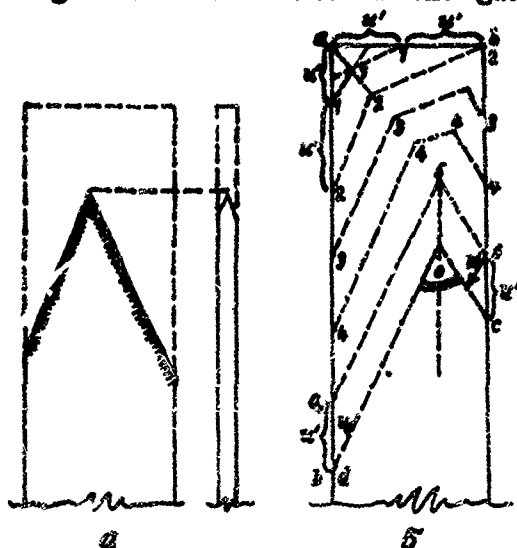


Fig. 8. Powder Strip burning in the open air.



Fig. 9 - Unburned grains of powder.

Fig. 9 Unburned grains of black powder.

At a density of 1.80 an exact proportion

$$\frac{t_2}{t_1} = \frac{a_2}{a_1}$$

was observed and at this density of powder Kasten observed the similarity of geometrical patterns between unburned grains and initial grains.

This result can be obtained only if burning occurs by parallel layers.

The following Table 6 sums up the results of the actual firings and the results of experiments in the manometric bomb.

Table 6

<u>No.</u>	<u>δ</u>	<u>Firing tests</u>	<u>Experiments in a manom. bomb</u>
1	1.64	no unburned grains	$t_1 \approx t_2$
2	1.72	unburned grains of irregular forms	$t_1 < t_2$, but $\frac{t_2}{t_1} \neq \frac{a_2}{a_1}$
3	δ > 1.80	unburned grains of regular form	$\frac{t_2}{t_1} = \frac{a_2}{a_1}$

These results show the direct dependence of time of burning on density of powder. Black powder is a mechanical mixture of sulphur, charcoal and potassium nitrate and the lower is its density (the smaller compression in the press) the more friable is the mass of the powder, and the time of burning cannot be affected by the size of a grain, which is easily crumbled even by a moderate pressure.

At a density $\delta = 1.70 - 1.72$ the pores of the powder mass are smaller and crumbling can be produced only under higher pressures. Only when the density is as high as $1.80 - 1.82$ is a compact mass of powder not crumbled even by high pressures but burns regularly in parallel layers.

Thus at higher pressures a general character of burning, and burning rate in particular, are definite results of density and, still more, of pressure - in fact an increased rate of burning is produced by an increased pressure. Thus Vielle's criterion can be formulated as follows: if in the same constant volume, with the same density of burning two powders of the same chemical composition with grains having unequal sizes but geometrically similar forms are burned, and if the observed times of their complete burning t_1 and t_2 are proportional to the sizes of their grains a_2 and a_1 , i.e. if $\frac{t_2}{t_1} = \frac{a_2}{a_1}$, then

this is evidence that the burning process in this case is occurring in parallel layers.

1.7 Smokeless powders. The experiments in the manometric bomb with smokeless powders show that in this case Vielle's criterion is perfectly satisfied and it can be safely assumed that smokeless powders do burn in parallel layers.

Although the rate of burning for smokeless powder in the open air is considerably lower than that for black powder, nevertheless its rate of burning in the closed volume is very high. A total duration of the actual firing or of the experiment in the manometric bomb is of the order of some thousandths of a second.

Since the strips of the smokeless powders are very strong and elastic, they do not crumble and burn in parallel layers.

Those unburned strips which are found after the actual firings are always of a similar shape to the original strips before firing. In the case of burning within the bore of a gun, but not in the open air, the strips of powder preserve their original parallelepiped forms but not of pointed prisms as is observed in the open air.

This sharpening, with the angle whose sine is the ratio $\frac{u}{u^1}$, is a result of a comparatively small difference ($u^1 - u$), but in a closed volume the rate of inflammation u^1 is incomparably higher than u because this inflammation is caused by the hot gases and a high enough ignition pressure - hence the strip of powder burns preserving its shape, its surface becoming slightly rougher.

If a strip of smokeless powder is ignited in the open air it burns very rapidly, being inflamed over all its surface. When the powder charge is in the gun's chamber or in the manometric bomb its inflammation is produced by the ignitor having its own additional charge of pyroxylin or black powder, developing at once large amounts of hot gas with the considerable pressure of 10-50 atm.

Under these conditions the charge is at once inflamed almost over its whole surface and the further burning goes on in parallel layers.

From his experimental results Vielle established his laws of burning of smokeless powders. His basic assumption was that the mass of powder is perfectly homogeneous in all directions and that all grains are identical in shape and size. Then the following principal laws are valid:

1. The inflammation of the powder in the closed volume is instantaneous.
2. The process of burning progresses by parallel layers with the same rate of burning over the whole surface at any moment of time.

The total amount of the developed gases depends on the change in volume of the burning grains. On the basis of the above formulated laws it is possible by means of purely geometrical considerations to find the relationship between the thickness of the burned layer of grain and the total volume of burned powder - this relationship is what is called the geometrical law of burning of the powder.

This law depicts only the external schematic aspect of the entire complex burning process of the whole powder charge, which is composed of grains or elements not quite identical in size or shape. For example - every strip pressed through the die has different strength along its length and breadth.

Besides this the inflammation of the large number of grains constituting a powder charge cannot be strictly simultaneous and instantaneous. Even though the actual process of the burning of a powder charge differs from

the schematic process assumed for a separate grain, nevertheless the geometric law of burning lays the foundation for a comprehensive evaluation of the effect produced by the forms on the development of pressure within the bore of a gun and sizes of the grains.

These purely geometric factors turn out to be effective means which can be used for the control of the whole process of gas formation and for the regulation of the basic process of firing.

In recent researches in the Twentieth Century the geometric law of burning was perfected in its details and was further developed by taking into account those factors which were omitted or overlooked in the earlier work. The geometric law was based on the study of the pyroxylin powder of a single form of grain (strip, tube, plate). Later on newly developed powders with a more complex form were considered. American powders with 3, 7 and 19 perforations; Russian grain developed by Kisnensky with 36 perforations; phlegmatized powder with nonhomogeneous distribution of the phlegmatizer within the mass of powder and nitroglycerine powders, in which nitroglycerine powders, in which nitroglycerine is unevenly redistributed during its storage. Certain new processes of surface

graphitization were introduced which inhibited the process of inflammation.

All these new factors resulted in new refinements of our practical methods and new corrections to our theoretical schemes.

1.8 Theory of the Burning of Powder. In 1908 Charbonnier in his "Interior Ballistics" brought out several critical views on the validity of the basic principles of the geometric law of burning. A careful inspection of thick strips of powder thrown out of the gun after firing disclosed that many of them had burned very irregularly; their webs were markedly different, and their surfaces had indentations obviously resulting in fragmentations of the strips into smaller splinters which were also found in sizable quantities at the front of the gun. A certain degree of imperfection in the manufacturing process of powder of course can be taken into account, but the fact remains that the ballisticians and artillerymen by all means must manipulate with real and not with ideal powders and here a question arises - is it justifiable to apply certain theoretical schemes devised for a separate grain (strip) to the whole powder charge consisting of a large bunch of powder strips or even of several such

bunches? The negative answer is unavoidable and it is easy to explain the necessary deviations from the elementary law controlling the burning of one isolated grain. A basic assumption of interior ballistics is that the ignition of the whole powder charge is instantaneous, i.e. the rate of spreading of the flame is incomparably greater than the rate of burning. This very assumption is not verified for open air burning, and there can be found no valid reason for assuming that under the high pressures the rate of spreading of a flame can be incomparably higher than the rate of burning.

It is more plausible that the first bunch of strips nearest to the igniter will be inflamed and burned ahead of the bunches which are nearest to the base of the projectile.

The first flame of ignition naturally is directed into the spaces between the grains and an orderly orientation of all grains along the axis of a chamber is liable to produce a much better effect of increasing the rate of ignition than the disorderly positions of all the grains poured into a chamber in a haphazard way.

The immediate contacts between the grains of powder and contacts of grains with the metal of the gun may result in certain deviations from the regularity of burning

by parallel layers.

Charbonnier himself, having stated all his objections and critical remarks, has failed to produce his own experimental results verifying his criticism. But these items have been discussed and investigated by other ballisticians.

More detailed investigations were made by M. E. Serebryakov (1924-1929) who introduced the use of a conical crusher, a very sensitive device registering as low a pressure as 5-7 kg/cm. (M. E. Serebryakov, "The Physical law of burning in Interior Ballistics" (1937-1940).

This new type of crusher permitted the registering of the whole curve of pressure from the very beginning until the end of powder burning. On the other hand, M. E. Serebryakov has worked out a new method of a more minute analysis of the process of burning attainable by a special analysis of the experimental curve of the pressure in the manometric bomb. Thus from the analysis of a series of experiments M. E. Serebryakov has established beyond a doubt that the ignition of powder is not instantaneous but depends on the gas pressure developed by the igniter and on the type of ignition.

This new method giving a more descriptive idea of the intensiveness of the gas formation process has established

not only a whole series of deviations from the "geometric law" of the powder burning but also presented plausible explanations, thus showing that the actual process of burning is much more complex than the assumption of the "geometric law" may imply.

It was found that the mass of a powder charge is not uniform from one layer to another and that the rate of burning of the outer layers is higher than the rate of burning of the inner layers. Special experiments have definitely established that the character of burning depends not only on the shape of a grain, but on the mutual positions of burning surfaces of grains. The closer these surfaces are to each other, the more vigorous is the burning. The phlegmatized powders have been also investigated and there were found certain peculiar features of their burning and a special method was devised for determining the depth of phlegmatization of the powder mass.

The powders with the long and narrow channels showed special peculiarities in their burning, and thus a special theory of a non-uniform burning with the intensity varying from one element of powder charge to another was established. This theory disclosed that the difference in intensity of burning inside the perforations of grains and on the surfaces of grain depends largely on the density

of loading and varies during the firing with the travel of the projectile.

All the experimental results definitely not consistent with the "geometric law" of burning were explained by certain specific propositions of the physico-chemical nature of powders or by certain physical characteristics of the powder gas. These results were systematized and formulated comprehensively as the "physical law" of the burning constituting the next necessary development of the previous incomplete and approximate "geometrical law" (details are shown in Section III).

Muraour, considering the process of powder burning in the light of physical chemistry, came to the following conclusions:

1. Powder burns because the newly formed molecules of gas by their bombardment bring its temperature up to the temperature of its disintegration.
2. There is a "contact layer" of gases in the proximity of the powder surface; the reactions of the disintegration are not yet completed, since NO_2 has not reacted with CO and H_2 ; the temperature of the "contact layer" controls the rate of burning, and this temperature is lower than the calculated temperature of explosion.
3. In the outer layers of gases, all the reactions are completed and these layers become hotter and hotter.

4. Contact with the colder walls of a manometric bomb produces a cooling effect on the gases, and their temperature falls.

Muraour also tried to take into account the effect of the radiating heat of the powder gases on the heating of the powder at low densities of loading.

Since 1939 several works were published by Russian scientists on the mechanics of the burning process in explosions: A. F. Belayev, D. A. Frank-Kamenetzky; Prof. J. B. Zeldovich.

Prof. Zeldovich began with the theory of volatile liquid explosives and applied his results to the theory of burning of powders.

This "thermal theory" considers the burning process as a result of the heating of the powder surface up to the temperature of its disintegration or transformation into gases, with their temperature still continuing to increase till the temperature of burning is reached.

A burning rate, being a function of the gas pressure, is also affected by the temperature of powder heated by the surrounding mass of gases. Certain details of this theory are particularly new and original as giving a comprehensive picture of the operating distribution of thermal energy between gases and powder, with the detailed

descriptions of the following active factors: the initial temperature of the disintegration of gases, specific heat and thermal conductivity of powder. This theory is not completed yet but is of considerable scientific interest because of its detailed and scientific account of the process of the burning of powder.

1.9 The modern theory of the burning of powder (After J. B. Zeldovich)

The following is a general picture of the powder burning process: as soon as the outer layer of the nitrocellulose is decomposed, then as a result the process of gasification begins over the surface of the powder - products of gasification react in their gaseous phases having a very rapidly rising temperature. However, the surface temperature, being the temperature of the initial decomposition of the nitrocellulose, remains considerably lower.

The distribution of temperatures is schematically shown on Fig. 10.

T_0 - temperature inside of powder

T_n - temperature of powder on the surface

T_r - temperature of gases

Shaded areas show the zones affected by the chemical reactions: zone 1 - gasification (in powder) and zone 2 - reaction of burning (outside of powder). The burning

surface of powder has a heating layer with its thickness X_r depending on the thermal conductivity (temperature coefficient) and rate of burning. Within the partial thickness $X_p \approx 0.05 X_r$ the actual reaction of gasification goes on.

One of the principal problems of this theory is the establishment of the functional relationship between the rate of burning and the kinetics of the chemical reaction.

An essential importance must be ascribed to the heating through the layer X_r not only because this heating shows the connection between the burning rate and the kinetics of gasification but also because here other problems also are involved: for instance - the problem of the inflammation, the problem of unstable burning, etc.

From the experiment made by O. J. Leypounski and Mrs. V. J. Aristov with the burning powders at the open air we have:

$$T_n = 252 \pm 48^\circ = 525 \pm 48^\circ \quad \text{-- for pyroxylin powder}$$

$$T_n = 330 \pm 45^\circ = 603 \pm 45^\circ \quad \text{-- for nitroglycerine powder}$$

Table 7 gives the physical characteristics of powders in the experiments of O. J. Leypounski.

Table 7

<u>Powders</u>	<u>Specific heat cal./gm.°C</u>	<u>Temperature Coefficient cm²/sec.</u>	<u>Thermal conduct- ivity cal.cm/sec.</u>	<u>Rate of burning at p=1 atm. m/m sec.</u>
Pyroxylin	0.29	1.2×10^{-3}	5.5×10^{-4}	0.51
Nitroglycerine	0.34	0.87×10^{-3}	4.8×10^{-4}	0.45

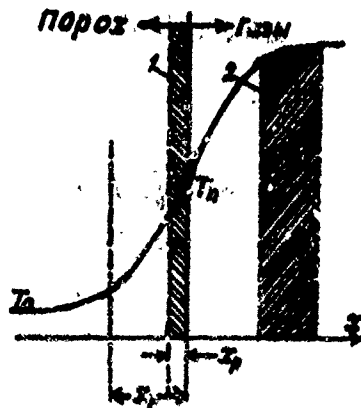


Fig. 10 The distribution of temperatures at the burning of powder.

Chapter 2, - The Characteristic Equation of the Powder Gases.

(Relationship between the pressure and loading conditions).

2.1 Powder gases developed under the high temperature and high pressure in a closed vessel are the subject of the general laws of physics and thermodynamics and they have as all other gases their characteristic equation expressing the form of the relationship between pressure, temperature and specific volume.

Clapeyron's equation: $p w = RT$

(ideal gases or rarified)

Van der Waal's equation: $(p + \frac{a}{w^2})(w - b) = RT$ (Real gases)
or: $p(w - b) = RT$

For ω_{ij} of powder burning in a volume W_0 at T_1 K°:

$$p \left(\frac{W_0}{\omega} - b \right) = RT_1$$

or:
$$p = \frac{\omega RT_1}{W_0 - b\omega} \dots (1)$$

2.2 Formula for the maximum pressure.

Empirical formula of Noble and Abel: $p_m = \frac{f \Delta}{1 - \alpha \Delta} \dots (2)$

or:
$$p_m = \frac{f \omega}{W_0 - \alpha \omega} \dots (2')$$

From (1) and (2'): $f = RT_i$ and $\alpha = \beta$

Since $R = \frac{P_1 V_1}{273}$ is the work done by the gas at

$P_1 = 1 \text{ atm} = 1.033 \times 10^6 \text{ dy/cm}^2$ when its temperature is raised 1° ,
 f is the work of 1 kg . of powder gas when heated at
 T_1° under a constant pressure P_1 .

From (2): $\frac{P_2}{\Delta} = f + \alpha P_m$ or: $y = f + \alpha x \dots (3)$

i.e. $\frac{P}{\Delta}$ is a linear function of P_m

For pyroxylin powder: $f = 900000$; $\alpha = 1$

nitroglycerine powder: $f = 1050000$; $\alpha = 0.8$

black powder: $f = 280000$; $\alpha = 0.5$

2.3 Determination of f and α for a given powder.

Having results of two experiments in manometric bomb at P_1 ,
 with Δ_1 , and at P_2 with Δ_2 we can find α and f
 for a given powder, from the equation (3) written for
 these experiments:

$$\alpha = \frac{\frac{P_1}{\Delta_1} - \frac{P_2}{\Delta_2}}{P_2 - P_1} \dots (4)$$

$$f = \frac{P_1}{\Delta_1} - \frac{P_2}{\Delta_2} \cdot \frac{\Delta_2 - \Delta_1}{P_2 - P_1} \dots (5)$$

$$\text{or: } f = \frac{P_1}{\Delta_1} - \alpha P_1 = \frac{P_2}{\Delta_2} - \alpha P_2 \dots (6)$$

2.4 The experimental errors in ρ_1 and ρ_2 affecting the calculated values of α and f .

Errors in f :

Denoting δf_1 , and δf_2 the absolute errors in f caused by the errors in ρ_1 and ρ_2 respectively we have from (5): differentiating with respect to ρ_1 :

$$\delta f_1 = \frac{\rho_2}{\Delta_2} \cdot \frac{\Delta_2 \Delta_1}{\Delta_1} \cdot \frac{\rho_1}{(\rho_2 - \rho_1)^2} \cdot \delta \rho_1,$$

and differentiating with respect to ρ_2 :

$$\delta f_2 = \frac{\rho_1}{\rho} \cdot \frac{\Delta_2 \Delta_1}{\Delta_1} \cdot \frac{\rho_2}{(\rho_2 - \rho_1)^2} \cdot \delta \rho_2 \quad (\Delta_2 > \Delta_1; \rho_2 > \rho_1)$$

Hence the relative errors in f will be:

$$\frac{\delta f_1}{f} = \frac{\rho_2}{\rho_2 - \rho_1} \cdot \frac{\delta \rho_1}{\rho_1} \quad \dots \quad (7)$$

For pyroxylin powders: $\Delta_1 = 0.15$; $\Delta_2 = 0.25$

$$\frac{\delta f_2}{f} = - \frac{\rho_1}{\rho_2 - \rho_1} \cdot \frac{\delta \rho_2}{\rho_2} \quad \dots \quad (8)$$

For nitroglycerine powders: $\Delta_1 = 0.12$; $\Delta_2 = 0.20-0.22$

Errors in α :

Differentiating (4) with respect to ρ_1 and ρ_2 we will have:

$$\delta \alpha_1 = - \frac{f}{\rho_2 - \rho_1} \cdot \frac{\delta \rho_1}{\rho_1} \quad \dots \quad (9)$$

and

$$\delta \alpha_2 = \frac{f}{\rho_2 - \rho_1} \cdot \frac{\delta \rho_2}{\rho_2} \quad \dots \quad (10)$$

from (7) and (9): $\frac{\delta f_1}{f} = - \frac{\rho_2}{f} \cdot \delta \alpha_1 = - \frac{\delta \alpha_1}{\frac{1}{\Delta_2} - \alpha} \quad \dots \quad (11)$

and:

$$\frac{\delta f_2}{f} = - \frac{\delta \alpha_2}{\frac{1}{\Delta_1} - \alpha} \quad \dots \quad (12)$$

2.5 Powder pressure lower than $\frac{p}{m}$. At any moment when a fraction $(\psi \cdot \omega)$ of the initial weight of charge ω_{ng} is burned we have the residual volume of bomb W_ψ instead of W_0 : $W_\psi = W_0 - \frac{f}{\delta} (1 - \psi) - \alpha \psi \omega$

and then the equation of the gaseous state will be:

$$p_\psi [W_0 - \frac{f}{\delta} (1 - \psi) - \alpha \psi \omega] = f \omega \psi$$

hence:

$$p_\psi = \frac{f \omega \psi}{W_0 - \frac{f}{\delta} (1 - \psi) - \alpha \psi \omega} = \frac{f \psi}{\frac{1}{\delta} - \frac{1}{\delta} - (\alpha - \frac{1}{\delta}) \psi} \quad (13), (14)$$

This is a general formula of Pyrostatics which at $\psi = 1$

gives: $p_i = \frac{f \Delta}{1 - \alpha \Delta}$

At the beginning of burning ($\psi = 0$): $W_\Delta = W_0 - \frac{f}{\delta}$

at the end of burning ($\psi = 1$): $W_i = W_0 - \alpha \omega$

Since for the pyroxylin and nitroglycerine powders

$\alpha = 1.0 - 0.8$; $\delta = 1.6$, $\frac{1}{\delta} = 0.625$ we have:

$$W_\Delta > W_\psi > W_i$$

2.6 The inverse relationship: ψ as a function of p . From (13) we have:

$$\psi = \frac{\frac{1}{\delta} - \frac{1}{\delta}}{\frac{1}{\delta} + \alpha - \frac{1}{\delta}} = \frac{p (\frac{1}{\delta} - \frac{1}{\delta})}{f + p (\alpha - \frac{1}{\delta})} \quad (15)$$

or substituting f from (2):

$$\dot{p} = \frac{1}{1 + \frac{1-\alpha A}{1-\frac{A}{B}} \cdot \frac{B-A}{B}} \quad (16)$$

$$\text{Here: } \frac{1-\alpha A}{1-\frac{A}{B}} = \vartheta = \frac{W_1}{W_2} = \frac{W_0(1-\alpha A)}{W(1-\frac{A}{B})} < 1$$

$$\text{At } A=0.25; \alpha=1; B=1.6: \vartheta=0.89$$

2.7 Evaluation of the effect of the igniter. In using the general formula of pyrostatics (14) we may neglect the value of the atmospheric pressure inside the bomb, but since the time of Nobel's experiments the ignition of the powder has been produced by a small separate charge of the black powder and the additional weight of the igniter was included in the total weight of powder charge. At present in the experiments with the bomb or in actual firing with the smokeless powder the igniter used is prepared from black or pyroxylin powder. Thus at the beginning we have a certain initial powder pressure and a certain mass of hot gases, produced by the igniter. The actual burning of the powder charge starts at a certain pressure p_B developed by the igniter.

Let us denote: the weight of the charge of the igniter W_B ; force of the igniter f_B ; covolume of the igniter α_B and the preliminary pressure of the

igniter p_0^* . Applying Noble's formula to the process of ignition only, we have: $p_0^* = \frac{f_0 \omega_0}{W_0 - \frac{f_0}{f} - \alpha_0 \omega_0} \approx \frac{f_0 \Delta_0}{1 - \frac{f_0}{f}}$

here $\Delta_0 = \frac{\omega_0}{W_0}$ and $\alpha_0 \omega_0$ are negligible.

For any intermediate moment the formula (13) will be:

$$p' = \frac{f_0 \omega_0 + f \omega_f}{W_0 - \frac{f_0}{f} - (\alpha - \frac{f_0}{f}) \omega_f - \alpha_0 \omega_0}$$

again neglecting $\alpha_0 \omega_0$ we will have:

$$p' = \frac{f_0 \omega_0 + f \omega_f}{W_f} = \frac{f_0 \omega_0}{W_f} + p$$

Here $p = \frac{f \omega_f}{W_f}$ is the gas pressure calculated without taking into account the effect of ignition; a decreasing value of W_f will increase the total pressure p' .

At the end of burning the total maximum pressure will be:

$$p_m = \frac{f_0 \omega_0 + f \omega_f}{W_0 - \alpha \omega - \alpha_0 \omega_0} = \frac{f_0 \omega_0}{W_0 - \alpha \omega} + \frac{f \omega_f}{W_0 - \alpha \omega} = p'_m + p_m$$

here: $p'_m = \frac{f_0 \omega_0}{W_0 - \alpha \omega} = \frac{f_0 \Delta_0}{1 - \alpha \Delta}$ and $p_m = \frac{f \Delta}{1 - \alpha \Delta}$

Since $1 - \alpha \Delta < 1 - \frac{\Delta}{f}$ we have $p'_m > p_0^*$

For smokeless powder the ratio $\gamma = \frac{1 - \alpha \Delta}{1 - \frac{\Delta}{f}} > 0.89$
 < 1.00

Hence: $\frac{p'_m}{p_0^*} \approx 1.10$

This result shows that with a sufficient accuracy we can assume that an additional pressure provided by the igniter can be considered as constant, while the actual value of this additional pressure is always found to be between 20 kg/cm² and 50 kg/cm² and even in exceptional cases never higher than 100 kg/cm².

Thus we have as a final estimate: $p_0 = p_0^0 = \frac{f_0 \omega_0}{W_0 - \frac{\omega_0}{\delta}}$

and our formulae taking into account the pressure developed by the igniter, will be:

Maximum pressure: $p_m' = p_0 + \frac{f \omega}{W_0 - \alpha \omega} = p_0 + \frac{f_0}{1 - \alpha \Delta}$

Igniter pressure: $p_0 = \frac{f_0 \omega_0}{W_0 - \frac{\omega_0}{\delta}}$

Intermediate pressure: $p_\psi' = p_0 + \frac{f \omega \psi}{W_0 - \frac{\omega}{\delta} - \omega(1 - \frac{\delta}{2})\psi}$

From the last equation:

$$\psi = \frac{\frac{1}{\Delta} - \frac{1}{\delta}}{\frac{1}{p - p_0} + \alpha \cdot \frac{1}{\delta}} = \frac{1}{1 + \frac{1 - \alpha \Delta}{1 - \frac{\delta}{2}} \cdot \frac{p_m' - p_0'}{p - p_0}}$$

Here pressures p_m' and p_0' are actual pressures registered by means of crusher or by any other instrument, and $p_0 \sim p_0' = p_0^0$. Since the last formula is somewhat unwieldy, special tables are prepared in order to simplify the calculations of series of ψ values. In

these tables (see appendix 1) the expression for ψ can be brought to such a form in which ψ will be a function of a constant parameter $\vartheta = \frac{1-\alpha\Delta}{1-\frac{\alpha}{\beta}}$ and a certain ratio of pressures: $\beta = \frac{p'_m - p_s}{p'_m - p_s}$

Here: $p'_m - p_s$ is a constant for a given experiment, p' is any pressure picked up from the pressure curve for which we want to find its corresponding value of ψ . A needed transformation of ψ is as follows:

$$\psi = \frac{1}{1 + \left(\frac{1-\alpha\Delta}{1-\frac{\alpha}{\beta}} \right) \cdot \left(\frac{p'_m - p_s}{p'_m - p_s} \right)} = \frac{p'_m - p_s}{(p'_m - p_s) + \vartheta (p'_m - p_s)} \cdot \frac{\left(\frac{p'_m - p_s}{p'_m - p_s} \right)}{\left(\frac{p'_m - p_s}{p'_m - p_s} \right) (1-\vartheta) + \vartheta} = \frac{\beta}{(1-\vartheta)\beta + \vartheta}$$

Here: β varies from 0 to 1; ϑ varies from 0.86 to 1. The tables are arranged like four figure logarithmic tables for each 0.001, and interpolated for the 4th figure.

From the series of calculated ψ we can calculate also the curve of $\left(\frac{d\psi}{dt} \right)$ or the rate of gasification. This rate is one of important characteristics which controls the inflow of gases, i.e. the process of the build of pressures.

Chapter 3 - Evaluation of the amount of heat transmitted through the walls of the manometric bomb.

3.1 During the burning of powder in the bomb, a certain amount of heat is lost by heating the walls of the bomb. As a result the actual pressure becomes somewhat lower than the theoretical maximum pressure, expected under the assumption that the total amount of heat derived from the powder gases has been utilized for the building up of gas pressure.

This sort of heat loss depends on the joint influences of several loading conditions. As early as 1895-96 the experiments of Prof. S. Voukoloff in the Russian Navy Laboratory showed at $\Delta = 0.20$ a marked difference of about + 8% in the maximum pressures observed in a bomb with an insulated inner surface (a layer of mica) as compared with the maximum pressure in an ordinary bomb. Any error made in the value of the maximum pressure p_m will affect the obtained value of "force" f and covolume α . At a pressure higher than 1000 kb/cm² Nobel's formula gives quite satisfactory results; at lower pressures with

$\Delta < 0.10$ our straight line $\frac{p_x}{\Delta} = f + \alpha p_m \dots (3)$ becomes a hyperbolic line.

More recent and detailed experiments of the docent A. J. Kokhanov in 1933 with the densities of loading varying from 0.015 up to 0.200 proved that a real relationship

walls of a bomb, we will have lower values of f for the powders having a larger web. This result can be foreseen a priori because a powder with a larger web will burn more slowly and the result will be affected by the walls of the bomb for a larger period of time, hence the heat loss will be greater.

If in these experiments we use two bombs of different inner volumes with the same powder at the same Δ , then in the larger bomb the weight of powder referred to the unit of surface will be smaller and heat losses will be less than in the smaller bomb - hence the obtained β will be higher in the larger bomb.

Several experimental investigations were made of this type of heat loss in the manometric bomb. All these attempts are not yet considered as final or completely satisfactory. As one of the most outstanding investigations of this kind we will mention the work of Muraour (1926-27).

According to Muraour the total loss of heat transmitted to walls of the bomb is proportional to the number of impacts of gas molecules against the inner surface of the bomb (S_g); to the gas pressure p and to the time t . When the pressure is variable, we consider $\int p dt$ which is independent of Δ .

Hence, the loss of heat through the walls of the bomb ΔQ will be constant for every ω and Δ . This conclusion was verified by Muraour's experiments made at various Δ .

Since the total amount of heat is proportional to ω the relative loss $\frac{\Delta Q}{Q}$ will be inversely proportional to ω and finally $\frac{\Delta Q}{Q}$ will be proportional to $\frac{3g}{\omega} \int p dt$

It is necessary to note that $\int p dt$ should not be affected by the cooling effect of the walls of a bomb. Any drop in pressure say at $n\%$ will increase the time of burning; thus the curve p as a function of time t will be somewhat deformed but the whole area $\int p dt$ will not be altered. This result was wholly confirmed by our experiments with bombs of various volumes. Hence a very important result follows, namely: the rate of burning u , referred to unit pressure can be calculated from

$$u_1 = \frac{c_1}{\int p dt}$$

and this value can be determined with the same degree of accuracy in larger and in smaller bombs without any account of heat losses through the walls of bombs.

3.2 Experimental investigations of Muraour. The volume of his bomb was 150 cm³. and $\Delta = 0.20$. One powder charge was burned in the bomb under normal conditions, and another charge of the same weight was burned

in a special pan with pins preventing its immediate contact with the inner surface of a bomb - as is shown on Fig. 17 (p. 76 - book).

In the first experiment the effective surface was $S_2 = S_1$ and the observed pressure p_1 ; in the second experiment the effective surface was $S_2 = S_1 + S_p$ where S_p is the surface of the pan and the observed pressure $p_2 < p_1$. The difference in pressures $\Delta p = p_1 - p_2$ was ascribed to the action of the difference in surface $S_2 - S_1 = S_p$.

In order to evaluate the pressure expected to be found in the absence of cooling we need to evaluate the additional pressure $\Delta p'$ which is due to the increase of the surface from S_p to S_2 so we write: $\frac{\Delta p'}{\Delta p} = \frac{S_2}{S_p}$
hence: $\Delta p' = \Delta p \frac{S_2}{S_p}$

Thus we have an uncorrected pressure ($p_1 + \Delta p'$)

and the relative correction in p_m : $\frac{\Delta p_m}{p_m} = \frac{\Delta p'}{p_1} = \frac{\Delta T}{T_1}$

These experiments with many powders differing in their compositions and sizes of webs at $\Delta = 0.20$ have established an important functional relationship between $\frac{\Delta p_m}{R_m}$ (losses in p_m) and durations of the burning process. The value of $\frac{S_2}{\omega}$ in these experiments was: $7.774 \frac{\text{cm}^2}{\text{g}_m} \approx 77.74 \frac{\text{dm}^2}{\text{kg}}$

In all these experiments cylindrical crushers were used and a very strong igniter made of black powder with its additional pressure of 250 kg/cm² and results were incorporated into "curve C" of $\frac{\Delta p_m}{p_m} = \frac{\Delta T}{T} \%$ as a function of the time of burning t_k in mill.-sec. (See Fig. 18) Page 76 (book).

The use of this curve is as follows: the powder to be tested first goes through the experiment at $\Delta = 0.20$ and burning time t_k is determined; then for this t_k on the "curve C" we find $C_H = \frac{\Delta p_m}{p_m} \%$

Under other conditions (another bomb and Δ)

$$\frac{\Delta p_m}{p_m} = \frac{\Delta T_i}{T_i} = \frac{C_H \%}{7.774} \cdot \frac{S_0}{W} = \frac{C_H \%}{7.774} \cdot \frac{S_0}{W_0} \cdot \frac{1}{\Delta} \dots (17)$$

Here C_H depends on thickness (web) of powder and its composition; $\frac{S_0}{W_0}$ is a relative surface of bomb =

$$= \frac{\pi d c + \frac{\pi d^2}{4} \cdot 2}{\frac{\pi d^3}{4} \cdot 2c}$$

The chamber of the bomb is a cylinder with d as its diameter and $2c$ its length. ($\beta = \frac{d}{2c}$)

$$S_0 = \text{surface of the chamber} = 2\pi d c + 2\left(\frac{\pi d^2}{4}\right)$$

$$W_0 = \text{volume of chamber} = \frac{W}{\Delta} = 2c \cdot \frac{\pi d^2}{4} = \frac{\pi}{2} c d^2$$

Formula (17) shows that the heat losses are particularly significant at the decreased value of Δ

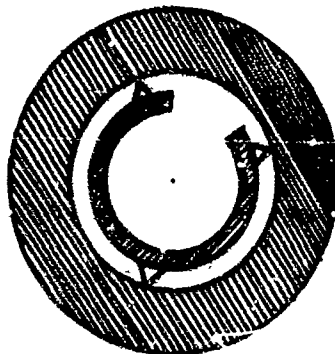


Fig. 17 - Manometric bomb used by Muracour

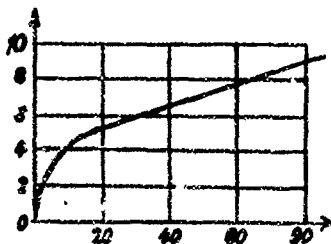


Fig. 18 - "C-curve"

$\frac{h}{R_0}$ as a function of t_k in mill. sec.
(as given by Muracour)

In the Russian experiments conical crushers are used and the pressure p is only as high as 100-120 kg/cm^2 (instead of 250 kg/cm^2).

In order to make Muraour's results applicable to our experiments with the pyroxylin powders the following Table 8 was prepared for the corrected values of G_M .

For the value of t_k the following formula was used:

$$t_k = 2.303 \tau \cdot \log \frac{A}{B}$$

here: $\tau = \frac{e_i}{u_i} \cdot \frac{1 - \epsilon_i A}{f_A} = \frac{e_i}{u_i} \cdot \frac{1}{\rho_m}$

Table 8 (p. 77 - book)

Table for G_M for the pyroxylin powders with a constant surface of burning.

phleg-
matized

web = $2e_i$ = in m/m	0.30	0.30	0.40	1.00	2.00	4.00
rate of burning						
$u_i \cdot 10^7 \frac{dA}{dt} : \frac{A}{A_m} =$	90	70	80	75	72	62
Coefficient $\frac{1}{\epsilon} =$	1220	950	813	305	146	69
Time of burning t_k in mill.sec.						
at $A = 0.20$, $p_s = 250$:	1.76	2.26	2.64	7.00	14.60	31.0
Coefficient $G_M\%$:	1.5	2.0	2.6	4.0	5.0	6.1

Here is shown the whole procedure of finding the corrections in f and in α due to heat losses through the walls of a bomb. Our bomb has volume $W_0 = 78.5 \text{ cm}^3$; two densities of loading were used: $\Delta_1 = 0.15$ and $\Delta_2 = 0.25$. Thickness of powder $2a_1 = 1 \text{ m/m}$. The corresponding maximum pressures were $p_{m1} = 1435 \text{ kg/cm}$ and $p_{m2} = 2760 \text{ kb/cm}^2$. $p_{m2} - p_{m1} = 1325$; $\frac{S_0}{W_0} = 1.30$; Table 8: $C_M = 4.0$

Calculate: $\frac{p_{m1}}{\Delta_1} = 9570$; $\frac{p_{m2}}{\Delta_2} = 11040$;

$$\frac{p_{m2}}{\Delta_2} - \frac{p_{m1}}{\Delta_1} = 1450$$

Formula (4): $\alpha = \frac{\frac{p_{m2}}{\Delta_2} - \frac{p_{m1}}{\Delta_1}}{p_2 - p_1} = \frac{1450}{1325} = 1.096$

Formula (6): $f = \frac{p_i}{\Delta_1} - \alpha p_i = 800000$

Formula (17): $\frac{\Delta p_m}{p_m} = \frac{S_0}{W_0} \cdot \frac{1}{\Delta} \cdot \frac{C_M}{7.774} = \frac{0.6692}{\Delta}$

$$\Delta p_{m1} = p_{m1} \cdot \frac{0.6692}{\Delta_1} = 64 \text{ kg/cm}^2; \quad \Delta p_{m2} = p_{m2} \cdot \frac{0.6692}{\Delta_2} = 74 \text{ kg/cm}^2$$

Thus we have: $\left. \begin{aligned} p'_{m1} &= p_{m1} + 64 = 1499 \\ p'_{m2} &= p_{m2} + 74 = 2834 \end{aligned} \right\} p'_{m2} - p'_{m1} = 1335$

$$\frac{p'_{m1}}{\Delta_1} = 10000; \quad \frac{p'_{m2}}{\Delta_2} = 11340$$

$$\frac{p'_{m2}}{\Delta_2} - \frac{p'_{m1}}{\Delta_1} = 1340$$

$$\alpha(\text{corrected}) = \frac{1340}{1335} = 1.004 \approx 1.0 \frac{dm^3}{kg}$$

$$f(\text{corrected}) = 1000000 - 1.004(1499) \cdot 100 = 1000000 - 150000 = 850000$$

Thus in the final result by the use of corrections we increased f from 800,000 to 850,000 i.e. about 6.25% and decreased α from 1.096 to 1.000 i.e. about 9.6%.

In experiments with another bomb having its volume $V_0 = 25.25 \text{ cm}^3$, the same powder at the same densities of loading gives us $p_{m1} = 1405 \text{ kg/cm}^2$, and $p_{m2} = 2725 \text{ kg/cm}^2$.

For this bomb $\frac{S_0}{W_0} = 1.89 \text{ cm}^2/\text{cm}^3$ and $f = 774000$;

$$\alpha = 1.160$$

Then our corrections will be: $\Delta p_{m1} = 95$ and $\Delta p_{m2} = 110$ and the corrected value of $f = 850,000$; and of $\alpha = 1000$ the same as before but the corrections themselves are larger, i.e. a smaller bomb gives a smaller value of f and a larger α .

Kokhanov's experiments with the low Δ and powders with large w_0 s showed the needs of very large corrections but the introduction of the above shown corrections transforms a hyperbolic curves of Kokhanov (Fig. 16) into a straight line.

Table 9 was calculated for values of $\frac{S_0}{W_0}$ and for various typical dimensions of the manometric bombs.

Table 9

Krupp's bomb

W_{0cm} :	21.80	25.25	78.5	120	146.5	216	3320
d_0 :	2.2	3.0	4.4	4.4	3.0	4.4	8.0
$\frac{S}{W_0}$:	2.17	1.89	1.30	1.16	1.48	1.05	0.53
$\frac{S}{\pi d_0 W_0}$:	0.279	0.243	0.1673		0.184	0.135	0.0682
				0.1495			

Since t_k , the time of the complete burning of powder, is in direct proportion to $I_k = \int_0^{t_k} p dt$ or the total impulse of pressure, it is possible to calculate "curve C" as a function of I_k i.e. independently of Δ . This work was done by Mrs. M. J. Samarin in the Artillery Scientific Research Naval Institute (ASRNI) in 1938. The pressures were registered by the use of conical crushers. She repeated the experiments with the use of an additional pan for the powder charges. The pressures were registered by the use of conical crushers. The obtained curve C (called "C-Curve") as a function of I_k , is given on Fig. 19.

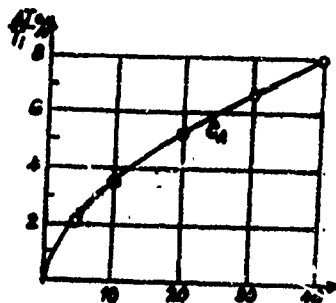


Fig. 19.- Curve C, a characteristic of the heat LOSS through the walls of gun.

Chapter 4 - The Law of Gas Formation (Gasification)

4.1 Definition. The study of gasification under simplified conditions within a constant volume makes possible the further development of the results obtained as modified for the more complicated conditions existing within a variable volume at firing.

The general formula of pyrostatics:

$$p = \frac{f\omega\psi}{W_0 - \frac{f\omega\psi}{\Delta} - (\alpha - f)\omega\psi} = \frac{f\omega\psi}{W_4}$$

shows that at given loading conditions ($W_0, \omega, f, \alpha, \delta$), the pressure is determined by the value ψ of the burned part of the powder, where $\psi\omega$ is the weight of gases and $f\psi\omega$ is the amount of energy of these gases. Since the value W_4 varies in the manometric bomb only slightly, we can assume that at given f and Δ the pressure is nearly proportional to ψ , and consequently the general character of the building up of the pressure with time or $(\frac{dp}{dt})$ is largely determined by the variation with time of $\frac{d\psi}{dt}$.

The variable $(\frac{d\psi}{dt})$ is called the velocity of gas formation or the "volumetric velocity of burning". We need a more detailed analysis of this variable.

4.2 The Velocity of Gas Formation. Let us derive a formula for $(\frac{d\psi}{dt})$ in terms of factors determining the mode of burning of powder by parallel layers. A given

grain of powder, having initial volume Λ_i and surface S_i , is supposed to be burned in concentric layers with the same rate of burning in all directions. At a certain moment of time, the grain will have a surface S and volume Λ (see Fig. 20). We suppose that in the time interval dt , the thickness of the burning layer will be de , then the burned element of volume will be $d\Lambda_e = Sde$.

hence: $\Lambda_e = \int S de$

and: $\psi = \frac{\Lambda_e}{\Lambda_i} = \frac{\int S de}{\Lambda_i}$

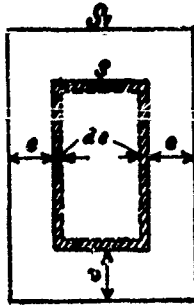


Fig. 20 Schematic view of burning by parallel layers.

Differentiating this equation with respect to time we will have:

$$\frac{d\psi}{dt} = \frac{S}{\lambda_1} \cdot \frac{de}{dt} = \frac{S}{\lambda_1} u = \frac{S_1}{\lambda_1} \cdot \frac{S}{S_1} \cdot u$$

Here: $\frac{S_1}{\lambda_1}$ - initial specific surface (or the initial "enuddation" of a grain) related to the unit of initial volume and depending on the shape and dimensions of the grain.

$\frac{S}{S_1}$ - relative surface of a grain varies with burning and depends only on the shape of the grain and the relative thickness of its burned layer, but not on the absolute dimensions of the grain.

The third factor $\frac{de}{dt}$ is the linear velocity of burning, depends on the nature of the powder, its temperature and on the pressure.

For the experimental estimation of u in a bomb at its variable pressure we have to know the variations of the thickness of the burning layer in unit time, i.e., we have to establish a definite geometrical relationship between the thickness and the volume of the powder gases.

The general scheme of such a study is as follows: having obtained from experiments in a bomb, a curve of pressure as a function of time we can calculate ψ for the varying time; then we will make use of the geometric

law of burning in order to establish the relationship between the thickness of powder (e), fraction ψ and $\frac{S}{S_1}$; next we have to find on the basis of the same geometrical law, the relationship between $\frac{S_1}{\lambda_1}$ and the shape and dimensions of the grain. Then the numerical differentiation of e and ψ with respect to time t makes it possible for us to establish the experimental values of $\frac{d\psi}{dt}$

and $u = \frac{de}{dt}$ and their variations with time. The establishment of all these relationships will enable us to control and regulate the amount and intensity of the gas formation; thus a complete mastery over the phenomenon of firing can be attained.

4.3 The effect of the geometric factors on Gas Formation.

Basic variables:

$$\psi = \frac{\lambda_1}{\lambda_2}$$

$$z = \frac{2e}{2e_1}$$

$$\bar{\sigma} = \frac{S}{S_1}$$

$$\Sigma = \frac{S_1}{\lambda_1} \cdot \frac{S}{S_1}$$

$\Gamma = \Sigma \cdot u = \frac{S_1}{\lambda_1} \cdot \frac{S}{S_1} \cdot u$ is the intensiveness of a gas formation.

Relationship between ψ and z .

$$\psi = \gamma_0 z (1 + \lambda z + \mu z^2) \dots (12)$$

here: γ_0 , λ , μ - the characteristics "of the form".

For strip powder (parallelepiped):

$$\left. \begin{array}{l} \text{Thickness } 2a, \text{ (web)} \\ \text{width } 2b \\ \text{length } 2c \end{array} \right\} \begin{array}{l} \alpha = \frac{2a}{2b} \\ \beta = \frac{2a}{2c} \end{array}$$

α is a relative decrease in width. β is a relative decrease in length.

$$\psi = (1 + \alpha + \beta)z \left[1 - \frac{\alpha + \beta + \alpha\beta}{1 + \alpha + \beta} z + \frac{\alpha\beta}{1 + \alpha + \beta} z^2 \right]$$

$$1 + \alpha + \beta = \gamma_0; \quad \frac{\alpha + \beta + \alpha\beta}{1 + \alpha + \beta} = \lambda; \quad \frac{\alpha\beta}{1 + \alpha + \beta} = \mu$$

hence: $\psi = \gamma_0 z (1 + \lambda z + \mu z^2)$

at the end of burning: $z=1$, $\psi=1$

so at the end of burning: $1 = \gamma_0 (1 + \lambda + \mu)$

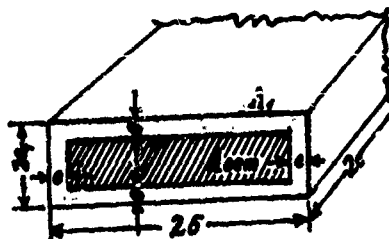


Fig. 21 - A burning strip of powder.

Formula (22) is a general formula applicable to all forms of powder grain provided the appropriate numerical values of γ , λ and μ are used.

Differentiating (22) with respect to z we have:

$$\frac{d\psi}{dz} = \frac{d\psi}{dt} \cdot \frac{dt}{dz} = \gamma \sqrt{1+2\lambda z+3\mu z^2} \quad (25)$$

Having also: $\frac{d\psi}{dt} = \frac{S_1}{\lambda_1} \cdot \frac{S}{S_1} \cdot u$; $u = \frac{dz}{dt}$; $\frac{dt}{dz} = \frac{1}{u}$

and: $\frac{de}{dz} = \frac{de}{z(\frac{S}{S_1})} = e$,

(25) can be rewritten: $\frac{S_1}{\lambda_1} \cdot \frac{S}{S_1} \cdot e = \gamma (1+2\lambda z+3\mu z^2) \quad (26)$

at $z = 0$, (26) will be: $\frac{S_1}{\lambda_1} e = \gamma \dots \quad (27)$

Dividing (26) by (27) we have: $\frac{S}{S_1} = \sigma = 1+2\lambda z+3\mu z^2 \dots \quad (28)$

the relative burning surface: σ

From (27) we have the initial specific surface

(initial "denudation" of grain): $\frac{S_1}{\lambda_1} = \frac{\gamma}{e} \dots \quad (29)$

During the burning (when z varies from 0 to 1) δ depends mostly on λ because μ is considerably smaller than λ . For powders with $\lambda < 0$ (strips, cubes, bars) δ is decreasing at burning and such forms of powder are called degressive forms; when $\lambda > 0$ (multiperforated grains) then δ is increased at burning and such forms are called progressive forms.

Function δ depends on the form of grain and its relations. Function $\frac{\delta_1}{\lambda_1} = \frac{\lambda_2}{\lambda_1}$ depends on the form of grain μ and on its absolute dimension (e). The smaller is e , the greater amount of gases per unit of time will be produced. From (28) and (25) we have:

$$\frac{\delta_1}{\lambda_1} = \lambda_2.$$

Functions ψ and z for other forms of grains.

A. Powder with one channel (tubes)

$2e$ - thickness of wall of cylinder

D - outside diameter

d - inside diameter

$2c$ - length of a tube

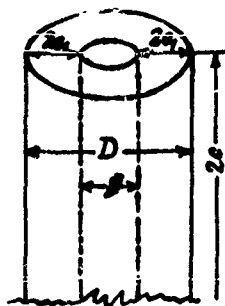


Fig. 22 Schematic view of a burning tube of powder.

$$\frac{2a}{2c} = \beta ; A_i = \frac{\pi}{4} 2c(D^2 - a^2) ;$$

$$\text{Remaining volume: } A_r = \frac{\pi}{4} (2c - 2a) [(D - 2c)^2 - (d + 2a)^2]$$

$$\psi = 1 - \frac{A_r}{A_i} = (1 + \beta)Z \left(1 - \frac{\beta}{1 + \beta} Z\right); \quad 1 + \beta = \gamma; \quad -\frac{\beta}{1 + \beta} = \lambda$$

We have: $\psi = \gamma Z (1 + \lambda Z)$ here $\mu = 0$

The tube is equivalent to a strip with an unchangeable width. ($b = \infty$) i.e., its $\alpha = \frac{c_1}{c} = 0$.

Thus the characteristics γ and λ for tube are not affected by the diameter but only by $2s$, and $2c$.

C. Forms of grain derivative from the strip.

1. square plate: $2b = 2c; \alpha = \beta$

2. square bar: $2a_1 = 2b$; $\alpha = 1$; $\beta > 0$

3. cube: $2a_1 = 2b = 2c$; $\alpha = \beta = 1$

Table 10 (p. 87 - book)

Form of grain:	χ	λ	μ	$\sigma_{\chi=1+2\lambda+3\mu}$
Tube	$1+\beta$	$-\frac{\beta}{1+\beta}$	0	$\frac{1-\beta}{1+\beta}$
Strip	$1+\alpha+\beta$	$-\frac{\alpha+\beta+\alpha\beta}{1+\alpha+\beta}$	$\frac{\alpha\beta}{1+\alpha+\beta}$	$\frac{(1-\alpha)(1-\beta)}{1+\alpha+\beta}$
Square plate	$1+2\beta$	$-\frac{2\beta+\beta^2}{1+2\beta}$	$\frac{\beta^2}{1+2\beta}$	$\frac{(1-\beta)^2}{1+2\beta}$
Square bar	$2+\beta$	$-\frac{1+2\beta}{2+\beta}$	$\frac{\beta}{2+\beta}$	0
Cube	3	-1	$\frac{1}{3}$	0

This table shows that the transition from the tube to the cube goes together with the increases in all characteristics: in χ from 1 to 3: in the absolute value of λ from a small fraction to 1, in μ from 0 to $1/3$.

Since at a given value of $2a_1$ the initial specific surface $\frac{S_i}{A_i}$ varies with χ and at the transition from the strip powder ($\chi = 1 + \alpha + \beta$) to the cube ($\chi = 3$) will be increased in 3 times: at the same time the increase in λ shows that the surface σ will be sharply decreased.

A tubular powder with the increased length of tubes has properties which approach those of a powder with the constant surface of burning with: $\lambda=1$; $\lambda=0$; $\mu=0$ and: $\psi=2$; $\phi=1$.

Any tube of powder in comparison with the strip of the same length has a smaller $\frac{S_i}{\lambda_i}$ and a smaller degreesiveness both of which can be increased by the decrease in the length.

The following Table 11 gives geometric characteristics of the form of various bodies of revolution (sphere, cylinder, tube).

Table 11 (p. 89 - book)

Characteristics:	$2e_i$	$2b$	$2c$	$\alpha=\frac{e_i}{c}$	$\beta=\frac{e_i}{c}$	$\alpha\beta$	$\lambda=\frac{\alpha}{1+\alpha\beta}$	$\mu=\frac{\beta}{1+\alpha\beta}$	$\psi=\frac{\lambda}{1+\alpha\beta}$
Bodies:									
Sphere	$2R$	$2R$	$2R$	1	1	1	3	$-\frac{3}{2}$	$-\frac{1}{2}$
Rod	$2R$	$2R$	$2c$	1	$\frac{R}{c}=\beta$	β	$2+\beta$	$-\frac{1+2\beta}{2+\beta}$	$\frac{\beta}{2+\beta}$
Solid cylinder $2R=2c$	$2R$	$2R$	$2R$	1	1	1	3	-1	$\frac{7}{3}$
Circular plate	$2e_i$	$2R$	$2R$	$\frac{e_i}{R}=\beta$	$\frac{e_i}{R}=\beta$	β^2	$1+2\beta$	$-\frac{2\beta+\beta^2}{1+2\beta}$	$\frac{\beta^2}{1+2\beta}$
Tube	$R-r$	∞	$2c$	0	$\frac{R-r}{2c}=\beta$	0	$1+\beta$	$-\frac{\beta}{1+\beta}$	0
Washer plate	$\frac{2e_i}{2c}$	∞	$R-r$	0	$\frac{2e_i}{R-r}=\beta$	0	$1+\beta$	$-\frac{\beta}{1+\beta}$	0

All curves: (σ, z) ; (ψ, z) ; (σ, ψ) are obtained from the above shown equations: $\psi = \chi z (1 + \lambda z + \mu z^2) \dots (22)$

and: $\sigma = 1 + 2\lambda z + 3\mu z^2 \dots (23)$

The third curve $\sigma = \varphi(\psi)$ can be constructed by calculating ψ and σ corresponding to the same value of z . These curves are shown on Fig. 24, Fig. 25 and Fig. 26 presenting: $\sigma = f(z)$, $\psi = F(z)$ and $\sigma = \varphi(\psi)$ respectively.

The following "degressive" forms of grains have their curves marked by: (1) tube, (2) strip, (3) square plate, (4) solid bar and (5) cube or sphere.

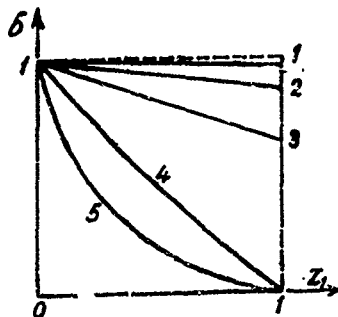


Fig. 24. $\sigma = f(z)$

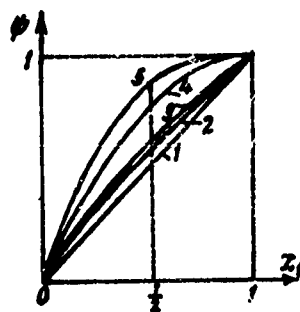


Fig. 25. $\psi = F(z)$

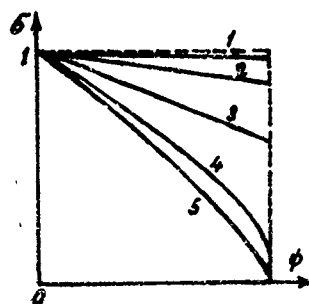


Fig. 26. $\sigma = \varphi(\psi)$.

We observe from Fig. 24 that the most degressive form is presented by cube or sphere (5) and the least degressive form is presented by tube (1). From Fig. 25 we observe that a more degressive form gives the larger amount of gas during the first half of the burning: at $z = 0.5$

$$\psi(\text{tube}) = 0.5005 \text{ and } \psi(\text{cube}) = 0.875. \text{ Curve } \delta = \varphi(\psi)$$

Fig. 26 is particularly valuable because it makes easier the comparison of the experimental data obtained in a manometric bomb with the readings on this curve: ψ is determined by the value of ρ observed in a bomb, and δ will be found from $(\frac{d\psi}{dt})$ obtained by the differentiation of ψ as a function of time. The binominal form of a function $\psi = F(z)$

$$\text{written as: } \psi = \alpha_0 z (1 + \lambda_1 z) \dots (22')$$

can be determined when the coefficients α_0 and λ_1 are found from the following two requirements: 1) at $z = 1$

ψ must be calculated from (22) and (22'):

$$\alpha_0 (1 + \lambda_1 + \mu) = 1 = \alpha_0 (1 + \lambda_1); \lambda_1 = \frac{\mu}{\alpha_0} - 1$$

and 2) at $z = 0.5$: $\alpha_0 \cdot \frac{1}{2} (1 + \lambda_1 \frac{1}{2} + \mu \frac{1}{2}) = \alpha_0 \cdot \frac{1}{2} (1 + \frac{1}{2})$

$$\text{Hence: } \alpha_0 = \alpha_0 (1 - \frac{\mu}{2}) \text{ and: } \lambda_1 = \frac{\lambda + \frac{3}{2}\mu}{1 - \frac{\mu}{2}} = \frac{1}{\alpha_0} - 1$$

and with these χ , and λ , our function $\psi = \chi, z (1 + \lambda, z)$ will give the same values of ψ which are obtained from $\psi = \chi z (1 + \lambda z + \mu z^2)$ for the three values of z : at $z = 0$: $z = 0.5$ and $z = 1$.

For the strip powders these two functions give almost identical results for the all values of z between $z = 0$ and $z = 1$. Thus we may use the functions:

$$\psi = \chi z (1 + \lambda z)$$

$$\sigma = \frac{1 + \lambda z}{1 + \lambda^2 z^2}$$

$$\sigma = \sqrt{1 + \lambda^2 z^2} \psi$$

4.4 Powders of Progressive Forms. All the degressive forms of powder, have their burning surfaces decreased. One form, however, the tube, is an exception because its inner surface is increasing at burning, thus compensating for the decrease of the external surface. If the tubes were not burned at their ends then the tube powder would be a powder with a constant burning surface.

The initial surface of a tube (neglecting the ends):

$$S_i = 2\pi R \cdot 2c + 2\pi r \cdot 2c = 2\pi(R+r)2c$$

(R and r are radii of the tube and $2c$ its length).

After a thickness e is burned from outside and inside, then the remaining surface is:

$$S = 2\pi(R-e)2c + 2\pi(r+e)2c = 2\pi(R+r)2c$$

If we have not one channel (perforation) but several of them, then their increased surfaces of burning will make up the decrease in surface on account of the burned length of the tube. This idea was realized by making a cylindrical grain with 7 perforations (See Fig. 27).

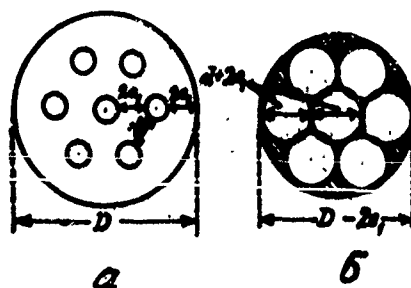


Fig. 27. Powder with 7 perforations.

At left - before burning, at right - at the moment of fragmentation.

This grain has one central perforation compensating for the decrease in the external burning surface and six perforations producing the increase in burning surface. The outer surface of a grain before burning is at distance $2e$, from the inner surfaces of perforation (Fig. 27 left side). When the thickness e , is burned out in both directions then the remaining grain is supposed to break down into 12 splinters (slivers) as is shown at the right

side of Fig. 27 by the shaded areas. These splinters, 6 large ones and 6 small ones, will burn with decreasing surface, just like ordinary bars and even more degressively on account of their sharp edges and protruding angles. This unavoidable final transition of the progressive mode of burning into a degressive one is a defect of the progressive powders.

Regular standard sizes of the diameter of the perforations and the thickness of the webs in 7-perforated cylindrical grain are: $2e, = 2d$; hence the outer diameter of a grain: $D = 3d = 4(2e) = 11e, = 11d$

The length of a grain: $2L = (2.0 - 2.5)D \approx 20 - 25d$.

At the moment of fragmentation (right side of Fig. 27)

$S_2 = 36.7\%$ i.e., 37% of the increase in the burning surface and at this moment ψ is about 85% (0.85). Therefore, 13% of the powder will burn degressively with a sharp decrease of the burning surface.

In practice however, the fragmentation does not begin simultaneously in all grains and S_2 must be somewhat lower than 37% and ψ is also lower than 85%.

Figure 28 presents a schematic view of the relative positions of an initial perforation (d -diameter) and a curvilinear splinter (a larger one).



Fig. 28. Results of fragmentation of a grain with 7 perforations.

A circle inscribed into a cross-sectional area of an outer sliver will have the radius $\rho = 0.1772(d+2e) = 0.532e$,

For an inner smaller aliver its inscribed circle will have its radius: $\rho' = 0.0774(d+2e) = 0.232e$,

Hence when the burning surfaces will meet in the center of the larger aliver (splinter) the total burned thickness $e_k = e + \rho = 1.532e$,

So the burning of the progressive powders goes on in the following two phases:

1. Before fragmentation: z varies from 0 to $Z_s = \frac{e}{e+\rho} = 0.68$

ψ varies from 0 to $\psi_s < 1$; the burn-

ing surface is increased, and

2. After fragmentation z varies from 1 to $z_k = \frac{S_0 \psi}{S_1}$;

ψ varies from $\frac{1}{2}$ to 1; the burning surface is decreased i.e., burning is degressive.

The fragmentation and degressive burning during the second phase of burning are marked defects of the progressive powders. Several remedies have been offered for these defects. Here will be described two of these remedies. One was proposed by Walsh ("rosette" grain), another by the Russian powder-maker Kisnemsky (1918) - 36 perforation grain.

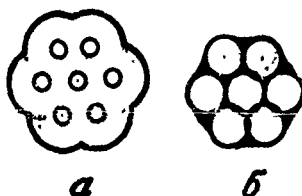


Fig. 29. Walsh's grain, is shown in two forms, at the left - Walsh's grain before burning; at the right - when fragmentation begins.

This grain is an improved 7 perforation grain with its outer surface not cylindrical but obtained as a combined result of 6 cylindrical surfaces. Each of these cylindrical surfaces has its radius $r = 2e + \frac{d}{4}$ with its center in the center of each perforation. This grain can be called a grain with a shaped contour. (See Fig. 29 left side). The dimensions of the splinter are markedly smaller than in the regular 7 perforation grain. The calculations show that $\frac{V}{V_0} = 0.95\%$. Thus only 5% of the powder burns regressively, and $\frac{S_1}{S_0} = 1.37$, the same as for a regular grain.

Kisnensky's grain. This grain was designed with a view to the diminution of fragmentation and the increase of the progressiveness of powder. This grain is a bar with quadratic cross section, and 36 quadratic perforations. Kisnensky expected that with burning by parallel layers the quadratic perforations would not produce any remaining fragments till the very end of burning. Besides this, a large number of perforations were expected to produce a higher progressiveness with $G_N = 2$. This powder was designed by Kisnensky for the gun for extra distance firing which was developed by Trofimov in 1918-26. Kisnensky's expectations did not, however, come true. The quadratic contours of the perforations failed to

remain quadratic - their angles became rounded (there is no reason to expect an increased burning rate along the direction of a diagonal).

Kisnemsky's powder failed in producing that high progressiveness which was expected.

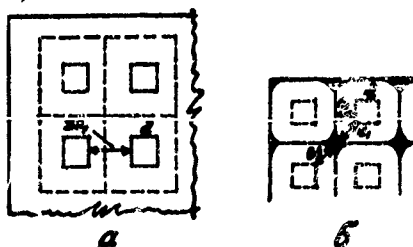


Fig. 30. Kisnemsky's grain. The right side shows the grains at the moment when fragmentation began. The remaining splinters constitute about 10% and $\psi_s = 0.90$.

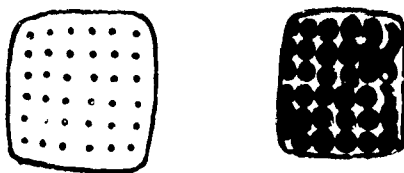


Fig. 31. A photographic picture of Kisnensky's grain before burning (at the left) and after as it was thrown out of a gun (at the right) with almost round perforations.

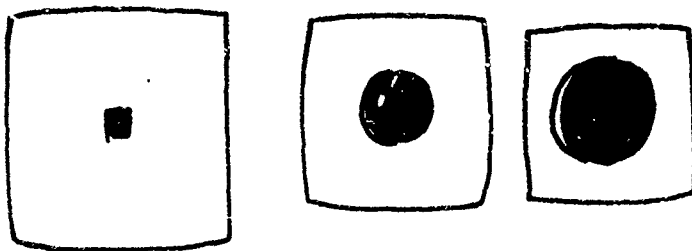


Fig. 32. A large grain with one quadratic channel gradually transformed by the burning into a cylindrical one.

The variations of the amount of burned powder and of the burning surface are given by the same formulae for the progressive form as for the degressive forms:

$$\psi = \chi Z (1 + \lambda Z + \mu Z^2)$$

$$G = 1 + 2\lambda Z + 3\mu Z^2$$

The only difference would be in the numerical values of the coefficients and their signs ($\lambda > 0$; $\mu < 0$).
Let us denote: thickness (web) $2e$; diameter of perforation d ; diameter of the grain D ; the length of the grain $2c$; the number of perforations n .

Then: the burned fraction of powder: $\psi = 1 - \frac{A_r}{A_i}$; $\frac{2e}{2c} = \beta$

and notations: $\frac{D + nd}{2c} = \Pi$; $\frac{D^2 - nd^2}{(2e)^2} = Q$,

or: $D + nd = 2c\Pi$, and: $D^2 - nd^2 = (2c)^2 Q$.

The initial volume of a grain: $A_i = \frac{\pi}{4} \cdot (D^2 - nd^2) 2c$

The remaining volume at any moment of burning of a layer with a thickness e : $A_r = \frac{\pi}{4} [(D - 2e)^2 - n(d + 2e)^2] (2c - 2e)$

Hence: $\frac{\Lambda_r}{\Lambda_i} = \frac{[D^2 - nd^2 - 2(D+nd)ze - (n-1)(ze)^2]}{D^2 - nd^2} \cdot \frac{ze \cdot ze}{ze}$

since: $\frac{ze}{ze} = \frac{ze}{ze} \quad \frac{ze}{ze} = \beta z$

we have: $\frac{\Lambda_r}{\Lambda_i} = \left[1 - \frac{2(D+nd)}{D^2 - nd^2} \cdot ze - \frac{n-1}{D^2 - nd^2} (ze)^2 \right] (1 - \beta z)$

or: $\frac{\Lambda_r}{\Lambda_i} = 1 - \left(1 + \frac{2n_i}{Q_i} \right) \beta z - \left(\frac{n-1-2n_i}{Q_i} \right) \beta^2 z^2 + \frac{n-1}{Q_i} \beta^3 z^3$

Thus, finally: $\psi = 1 - \frac{\Lambda_r}{\Lambda_i} = \frac{Q_i + 2n_i}{Q_i} \beta z \left[1 + \frac{n-1-2n_i}{Q_i + 2n_i} \beta z - \frac{(n-1)\beta^2}{Q_i + 2n_i} z^2 \right]$

Here: $\frac{Q_i + 2n_i}{Q_i} \beta = \gamma$

$\chi = \frac{Q_i + 2n_i}{Q_i} \beta$

$\beta \frac{(n-1) - 2n_i}{Q_i + 2n_i} = \lambda$

at $n = \gamma$: $\lambda = \frac{2(\beta - n_i)}{Q_i + 2n_i} \beta$

$-\frac{(n-1)\beta^2}{Q_i + 2n_i} = \mu$

$\mu = -\frac{6\beta^2}{Q_i + 2n_i}$

Thus the general formula, has the same appearance as for the degressive powders: $\psi = \chi Z (1 + \lambda Z + \mu Z^2)$

and: $\sigma = 1 + 2\lambda Z + 3\mu Z^2$

For these powders $\mu < 0$ and λ will be 0 at:

$$n - 1 - 2n = 0 \text{ or: } \frac{n-1}{2} = \frac{D+nd}{2c}$$

Therefore, under these conditions the powder ceases to be progressive because then: $\frac{d\sigma}{dZ} < 0$

For example: 7 perforation grain for which $D = 11d$; condition $\chi = 0$, means that $6 - 2n = 0$ i.e., $6 - \frac{D+nd}{c} = 0$, or $6c = D + 7d = 18d$; $2c = 6d$; $\beta = \frac{1}{3}$; $a_1 = d$; $\mu < 0$

An analysis of the structure of the coefficient shows that the progressiveness of the form is increased with the number of perforations, with a decrease of the diameter of the perforation, (with the same $2c$), and with the length of a grain ($2c$).

In a grain with rectangular cross-sections (Kisnensky's grain), n , is the ratio of the perimeter of the grain cross-section to the perimeter of a square with its side equal to length $2c$, and q , is the ratio of the cross-sectional area to the area of the same square ($4c^2$). If the side of a cross-sectional quadratic area of a

grain is A_g , and the side of the quadratic perforation a_p , the length $2c$ and the total number of n horizontal and n vertical perforations is denoted by n^2 , Then:

$$n_1 = \frac{A_g + n^2 a_p}{2c} ; \quad Q_1 = \frac{A_g^2 - n^2 a_p^2}{(2c)^2} ; \quad \beta = \frac{2e}{2c}$$

For Walsh's grain, we have: $\beta = \frac{2e}{2c}$ and

for n_1 and Q_1 , we will have: (see Fig. 33)

$$n_1 = \frac{P}{2\pi c},$$

where P is the perimeter of the grain and $2c$, its length

$$Q_1 = \frac{S_r}{\frac{\pi}{4} \cdot (2e)^2}$$

where S_r is the cross-sectional area of the grain; diameter of the perforation is d_p ; web = $2e = \alpha_p \cdot d_p$.

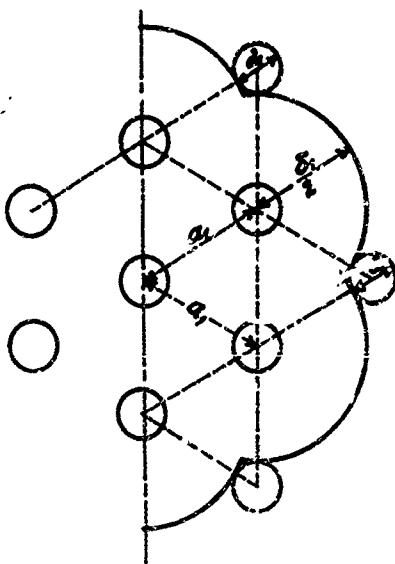


Fig. 33. Schematic view of Walsh's grain.

S_T is the sum of: (1) 12 triangles (equilateral) with their sides equal to a , each reduced by 3 circular sections of 60° and radius $\frac{d_1}{2}$, $a_1 = 2a + d_1$; (2) 6 sectors of 120° with diameter $d_1 = d_1 + 2 \cdot 2e$, each reduced by a sector of 120° with diameter d . Thus

$$S_T = 12 \left(\frac{\sqrt{3}}{4} a^2 - 3 \cdot \frac{1}{6} \cdot \frac{\pi}{4} d_1^2 \right) + 6 \cdot \frac{1}{4} \cdot \frac{\pi}{4} (d_1^2 - d^2) = \frac{\pi}{4} \left(\frac{12\sqrt{3}}{4} a^2 - 8d_1^2 + 2d^2 \right)$$

Perimeter P is the sum of: (1) 6 arcs of 120° with the circle diameter d_1 ; (2) 7 circles of diameter d_1 ; (3) 6 arcs of 60° with the circle diameter d . Thus:

$$P = \pi \left(6 \cdot \frac{1}{3} d_1 + 7d_1 + 6 \cdot \frac{1}{6} d \right) = \pi \cdot 2 (d_1 + 4d)$$

Then we will have: $\Pi_1 = \frac{P}{\pi 2c} = \frac{2(d_1 + 4d)}{2c}$

$$Q_1 = \frac{S_T}{\frac{\pi}{4} (2c)^2} = \frac{\frac{12\sqrt{3}}{4} a^2 - 8d_1^2 + 2d^2}{(2c)^2}$$

and: $\beta = \frac{2e}{2c}$

Since the value of μ for the 7 perforation grain is a small one we may use a simplified binomial formula for

$$\psi = X_0 (1 + \lambda_1 z)$$

and the coefficients X_0 and

λ_1 can be determined from the same two conditions as we have used above in the case of degressive forms.

$$\text{At } z = 0.5: \frac{x_0}{2} \left(1 + \frac{1}{2} + \mu \frac{1}{2}\right) = \frac{x_0}{2} \left(1 + \frac{1}{2}\right)$$

$$\text{at } z = 1: x_0(1 + \lambda + \mu) = \frac{x_0}{2} \left(1 + \frac{1}{2}\right) = \psi_5$$

$$\text{Hence: } x_0 = \left(1 - \frac{\mu}{2}\right)x_0 \quad \text{and} \quad \lambda_1 = \frac{\psi_5}{x_0} - 1.$$

$$(\text{for progressive powders we had: } \lambda_1 = \frac{1}{x_0} - 1)$$

For example: for the 7 perforation grain:

$$2e_1 = 1; d = 0.5; D = 5.5; 2c = 12.5 \quad \text{all in mm.}$$

$$\beta = \frac{2e_1}{2c} = 0.08; \pi_1 = \frac{D+7d}{2c} = 0.720; 2\pi_1 = 1.440$$

$$Q_1 = \frac{D-7d^2}{(2c)^2} = 0.1824; Q_1 + 2\pi_1 = 1.6224$$

$$x_0 = \frac{Q_1 + 2\pi_1}{\beta} = 0.712; \lambda = \frac{(n-1) - 2\pi_1}{Q_1 + 2\pi_1} = 0.225$$

$$\mu = -\frac{(n-1)^2}{Q_1 + 2\pi_1} \beta^2 = -0.0237$$

$$\psi_5 = x_0(1 + \lambda + \mu) = 0.885; \psi_5 = 1 + 2\lambda + 3\mu = 1.379$$

From a binomial formula: $\chi_1 = \chi (1 - \frac{\lambda}{2}) = 0.720$

$$\lambda_1 = \frac{\psi_1}{\chi_1} - 1 = 0.1873$$

$$\psi_2 = \chi_1 (1 + \lambda_1) = 0.855 ; \sigma_2 = 1 + 2 \lambda_1 = 1.375$$

The products of fragmentations (the second phase) are of two sorts - small slivers (see Fig. 27 - 6 small inner slivers), and larger slivers, 6 larger slivers on the same Fig. 27.

Prof. G. V. Oppokov has shown that assuming burning by parallel layers, it is possible to find a general expression for the burning of the smaller slivers together with the larger ones, and the next final period of burning only of the remnants of the larger slivers.

The results obtained by G. V. Oppokov show that the burning of the products of fragmentation goes on almost as degressively as for a cubic grain, i.e., more degressively than for a prismatic bar.

We will use the binomial formula:

$$\psi = \chi_2 Z (1 + \lambda_2 Z)$$

Changing the origin of coordinates to the point of the beginning of fragmentation: $Z_s = 1 ; \psi_s = \psi$

$$\text{we will have: } \psi - \psi_s = \chi_2 (Z-1) [1 + \lambda_2 (Z-1)]$$

differentiating this equation:

$$\frac{d\psi}{dz} = \frac{S}{\lambda_1} e_1 = \alpha_2 [1 + 2\lambda_2 (z-1)]$$

and bringing in our two basic requirements:

1. for $z = z_K$, $\psi = 1 =$

$$\text{i.e.: } 1 - \psi_0 = \alpha_2 (z_K - 1) [1 + \lambda_2 (z_K - 1)]$$

2. for $z = z_K$, $\sigma = 0$

$$\text{i.e.: } 1 + 2\lambda_2 (z_K - 1) = 0$$

From these two equations we find α_2 and λ_2

$$\lambda_2 = -\frac{1}{2(z_K - 1)} ; \quad \alpha_2 = \frac{2(1 - \psi_0)}{(z_K - 1)}$$

For example, for a standard 7-perforated grain:

$$\begin{aligned} \text{at } z_K = 1.532 \text{ and } \psi_0 = 0.855 \\ \lambda_2 = -0.94 \text{ and } \alpha_2 = 0.545 \end{aligned}$$

For Walsh's grain: at $z_K = 1.232$; and $\psi_0 = 0.95$

$$\lambda_2 = -0.216 \text{ and } \alpha_2 = 0.432$$

For curves (σ, z) , (ψ, z) and (σ, ψ) we will use the general relationships: $\psi = \alpha_2 z (1 + \lambda_2 z + \mu_2 z^2)$

$$\text{and: } \sigma = \frac{S}{S_1} = 1 + 2\lambda_2 z + 3\mu_2 z^2$$

Then our curves will be obtained as is shown in Figs. 34, 35 and 36.

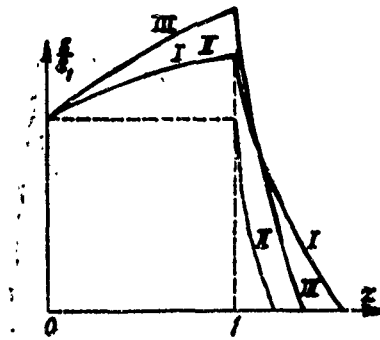


Fig. 34.

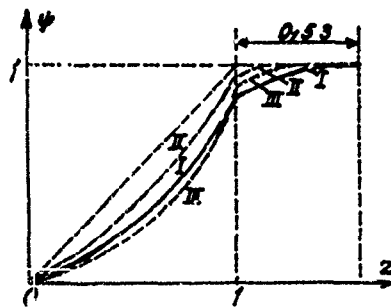


Fig. 35.

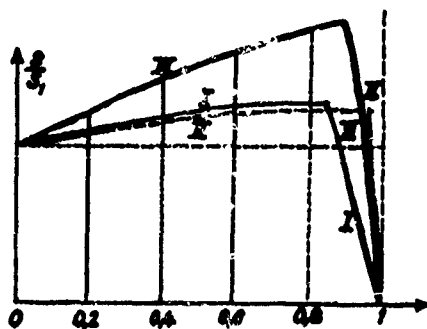


Fig. 36.

Where curves marked I refer to 7-perforated grain curves marked II refer to Walsh's grain, and curves marked III refer to Kisnensky's grain.

Coated tubular powders of the high progressiveness were proposed in Russia after the results of Kisnensky's powder proved to be below expectations. Then Prof. O. G. Philippov of the Artillery Academy proposed the coated powder which is a regular tubular powder with its outer surface covered with a non-burning layer. Then the burning affects only the internal surface of the grain which is continually increased till the end of burning. The increase in the burning surface is proportional to the ratio of the external and internal diameters for the

cylinder with one perforation with its $D_0 = 3e_0$ and $e_0 = d_0$ i.e., $\frac{S_N}{S_1} = \frac{D_0}{d_0} = 3$

The progressiveness is much higher than for Kisnensky's grain with its 36 perforations.

Practice, however, has shown that there was a certain snag in this otherwise very promising procedure; there was a practical difficulty in the preparation of such a layer which should not be burned at all and should be strong enough in its resistance to mechanical strains and friction during its storage and transportation as well as to disruption by the moving powder gases. Besides this there was observed an increased smokiness on account of the pulverized remnants of the protective layer thrown out of the gun during firing.

The whole outer surface (cylindrical) and both circular plates of the ends do not burn, and the inner cylindrical surface can be burned only through the thickness e_0 (not $3e_0$)

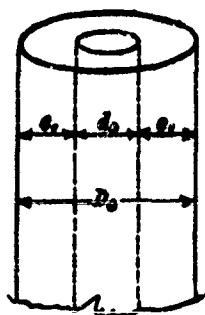


Fig. 37. A coated tubular powder.

We have: (see Fig. 37)

$$\Lambda_1 = \frac{\pi}{4} [(d_0 + 2e)^2 - d_0^2] 2c = \pi \cdot 2c [d_0 e + e^2]; \quad z = \frac{e}{d_0}$$

$$\Lambda_2 = \frac{\pi}{4} [(d_0 + 2e)^2 - (d_0 + 2e)^2] 2c = \pi \cdot 2c [d_0 e + e^2 - (d_0 e + e^2)]$$

$$\text{Hence: } \frac{\Lambda_2}{\Lambda_1} = 1 - \frac{d_0 e + e^2}{d_0 e + e^2} = 1 - \frac{z + \frac{e}{d_0} z^2}{1 + \frac{e}{d_0} z}$$

$$\text{and: } \psi = 1 - \frac{\Lambda_2}{\Lambda_1} = \left(\frac{1}{1 + \frac{e}{d_0} z} \right) z \left(1 + \frac{e}{d_0} z \right)$$

$$\text{at } z=1, \quad \psi=1.$$

Comparing this result with our formula: $\psi = \chi z / (1 + \lambda z)$

we see that: $\lambda = \frac{g_1}{a_0}$

$$\text{and } \chi = \frac{1}{1 + \lambda}$$

$$\text{Then } \sigma = \frac{z}{g_1} = 1 + \lambda z = 1 + 2 \frac{g_1}{a_0} z ; z_K = 1 + \frac{z}{a_0} = \frac{2a_0}{a_0}$$

$$\text{If } g_1 = a_0 ; \lambda = 1 ; \chi = 0.5 ; \sigma_K = 3$$

$$\text{at: } g_1 = 2a_0 , \lambda = 2 , \chi = \frac{1}{3} ; \sigma_K = 5$$

- more

progressive than for $g_1 = a_0$

Chapter 5 - The Rate of Burning Law.

5.1 The principal factors in determining the rate of burning are, - the nature of the powder and its temperature and the temperature and pressure of the surrounding gases.

Since the immediate measurement of the temperature of gases during the burning of powder is still beyond our experimental technique we must deal with the functional relationship of the character of powder and gas pressure measurable and registerable in experiment.

The basic "law of the ratio of burning" is represented in the form of : $u = f(p)$

Various forms for expressing this relationship are used in practice.

The first step is the experimental recording of the pressure in a bomb as a function of time. The form of powder usually taken for these experiments can be strip, plate, or tube, preferably of uniform thickness; all the average dimensions are carefully measured (2a, 2b, 2c, D, d, etc.); the characteristics X_0 and λ (in the binomial formula) are calculated and the curve $\psi = f(z)$,

$z = \frac{e}{a}$ is drawn. Then the powder is burned in a manometric bomb using a strong igniter which will give a simultaneous inflammation of the whole powder surface.

Next the curve of p as a function of time t is taken and using the diagrams of $\psi = f(z)$ or $\psi = F(e)$ and the rate of burning $u = \frac{\Delta e}{\Delta t}$ is determined by the immediate measurements of Δe and Δt with the average value of p on this interval Δt i.e., the curve $u = f(p)$ can be constructed.

2.2 Vielle's formula:

$$u = A p^{\gamma}$$

here A and γ depend on the nature of powder and γ can be 1. The smaller γ is the less sensitive is the powder to the variations of pressure. Vielle used

$\gamma = \frac{1}{2}$ for black powders and $\gamma = \frac{2}{3}$ for smokeless. We use, for our slow burning black powders used in a time fuse $\gamma = \frac{1}{3}$. Prof. G. Zabudsky used for pyroxylin powders $\gamma = 0.93$, for cordites $\gamma = 1$, for ballistite $\gamma = 1.107$.

2.3 Binomial formula:

This formula was used by Prof. S. Voukolov (1891-1897); by Prof. Wolf (1903) and by Prof. I. P. Grave (1904). Mouracour also used this formula (1930-1935). Prof. Grave (1904) carried out many experiments for the comparison of formulas $u = A p^{\gamma}$ and $u = a p + b$ his conclusion was: "Both formulas can be considered

equally adaptable for the expression of that law which controls the variations in the rate of burning as a function of the variation of the pressure. The mean errors involved in working with these formulas in general are alike and both formulas lead to almost identical results.

An apparent contradiction involved in this statement is that a straight line ($u = ap + b$) not passing through the origin cannot be equivalent to a parabolic curve ($u = Ap^2$) passing through the origin.

Fig. 38 explains at least the degree of validity of the above contradiction. In the earlier experiments with bombs (1880) the crusher did not register pressures lower than 300-400 kg/cm² and as a result of this omission of the lower pressures, the linear law ($ap + b$) experimentally was just as good as the parabolic law ($u = Ap^2$) for pressures lower than 300-400 kg/cm². Translator's note:

Another contradiction involved in formula $u = ap + b$ is, that this law appears to be physically inadmissible, as it implies the burning of propellant under no pressure, at $p = 0$, $u = b$ (constant). Direct evidence on this point is available, as Noble ("Artillery and Explosives", pp. 523-524) gives an account of an attempt

of Abel's to burn cordite in a vacuum. The attempt failed, but Noble made no deduction from the negative result!

5.4 Formula: $u = Ap$

Charbonnier (1908) in the beginning of his research used a more general law: $u = Ap^{\gamma}$. After the analysis of his experimental curves it was found that for the french strip powders of that time the exponent γ could be taken as 1. Prof. N. Drosdov (1910) also used $u = Ap$ in his work.

5.5 Schmitz's criterion. In 1913 Schmitz, experimenting with a large Krupp's bomb and measuring pressures not with crushers but by means of optical recording of the elastic deformations of a special elastic bar, succeeded in determining all the pressures from the very beginning of burning. He has introduced another criterion for the selection of the appropriate law of the rate of burning and he assumed the law: $u = Ap$.

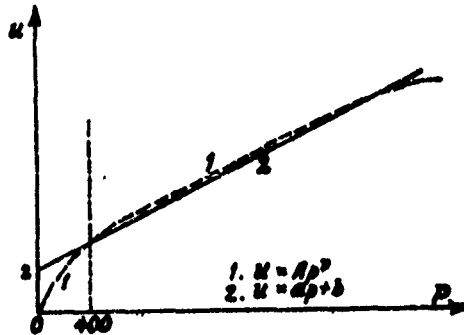


Fig. 38.

Assuming that the law $u = Ap$ is correct, then

$$u = \frac{ds}{dt} = Ap$$

and: $e = A \int p dt$ or: $\int p dt = \frac{e}{A}$

Hence:

for complete burning: $e_c = A \int_0^{\tau_n} p dt$

and: $\int_0^{\tau_n} p dt = \frac{e_c}{A}$ is constant

for the given powder. Since e_c and A are characteristic of powder but not of the loading conditions we are justified in stating that if the law $u = Ap$ is correct then the impulse of gas pressures does not depend on the loading conditions, and this impulse is equal to the ratio of one-half of the web to the coefficient A .

From the whole series of experiments in the Krupp bomb with varying densities of loading from $\Delta = 0.12$ up to $\Delta = 0.26$, Schmitz found that the areas of curves $p = f(t)$ or $\int_0^{t_K} p dt$ for all these firings are all equal. See Fig. 39.

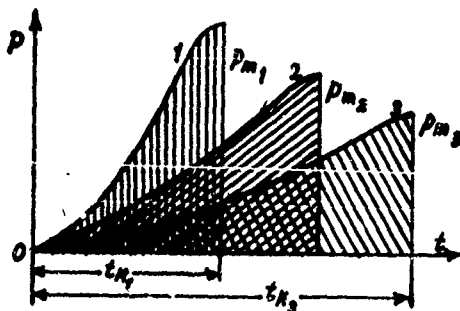


Fig. 39. Curves $p = f(t)$ for various densities of loading.

These results prove that the law $u = \Delta p$ is correct.

If another law: $u = ap + b$ was correct then:

$$de = ap dt + b dt$$

and : $e_i = a \int_0^{t_K} p dt + b t_K$

Hence: $\int_0^{t_k} p dt = \frac{a_1}{a} - \frac{a}{a} t_k$

Since t_k is decreased with the increased Δ then $\int_0^{t_k} p dt$ must be increased with Δ .

An analogous result can be obtained for the law $u = Ap^y$ with $y < 1$.

After Schmitz's work many other researches were conducted along this line. Muraour (1927-28) investigated the rates of burning of colloidal powders and in (1924 - 25) he evaluated the heat loss through the walls of a bomb.

The experiments of M. E. Serebryakov with pyroxylin and nitroglycerine powders completely verified the law $u = Ap$; here $A = \frac{u}{p}$ can be taken at $p = 1$, when $u = u_1$ i.e., $A = \frac{u_1}{1}$. Here the velocity of burning is referred to the unit of pressure.

Then: $u = Ap = u_1 p$

and $u_1 = \frac{u}{p} \cdot \left(\frac{\frac{dm}{dt}}{\frac{dm}{dt}} \right)$

In other words u_1 is a velocity of burning referred to the unit of pressure. Thus the value of u_1 , together with the values of f ("force" of powder) and covolume α is a ballistic characteristic of powder of a physico-

chemical nature. The value of u , for pyroxylin powders varies from 6×10^{-6} to 9×10^{-6} $\left(\frac{\frac{dm}{dm^2}}{\frac{dm}{dm^2}}\right)$

The larger is the web, the larger is the amount of volatiles, the slower does the powder burn; the higher is the percentage of nitrogen the higher is u . For nitroglycerine powders the percentage of nitroglycerine is the most important factor directly affecting its u .

The amount of volatiles is also very important: for example in the pyroxylin powder an increase of 1% of volatiles cuts down u , by 10-12%.

In American literature the following formula is used for pyroxylin powder

$$u = \frac{0.0025 E}{48(180 - t^{\circ}) + 256(h + 908.5h')} 10^{-4}$$

here $E = 69400(N - 6.37)$ - the energy of powder $\frac{Kg.m.}{Kg.}$

t° = temperature of the powder.

h = % of volatiles removable by 6 hour drying.

h' = % of volatiles remaining in powder after 6 hours of drying.

N = % of Nitrogen

For the Russian pyroxylin powders another formula is more suitable: $u = \frac{10^{-4} \cdot 0.175(N - 6.37)}{0.04(220 - t^{\circ}) + 3h + h'} \cdot \frac{\left(\frac{dm}{dm^2}\right)}{\left(\frac{Kg.}{dm^2}\right)}$

Here 220° is the temperature of the inflammation of the powder and $\bar{E} = 700000$ ($N=6.37$) $\frac{M_0 \cdot d_m}{R \cdot T}$.

Letang using the principles of the kinetic theory of gases and considering that the burning of powder is a process of detaching powder molecules by the impacts of gas molecules, gives his formula for u_1 :

$$u_1 = \frac{g}{\rho \sqrt{\pi} c_p} \left(1 + \frac{c_1^2}{c_p^2} \right) e^{-\frac{c_1^2}{c_p^2}}$$

Here:

g - acceleration of gravity

ρ - density of powder

c_p - probable velocity of gas molecules

c_1 - velocity of molecules sufficient for the

detaching of at least one molecule of powder.

Schmitz in his experiments used densities of loading from $\Delta = 0.12$ to $\Delta = 0.25$. There were, however, some experiments later on with Δ as low as 0.015.

The results of these experiments gave $\int_0^{t_k} p dt$, a total impulse of gases varying along the law of a straight line:

$$\int_0^{t_k} p dt = S_0 - \pi t$$

this function verifies the law: $u = ap + b$.

The experiments conducted by M. E. Serebryakov and A. Kokhanov (1937-1940) indicated that $\int_0^{t_k} p dt$ varies with the time of burning only for powders having a considerable web ($2e, > 0.5$). For very thin powders with higher rate of burning $\int_0^{t_k} p dt$ is not affected even by a very small Δ . This result shows that it is important to take into consideration the speed of the process of the heating of the powder mass laying close to the burning surface: then its u_1 is increased and

$$\int_0^{t_k} p dt = \frac{G}{u_1} \quad \text{is decreased.}$$

Special experiments were conducted to demonstrate the influence of the powder temperature on the rate of burning at constant atmospheric pressure. The time of complete burning of a strip of powder of the same length at $t^\circ C = 15^\circ$ was 14 sec.; and at $50^\circ C$. the time was 9.4 sec., which means that the rate of burning was increased 1.5 times so the integral was decreased 1.5 times.

The way in which the heating of powder affects the rate of burning is very clearly seen when series of experiments are made in one and the same bomb which is gradually heated by the burning process within its walls, and is not given time enough to be cooled between the experiments. A powder introduced for the experiment is

always kept a few minutes before the experiment starts, and thus the powder temperatures each time become higher and higher, with the result that the values of $\int_0^{t_k} p dt$ are gradually decreased because the higher temperature of powder increases the rate of burning and

$\int_0^{t_k} p dt = \frac{c}{u}$, becomes smaller and smaller.

Since the integral $\int_0^{t_k} p dt$ is decreased with

the decreasing Δ this means that, formally speaking, this result can occur in both cases: for the law: $u = \Delta p$ as well as for the law: $u = a p + b$

M. E. Serebryakov (1932) has demonstrated that at

$p_m > 1000 \text{ kg/cm}^2$ the law $u = \Delta p$ can be accepted and at $p_m < 1000 \text{ kg/cm}^2$ the law: $u = A p^{0.32}$ is more accurate.

For very low pressures (from 5 atm. to 250 atm.) Prof. I. M. Shapiro used the law $u = 0.37 p^{0.7}$ which is not in agreement with the law: $u = \Delta p$. It has already been shown above that the decrease of the integral $\int_0^{t_k} p dt$ for the small Δ is explainable by the increase in the rate of burning.

Summing up these results we must admit that we do not yet have one general law for the burning rate as a function of pressure. But since for the practical firings of

guns, all powders are burned at higher densities of loading and pressures, we may safely use for these cases the law: $u = u, p$

We had the expression for the rate of gasification:

$$\frac{d\psi}{dt} = \frac{S_1}{\lambda_1} \cdot \frac{S}{S_1} u \dots (31)$$

now we rewrite it: $\frac{d\psi}{dt} = \frac{S_1}{\lambda_1} \cdot \frac{S}{S_1} u, p$. Since: $\frac{S_1}{\lambda_1} = \frac{\alpha}{e}$,

and that $I_x = \int_0^{t_x} p dt = \frac{e}{u}$,

we have (31): $\frac{d\psi}{dt} = \frac{\alpha}{e} \cdot u \cdot \frac{S}{S_1} p = \frac{\alpha}{I_x} \sigma p \dots (32)$

here: $\frac{S_1}{\lambda_1}$, $\frac{S}{S_1}$ depend on the geometric characteristics of powder.

u , - rate of burning at $p = 1$, this is a characteristic of the nature of the powder and the degree of its warming up.

p - pressure at which the burning is going on;

the pressure is characteristic of the medium in which the powder is placed and it depends on $\Delta, f, \alpha, \delta, \psi$.

Chapter 8 The law of the variation of the pressure as function of time

From: $\frac{d\psi}{dt} = \frac{S_1}{\lambda_1} \cdot \frac{S}{S_1} \cdot u, p = \frac{\gamma_0}{e} u, \sigma p = \frac{\gamma_0}{I_n} \sigma p \dots (32)$

and: $p = p_B + \frac{f \Delta \psi}{1 - \frac{\Delta}{f} - \Delta(\alpha - \frac{1}{f}) \psi} = p_B + \frac{f \Delta \psi}{\lambda_\psi} \dots (34)$

here: $\lambda_\psi = 1 - \frac{\Delta}{f} - \Delta(\alpha - \frac{1}{f}) \psi$
(relative free volume of a bomb);

by differentiating (34) with respect to t, we have:

$$\frac{dp}{dt} = \frac{f \Delta}{(1 - \alpha \Delta)} \cdot \frac{1 - \frac{\Delta}{f}}{\lambda_\psi} \cdot \frac{1 - \alpha \Delta}{\lambda_\psi} \cdot \frac{d\psi}{dt} \dots (34')$$

here: $(1 - \frac{\Delta}{f})$ is λ_ψ at the beginning and

$(1 - \alpha \Delta)$ is λ_ψ at the end of burning and

$$1 - \frac{\Delta}{f} > \lambda_\psi > 1 - \alpha \Delta$$

Hence with a very good approximation: $\frac{1 - \frac{\Delta}{f}}{\lambda_\psi} \cdot \frac{1 - \alpha \Delta}{\lambda_\psi} \approx 1$

and then using (33) we have:

$$\frac{dp}{dt} = \frac{f \Delta}{1 - \alpha \Delta} \cdot \frac{u_1}{e} \approx \sigma p \dots (35)$$

For powders with a constant surface of burning: σ is constant but $\sigma_0 = 1$ and $\sigma_1 = 1 + 2\lambda$, so we take

$$\sigma_{ave} = \frac{\sigma_0 + \sigma_1}{2} = 1 + \lambda$$

and from: $\psi = \chi z (1 + \lambda z)$ at $\psi = 1$

we have: $1 = \chi (1 + \lambda)$

hence: $\chi = \frac{1}{1 + \lambda}$

and finally $\chi \sigma$ in (35) will be: $\frac{1 + \lambda}{1 + \lambda} = 1$

and (35) will be rewritten:

$$\frac{dp}{dt} = \frac{f \Delta}{1 - \alpha \Delta} \cdot \frac{u_1}{e_1} p = \frac{p_m p_b}{I_N} \cdot p \quad (36)$$

Finally introducing a notation:

$$\tau = \frac{e_1}{u_1} \cdot \frac{1 - \alpha \Delta}{f \Delta} = \frac{I_N}{(p_m p_b)} \text{ (seconds)} \quad (37)$$

thus τ is the time of the complete burning at the constant pressure ($p_m = p_b$) we have the basic equation:

$$\frac{dp}{p} = \frac{dt}{\tau} \dots (38)$$

Having integrated (38) we have: $\log_2 \left(\frac{p}{p_b} \right) = \frac{t}{\tau}$

hence: $t = 2.303 \tau \log \left(\frac{p}{p_b} \right) \dots (39)$

$$t_k = 2.303 \tau \log \left(\frac{p_m}{p_b} \right) \dots (40)$$

$$p = p_b e^{\frac{t}{\tau}} \dots (41)$$

$$P = P_0 e^{\frac{\Delta t}{\tau}} \dots \dots \dots (42)$$

The following set of 3 groups of curves (Fig. 40, Fig. 41, and Fig. 42) presents various shapes of the exponential curves expressing pressures as functions of time under various loading conditions: Fig. 40 - a constant P_0 and various Δ Fig. 41 - constant Δ and various P_0 ; Fig. 42 - constant Δ and various e, \dots

Thus the final conclusion is: by the appropriate use of the ballistic characteristics $f, \alpha, u,$ of the forms and dimensions of grain ($\chi, \sigma, e,$) and of density of loading Δ it is possible to control and regulate both-the rate of increase and absolute value of gas pressure-in a closed volume (of a bomb), which is another way of saying that both phenomena-the burning of powder and formation of gases-can be brought under our complete and effective direction.

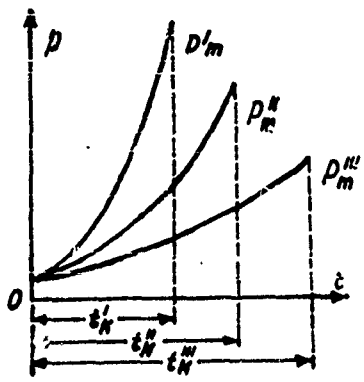


Fig. 40 - Curves (p,t) at different Δ and same p_B .

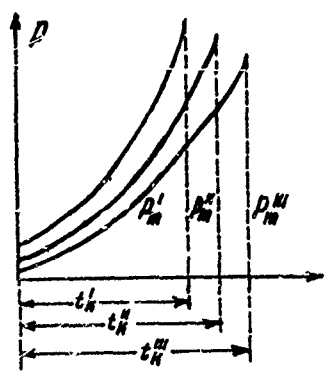


Fig. 41 - Curves (p,t) at different p_B and same Δ .

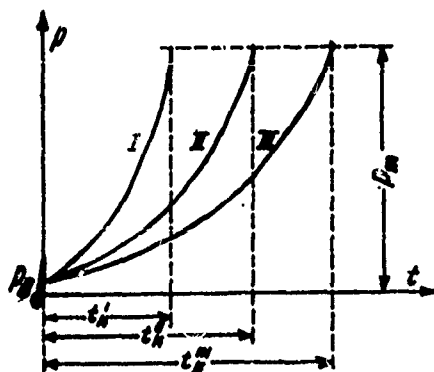


Fig. 42 - Curves (p, t) for different e , and same Δ .

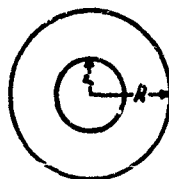


Fig. 43 - Scheme of a burning sphere or cylinder.

Section III - Ballistic Analysis of Powders based on the Physical Law of Burning. (p. 113-171)

(See "Physical Law of Burning in Interior Ballistics" by M. E. Serebryakov (1937-40))

Chapter 1 Development of Method for the Ballistic Analysis of Powders.

1.1 An attempt to adjust the theoretical law to experiments in the manometric bomb.

All the pressure curves calculated from: $p = p_0 e^{\frac{t}{\tau}}$ have their slopes $(\frac{dp}{dt})$ continually increasing up to the final value: $(\frac{dp}{dt})_{\infty} = \frac{p_m}{\tau}$

All the pressure curves obtained experimentally in bomb show their slopes definitely reaching their maxima at certain $p_i < p_m$ and after this point of inflexion $(\frac{dp}{dt})$ gradually falls down not infrequently reaching its final value $(\frac{dp}{dt})_{t_K} = 0$ when $p = p_m$

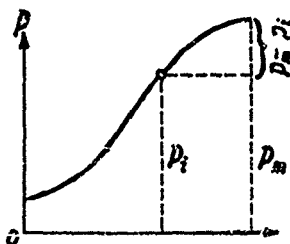


Fig. 44 - Curve (p,t) with a point of inflexion.

As a necessary remedy against this discrepancy Charbonnier introduced certain "function of form" which presented a relationship between $\frac{S}{S_i}$ (the relative surface) and ψ (the fraction burnt) in form:

$$\frac{S}{S_i} = (1 - \psi)^\beta$$

where the exponent β is determined not by the geometry of a grain but by an experiment in the manometric bomb.

From purely geometric considerations it is easy to show that:

for the solid sphere: $\frac{S}{S_i} = (1 - \psi)^{\frac{1}{3}}$; $\sigma = (1 - \psi)^{\frac{2}{3}}$; $\beta = \frac{2}{3}$

for the solid cylinder: $\frac{S}{S_i} = \sigma = (1 - \psi)^{\frac{1}{2}}$; $\beta = \frac{1}{2}$

for the infinitely wide trip: $\frac{S}{S_i} = \sigma = (1 - \psi)^0 = 1$; $\beta = 0$
(constant S)

But Charbonnier's experimental determination of β consisted in calculation of β by means of the pair of pressure values: p_i at the point of inflexion and p_m maximum pressure at the moment t_K (end of burning) from his *a priori* formula: $\beta = \frac{p_m - p_i}{p_m} \dots (48)$

The more uniformly powder burns, the closer β_c is to β_m and the lower the value of β is found ($\beta = 0$ for the constant surface of burning).

Fig. 45 shows experimental curves $\sigma = f(\psi)$: 1 and 2 for $\beta = 0.2$ and $\beta = 0.5$ respectively for the french strip gun powder and plate powder for small arms. On the same Fig. 45 in dotted lines 1' and 2' are shown $\sigma = f(\psi)$ obtained from the geometrical law of burning as it is applied in cases of strip powder (curve 1') and plate powder (2')

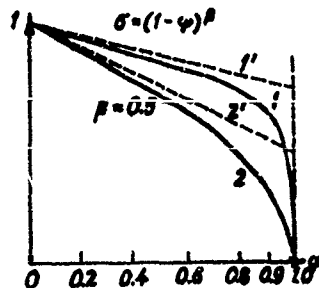


Fig. 45 - Function of form: $\sigma = f(\psi)$.

Conclusion drawn from Charbonnier's experiments:

1. The burning surface of all powders approaches zero (at $\psi = 1$) and the more degressive powder is the more rapid is the slope of curve $S=f(\psi)$ to the point at $\psi = 1$.
2. Actual burning is always more degressive than can be expected in accordance with the geometric law.
3. Such a discrepancy can be a result of not homogeneous enough mass of the powder as well as of not instantaneous inflammation of all the elements of the whole powder charge.
4. The experimental curves (p, t) presenting the actual variations of pressures with time establish a direct connection between the theoretical formula and experimental results of the manometric bomb.

Thus Charbonnier introduced the evaluation of the powder progressiveness by means of experiments but not by the geometric relationships of elements of the form of a powder grain.

The progressiveness of the form by no means can be taken as the complete expression of the progressiveness of the burning process. This process involves not only the geometry of the grain but its Physics and Chemistry

as well; besides this there is a very imposing complex of the loading conditions, of the initial ignition and inflammation which all markedly affect the progressiveness of the burning process.

With all due credit to Charbonnier's ingenious invention of his "function of form" it must be admitted that this function did not reflect the entire real character of the burning in all details. And hardly could this be expected because this function after all takes into consideration only two elements p and p_m both located rather at the very end of the analysed process of burning.

The whole curve (p, t) was not explored and particularly important was the absence of recorded pressures in the beginning of burning, when the cylindrical crushers were unable to register low pressures.

Exactly this point has been picked up by Prof. M. Serebryakov in 1923-24 who started his experiments in the manometric bomb, using his conical crushers, thus establishing a new method of the analysis of the powder burning, applied along the entire curve (p, t) from the beginning to the end of burning.

Prof. M. Serebryakov introduced a new experimental characteristic of the progressiveness of the burning --

this characteristic shows the variations of the intensiveness of gas formation during the whole course of the process of burning.

The applications of this new method made observable for further studies some new facts which could not have been foreseen by the geometric theory; also some new experimental deviations from the geometric formula were found and several hypothetical propositions given a priori by Charbonnier, were proved and verified by the experimental results obtained by Prof. Serebryakov.

1.2 The experimental characteristic of the progressiveness of the burning process - the function \sqrt{t} .

Practical application of the function \sqrt{t} for the analysis of the burning process of powder: The derived experimental characteristic must be constructed, as to its form, that in the ideal case it could be determined by its geometrical factors, assuming that the whole mass of powder is strictly homogeneous.

On the other hand the numerical value of such a characteristic must be calculated using only those experimental results obtainable in the manometric bomb, which are truly reliable.

From the results of burning the powder in the bomb we obtain data in the form of the pressure - time curve, which gives us the recorded pressure at any moment of time with a definite degree of accuracy.

Assuming that f and δ are constant through the whole mass of powder and that there is no cooling effect of the walls, we may apply the general formula of Pyrostatics:

$$p - p_0 = \frac{f \Delta \psi}{1 - \delta - \delta(\alpha - \frac{1}{2})\psi}$$

Here the pressure is a function of the burned fraction of the powder charge ψ .

But the very process of building up of the pressure p is given by $\frac{dp}{dt}$ and therefore by $\frac{d\psi}{dt}$.

All the experimental variations of $(\frac{d\psi}{dt})$ in form of $(\frac{\Delta \psi}{\Delta t})$ can also be taken from the experimental values of p ,

from:
$$\frac{d\psi}{dt} = \frac{S_1}{\lambda_1} \cdot \frac{S}{S_1} u, p$$

and for the comparison for successive values of $\frac{d\psi}{dt}$

these values must be related to their corresponding

pressures p , i.e., the ratio $\frac{(\frac{dy}{dt})}{p}$ is a true measure of the increase or the decrease in the rate of gas formation: if during the process of burning the ratio $\frac{(\frac{dy}{dt})}{p}$ is increased, this increase proves that the powder burns progressively if the ratio $\frac{(\frac{dy}{dt})}{p}$ is decreased our powder burns degressively.

This ratio we denote by $\Gamma = \frac{1}{p} \cdot \frac{dy}{dt}$

Thus Γ is a specific rate of gasification per unit pressure and is called - the intensiveness of the process of gasification; its variability during the process of gasification does characterize the powder from the viewpoint of the progressiveness of the powder itself but not of the form of its grains.

The dimensional structure of Γ is reversed in comparison with the dimensionality of the impulse: $\frac{1}{(\frac{dy}{dt}) \text{ sec.}}$

When the pressure is constant, Γ varies in proportion with the surface of powder as it should be in accordance with the geometric law and in this case Γ is a characteristic of the progressiveness.

If the ignition were really instantaneous over the whole powder surface and the pressure were constant at its

value ρ then the powder, being perfectly homogeneous, could have been burned strictly in parallel layers and the intensiveness of gasification would have been varied in proportion with the powder surface. If:

$$\frac{d\psi}{dt} = \frac{S_1}{\lambda_1} \cdot \frac{S}{S_1} \cdot u \cdot \rho$$

hence: $\Gamma = \frac{1}{\rho} \cdot \frac{d\psi}{dt} = \frac{S_1}{\lambda_1} \cdot \frac{S}{S_1} \cdot u$ - here the only variable is S - surface of powder or $\frac{S}{S_1}$

In this case Γ varies proportionally to $(\frac{S}{S_1})$ i.e., the characteristic of progressiveness conforms with the geometric characteristic of the form of a grain.

For this reason we will take $\Gamma = \frac{1}{\rho} \cdot (\frac{d\psi}{dt})$

the intensiveness of the gasification, as the experimental characteristic of the progressiveness of the powder burning.

Function Γ is determined at intervals of time on the pressure curve by ψ , calculated at the corresponding intervals, thus without any reference to the geometric factors of a powder. This is the reason for considering this function as the expression of the basic experimental, physical law of the burning process. The following three curves present the characteristics of the actual burning of powder:

$$P = f_1(\psi) \quad ; \quad P = f_2(t);$$

$$\text{and: } \int_0^t P dt = f_3(\psi).$$

Graphs (Fig. 46, 47, 48, 49) present pressure - time curves (solid lines) and \bar{P} curves in dotted lines, for the following powders: Fig. 46 - tubular powder; Fig. 47 - strip powder; Fig. 48 - 7-perforation grain powder and Fig. 49 - Kisnemsky's powder with 36 perforations.

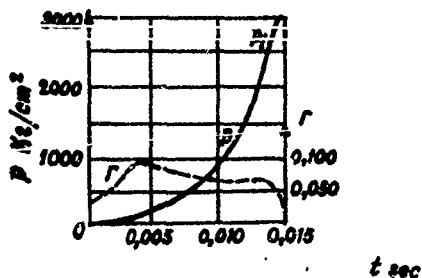


Fig. 46 - Characteristic ($\bar{P}; t$) for the tubular powder.

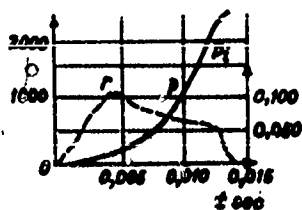


Fig. 47 - Characteristic (F, t) for the strip powder.

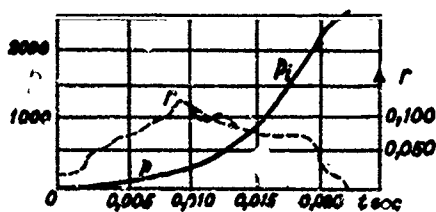


Fig. 48 - Characteristic (F, t) for a 7 perforation grain.

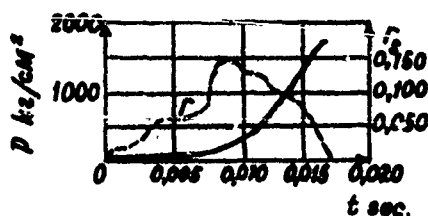


Fig. 49 - Curve (P, t) for Kisremsky's grain with 36 channels.

Considering the value
$$\bar{P} = \frac{S_i}{\lambda_i} \cdot \frac{S}{S_i} \cdot u,$$
 at the constant u , we may expect that \bar{P} for strips and plates will start at its maximum and very slowly will fall down to its minimum value about $\frac{S_i}{S} = 0.90$. But the experimental curves all show their starts at small initial values, then they reach their maximum at the pressures 150-170 kg./cm² and after a gradual depression they sharply fall down at the moment of time corresponding to the point of inflexion at the pressure curves.

For the multiperforated powders (Fig. 48 and 49) these deviations of curves from the theoretical patterns are still more noticeable.

The beginning of the final sharp downgrade corresponds to the beginning of the fragmentation of the grains into slivers and the resulting more degressive burning of these sharp-edged minute remnants.

Thus, generally speaking, the perforated grains burn after the pressure reaches 200 kg./cm as if their burning surface was decreasing all the time whereas theoretically this surface should be increased up to the moment of fragmentation.

A more detailed comparison of theoretical and experimental data can be made using curves (P, ψ) instead of (P, t) . Curves (P, t) are somewhat distorted in the direction of the t-axis: the intervals closer to the beginning with lower pressures are stretched and intervals closer to the last higher pressures are compressed.

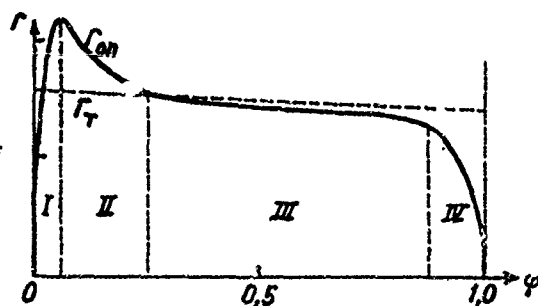


Fig 50 - Curve (P, ψ) for tubular powder.

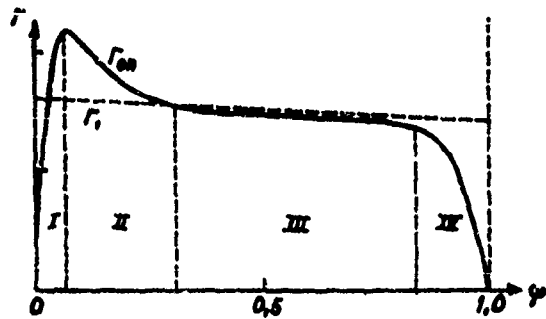


Fig. 51 - Curve (Γ, ψ) for strip powder.

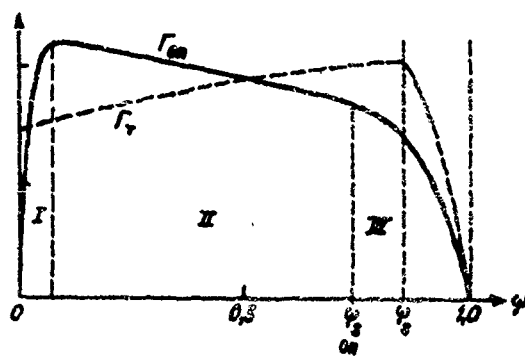


Fig. 52 - Curve (Γ, ψ) for 7 perforation grain.

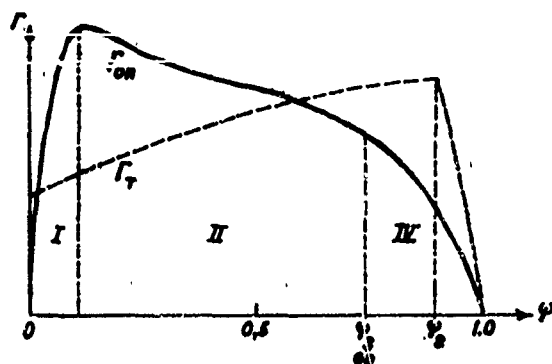


Fig. 53 - Curve (r, ψ) for Kisenemsky's grain
with 36 channels

The curves (r, ψ) are shown in solid line at Fig. 50, 51, 52, 53 together with theoretical $r = \frac{S_i}{\lambda} \cdot \frac{S}{S_i} \cdot u$ (dotted lines) which have their $\frac{S}{S_i}$ varied in accordance with the geometric law with $u = 0.075$ mm/sec. for pyroxylin powders. For tubular and laminar powders (Fig. 50, 51) we have 4 distinctly different sections.

Section I: The curve starts not from the maximum but from the small initial value growing rapidly up to the maximum (at $\psi = 0.05 - 0.08$) which is considerably larger than the theoretical at the beginning ($\psi = 0$).

Section II: is a smooth fall in r to the theoretical curve; there is an interval of the accelerated burning (with the "hump") from $\psi = 0.005 - 0.03$ to $\psi = 0.30$.

Section III: represents normal burnings in accordance with the theoretical geometric law; here ψ varies from 0.30 to 0.85 - 0.90.

In Section IV the experimental curve falls sharply, down from the theoretical to $R = 0$ at $\psi = 1$. Curves (R, ψ) for the multiperforated powders are shown on Fig. 52 (7-perforation grain) and Fig. 53 (Kisnensky's powder with 36 perforations). These curves are even more distinct from the theoretical ones; besides this the down-grade (without any sharp turning point) at the beginning of fragmentation starts at $\psi = 0.70 - 0.75$ and fragmentation itself is more gradual and moderate on account of different webs sizes - a partial fragmentation starts when the smallest webs are burned out, then the webs of the next size burn, etc. thus the progressive burning proceeds along together with the degressive burning of slivers.

Chapter 2 Ballistic Analysis of the Actual Burning of Powder.

2.1. Experiments investigating the ignition of powders. The time (in sec.) of the complete burning of powder is given by: $t_K = 2303 \cdot c \cdot \log \left(\frac{P_m}{P_0} \right) \dots (40)$

under the condition of the instantaneous ignition of the whole powder (here P_0 is initial pressure produced by the igniter). Calculations of t_K for $\Delta = 0.20$; $P_m - P_0 = 2000 \text{ kg/cm}^2$ and P_0 varying from 20 up to 140 kg/cm^2 are given in the following Table 14.

Table 14 (theoretical)

$P_0 \text{ kg/cm}^2 :$	20	40	60	120
$t_K \text{ sec.} :$	0.0140	0.0119	0.0107	0.0087
$\frac{t_K}{(t_K)_{120}} :$	1.61	1.37	1.23	1.00

This table shows that theoretically by decreasing P_0 from 120 kg/cm^2 to 20 kg/cm^2 , we will increase the time of the complete burning at 61%. Whereas the experimental results with the same igniter pressure give entirely different effects.

In the manometric bomb with $\Delta = 0.20$ and with the amounts of igniting dry pyroxylin powder producing the same pressures p_s as they are in Table 14 and using a charge of the strip powder with web $2\varphi = 1$ m/m (148x40) the following results were obtained as they are shown in Table 15.

Table 15 (experimental)

p_s kg/cm ² :	20	40	60	120
t_x (Table 14):	0.0140	0.0119	0.0107	0.0087
$\frac{t_x(\text{exp.})}{t_x(\text{theor.})}$:	3.11	1.78	1.48	1.00

Analogous results have been obtained with other igniters.

Theoretical curves (p, t) on the whole course of burning after the instantaneous ignition must begin at their maximum value and the shapes of these curves must not be affected by the amount of powders in the igniter because regardless of the value of p_s after the instantaneous ignition of the whole surface, its burning will proceed in such a way that only the lengths of curves will be shorter at the higher igniter pressures. Fig. 54 shows

this for the $p_B = 20 \text{ kg/cm}^2$, $p_B = 50 \text{ kg/cm}^2$ and $p_B = 120 \text{ kg/cm}^2$.

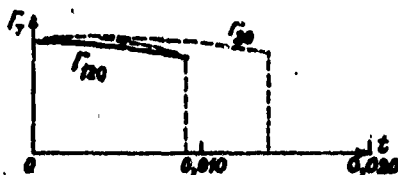


Fig. 54. Theoretical curves (Γ, t) at various p_B
 $20 \frac{\text{kg}}{\text{cm}^2}$ and $120 \frac{\text{kg}}{\text{cm}^2}$.

Experimental curves for $p(t)$ and $\Gamma(t)$ for various igniter pressures: 1 - for $p_B = 20 \text{ kg/cm}^2$; 2 - for $p_B = 50 \text{ kg/cm}^2$ and 3 - for 120 kg/cm^2 are shown in Fig. 55 where, using the same scale for t the curves (p, t) are drawn at upper part and (Γ, t) at the lower part marked accordingly by 1, 2 and 3.

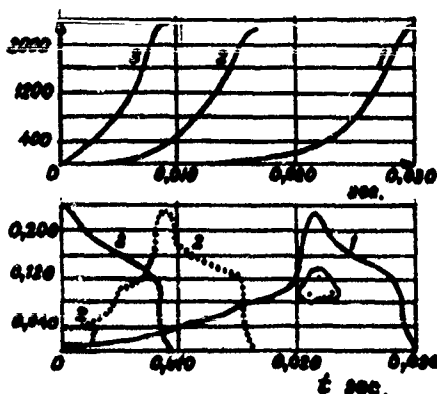


Fig. 55 - Upper part, experimental curves (p, t)
Lower part, experimental curves (r, t)

1 - $p_0 = 20$; 2 - at $p_0 = 50$; 3 - at $p_0 = 120$
kg./cm².

At the lowest igniter pressures 20 kg/cm² the curve $r(t)$ (marked by 1) begins at a very small ordinate and gradually goes up until the powder pressure is about 225 kg/cm² when a very steep rise follows to the maximum with immediate dropping down to 0. The gradual initial increase in ordinates is indicated on the gradual increase of burning surface i.e., its gradual ignition.

Curves $r(t)$ marked by 2 ($p_0 = 40$ kg/cm²) in dotted line has a larger initial ordinate, a shorter length of the interval corresponding to the gradual (and steeper) rising to the same maximum as on the curve 1 and almost

identical course of falling down to zero - as if curve 1 was simply removed to the left along the time scale, which means that a larger initial burning surface takes place in this case in comparison with curve 1. Curve 3 (with the weight of igniter 6 times larger than in case 1, and with igniter pressure $p_s = 120 \text{ kg/cm}^2$.) begins with the same maximum as the preceding curves and with the same shape of falling down to zero.

These results clearly show that only at the igniter pressure $p = 120 \text{ kg/cm}^2$ may we have almost instantaneous ignition, but in the artillery practice the igniter pressures are never higher than $40\text{-}50 \text{ kg/cm}^2$ and as normally $10\text{-}25 \text{ kg/cm}^2$; so that ignition cannot be assumed to be instantaneous. The curves $\gamma(\psi)$ constructed for the cases presented in Table 15, i.e., for the igniter pressures 20, 40, 60 and 120 kg/cm^2 are shown in Fig. 56.

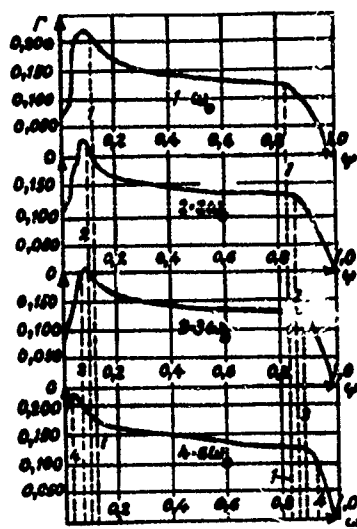


Fig. 56 - 1 - ω_0 ; $p_B = 20 \frac{\text{kg}}{\text{cm}^2}$

2 - $2\omega_0$; $p_B = 40 \frac{\text{kg}}{\text{cm}^2}$

3 - $3\omega_0$; $p_B = 60 \frac{\text{kg}}{\text{cm}^2}$

4 - $6\omega_0$; $p_B = 120 \frac{\text{kg}}{\text{cm}^2}$

These curves are analogous to curves $\frac{S}{S_i} = f(\psi)$ for strip powder but there are certain deviations: $f'(\psi)$ maximum removes from $\psi = 0.1$ to $\psi = 0.05$, and the final downgrade also moves from $\psi = 0.85$ toward the end. These peculiarities show that: (1) not before 5% or 10% of the whole charge is burned, is the whole surface of the powder ignited; and (2) the larger the igniting charge the quicker is the ignition flame spread over the whole surface, and the more time elapses before the beginning of fragmentation and final burning of slivers. These points of the beginning of the fragmentation correspond to the points of inflexion of (pt) curves which are obtained at $\psi = 0.85$, at $\psi = 0.875$, at $\psi = 0.90$ and $\psi = 0.92$ for the corresponding igniting charges ω_0 , $2\omega_0$, $3\omega_0$, and $6\omega_0$, which means that the smaller the igniting charge is, the longer the time for the ignition of the whole surface is, the more webs become varied and the shorter time is required for fragmentation at the point of inflexion for curve (pt).

The exponent β (48) in the function of form is

$$\beta = \frac{R_m - R_i}{R_i} = \frac{R_m}{R_i} - 1 \sim \frac{1}{\psi_i} - 1$$

Hence this coefficient will be for our four cases:

(1) $\beta = 0.18$; (2) $\beta = 0.14$; (3) $\beta = 0.11$ and (4) $\beta = 0.09$.

The greater β is, the more degressive is burning (the change from the curve 4 to the curve 1.)

The experiments show that a non-instantaneous ignition is more pronounced at smaller igniting charges.

Comparing diagrams of Fig. 56 with those of Fig. 45 (graph of the "function of form"), we see that the "function of form" for the cases when $\beta = 0.2$ ($p_0 = 20$ kg/cm²) is very close to $f(\psi)$ marked 1 at their middle parts and ends but are essentially different in their initial part ($\psi = 0$): (1) $f(\psi)$ has its initial rise which is absent in the "function of form":

$$\frac{S}{S_1} = (1-\psi)^0 \approx (1-\psi)^{0.2}$$

and (2): there is a noticeable "hump" in ordinates in the interval from $\psi = 0.1$ to $\psi = 0.3$ over the ordinates at the same interval of ψ in the "function of form". This abnormal increase in the ordinates in $f(\psi)$ was unknown to earlier investigators but at present this particular part of the curve $f(\psi)$ shows the effect of the gradual ignition, i.e., of a gradual increase in the burning surface of the powder, and proves the non-existence of the instantaneous ignition of the igniter pressures lower than 120-150 kg/cm².

Using the igniters made of black powder and pyroxylin producing the same β we will find that the ignition of black powder is more intensive because this ignition is a result of action not only of hot gaseous molecules but of the hot solid particles absent in the pyroxylin igniter.

12.2 Nature of "The Hump". This "hump" in Section II (Fig. 51 and 56) of the experimental $P(\psi)$ curves over the smooth contours of theoretical curves of the "function of form" can be found in smokeless powders with volatile solvent.* Powders with solid solvent (tetryl + pyroxylin) are burning closer to the geometric law and their curves $P(\psi)$ have almost no humps.

Let us consider two tubular powders of the same dimensions: one powder (1) is prepared with volatile solvent, another (2) with the solid solvent.

Since the geometric factors are identical in both powders their
$$P = \frac{S_i}{A_i} \cdot \frac{S}{S_i} u$$
 may be affected only by the value of u , (burning rate at the unit pressure). Both curves marked 1 and 2 are shown in Fig. 57. Curve 1 has a very pronounced hump, curve 2 has hardly any.

* Powders with larger webs have larger "humps". Pyroxylin powders have larger "hump" than nitroglycerine powders.

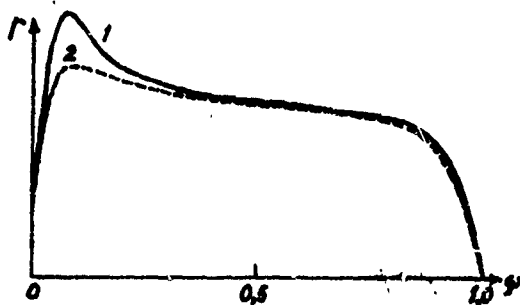


Fig. 57. The intensiveness of gas formation for two chemically different powders of the same dimensions.

1 - volatile solvent

2 - solid solvent

Differences in ordinates of these curves in the intervals of t from 0.1 to 0.3 are attributed to differences in the burning rates u_1 and this difference in u_1 is explainable by the more noticeable heterogeneity of the mass in the powder (1) than in powder (2). Powder with volatile solvent is washed for a long time in water; during this process the powder becomes more porous and its u_1 is increased over the outer layers. When burning penetrates into deeper layers, u_1 becomes lower. The inner parts of powder grain are not affected by water and are burned normally.

Powders with the solid solvent are more homogeneous but some increase in u_1 during the initial intervals when the powder pressure is not high (lower than 500 kg/cm²) can be produced by more intensive heating through the outer layers. When the pressure goes over 500 kg/cm², the heating through the outer layers is not so intensive and not so deep, and u_1 becomes smaller and $f(\psi)$ falls down. This explanation was suggested by M. Serebryakov in 1937, and verified later on by Prof. J. B. Zeldovich in 1942, but a general theoretical and detailed experimental investigation of this problem is still in process of development. At any rate one causative definition of the humped part of the $f(\psi)$ curve for powders with volatile solvent is this; This excessive growth of the ordinates is produced by the accelerated burning of the outer layers of powder at the lower gas pressures, mostly observable in the case of powders with volatile solvent. The larger the web size, the smaller is u_1 , the more pronounced is the hump of the $f(\psi)$ curve.

At pressures higher than 500 kg/cm² and with increasing u_1 , the humps are tapered down to zero.

The following empirical formula was developed from experimental data:

$$u_1 = u'_1 e^{-a\sqrt{z}}$$

here: u'_1 = burning rate of the outer layer;

almost for all pyroxylin powders $u'_1 = 0.0000120 =$

$$0.0000125 \frac{\text{dm/sec}}{\text{kg/dms}}$$

z - relative thickness of the burned layer, which for tubular and strip powder is nearly ψ (for tubular powder $z = \psi$)

a - characteristic of the decreasing rate of burning given by formula:

$$a = \frac{b_{21}(\frac{u'_1}{u_1})}{\sqrt{z_c}}$$

u - a constant rate of burning of the inner layers after $z = z_0$.

This formula is good enough for z varying from $z = 0$ to $z = 0.3$.

Fig. 58 shows curves $u_1(z)$ for the two different powders: one powder SN : $2 e_1 = 1$ m/m; $u'_1 = 0.0000120$ $u_1 = 0.0000075$; $a = 0.858$. Another powder B_{14} contains a larger amount of volatiles than powder SN and its average u_1 (0.0000060) is lower than u_1 of powder SN . On the other hand powder B_{14} with its thick web (6 m/m) was washed in water much longer than powder SN and its u_1 of the outer layers is 0.0000125 higher than u_1 for powder SN .

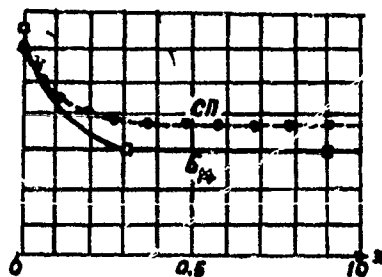


Fig. 58 Variations in u_1 for powders SN and B_{14}

Solid line - powder B_{14}

Dotted line - powder SN

For powders with a volatile solvent their rate of burning is not constant but is higher for the outer layers than for the inner ones where it finally becomes constant. This makes the burning of these powders more degressive than would be expected on the basis of a constant rate of burning and purely geometric changes in surface S .

Thus if the deviations from the geometric law are caused by the heterogeneity of mass of powder and by variations in the thickness of powder grains, then we may question whether it is possible or not to have our $f(\psi)$ curve without its hump, and if it is possible at all to realize experimentally the geometric law of burning.

To answer these questions a special experiment was conducted with a powder charge made in form of a rod with rounded ends of 7.5 mm diameter and 42 mm length. The powder used for the experiment was without any solvent. This charge was placed in the middle of the bomb having its inner volume of 21.5 cm³. Thus the very best requirements in respect to uniformity and equality of all conditions of burning were met.

The igniter was able to develop its pressure $p_i = 160 \text{ kg/cm}^2$, guaranteeing instantaneous ignition.

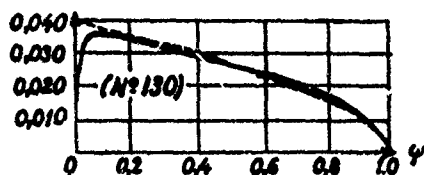


Fig. 59 Experimental curve $I'(\psi)$ in solid line
Geometric law curve - in dotted line

Fig. 59 shows the $\Gamma(\psi)$ curve obtained in this case without any hump together with the curve calculated on the basis of the geometric law for $u_1 = 0.069$ mm/sec. This result gives a definite answer to the above questions. It is possible to realize the burning in perfect agreement with the geometric law. But in practice we always have powder with volatile solvent; our actual charges are placed within their chambers without any special precautions of guaranteeing the unrestricted uniformity and easiness of gas formation and gas motion. On account of these unavoidable practical complications of the total circumstances surrounding the process of burning of powders in guns, the geometric law of burning cannot be realized and all deviations from this law are the more noticeable the more are the difference between conditions of burning in the different parts of a powder chamber.

3.3 The point of inflexion on the (p,t) curve. From

formula (49):
$$\frac{dp}{dt} = \frac{f_A}{1-\alpha_A} \cdot \frac{u_i}{e_i} \cdot \frac{S}{S_i} p;$$

and for tubular or strip powders which have $(\frac{S}{S_i})$ constant for all increasing p's, $(\frac{dp}{dt})$ must be increased to the end of burning. But the numerous experiments show that for these powders the curve (pt) always has a point of inflexion after which $(\frac{dp}{dt})$ is decreased and sometimes becomes zero.

Charbonnier used the location of this point for determining the exponent :
$$\beta = \frac{P_m - P_i}{P_i}$$

At the point of inflexion $(\frac{d^2p}{dt^2}) = 0$, this means that in (49), $(\frac{S}{S_i}) \cdot p$ must be constant at the moment when $p = p_i$; therefore at this point S, a burning surface must be rapidly decreasing because pressure p is rapidly increased. If the rate of decrease in S is greater than $(\frac{dp}{dt})$ then Sp and $(\frac{dp}{dt})$ will be decreased and the curve (pt) will have its curvature changed, i.e., (pt) curve will be bent down.

Such curves are observed for multiperforated powders whose burning surface decreases rapidly after the fragmentation of grains.

By the proper selection of equal webs of strip powder and by special arrangement of mutual positions of strips in a charge, it becomes possible to help the ignition (with high pressure p_B) to spread at once over the whole surface of powder. And then the curve (pt) will not have any point of inflexion and will proceed with it ~~the~~ $\frac{dp}{dt}$) increasing to the end.

And, inversely by selecting strips with varying webs, it is possible to obtain the inflexion point even much earlier (for lower p_1).

It is even possible by using combination of strips of various powders, to transform the (pt) curves at the long interval into a straight line as the continuous row of inflexion points.

The following Table 16 presents some of the experimental results obtained by M. E. Serebryakov in his investigations of factors producing the points of inflexion.

(Powder CH ; $\Delta = 0.20$; the igniter dry pyroxylin; $W_0 = 78.5 \text{ cm}^3$.) Experiment No. 1: Strips with varying webs, igniter very weak (20 kg/cm^2). Experiment No. 2: Strips with strictly constant webs, the same igniter. Experiment No. 3: The same strips as in No. 2, with the strong igniter ($p_B = 123 \text{ kg/cm}^2$).

Table 16

$$W_0 = 78.5 \text{ cm}^3.$$

No.	$2e, \text{ mm}$	$\rho_0, \frac{\text{kg}}{\text{cm}^3}$	$\Delta \tau, \frac{\text{cm}^2}{\text{sec}}$	ρ_m	ρ_i	$\left(\frac{dp}{dt}\right)_{\text{max}}$	ψ_i	$t_k, \text{ sec.}$	β
1	0.92-1.07	20	0.201	2115	1717	428	0.82	0.0355	0.230
2	1.00-1.01	20	0.201	2150	1950	480	0.92	0.0348	0.103
3	0.98-1.00	125	0.211	2310	2190	540	0.95	0.0084	0.055

Curves (p, t) (Γ, t) and (Γ, ϕ) are given in Fig. 60 (only No. 1 and No. 3) and Fig. 61.

In experiment No. 1, the curve (p, t) after the point of inflexion smoothly changes its curvature with its $\left(\frac{dp}{dt}\right)$ nearing 0 at t_k . In experiment No. 3, the ignition is instantaneous, point of inflexion is moved to the end of the curve.

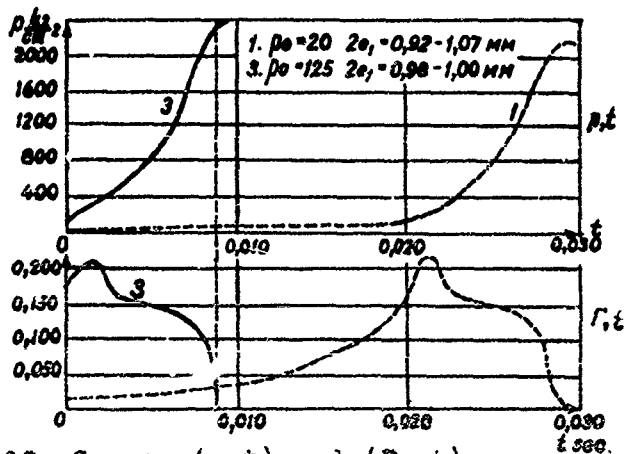


Fig. 60 Curves (p, t) and (Γ, t)
Table 16: No. 1 and No. 3.

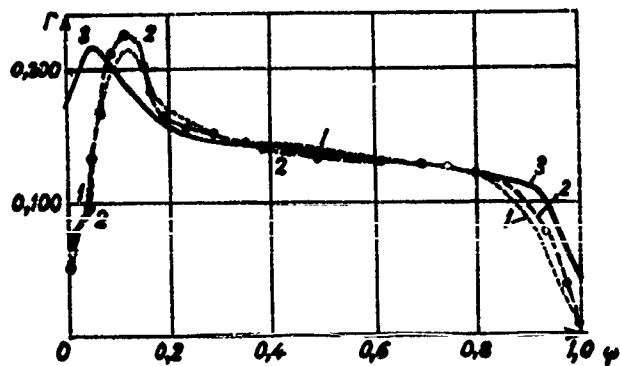


Fig. 61 Curves (r, ψ) at various p_s and $2e$, ,
Table 16: No. 1, No. 2, No. 3.

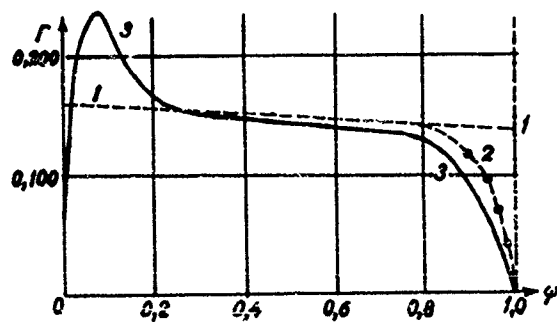


Fig. 62 Curves (r, ψ) at the burning out of strips
with various webs.

Conclusions:

1) The point of inflexion marks a sudden decrease in the burning surface of a powder;

2) The location of the point of inflexion depends on the degree of uniformity in the sizes of webs of laminar or tubular powders at the last phases of burning.

3) By the proper selection of the conditions of ignition and sizes of webs the location of the point of inflexion can be widely moved on the (pt) curve.

This point always is a result of the irregularity of web sizes and in multiperforated powder it follows the sharp decrease of the burning surface of slivers.

4.4 On the rapid decrease of the intensiveness of gas formation in the last phases of burning. For the degressive powders their experimental curves $\dot{V}(\psi)$ are almost identical in their middle sections from $\psi = 0.3$ to $\psi = 0.8 - 0.9$; then the experimental curves begin their steep downgrades to 0 at $\psi = 1$.

This is the result of the variety in web sizes in powder grain (strips). The smaller the web of a strip, the quicker this plate burns out, and at the end of burning the decrease in burning is very abrupt and the function $\dot{V} = \frac{S_i}{\lambda_i} \cdot \frac{S}{S_i} u_i$ rapidly falls.

The more varied are the web sizes, the sooner occurs the decrease in the intensiveness of gas formation. It is also not amiss to note that even over the surface of a single strip its webs as a rule are larger in their middle parts and smaller along the edges of a strip (as a result of the drying process).

In tubular powders an even wider variety in the web sizes is produced by the eccentricity of the inner and outer surfaces. This can be seen in Fig. 61.

The following Table 17 shows the results of calculations of $\Gamma = \frac{S_i}{\lambda_i} \cdot \frac{S}{S_i} u_i = \frac{S}{\lambda_i} \cdot u_i$ for the charge of strip powder with varied webs from 0.92 mm. to 1.7 mm. All strips have been distributed in six groups as shown in Table 17: 15% with $2e_i = 0.92$; 15% with $2e_i = 1.12$ and 15% with $2e_i = 1.17$. Average $2e_i = 1.05$ mm.

Theoretically for the powder with the constant average web, the ratio $\frac{S}{\lambda_i}$ varies during the burning from 2.07 to 1.76 mm²/mm². and the function Γ from 0.130 to 0.136 at $u_1 = 0.0775$ mm/sec.

Table 17

No. of Groups :	1	2	3	4	5	6	Re- marks
Web $2e_1$: mm	0.92	0.97	1.02	1.07	1.12	1.17	($2e_1$) aver. = 1.05
% of strip : with their web $2e_1$ in a total charge	15%	15%	20%	20%	15%	15%	
ψ_i :	0.894	0.931	0.961	0.982	0.994	1.000	
$\frac{S_i}{\lambda_i}$:	1.526	1.250	0.887	0.530	0.263	0	Theor- etical Γ at the begin- ning ($\Gamma_{\text{aver.}}$) = 0.160.
$\frac{S_i}{\lambda_i} u_i = \Gamma_i -$	0.118	0.097	0.069	0.041	0.020	0	Theor- etical Γ at the end (Γ) aver. = 0.136
(curve 2 on Fig. 62)							

Fig. 62 shows theoretical curve for Γ (in dotted line) marked 1. The ascending part of the curve marked 2 (in dotted line with circles) represents the results

calculated in Table 17 and a solid curve marked 3 is obtained from the results given by the experiments in the manometric bomb.

A very good fitting of curves 2 and 3 is somewhat distorted at the end because the igniter was not strong and a slowed down ignition increased the actual deviations in webs beyond the prescribed limits shown in Table 17.

The results shown above can be summed up as follows:

1) A very steep rise of the curve $I(\psi)$ in the beginning is a result of the gradual ignition. The instantaneous ignition and the beginning of the curve $I(\psi)$ with its maximum can be obtained only with the high pressure igniter (120-150 kg/cm²).

2) The "hump" of the curve $I(\psi)$ is an indication of accelerated burning at lower pressures in the presence of uneven sizes of webs and also a result of washing out in water of the volatile solvent and intensified heating at the low rate of burning.

3) An inflexion point on the (pt) curve and a corresponding sharp decline of the intensiveness of gasification at the end of burning are produced by the uneven burnings of various webs of the powder. The small igniter and a large variety of webs produce the inflexion points

earlier than they are produced (if at all) by the stronger igniter and even sizes of webs.

18.5 Application of ballistic analysis. A progressive burning of powder can be attained by the process of phlegmatization, i.e., by the infusion of certain material retarding the rate of burnings of the outer layers. The distribution of the phlegmatizer in powder grain must not be uniform - its concentration in the powder mass should decrease from the outer surface to the inner layers. Thus the rate of burning u_1 (at $p = 1 \text{ kg/cm}^2$) depending on the nature of the powder will be gradually increasing from its minimum on the outer surface to its maximum in the depth of a grain and this process is controlled not by the shape of a powder but by the particular chemical composition of the mass of powder.

The process of phlegmatization, like every other technological process, is liable to be imperfect within certain limits and insufficient phlegmatization can be just as undesirable as overphlegmatization, going through the whole mass of a grain and making the whole of it a slow burning grain but not a progressively burning one.

Hence a very important practical problem arises - the problem of the determination of the actual depth of grain

affected by the presence of phlegmatization. The simplest procedure consists in coloring the mass of phlegmatizer with fuchsin; after the process of phlegmatization is over, a dry powder grain is dissected and under the microscope the thickness of the colored layer is measured. But this method is not a very accurate one because the fuchsin and phlegmatizer have different penetrating powers; besides this, a measured depth of penetration contains no information concerning the character of distribution of phlegmatization in a powder.

The use of experiments in the manometric bomb and their analysis by means of the function $\Gamma(\psi)$ give results very accurately representing the real nature of the distribution of phlegmatization within the grain, and its effect on the rate of burning.

Fig. 63 presents two curves $\Gamma(\psi)$ for seven perforation powder grain. Curve 1 is computed from an experiment in the manometric bomb with powder without phlegmatizer in its mass; curve 2 (in dotted line) is computed from an experiment in the manometric bomb with phlegmatized powder. Curve 1 is a regular $\Gamma(\psi)$ curve havint its hump and depressior at $\psi = 0.50$; the curve 2 has no hump, its ordinates are increased from the lower initial value

of \dot{r} up to \dot{r} equal to \dot{r} of the curve 1 (at $\psi = 0.50$) and for the larger ψ both curves become identical.

This picture says that the phlegmatization is active till $\psi = 0.5$ is reached, i.e., powder is burning progressively until the half of a grain is burned.

Since both grains in this experiment have the same size and shape, their functions \dot{r}_1 and \dot{r}_2 contain only factors $(u_1)_1$ and $(u_1)_2$ which are different.

So we have:
$$\frac{\dot{r}_2}{\dot{r}_1} = \frac{(\frac{S}{\lambda_1} u_1)_2}{(\frac{S}{\lambda_1} u_1)_1} = \frac{(u_1)_2}{(u_1)_1}$$

Taking this ratio from the curves 1 and 2, we may draw the curve shown on Fig. 64 which represents the relative variation of the rate of burning affected by the phlegmatization.

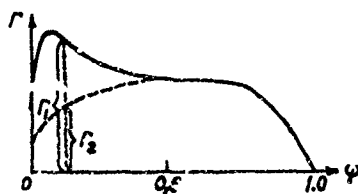


Fig. 63 Curves \dot{r}/ψ before (1) and after (2) phlegmatization of powder.

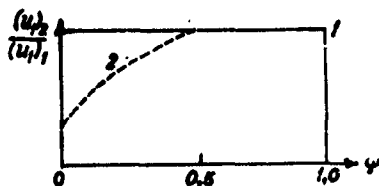


Fig. 64

Ratio of rates of burning $\frac{(u_2)_2}{(u_1)_1}$ taken from the curves in Fig. 63.

This curve shows that the phlegmatization is strong (its concentration is high) at the outer surface where the rate $(u_2)_2$ is a fraction of $(u_1)_1$ and at $\psi = 0.50$, $(u_2)_2$ becomes equal to $(u_1)_1$ which means that phlegmatization does not penetrate deeper than the surface of grain holding one half of the weight of grain.

Thus by using phlegmatization, it is possible to cut down the intensiveness of gas formation during the first half of the burning process; the practical significance of this result is the possibility of an increase in the powder charge without any increase in the maximum pressure, but with an increase of the muzzle velocity.

But phlegmatization also cuts down the force, f , of powder; therefore, a certain part of our increase in the powder charge will work on the preservation of the same muzzle velocity which was attained by the unphlegmatized powder, but still we will have some gain in having lower maximum pressure.

Making comparative experiments with powder which is uniformly permeated with the phlegmatizer and a powder in which the concentration of phlegmatization varies from one layer to another, we may determine how this later phlegmatization is numerically distributed from one layer to another.

By prolonging the process of phlegmatization for a long enough time, we may obtain a powder so uniformly phlegmatized through its whole web that this powder will be a slow burning but not a progressive one.

An analysis made by means of the application of the function $f(\psi)$ has disclosed that the British tubular cordite, despite its degressive form after burning up to $\psi = 0.3$, becomes a progressively burning powder.

Special experiments show that a freshly prepared cordite, after the removal of the excess of its solvent (acetone), produces a regular $f(\psi)$ curve identical with

the curve obtained for tubular pyroxylin powder (see Fig. 65). But after keeping this powder in the thermostat at 50°C., we will find that its "force" is decreased and the ordinates of its curve $f(\psi)$ (curve 2) after the hump and depression will be again increased along the interval of ψ from 0.3 up to 0.9 and then will sharply fall to zero.

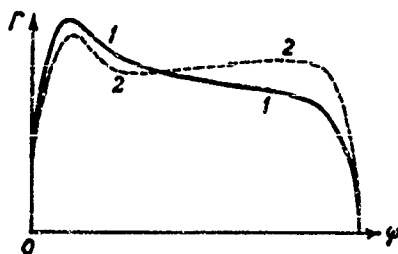


Fig. 65 Curves $f(\psi)$ for nitroglycerine powder
(cordite)

Curve 1 - freshly prepared cordite after removal of excess acetone.

Curve 2 - the same cordite after keeping in thermostat

The marked drop in f shows that the powder lost some of its nitroglycerine through its outer surface when heated up to 50° C. The remaining nitroglycerine has been redistributed along the thickness of a grain.

Since the rate of burning of a layer depends on the amount of nitroglycerine in this layer we observe the increase of the rate of burning with the penetration of burning in the inner layers of a grain and as a final result the ordinates of Γ are increased and the burning becomes progressive.

The conclusion is that the length of time and mode of keeping the powder in storage may affect the character of the burning of cordite and using the function $\Gamma(\psi)$ as a means of analysis, it is possible to detect any changes in the character of burning of a powder.

Chapter 3 - Special Features of Burning of Multiperforated Powders

We have already seen (Figures 48, 49, 52, 53) that the experimental curves $\Gamma(\psi)$ for the multiperforated powders deviate more markedly from the theoretical geometric law than the experimental $\Gamma(\psi)$ curves for the powders with simpler forms of grains (strips, tubes) and the longer are the inner channels in grain, the more conspicuous are these deviations. The most puzzling facts from the viewpoint of the geometrical law of burning are the degressive parts of the experimental $\Gamma(\psi)$ curves for the powders in which the inner surfaces of the channels in accordance with the theory should be increased during the burning until the fragmentation begins. Thus it seems that the fragmentation of the powder grain begins immediately after its inflammation and then the slivers have their surfaces burning degressively. Such fragmentation during the initial phase of burning can be attributed to the accelerated gas formation within the long and narrow channels, in which a higher pressure can develop with the resulting higher rate of burning, on the other hand the resistance of the walls of grain becomes insufficient against the increased pressure, the grain is crushed and the burning of slivers becomes degressive.

Such an explanation of the degressiveness of $\Gamma(\psi)$ curves seemed to be natural and acceptable as far as it deals with the decreasing burning surface. But the facts definitely disagree with the very hypothesis of the immediate fragmentation during the initial phase of burning: the powder grains picked up from the ground after the firing show very convincingly that even a very considerable burning out of the inner surfaces of channels, amounting to 60% of the total mass of a grain still does not destroy the grain. This fact means that the burning process in case of the multiperforated grains is much more complex process requiring a more detailed analysis of the specific factors involved in the process of burning of the multiperforated powders.

3.1 The influence of close contact between the burning surfaces. Two strips of powder can burn quietly beside each other without any reciprocal reaction, but if one of the burning strips is put on the other, mutual interference begins immediately. The burning becomes very intense; gases are violently ejected from the cracks all along the contours of the contiguous surfaces. Thus we may suppose that the gas pressure between the strips is markedly raised. In order to verify this assumption, special experiments have been made.

Two parallel burnings were observed in a small manometric bomb with $W_0 = 21.5 \text{ cm}^3$. (1) For the first burning two "grains" of nitroglycerine powder (cordite) were used - one grain was made in the form of a tube, another in the form of a rod which can be easily inserted in that tube but during the first burning these two "grains" lay freely one beside the other. (2) For the second burning the rod was put inside the tube. The results are reproduced in Fig. 66, curves (p, t) and (Γ, t) marked by 1 and 2 and Fig. 67, curves (Γ, ψ) . Curve $(p, t)_2$ on Fig. 66 after $p = 100 \text{ kg/cm}^2$ goes all the time above curve $(p, t)_1$ and curve $(\Gamma, t)_2$ has its hump in the beginning of its rise almost twice as high in comparison with $(\Gamma, \psi)_1$.

Fig. 67 shows also almost a doubled hump for $(\Gamma, \psi)_2$ at $\psi = 0.03 - 0.04$ and after $\psi = 0.06$ both curves are very close to one another.

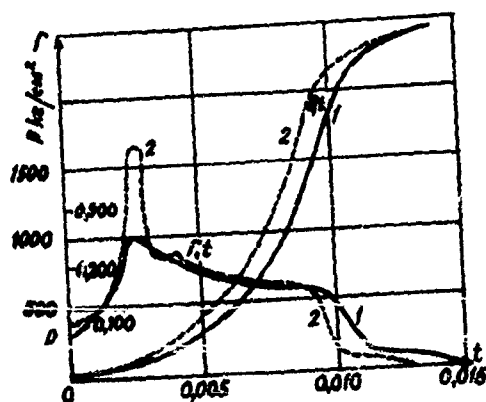


Fig. 66 Curves (p, t) and (Π, t) . 1) a rod and a tube lying beside each other. 2) a rod inside a tube.

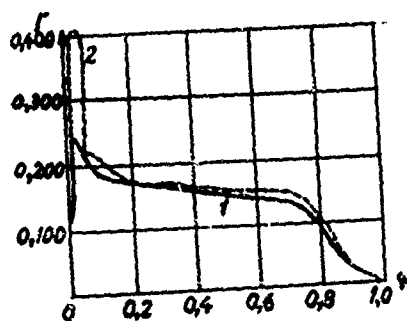


Fig. 67 Curves (Π, ψ) . 1) a rod and a tube lying beside each other. 2) a rod inside a tube.

This experiment with a rod burning inside a tube was repeated in the open air. As soon as both ends of the tube were ignited simultaneously, the rod was violently ejected from the tube, obviously because of the difference in pressures instantaneously formed at the ends of that narrow crack remaining between rod and tube.

During the burning in the bomb the analogous ejection of a rod took place in the beginning of burning at $\psi = 0.03 - 0.04$; a sudden hump on the $\Gamma(\psi)$ was formed, but immediately after this disturbance the normal burning was restored and both $\Gamma(\psi)$ curves continued their parallel courses.

Besides this a somewhat shorter time of burning $t_k = 0.0130$ sec. in the second experiment against $t_k = 0.0140$ in the first one shows that a more intensive burning took place, when the rod was inside the tube.

These experiments are particularly interesting and valuable because they have established the important fact of the sudden increase of the gas formation caused not by the increase in the burning surface but by the increase of the burning rate affected by the excess in pressure inside the narrow crack between the two contacting surfaces. As soon as such a contact is eliminated, the burning

process resumes its normal course. According to the geometric law of burning, all the surfaces of powder grains are supposed to burn at the same rate. Any change in the relative positions of grains does not affect the geometric law of the gas formation process.

Proximity between burning surfaces occurs also within the perforations of grains, especially within the long narrow perforations: the smaller the diameter of perforation, the closer are the parts of burning surfaces within it and the more intense is the burning. But during the burning itself, the diameters of channels are increased, and the intensity of burning falls together with the ordinates of the curve $\Gamma(\psi)$.

All powders with channels have a higher rate of burning than strip powders. For example Kisenemsky's powder with 36 perforations has its rate of burning before fragmentation begins (before the point of inflexion on the (pt) curve) $u_1 = 0.100$ mm/sec., whereas for the strip powder prepared out of the same mass $u_1 = 0.075$ mm/sec.

3.2 The relationship between the progressiveness of powder burning and the length of perforations. From the geometric law of burning it follows that the narrower and longer the channel, the more progressive is the form of a

grain having such a channel. But on the other hand the narrower and longer the channels within the grain, the more obstructed is the burning and ejection of gases out of these channels and the geometric law itself becomes less applicable and such grain burns less progressively.

Here are presented the experimental results obtained in the manometric bomb in the form of four curves $\Gamma(\psi)$ and four curves $(\frac{S}{S_0}, \psi)$ for the multiperforated grains (in the form of bars), having the same cross sectional areas but having four different lengths ($2c$, $\frac{2c}{2}$, $\frac{2c}{3}$ and $\frac{2c}{4}$); number of quadratic perforations 36; (side of square $\frac{16}{10}$ $a_0 = 0.42$ mm).

Powder charges for four experiments in a bomb were made of four different relative lengths of powder bars:

- | | |
|--|-----------------------------|
| 1) normal length $\frac{2c}{a_0} = 90$; | 2) $\frac{2c}{a_0} = 22$; |
| 3) $\frac{2c}{a_0} = 11$ | and 4) $\frac{2c}{a_0} = 9$ |

Table 18

	$2c$	$\frac{2c}{4}$	$\frac{2c}{8}$	$\frac{2c}{10}$
$\frac{2c}{a_0}$	90	22	11	9
S_1	1.37	1.53	1.76	1.89
Geometrical progressiveness Sk/S_1	2.17	1.83	1.39	1.20

Fig. 68 presents four curves $(\frac{S}{S_1}, \psi)$ and four curves (Γ, ψ) . Geometrical curves of progressiveness $(\frac{S}{S_1}, \psi)$ at the left side of Fig. 68 all begin at $\frac{S}{S_1} = 1$;

$\psi = 0$; they go regularly increasing their ordinates and being more curved (progressive) for larger relative lengths of grains (1) and almost flat for the shortest length (4).

From the experimental curves (p, t) ordinates were obtained for $\Gamma(\psi) = \frac{S}{S_1} \cdot \frac{S_1}{\lambda_1} u_1$, or of $\frac{\Gamma(\psi)}{(\frac{S}{S_1})} = \frac{S}{S_1} u_1 = \Gamma_s = \frac{\Gamma(\psi)}{S_1} \cdot \lambda_1$

If the geometric law is applicable, Γ_s will vary with constant u_1 only with $\frac{S}{S_1}$, i.e., $\Gamma_s(\psi)$ should have the same shape as the curve $(\frac{S}{S_1}, \psi)$ on the left

side of Fig. 68, but actual curves (Γ, ψ) are shown on the right part of Fig. 69.

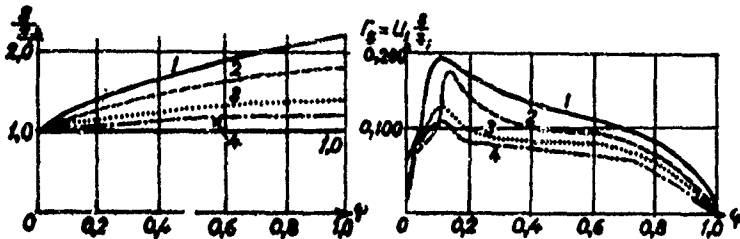


Fig. 68 The intensiveness of gas formation as affected by the length of channels in grains. At the left side: theoretical progressiveness (geometric law: $\Gamma = \frac{S_1}{\lambda_1} \cdot \frac{S_3}{S_4} \cdot u_1$) at the right side: experimental progressiveness: $u_e \cdot \frac{S_3}{S_4} = \Gamma_e$

All these curves have pronounced humps at $\psi = 0.1$, with the ensuing progressive course along which they run as a convergent pencil; the curve (1) corresponds to the largest relative length of channel $\frac{2c}{a_0} = 90$, the curve (4) is for the shortest $\frac{2c}{a_0} = 9$. For smaller lengths we

observe the smaller depressiveness; thus a short grain (No. 3) gives almost a horizontal part for its $\Gamma(\psi)$ curve (for $\psi = 0.4$ to $\psi = 0.6$).

Thus we reach the general conclusion that in their burning the longer grains deviate more from the geometric law than do the shorter grains, and that they are more depressive at the end of burning. In other words for burning in the manometric bomb the more progressive is the form of the grains the more depressive is the intensity of burning: the real physical law of burning produces the results which are opposite to the results of the geometric law.

A more detailed analysis of all 4 curves (Γ, ψ) however, shows that the curve 4 (for relative length = 9) is more depressive than the curve (3) for the relative length 11, which means that the decrease in depressiveness with the shortening of a grain passes through its minimum somewhere at $\frac{20}{a_0} \sim 20$, i.e., at a given cross section of a grain there can be found such an optimum length which produces the minimum of depressiveness or the maximum of progressiveness in the intensity of gas formation. Such paradoxical results of experiments in the manometric bomb have been checked by the actual firing.

Table 19

The results of firing tests with the powders having grains with constant cross section and various lengths ($2c/a_0$).

Powders	$\frac{2c}{a_0}$	ω_{kg}	$p_m \frac{kg}{cm^2}$	$v_{\frac{m}{sec}}$	$\frac{S_1}{\Delta_1}$	$\frac{S_1}{S_2} = \sigma$
1. long ($2c = 10 a_0$)	220	0.950	2285	613	1.39	1.89
2. shorter ($2c = 3a_0$) 36 perforation grain	66	1.150	2290	655	1.44	1.81
3. short ($2c = a_0$)	22	1.100	2285	648	1.59	1.54
4. Brand 9/7 (7 perforations)	24	1.200	2290	655	1.40	1.37

All tested powders have produced the same p_m but the most progressive (and the longest) - No. 1 gave its p_m at the smallest weight of charge (0.950 kg) with the lowest $v_{\frac{m}{sec}}$ (613 m/sec.)

The shortened powder (No. 2) with a lower progressiveness $\frac{S_1}{S_2} = \sigma$ by the use of heavier charge (with the same p_m) gave a higher $v_{\frac{m}{sec}} = 655$ and in fact is a more progressive powder than No. 1. But No. 4 with 7 perforations instead of 36 in No. 2 being markedly simpler in the process of manufacturing and, having a lesser

progressiveness than No. 2, gives the same ballistic results -- p_m and U_g .

Powder No. 3 is somewhat worse than No. 2 because at the same p_m with a smaller ω it produces a lower $U_g = 648$ m/s.

Thus the actual firing test shows that powders with narrow channel in a bomb and also in a gun give like results and that powders with too long and narrow channels being geometrically progressive are in fact disadvantageous. It is also important to note that there is always certain optimum grain length, at which the burning is most progressive and in guns with higher Δ this optimum length is not the same as can be found for a manometric bomb using a lower Δ .

Analogous tests with tubular powders verified this result: that at the same powder charge the longer tubes produce both higher p_m and higher U_g than the short ones. A general conclusion is that the burning of powders with the narrow channels does not follow the geometric law and the longer and narrower the channels, the larger are the deviations from the geometric law.

3.3 The basic principles of the theory of the non-uniform burning of perforated powders. The above described results show that even powders with the simplest form of grains deviate in their burning from the normal way prescribed by the geometric law of burning. These deviations become still more pronounced in the cases of powder grains having numerous long and narrow channels, and a natural question arises - how can these deviations be explained?

The fundamental assumption of the geometrical law is that at any given moment the acting pressures over all elements of a burning surface are equal and produce equal rates of burning, i.e., $u = u_1 p$ is constant over the whole burning surface. This assumption might have been true if the process of burning was so slow that all arising irregularities or inequalities might always have time enough to be distributed evenly and to become equal over the whole burning surface which may happen only if the burning process could be considered as analogous with a certain static process.

The actual burning process takes place abruptly and violently. The pressures at various parts of a charge or even at parts of a separate grain are different as well as are different rates of burning and all these differences

have not time enough for their leveling and the differences in the intensity of gas formation are particularly effective and significant in the narrow channels of powder grains.

In a powder with a perfectly homogeneous chemical composition the rates of burning can be equal only if and when the acting pressures are equal. But if a pressure p'' inside a channel were equal to a pressure p' outside this channel, the gases inside the channel could not escape and a physically unrealizable situation must have occurred: the volume of the manometric bomb should have been filled by the gases formed only from the outer surfaces of the grains and gases formed inside the channels of the grains must have been supposed to remain immovable within the channels. The only conclusion is that the pressures p and their $\frac{dp}{dt}$ outside and inside of channels, as well as the ratio of burning, cannot be equal. Let us apply the formulas of the pyrostatics to the inner surface of a channel and to the outer surface of a grain in order to prove the above conclusion. From (33) and (34') we have the following formula:

$$\frac{dp}{dt} = \frac{f\Delta(1-\frac{\Delta}{\tau})}{\Lambda_{\psi}^2} \cdot \frac{S_i}{\Lambda_i} \cdot \frac{S}{S_i} \cdot u_i \cdot \rho$$

for the rate of the increase in pressure in the relative free volume Λ_ψ of a bomb in which the powder is burning;

$$\text{Here: } \Lambda_\psi = 1 - \frac{\Delta}{f} - \Delta \left(1 - \frac{1}{f}\right) \psi = \frac{W_\psi}{W_0}$$

For the initial phase of burning: $S=S_1$; $\Lambda_s = 1 - \frac{\Delta}{f}$

$$\text{then: } \frac{dp}{dt} = \frac{f\Delta}{(1 - \frac{\Delta}{f})} \cdot \frac{S_1}{\Lambda_1} \cdot u_1 p = \frac{f\omega}{W_0 - \frac{\omega}{f}} \cdot \frac{S_1}{\Lambda_1} \cdot u_1 p$$

Since $\frac{\omega}{\Lambda_1} = \delta$ (density of powder):

$$\frac{dp}{dt} = f\delta u_1 \frac{S_1}{W_0 - \frac{\omega}{f}} \cdot p \dots (50)$$

Denoting $W_0 - \frac{\omega}{f} = V$ we will have finally:

$$\frac{dp}{dt} = f\delta u_1 \frac{S_1}{V} p \dots (50')$$

Thus we have that at given f , δ and u_1 and p , the rate of increase in p , i.e., $\frac{dp}{dt}$ is determined by the

$\frac{S_1}{V} = \gamma = \frac{S}{V}$ which is the ratio of the burning surface to that volume in which gases are emitted from the surface of powder.

The burning process going on within the channel can be considered as consisting of the two processes: 1) the emission of gases from the surface of a channel within

the volume of a channel and 2) the escape of gases from the channel under the inner pressure which is higher than the pressure outside of the grain.

Let us evaluate $\left(\frac{dp}{dt}\right)$ at the beginning of burning using the formula (50) first applying it to the inner surface of a channel and secondly to the outer surface of a grain. Denoting the initial volume of each channel by W_0 , its surface by S_0 , the total number of grains in the powder charge by N and the number of channels in a grain by n and assuming that the pressure of the igniter p_B is the same inside of channels and outside of a grain we will have for the channel:

$$\frac{dp''}{dt} = f \delta u \cdot p_B \bar{z}''$$

where: $\bar{z}'' = \frac{S_0}{W_0} = \frac{\pi d^2 c}{\frac{\pi}{4} d^3 c} = \frac{4}{d}$

For the outer surface S' of a grain: $\frac{dp'}{dt} = f \delta u \cdot p_B \bar{z}'$

where $\bar{z}' = \frac{S'}{W_0 - \frac{W}{f} - NnW_0}$

since $\frac{W}{f} = \Lambda_1$ and Λ_1 is the volume of the whole charge we have, after dividing the numerator, and denominator by Λ_1 : $\bar{z}' = \frac{S_1 S'}{\Lambda_1 S_1} \cdot \frac{1}{W_0 - 1 - \frac{NnW_0}{\Lambda_1}} = \frac{S_1}{\Lambda_1} \cdot \frac{S'}{S_1} \cdot \frac{1}{\frac{W_0}{\Lambda_1} - 1 - \frac{NnW_0}{\Lambda_1}}$

Now having these expressions for the numerical values of \bar{z}' and \bar{z}'' , for a given powder (for example for 7 perforation grain at $\Delta = 0.20$) after all the necessary calculations we will have that $\bar{z}'' \sim 70 \bar{z}'$ which means that $\left(\frac{dp''}{dt}\right)$ is about 70 times larger than $\left(\frac{dp'}{dt}\right)$ and the pressure p'' inside of a channel is in the same proportion higher than p' on the outer side of a grain, and the same ratio will hold for the rates of burning $u' = u_1 p'$ and $u'' = u_1 p''$. Thus if even at certain moment in the beginning of burning the pressure p' and p'' became equal, at the next moment this equality will be disrupted and the pressure within the channels p'' will be larger than p' and $u'' > u'$. On the other hand, the gases ejected from the channel will increase the inner volume W_0 and decrease the free volume outside of grains, thus the difference in conditions of burning tend toward pressure equalization. But the rate of burning inside of channels will prevail over the rate of burning on the surface of the grains.

Thus the presence of narrow and long channels in powder unavoidably creates the conditions of non-uniformity

of burning in channels and over the surfaces of grains. Thus non-uniformity is the main cause of these abnormal curves (Γ, ψ) of the progressiveness which were presented in Figs. 48, 49, 52 and 53.

The increase in Δ does not affect $\bar{z}'' = \frac{4}{\alpha}$ but \bar{z}' will be increased and the ratio $\frac{\bar{z}''}{\bar{z}'}$ will be decreased approaching 1. All the experiments show that the curves $\Gamma(\psi)$ at small Δ are more degressive.

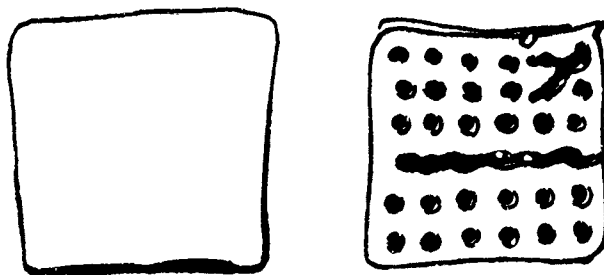


Fig. 69 - Burning of Kisnemsky's powder with very narrow channels.

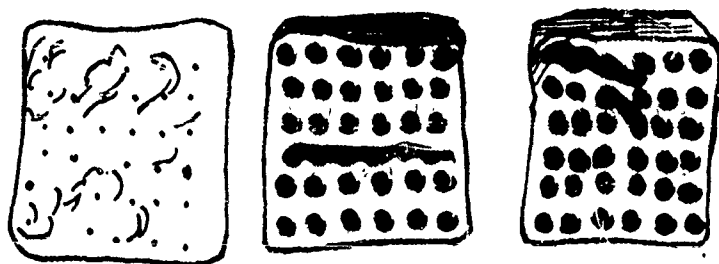


Fig. 70 - Burning of Kisnemy's powder with very narrow channels.

The presence of a marked increase of the pressure in the very narrow and long channels of the Kisnemy's powder is shown in Fig. 69 and Fig. 70 presenting photograph pictures of the incompletely burned grains thrown out of the gun during the actual firing. On the left parts of both pictures are shown unburned grains with almost invisible small square perforations (0.1 - 0.2 mm). At the right parts are shown incompletely burned grains with enlarged and burned through channels which are almost cylindrical in form.

3.4 How the shape of curve (Γ, ψ) is affected by the irregularities of burning of the multiperforated powders. Let us denote:

S' = the outer surface of the burning grain.

S'' = the total surface of channels of a grain.

$S = S' + S''$ = total surface of a grain.

Λ_1 = the initial volume of grain.

$u' = u_1 p'$ = rate of burning on the outer surface of grain. (p' is recorded by the crusher).

$u'' = u_1 p''$ = rate of burning inside of channels.

Let us assume that u' and u'' at any moment do not vary from point to point over their surfaces, i.e., u'' is the same in all channels and u' is the same over the whole outer surface. The first one (I) is the case of determining the numerical value of the function $\Gamma_I(\psi)$ - or the ordinates of the curve of the progressiveness corresponding to the geometric law - with constant rate of burning over the whole surface of grain.

The second case (II) is the case of determining the numerical value of the function $\Gamma_{II}(\psi)$, or the ordinates of the curve of the progressiveness corresponding to the actual physical burning taking place with different rates of burning in channels and outside of channels.

The general form of the function Γ is this:

$$\Gamma = \frac{1}{\rho} \cdot \frac{d\psi}{dt}$$

We are interested in: $\Gamma_I = \frac{1}{\rho'} \cdot \left(\frac{d\psi}{dt}\right)_I$

and in: $\Gamma_{II} = \frac{1}{\rho''} \cdot \left(\frac{d\psi}{dt}\right)_{II}$

Crushers are registering the outside pressure p' :

$$\text{Case I: } u'' = u' = u, \rho' : \left(\frac{d\psi}{dt}\right)_I = \frac{S}{\lambda_1} u' = \frac{S' + S''}{\lambda_1} u'; \quad \Gamma_I = \frac{1}{\rho'} \cdot \frac{S' + S''}{\lambda_1} u, \rho'$$

$$\text{or: } \Gamma_I = \frac{S' + S''}{\lambda_1} u.$$

$$\text{Case II: } u'' > u'; \rho'' > \rho'; \left(\frac{d\psi}{dt}\right)_{II} = \frac{S u' + S'' u''}{\lambda_1} = \frac{S' + S'' \frac{u''}{u'}}{\lambda_1} u'$$

$$\text{or: } \Gamma_{II} = \frac{S' + \frac{\rho''}{\rho'} S''}{\lambda_1} u,$$

The only difference in the analytical expressions of Γ_I and Γ_{II} is the factor $\left(\frac{\rho''}{\rho'}\right)$ multiplied by S'' , which means that Γ_{II} has its distinguishing features in the increase of the value of total surface of all channels which is now not S'' but $\left(\frac{\rho''}{\rho'} S''\right)$.

Thus in actual burning the powder acts as if the total surface of its channels were increased in the ratio of $\frac{\rho''}{\rho'}$. Therefore in the burning of a powder there is

some non-uniformity and the gas pressure and rate of burning inside of channels are greater than on the outer surface. Then at a given ψ the intensity of gas formation, i.e., the function Γ_H is greater than Γ_I , calculated under the assumption of uniform burning.

The value of ratio $\frac{u^*}{u} = \frac{p^*}{p}$ will affect the difference in intensities of gas formations in the real burning process and in the "geometric" description of this process. With the burning the diameter of a channel is increased and the ratio $\gamma = \frac{a}{d}$ is decreased and ratio $\frac{\gamma''}{\gamma}$ together with $(\frac{p^*}{p})$ will also be decreased, which means that the curves Γ_H and Γ_I will run closer and closer to each other.

Thus in the case of real burning in a closed vessel of a progressive powder with the narrow channels, the intensity of gas formation in the beginning will be markedly higher than is prescribed by the geometric law and the ordinates of curve $\Gamma_H(\psi)$ will be much higher than the ordinates of the theoretical curve. As the burning proceeds this difference in ordinates will be reduced and the actual intensity will be closer to the theoretical one. In other words, during the whole process of burning of a progressive powder the value of the function $\Gamma(\psi)$ will diminish and actual burning will be degressive.

The narrower are the channels and the greater their number, the greater will be the ratio $\frac{S''}{S}$ and the real burning will not be uniform at all.

Thus the powder seemingly progressive as judged by its form, as is the Kisenemsky's powder, in practice will burn markedly degressively.

3.5 Burning of the powder with narrow channels during the actual firing. It follows from the experiments that the degressiveness of the curves $P(\psi)$ is decreased by the increase of their parameter Δ .

This fact is very important for the actual firing in which the parameter Δ is decreased with the shot travel in the bore of a gun. The actual firing takes place at Δ as high as 0.50 to 0.70 and this Δ is decreased with the motion of the projectile. We have seen already in the physical theory of the burning process that with decreasing Δ the ratio $\frac{\gamma''}{\gamma'}$ is increased, i.e., the intensity of gas formation within the channels of grains becomes larger than the intensity of gas formation outside the grains. For the 7 perforation grains at $\Delta = 0.20$ $\gamma'' = 70 \gamma'$ and the curve $P(\gamma')$ is degressive; when $\Delta = 0.70$, we will have $\gamma'' = 8 \gamma'$ which means a considerable levelling in conditions existing

within the grains and outside of them and if $\Delta = 0.70$ could be kept constant, then the burning will proceed under more favorable uniform conditions.

Since $\Delta = \frac{\omega}{W_0 + 32}$ is continually decreased with the increase of l - shot travel in bore - we will have the ratio $(\frac{f''}{f})$ continually increased and the intensity of gas formation will also be increased with the increased progressiveness of burning.

Thus we arrive at the conclusion that our analysis of the burning process in the manometric bomb cannot be completed with the results obtained using just one value of

Δ . Our curve $f(\psi)$ must be constructed as a result of a series of curves with various parameters $\Delta : f(\psi, \Delta)$

In other words Δ itself must be treated as a variable.

The results obtained from the experimental curves

$f(\psi)$ for several Δ should be put through the interpolation and extrapolation procedures, and only then may we have a comprehensive picture of the real process of burning during the firing with Δ continually varying with the motion of a projectile along the bore of a gun. Thus the final one curve $f(\psi, \Delta)$ will represent a summary of results of all other curves as its components.

Fig. 71 shows a summary $\Gamma(\psi, \Delta)$ (in solid line) with the variable Δ for five partial curves (in dotted lines) constructed at various Δ 's: $\Delta = 0.65$; $\Delta = 0.40$; $\Delta = 0.25$; $\Delta = 0.15$; $\Delta = 0.05$. This summary curve $\Gamma(\psi, \Delta)$ may be distinctly different from each of its components. For example Fig. 71 shows the curve

$\Gamma(\psi, \Delta)$ with its variable Δ as a distinctly progressive curve which is obtained when the initial density of loading was $\Delta = 0.65$. Fig. 72 shows another $\Gamma(\psi, \Delta)$ for the case of a maximum density of loading $\Delta = 0.40$ and here we have $\Gamma(\psi, \Delta)$ as a markedly degressive curve with its variable density of loading. In firing practice we have a case in which the multiperforated Kisnemy's powder (with 36 perforations) on firing with a high density of loading, produced better results than the results of an ordinary strip powder (the same muzzle velocity at a lower p_m); in another case of firing from another gun with the lower density of loading, Kisnemy's powder was markedly worse than a strip powder (the same U_0 at a higher p_m)

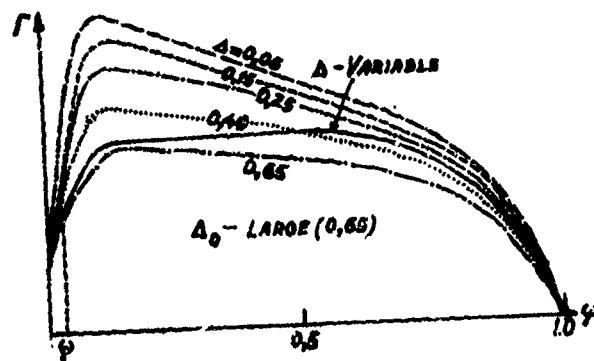


Fig. 71 Δ summary curve (Γ, ψ) in solid line at the initial $\Delta = 0.65$.

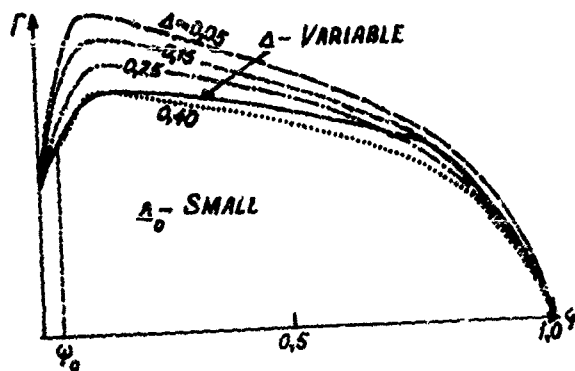


Fig. 72 Δ summary curve (Γ, ψ) in solid line at the initial $\Delta = 0.40$.

The larger Δ is, the more uniform are the conditions of the burning within the channels of grains and outside of grains; and the actual burning more and more approaches the burning prescribed by the geometric law.

Only by taking into consideration the totality of various factors of loading and firing conjointly affecting the process of burning, it becomes possible by the application of the theory of non-uniform burning to arrive at the correct conclusions concerning the actual burning of a powder in the bore of a gun during the firing.

Only this theory of the non-uniform burning gave the principal rules governing the burning within the narrow and long channels in powder grains and only this theory gave the sound explanation of the unsatisfactory progressiveness of Kienemsky's powder.

Chapter 4. - The Application of the Integral Diagrams.

4.1 The impulse of the powder gases as a characteristic of the powder burning. From the pressure curve $p(t)$ as a result of the experiment with the manometric bomb we also have $\Gamma = \frac{1}{\rho} \cdot \frac{d\psi}{dt}$ as the experimental characteristic of progressive burning, which can be constructed as $\Gamma(t)$ as well as $\Gamma(\psi)$. In the same way we find $\int p dt = I$ which is the impulse of the gas pressure. This impulse also can be considered as $I(t)$ or $I(\psi)$.

The function Γ has already been considered in its general application as an analyzer of the process of burning disclosing the influences of various factors affecting this function Γ . The integral curve $I(\psi)$ is another characteristic of the burning process, also affected differently by different factors of the burning process as well as of the nature of the powder itself.

From $I = \int_0^t p dt$, it follows: $\frac{dI}{d\psi} = \rho \frac{dt}{d\psi} = \frac{1}{\Gamma} = \tan \beta$ where β is an angle between the tangent line to the curve $I(\psi)$ and the horizontal axis, Hence: $\Gamma = \cot \beta$ (See Fig. 73.)

Since at the progressive burning Γ is increased and at the degressive burning Γ is decreased, we will have

that at the progressive burning $\frac{dI}{d\psi}$ is decreased and at the degressive burning $\frac{dI}{d\psi}$ is increased, i.e., the curve $I(\psi)$ may also give us an indication of the progressiveness of a powder.

Fig. 74 and Fig. 75 present $I(\psi)$ and $I'(\psi)$ determined for two different cases - namely the case of a weak igniter (Fig. 74) and that of a strong igniter (Fig. 75). In the case of a weak igniter the curve $I(\psi)$ at the beginning runs higher than $I(\psi)$ for the stronger igniter and the point of inflexion (a) corresponds to the "hump" of $I'(\psi)$ - point a'.

At the initial stage when the igniter's work is so important for the building up the curve $I(\psi)$, it is advisable for the experiments in the bomb to take the igniter pressure equal to the igniter pressure which is expected to be used in the actual firing.

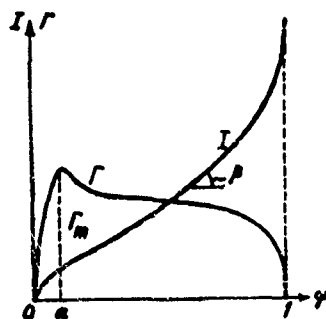


Fig. 73 Curves $I(\psi)$ and $\Gamma(\psi)$

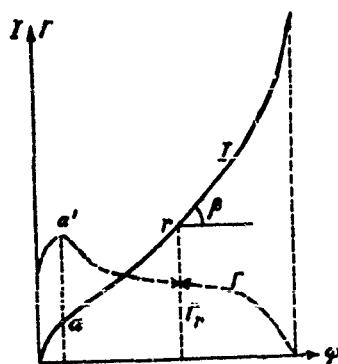


Fig. 74 Curves $I(\psi)$ and $\Gamma(\psi)$ -
- case of a weak igniter.

We have (44): $I_K = \frac{e_1}{u_1}$ and: $I = \frac{e}{u} = \frac{e_1}{u_1} \cdot \frac{e_2}{e_1} = I_K \cdot Z$

which shows that I is proportional to Z and therefore the curves $I(\psi)$ and $Z(\psi)$ are analogous. We have already the curves $\psi(Z)$ on the Fig. 25 or Fig. 35 which easily can be transformed in curves $Z(\psi)$.

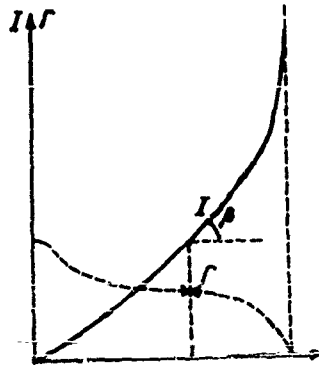


Fig. 75 Curves $I(\psi)$ and $\Gamma(\psi)$ -
- case of a strong igniter.

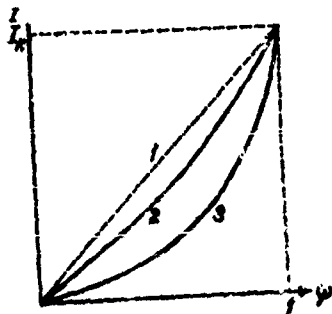


Fig. 76 The relative impulse $\frac{I}{I_K}$ as a function of ψ .

Fig. 76 shows the curve $\frac{I}{I_K}(\psi)$ at the same $\bar{I}_K = \frac{e_i}{u_i}$ for three different powders: 1) tubular powder; 2) strip powder, 3) cubes.

The larger the web $2e_i$ of a powder at a given u_i , the higher are the ordinates of (I, ψ) ; the higher is u_i at a given web, the smaller are the ordinates of (I, ψ) .

4.2 The application of $\int_0^t p dt = I$ for calculation of the rate of burning u_1 . The rate of burning u_1 at $p = 1$ is calculated from:

$$u_1 = \frac{e_1}{\int_0^{t_K} p dt} = \frac{e_1}{\int_0^I p dt} = \frac{e_1}{I_K}$$

If the ignition is instantaneous and if the web of powder is strictly constant or has a definite average value for the whole charge, then the above formula can be directly applied.

But the powder web is never constant even over a single strip in the powder charge. And the burning in the manometric bomb gives results related to the end of the burning of the elements with the maximum sizes of their webs. If, by the actual measurement we will establish a reliable average value of the web e_0 , then this web should be used for the construction of the curve:

$$\int p dt = f(\psi, e_0) \quad . \quad \text{See Fig. 77. And this integral}$$

$\int p dt$ should be taken according to the average value of e_0 , i.e., $\int p dt = I_{\text{aver}}(e_0)$.

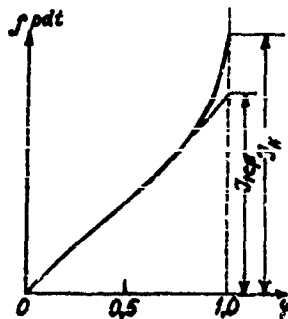


Fig. 77 Taking an average $(I_L)_{\text{aver}}$ at the figure
 $I_{L \text{ op}}$

The last part of curve $I(\psi)$ for ψ approaching 1.0 has a very steep rise corresponding to the burning of the last remnants of maximum webs. At the point $\psi = 0.9$, the curve should be prolonged tangentially up to intersecting the last ordinate corresponding to $\psi = 1$. This intersection will mark the average value of $(\int_0^{\psi} p dt)_{\text{aver}}$ corresponding to the average web $z = z_0$, and the above formula for u_1 will be rewritten: $u_1 = \frac{e_0}{(I_L)_{\text{aver}}}$.

In the cases with the weak igniters at the small initial values of $\psi < 0.10$, the separate curves are likely to be unduly diverse, then the following method

will bring more reliable results.

For a given powder, knowing its dimensions, we may find the values χ_0 and λ for short tubes, stripes or plates and χ_0, λ and μ for bars and cubes, then by using the formula: $\psi = \chi_0 \chi + \chi_0 \lambda \chi^2$ we calculate χ for $\psi = 0.1$ and for $\psi = 0.9$. Then we find $e_{0.1}$ and $e_{0.9}$ from the relationships: and

$$e_{0.1} = e \cdot \chi_{0.1} \quad \text{and} \quad e_{0.9} = e \cdot \chi_{0.9}$$

$$\text{Hence: } u_1 = \frac{e_{0.9} - e_{0.1}}{\int_{0.1}^{0.9} p dt}$$

where $\int_{0.1}^{0.9} p dt$ is taken from the Fig. 78.
(using the interval between $\psi = 0.1$ and $\psi = 0.9$)

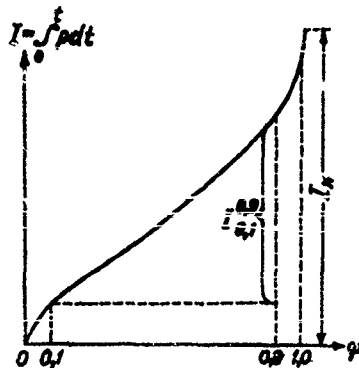


Fig. 78 Evaluation of u_1 in case of a weak igniter pressure.

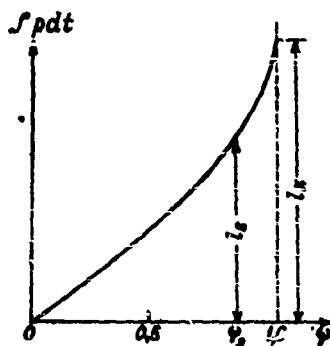


Fig. 79 Evaluation of u_1 for the progressive powder.

If we have to deal with the progressive form of a grain, then assuming the burning prescribed by the geometric law we will calculate ψ_s corresponding to the moment of the beginning of fragmentation and from the curve

$\int p dt = f(\psi)$ we will take (see Fig. 79.) $I_s = \int_0^{\psi_s} p dt = F(\psi_s)$; then assuming that up to this moment the

average web $(2e_1)_{\text{aver.}}$ will be burned out, we will have

u_1 from the formula:

$$u_1 = \frac{(e_1)_{\text{av.}}}{I_s}$$

We should not forget that powders with narrow channels are burning with different u_1 within the channels and on the outer surfaces of grain, therefore, the calculated u_1

in fact being affected by Δ can only be used conditionally and gives only comparative results at a given Δ .

4.3 Integral curves used as a criterion for checking this law of the rate of burning. From the formula $\int_0^{t_k} p dt = \frac{e_i}{u_i}$, it follows that the impulse $\int_0^{t_k} p dt$ is not affected by the density of loading, but that this is true only as far as we have assumed that the law of the rate of burning has the form of: $u = u_1 p$.

If the law of the rate of burning is assumed to be $u = Ap^y$ or $u = ap + b$, we will find other formulas for the impulses:

$$1. \text{ For the law: } u = ap + b = \frac{de}{dt}$$

we have: $de = ap dt + b dt$

$$\text{hence: } e_i = a \int_0^{t_k} p dt + b t_k$$

$$\text{and } \int_0^{t_k} p dt = I_k = \frac{e_i}{a} - \frac{b}{a} t_k$$

Since $t_k = 2,303 \tau \log\left(\frac{p_m}{p_0}\right) \dots (40)$ and $\tau = \frac{e_i}{u_i} \cdot \frac{1-\alpha\Delta}{f\Delta}$

(37) we infer that t_k is decreasing with

increasing Δ , i.e., I_k is increased with Δ .

2. For the law: $u = Ap^v = \frac{de}{dt}$; $de = Ap^v dt$

$$\text{or: } \int_0^{t_k} de = e_k = A \int_0^{t_k} p^v dt = A \int_0^{t_k} \frac{p^{v+1}}{p^{v+1}} p^v dt = \frac{A}{(p^{v+1})_{\text{av}}} \int_0^{t_k} p^{v+1} dt = \frac{A}{(p^{v+1})_{\text{av}}} I_k$$

$$\text{and } I_k = \frac{e_k}{A} (p^{v+1})_{\text{av}}$$

where $(p^{v+1})_{\text{av}}$ is an average value on the interval of t from 0 to t_k . Hence we see that I_k is increased with p and therefore with Δ . Therefore we may say that: (1) if I_k is independent from Δ , our law of burning is $u = u_0 p$ (2) if I_k is increased with Δ , our law of burning can be: $u = Ap^v$ or: $u = ap + b$

In other words, if with the increased Δ , our integral curves $\int p dt = f(\psi)$ are all identical, then we have to deal with the law of burning $u = u_0 p$; if our integral curves (I, ψ) with increased Δ are represented by the set of diverging curves all beginning in the origin ($\psi = 0$) with higher curves corresponding to higher

Δ , the law of burning must be: $u = Ap^v$ or $u = ap + b$.

4.4 Practical use of the integral curves for the verification of the law of the rate of burning. Special experiments were conducted by Prof. M. Serebryakov in 1924-25 to establish a reliable law of the rate of burning, under simpler conditions, when powders have no long and narrow channels (strips, short tubes).

For the first experiment the strip powder $C\pi$ ($2\phi_1 = 1$) was used; this particular sort is very uniform in the thickness of its strips; the experiments were made with the three densities of loading: $\Delta = 0.159$; $\Delta = 0.209$ and $\Delta = 0.259$ and with a very strong igniter ($p_B = 120 \text{ kg/cm}^2$).

The curves (I, ψ) obtained for each density of loading were marked by 1, 2, and 3 and are shown on left side (Fig. 80).

For the second series of 3 experiments one and the same $\Delta = 0.209$ was used - these three curves are shown on the right side of Fig. 80. As is clearly seen, there is no difference whatsoever between these groups of curves. Thus a complete independence of I_k from Δ is established, and the conclusion is, that this pyroxylin strip powder has its law of the rate of burning in the form of $u = u_1 p$.

The following three series of experiments have been designed, having in view a more varied material in sort of powder as well as in the sizes of the webs.

1. Powders with the simple degressive forms - strip, cord, short tube with a wide channel: they all are burning in such a way that from $\Delta = 0.12$ up to $\Delta = 0.25$, their impulses are not affected by Δ ; their integral curves $I(\psi)$ are almost identical (Fig. 81 and Fig. 82) at the ignition with its pressure $p_B = 100$ to 150 kg/cm².

Tubular powders having the fixed (trotyl + pyroxylin) solvent have their $\Gamma(\psi)$ curves without any pronounced hump and their integral curves (I_k, ψ) are concurrent straight lines from $\psi = 0$ up to $\psi = 0.90$ to 0.95 . (Fig. 81). Tubular powder having volatile solvent always have $\Gamma(\psi)$ curves with humps but their integral curves are almost identical, as shown in Fig. 82.

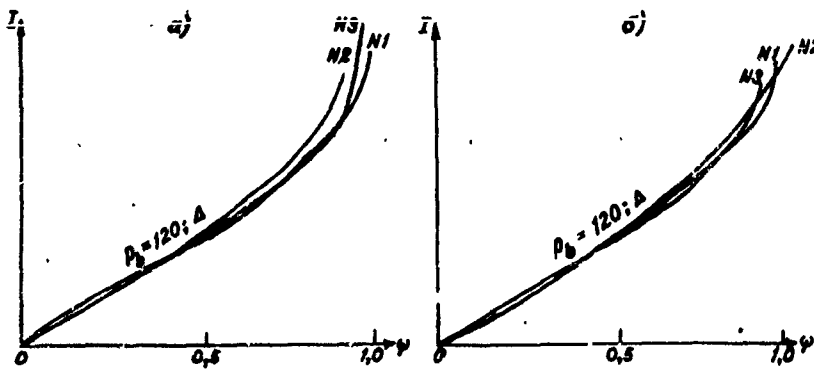


Fig. 80 Integral curves (I, ψ) at left (a) with three different Δ (0.159; 0.209; 0.259), $p_B = 120 \text{ kg/cm}^2$ at right (b) with one $\Delta = 0.209$; $p_B = 120 \text{ kg/cm}^2$.

Thus a general conclusion concerning tubular pyroxylin powders and powders with the fixed solvent in form of short tubes is, that for Δ varying from 0.15 to 0.25, the same law of rate of burning is valid: $u = u_{1p}$.

2. The same powders of simpler forms without narrow channels with the low density of loading $\Delta < 0.10$ are burning in such a way that their impulse I_k is decreased with the decrease in Δ which means that at the law: $u = u_{1p}$ the rate of burning u_1 will be increased with the decreasing Δ .

Fig. 83a and Fig. 83b show the character of varying in the ordinates of the integral curves $\int_{\psi=0.05}^{\psi=0.75} p dt$ for the

powder CΠ ($2 e_1 = 1 \text{ m/m}$) and variations in u_1 from 0.120 at $\Delta = 0.02$ to $u_1 = 0.077$ at $\Delta = 0.12$;

at the higher Δ both I_k and u_1 stay constant. The same even more pronounced effect is shown in Fig. 84

for the powder with $2 e_1 = 2.4 \text{ m/m}$: at $\Delta = 0.12$ to

$\Delta = 0.22$ the integral I_k is constant; at $\Delta = 0.02$ the integral I_k drops to $1/4$ of its former value. Such a sharp drop in value of $\int p dt$ at small Δ is observable only for the web $2 e_1 > 0.7$ to 1 m/m .

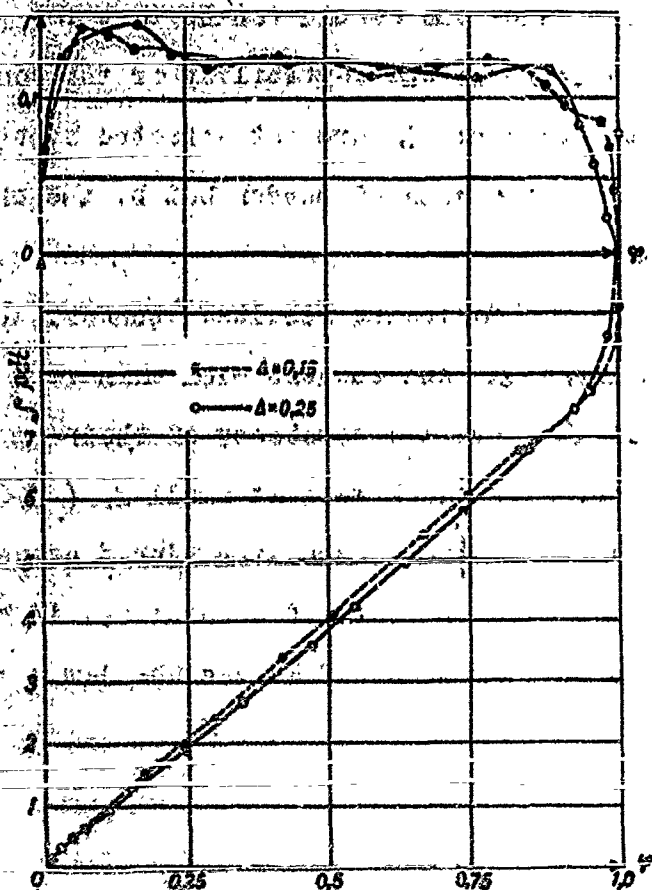


Fig. 81 Curves $f(\psi)$ and (f_{pdt}, ψ) for $\Delta = 0.15$ and $\Delta = 0.25$. Tubular powder with the fixed solvent.

3. For fine pyroxylin powders, in the shape of small thin plates, I_k does not change at the varying Δ from 0.157 to 0.020. Hence the conclusion is that for pyroxylin powders of simpler forms the variability or the constancy of $\int p dt$ at the varying Δ are not affected by the chemical nature of the mass of powder but by the character of the burning.

Thus we have the following results: powders with large webs at large Δ and powders with thin webs at both large and small Δ have the constancy of their impulse $\int p dt$. Powders with thick webs at small Δ ($\Delta < 0.10$) have their impulses $\int p dt$ decreasing with decreasing Δ , which means that the rate of burning u_1 , in this case, must also be increased, if we use the law $u = u_1 p$.

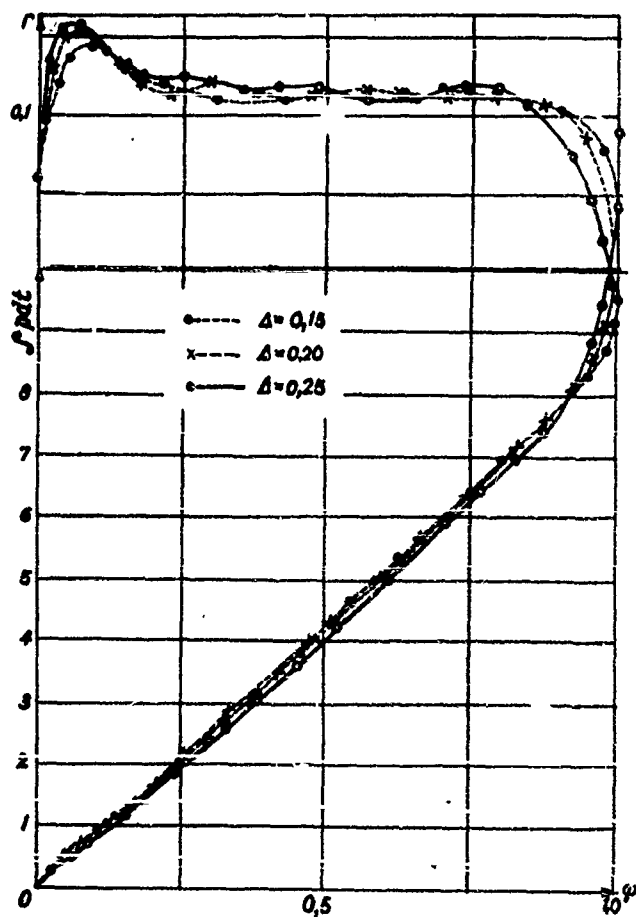


Fig. 82 Curves $\Gamma(\psi)$ and $(\int p dt, \psi)$ for $\Delta = 0.15$; $\Delta = 0.20$; $\Delta = 0.25$. Tubular powder with a volatile solvent.

What is the explanation of these results? The explanation is based on a very probable and natural assumption that at the slow burning of the thick powder in the beginning at the lower pressures the burning layers, despite their low thermal conductivity, are heated through by the hot gases and their reaction, i.e., their burning, like every other chemical reaction, will be accelerated with the corresponding decrease of Δ and of gas pressure with the decreased rate of shifting (u) of the burning layer inside of a grain and with the increased depth of heated layer with the increase of the temperature of these layers. A formal mathematical expression of the above physico-chemical scheme can be summarized in the geometric fact of the divergency of the integral curves $(\bar{I}_x, \bar{\psi})$ at various Δ which is an immediate result of the general transference of the observed situation from the province of the basic law $u = u_1 p$ to another law $u = \Delta p^\psi$ with $\psi < 1$.

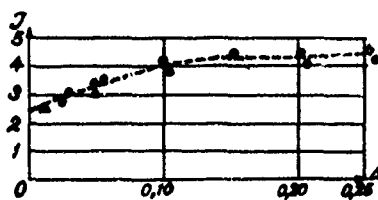


Fig. 83a $\int p dt$ as a function of Δ

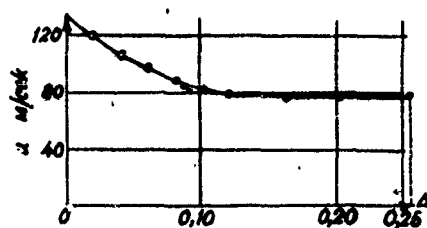


Fig. 83b u_1 as a function of Δ

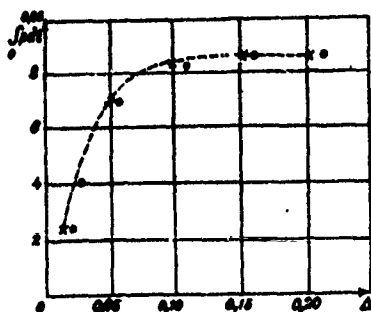


Fig. 84 $\int p dt$ as a function of Δ

Professor Serebryakov's experiments with the strip powder with the fixed solvent show that at $\Delta > 0.10$ and $p > 1000 \text{ kg/cm}^2$, the law is $u = u_1 p$, but for $\Delta < 0.10$ and $p < 800\text{--}1000 \text{ kg/cm}^2$, the law is $u = \Delta p^{0.83} = 0.240 p^{0.83}$.

In the same way experiments of Professor Pobedonostzev for the low pressures give the law $u = 0.063 p + 3$; u mm/sec and p kg/cm², and Professor Shapiro for the same case gives $u = 0.37 p^{0.7}$.

These formulas gave identical results for all p between 25 kg/cm^2 and 300 kg/cm^2 .

Thus a general resume is this: For the pyroxylin powders of simpler forms with fixed solvent (trityl + pyroxylin) at $\Delta > 0.10$ and pressures $p > 800 \text{ kg/cm}^2$, the law of the rate of burning must be assumed as $u = u_1 p$.

For the same powders at the pressures $p < 800 \text{ kg/cm}^2$ the law of the rate of burning is $u = \Delta p^\gamma$, $\gamma < 1$. (The higher is pressure, the closer γ is to 1.0).

This result means that the law of the rate of burning is not expressible in one and the same form for all different conditions of burning, but this form should be modified with the transition of the pressure from one range to another.

As was shown earlier the integral curves (I, ψ) for the pyroxylin multiperforated powders with the progressive forms of grains are running as a divergent set of curves, becoming almost parallel only for $\psi = 0.60$ to 0.65 . (Fig. 85 and 86). (The larger Δ , the higher is the curve).

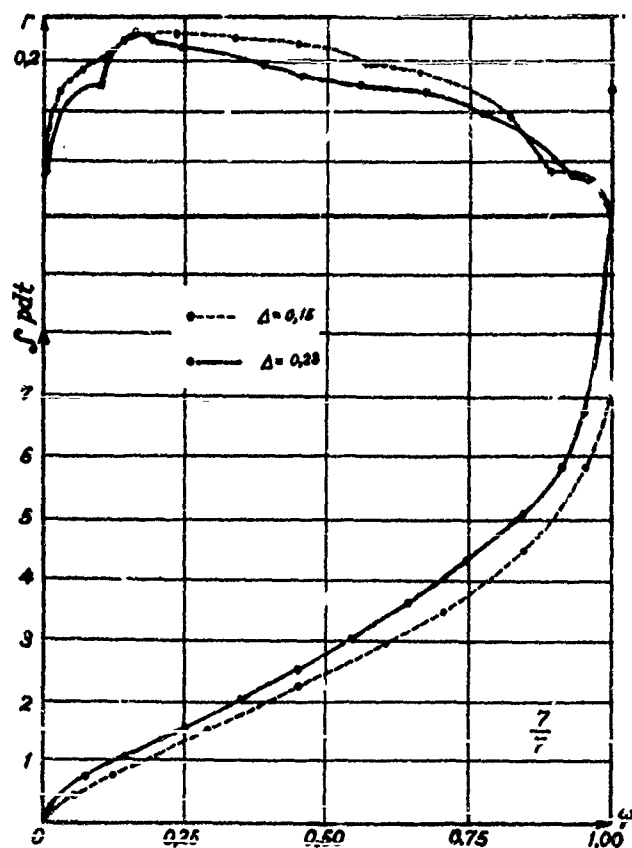


Fig. 85 Curves $(\int p dt, \psi)$ and (Γ, ψ) .
Powder 7/7 for $\Delta = 0.15$ and 0.23

As we know this divergency of $(\int p dt, \psi)$ curves leads to the acceptance of the law of the rate of burning in the form $u = \Delta p^\gamma$, with $\gamma < 1.0$. Professor Serebryakov's numerous experiments with a large number of different types of pyroxylin multiperforated powders (more than 100) gave for the 7 perforation grains the value of $\gamma = 0.83 \approx 5/6$.

Thus we have for the pyroxylin powders with the simple forms (strips, short tubes) of a grain for $\Delta > 0.12$; $u = u_{1p}$, and for the same pyroxylin powders with the narrow channels at the same $\Delta > 0.12$, we have $u = \Delta p^\gamma$, and the (I, ψ) curves are running as a divergent set with the higher curve having larger Δ .

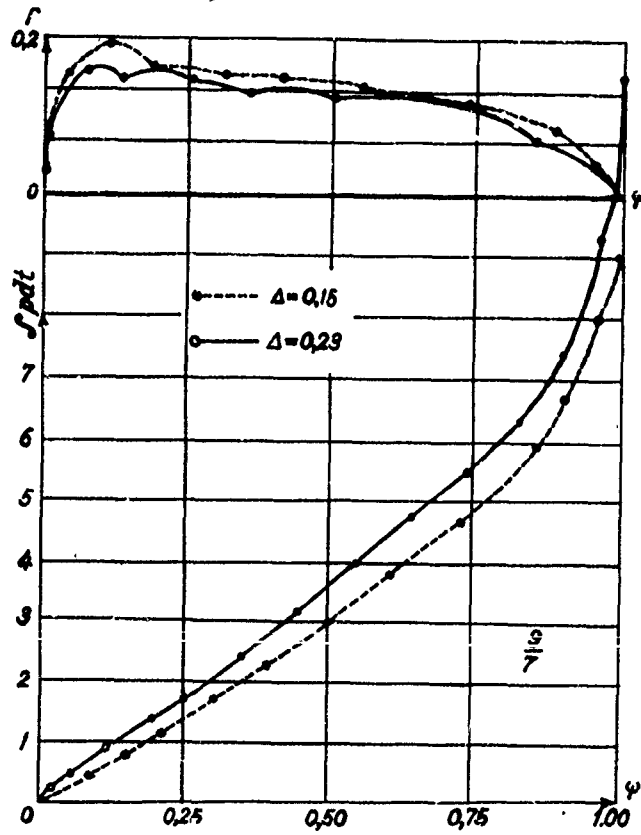


Fig. 86 Curves $(\int p dt, \psi)$ and (r, ψ)
 for the powder 9/7 $\Delta = 0.15$ and $\Delta = 0.23$.

These results which seem to be inconsistent will immediately be clarified on the basis of the theory of non-uniform burning, if we recall the property of the curves (Γ, ψ) to have their ordinates decreased by the increased Δ , but (Γ) geometrically speaking is a cotangent of the angle of a tangent line to the curve $(\int p dt, \psi)$ or: $\Gamma = \text{Cotang } \beta; \beta = \text{Arc Cotang} \left(\frac{dI}{2\psi} \right)$
 $I = \int p dt.$

Hence at the increasing Δ , Γ is decreased and the steepness of the $(\int p dt, \psi)$ curve is increased and these curves will be running higher and steeper in shape of a divergent set of curves. Thus at the law $u = u_1 p$, corresponding to the nature of a powder and loading conditions ($\Delta > 0.12$), the integral curves still are running as the divergent set, because of the non-uniform burning within the narrow channels at various

Δ and instead of the law $u = u_1 p$, we have in actual operation the law $u = A p^\gamma$ with $\gamma < 1$.

For the colloidal powders the law of the rate of burning is $u = u_1 p$. Here u_1 is a constant for the powders with the fixed solvent but for the ordinary pyroxylin and nitroglycerine powders u_1 is a variable during the first third of the burning process, where u_1 is affected

by the nature of powder and various conditions of burning. The integral curves in this case when u_1 is not constant still are running at various Δ as a convergent set. All the deviations from this norm in form of the divergency of curves ($\int p dt, \psi$) for the powders of simpler form with lower Δ can be explained by variations in the rate of burning u_1 caused by the heating through the layers of a grain at the slow burning.

The analogous divergency of the integral curves for the powders of the progressive form at larger Δ and an apparent deviation from the law $u = u_1 p$ are the results of the non-uniform distribution of pressure within the channels and on the outer surfaces of grains.

This apparent deviation from the law $u = u_1 p$ can be expressed in a purely formal way by the formula $u = \Delta p^\gamma$, but the law of the rate of shifting of burning surface into the depth of a grain still remains the same, $u = u_1 p$, where p can be varied over the whole surface and u_1 can be varied from one layer to another and affected by the temperature of the nearest burning surface. For 7 per foration grain powder the exponent $\gamma = 0.80$ to 0.83 and the coefficient Δ depend on the nature of the powder (percentages of nitrogen and volatiles.)

The above shown relationships and methods of pyrostatics enable us, from the experiments in the manometric bomb to make a complete analysis of the ballistic characteristics of a powder and its actual law of burning.

The ballistic characteristics "force" f , and co-volume ϕ can be determined in a bomb using two or three different Δ with 3 - 5 experiments for each Δ . The obtained values of p_m , f and ϕ are corrected by taking into account the losses through the walls of the bomb.

The rate of burning u_1 at the unit pressure, ($p=1$), is determined from the integral curve ($\int p dt, \psi$).

$$u_1 = \frac{(e_1)_{av}}{I_{av}} \quad \text{where } (e_1)_0 \text{ is an average web and } I_{av}.$$

is an average impulse (Fig. 77, 78 and 79.)

The actual law of burning is characterized by:

(1) the curve of the intensity of the gas formation

$$r = \frac{1}{p} \cdot \frac{d\psi}{dt} \quad \text{as a function of } \psi \quad \text{and as a function}$$

of t , and (2) the curve of the impulse $\int p dt$ as a function of ψ .

A specific form of the law of the rate of burning $u = u_1 p$, $u = A p^y$, or $u = a p + b$, is determined by the type of divergence or concurrence of the integral curves (I, ψ).

The curve (Γ, ψ) provides a method of analyzing the processes going on in the burning of powder. This curve makes possible the consideration of various factors which not long ago were left without evaluation (the process of the gradual inflammation, variation in the rate of burning, the effect of the phlegmatization, etc.)

In order to form our idea of the actual burning of a powder in a gun we still need the experiments conducted in a manometric bomb at various densities of loading. Hence we determine the influence of Δ on the variations in the progressiveness of burning. From comparison and analysis of this kind of data we arrive at a definite conclusion as to the burning of powder in the variable volume. Such is a general outline of the method of ballistic analysis of powder. Such a method which makes possible a taking into account various changes and factors, can be highly valuable at the powder plants. Having results obtained with the experimental powder in a manometric bomb, we can compare them with the results of a normal powder used in the field service and this comparison may lead to valuable more detailed knowledge of the experimental powder. Here is given the formula which may serve as a practical aid for utilizing the results of the ballistic analysis made in the laboratory

instead of more costly results of firing tests when it is desired to determine the weight of a charge of an experimental powder producing the same maximum pressure and the same muzzle velocity which are obtainable from a powder which is already used in service.

Notation: Powder adopted in service: ω' , f' , I_K'
and experimental powder: ω'' , f'' , I_K''

All six of these values are known from experiments with the manometric bomb.

Then we have:

$$\frac{\omega''}{\omega'} = \frac{\frac{f'}{f''} \cdot \frac{I_K''}{I_K'}}{1 + \frac{\Delta'}{\sigma} \left(\frac{f'}{f''} \cdot \frac{I_K''}{I_K'} - 1 \right)}$$

and here Δ' is a density of loading of a charge ω' .

In order to make use of only the most reliable part of the integral curve (I_K, ψ) we will take its values on the shortened interval of ψ starting at $\psi = 0.05$

and ending at $\psi = 0.75$. Thus we eliminate the uncertainties and non-uniformities associated with the action of not very strong igniters (pg smaller than 50 kg/cm²).

This formula gives a good approximation of the desired experimental weight of powder charge producing the same maximum pressure and muzzle velocity which are obtainable from the powder adopted in actual service.

Section IV - Physical Principles of Pyrodynamics

Chapter 1-

The firing process and its principal relationships.

Pyrodynamics is the study of the phenomena going on within the barrel of a gun during the firing; this study leads to the establishment of some definite relations between the loading conditions and various physico-chemical and mechanical processes constituting in their totality the firing of a gun. In the firing as in the process we observe a complex interdependence of many factors and elements. For example: the motion of a projectile depends on the gas pressure but this gas pressure depends on the powder burning as well as on the volume behind the moving projectile and this volume depends on the motion of a projectile.

The following periods can be noted in the process of firing:

1. The preliminary periods (static period, and forcing period - for details see Section XI). From the beginning of burning until the gas pressure becomes $p_0 = \frac{n_0}{s} \frac{\text{kg}}{\text{cm}^2}$

where n_0 is the force necessary for producing the complete engraving of the driving band at the full depth of rifling. The pressure p_0 is "the

forcing pressure (from $200 \frac{\text{kg}}{\text{cm}^2}$ to 500). See



Fig. 101. Schematic view of the driving band and rifles. During this period the projectile moves at the distance between the initial position of the rear edge of the driving band (point a) to the cross-section of the bore, where the full depth of rifling begins (point b). The end of this period is the moment t_0 .

2. The first period - is the period of burning of the powder charge. Gas pressure p varies from p_0 to the maximum pressure p_m and falls to p_k at the moment of the end of burning; at this moment the travel of projectile is l_k and its velocity v_k .

3. The second period - the period of the adiabatic expansion from the moment t_k to the moment t_2 when the bottom of projectile leaves the muzzle.

$$\text{From: } p \cdot S \cdot dl = d\left(\frac{mv^2}{2}\right) \quad \text{hence: } v_2 = \sqrt{\frac{2S}{m}} \cdot \sqrt{\int_0^{l_2} p \cdot dl}$$

$$\text{From: } p \cdot S = m \frac{dv}{dt} \quad \text{hence: } v_2 = \frac{S}{m} \cdot \int_0^{t_2} p \cdot dt$$

4. The third period - the period of the "after-effect".

At the end of this period $v_{\max.} > v_2$.

The principal phases of the firing process and their relationships.

1. The expanding powder gases are the source of the energy utilized or converted into necessary work and in pyrostatics we have the following relationships:

a. Gas formation as a function of the burnt fraction of grain: $\psi = \gamma z (1 + \lambda z + \mu z^2) = \gamma_1 z (1 + \lambda_1 z)$

here: $z = \frac{r}{r_0}$; $\psi = \frac{\Delta V_{\text{gas}}}{V_1}$ z is a relative burnt thickness.

ψ is a relative burnt volume.

b. Rate of burning: $u = u, p$

c. Rate of gas formation: $\frac{d\psi}{dt} = \frac{S_1}{A_1} \cdot \frac{S}{S_1} \cdot u, p = \frac{\gamma}{\gamma_1} \cdot \frac{S}{S_1} \cdot p$

Physical law of burning provides the relations:

$\psi = f(I)$; $I = F(\psi)$; $\frac{d\psi}{dt} = \Gamma \cdot p$, or: $\Gamma = \frac{1}{p} \cdot \frac{d\psi}{dt}$.

2. Transformation of Energy.

If: Q the amount of heat applied to the system

U the internal energy of the powder gases

ΣL total sum of all works produced by gases

and spent on the overcoming of resistances

A an inverse value of $E = 4270 \frac{\text{kg. dm.}}{\text{cal.}}$ (mechanical equivalent of heat), then we have: $Q = U + A \Sigma L$

3. Equations of motion: $p.s = m \frac{dv}{dt}$

$$ps = mv \cdot \frac{dv}{dl}$$

4. Equation of momentum: $mv + \mu U + MV = 0$

here: m - mass } of projectile
 v - velocity }

μ mass } of the
 U velocity } powder charge

M - mass } of the
 V - velocity } recoiling parts

5. Equation of the rotational motion:

r - lever arm of the rotating force

$r.N = J \cdot \frac{d\omega}{dt}$ here: N - rotating force

J - moment of inertia of projectile

ω - angular velocity; $\frac{d\omega}{dt}$ - angular acceleration

Chapter 2 - Energy balance during firing

1) $E_1 = 4270 \frac{\text{kg. dm.}}{\text{cal.}} \bar{C}_w T_1 \omega \psi \text{ kg. dm.}$ is the total amount of available energy when $\omega \psi \text{ kg.}$ of powder is burned at temperature T_1 and cooled down to the absolute 0° . 2) $E = 4270 \frac{\text{kg. dm.}}{\text{cal.}} \bar{C}_w T \omega \psi \text{ kg. dm.}$

is amount of energy not utilized yet after certain work has been done but cooling was not to 0° but to temperature $T < T_i$

Hence $(E_i - E)$ is the amount of energy spent on producing all the works, or: $E_i - E = 4270(T_i - T)\omega\psi c'_w$

where c'_w is a certain average specific heat at the interval from T_i to T .

Thus we have: $4270 c'_w (T_i - T) \omega \psi = \sum E_i$

where $\sum E_i$ is the total sum of works produced by the powder gas on firing including all the resistances involved. These works are as follows:

1. E_1 is the energy of the translational motion of the projectile measured by $(\frac{mv^2}{2})$
2. E_2 is the energy spent on the rotational motion of the projectile.
3. E_3 is the energy spent on the resistance of friction between the driving band and the surface of the bore (rifling included).
4. E_4 is the energy spent on the moving gases themselves and unburnt yet part of the powder.
5. E_5 is the energy spent on the moving of recoiling parts.

6. E_6 is the energy spent on the engraving of the driving band.

7. E_7 is the energy lost on the heating of the walls of barrel, of cartridge case and projectile.

8. E_8 is the energy lost through the leakage of gases.

9. E_9 is the energy spent on the overcoming of the air resistance within the bore and on the propelling this air out of the bore. The first five of these expenditures are all expressible in terms of E_1 or $\frac{mv^2}{2}$ as

as $\sum_i K_i \left(\frac{mv^2}{2}\right)$. E_6 and E_7 are usually accounted for not by the direct evaluations but by indirect comparative methods; E_8 and E_9 can be entirely omitted as negligible quantities.

Thus we have: $\sum_i E_i = \frac{mv^2}{2} (1 + K_2 + K_3 + K_4 + K_5) = \varphi \left(\frac{mv^2}{2}\right); \varphi > 1$.

In 1894, Prof. N. Zabudsky introduced the concept of the "effective mass" of a projectile which in the above notation will be φm and the factor φ is called "the coefficient of the effective mass" or "the coefficient accounting for the secondary works" as they are compared with the principal one taken as unity. Now the equation of the energy balance will be:

$$4270 C'_p T_1 \omega \psi - 4270 C'_w T \omega \psi = \varphi \left(\frac{mv^2}{2} \right) (\text{in kg.dm})$$

which means that the difference between the two thermal states of the powder gases is converted into the sum of the external works. The practical value of φ is between 1.02 and 1.20 and even larger.

The basic equation of Pyrodynamics.

From thermodynamics we have: $4270 [C_p - C_w] = R$
(constant of gases)

we rewrite it: $4270 = \frac{R}{C_p - C_w}$

$$\text{or: } 4270 C_w = \frac{R C_w}{C_p - C_w} = \frac{R}{\frac{C_p}{C_w} - 1} = -\frac{R}{\theta}$$

$$\text{where: } \theta = \frac{C_p}{C_w} - 1 = K - 1$$

$$\text{here: } K = \frac{C_p}{C_w}$$

is the exponent of the adiabatic curve;

$$\theta \sim 0.2 ; C_p = A_2 + BT ; C_w = A_1 + BT$$

Then the equation of the energy balance will be:

$$\frac{R}{\theta_0} T_1 \omega \psi - \frac{R}{\theta_0} T \omega \psi = \varphi \frac{mv^2}{2} \dots (52)$$

Here θ_0 is a certain average value of θ for temperature $T_0 = \frac{T_1 + T}{2}$

$$\text{Here: } R T \omega \psi = p W = p [W_0 + s \ell - \alpha \omega \psi - \frac{\omega}{2} (1 - \psi)] = p (W_0 + s \ell)$$

for the moment when $\omega \psi$ of powder is burnt and W_0

is a free volume of the chamber at this moment. Strictly speaking this relationship exists for the static gaseous process but we assume that this relationship exists also in our case, when the gas formation proceeds under varying conditions of pressure as well as of volume, and the equation of the balance will be rewritten:

$$\frac{R}{\theta_0} T_1 \omega \psi - \frac{p}{\theta_0} (W_\psi + s\ell) = \varphi \cdot \frac{mv^2}{2}$$

Remembering, that $RT_1 = f$ finally we have:

$$\frac{f}{\theta_0} \omega \psi - \frac{p(W_\psi + s\ell)}{\theta_0} = \varphi \frac{mv^2}{2} \dots (52')$$

This is the basic equation of pyrodynamics given by

Resal in 1864 in another form:

$$ps(\ell_\psi + \ell) = f\omega\psi - \frac{\theta_0}{2} \varphi mv^2 \dots (53)$$

here W_ψ was replaced by $s\ell_\psi$ and ℓ_ψ is the effective length of the free volume of the chamber at the moment when $\psi\omega$ of powder is burnt (ℓ_ψ is a function of ψ).

Here we have the following 4 variables involved in the process of burning as well as in the process of motion of the projectile: burnt fraction ψ , pressure p , travel of projectile ℓ and its velocity v .

A factual independent variable is ψ but all 4 variables are mutually interdependent.

Additional equations mentioned above (relationships in

the process of burning and equations of motion of the projectile) must be used for establishing definite relationships between our four basic variables.

Comparing

$$p = \frac{f\omega\psi - \frac{1}{2}\varphi m v^2}{W} \quad \text{from (52')}$$

$$\text{with : } p = \frac{f\omega\psi}{W_\psi} \quad \dots (13) \text{ given in pyrostatics}$$

we immediately see that at the same loading conditions the pressure in the gun with moving projectile all the time is lower than it is in the constant volume of a bomb.

Chapter 3 - The study of the principal relationships.

1. The principal characteristics involving the evaluations of the energy.

The equation of the balance (52) written for $\psi = 1$ (adiabatic process) gives: $\frac{f\omega}{\theta} - \frac{RT\omega}{\theta} = \varphi \frac{mv^2}{2}$, here: $f = RT$,

$$\text{or: } \varphi \frac{mv^2}{2} = \frac{f\omega}{\theta} \left(1 - \frac{T}{T_0}\right) \quad \dots \dots \dots (54)$$

Thus the maximum of the left part can be obtained at

$T = 0^\circ$ i.e. when the cooling of the gases will reach the absolute zero then the velocity v will reach its ideal limit (v_{max} .)

$$\frac{\varphi m}{2} (v_{am})^2 = \frac{f\omega}{\theta} \dots (55)$$

or:

$$v_{am} = \sqrt{\frac{2}{\varphi} \cdot \frac{f}{\theta} \cdot \frac{\omega}{m}} = \sqrt{\frac{2}{\varphi} \cdot \frac{f}{\theta} \cdot \frac{1}{\frac{m}{\omega}}} \dots (56)$$

The value $f\omega$ is called "the total reserved energy" in ω_{kg} of powder, and $\frac{f}{\theta}$ is called the potential of $1kg$ of powder. Even if this potential cannot be practically used but a practically important result is that by increasing f of powder or by decreasing θ we always can raise the efficiency of powder.

Since $f = \frac{R W_1 T_1}{273}$ we can by increasing W_1 or T_1 have a powder with a higher f .

From expression for $\theta = \frac{C_p}{C_w} - 1 = \frac{C_p - C_w}{C_w} = \frac{(A_1 + A_2 T) - (A_2 A_1 T)}{A_2 + B_1 T} = \frac{1}{A + B T}$

where: $A = \frac{A_2}{A_1 A_2}$

and $B = \frac{B_1}{A_1 A_2}$

During the firing θ is varied with T and since this variation is very limited it is advisable to use an average $\bar{\theta}$, evaluated as follows:

$$\bar{\theta} = \frac{1}{T - T_i} \int_{T_i}^T \frac{dT}{A + BT} = \frac{A_1 - A_2}{T - T_i} \int_{T_i}^T \frac{dT}{A_2 + B_1 T} = \frac{2.303(A_1 - A_2) \log \left(\frac{A_2 + B_1 T}{A_2 + B_1 T_i} \right)}{B_1(T - T_i)}$$

Table 20 gives the variations with temperature of $\bar{\theta}$ for the pyroxylin powders

Table 20

$(\frac{T}{T_i}) \rightarrow$	1.0	0.90	0.80	0.70	0.60	0.50	0.10
$T_i, K \rightarrow$	2700	2430	2160	1890	1620	1350	270
$\bar{\theta} \rightarrow$	0.185	0.190	0.196	0.202	0.208	0.215	0.252

In most practical cases $\frac{T}{T_i} \sim 0.70$ and $\bar{\theta} = 0.20$. It is advisable to use two values for $\bar{\theta}$: one during the first period when the cooling of the gases is not so great and another $\bar{\theta}$ during the second period when the cooling is more pronounced.

It is not amiss to point out that the coefficients A_1, A_2 and B_1 in the linear expressions for C_p and C_w are not the same in the works of various authors and besides this not all authors use the linear forms for thermal variations of C_p and C_w .

The linear form gives a good approximation for C_p and C_w only within the range $3000^\circ - 1500^\circ$ of

temperature; for lower temperatures the deviation from the linear forms becomes more significant.

The efficiency of the work done by the powder gases is the ratio of the useful work obtained to the total amount of energy available in a given powder charge; thus the efficiency $\eta_0 = \frac{m \psi_0^2}{2f\omega} = \frac{\theta m \psi_0^2}{2f\omega}$ varies between 0.20 to 0.33. Other authors assume:

$$\eta'_0 = \frac{\psi_0^2}{(\psi_{\text{lim}})^2} = \frac{\theta m \psi_0^2}{2f\omega} = \left(1 - \frac{T}{T_1}\right)$$

but $\left(1 - \frac{T}{T_1}\right)$ is the "economy co-

efficient" of the Carnot cycle in case of the ideal gas working without any "secondary works" and resistances.

Thus the introduction of the factor φ cannot be justified in the evaluation of the efficiency of work done by the powder gases. Sometimes the total amount of available energy is expressed by $\Pi' = E Q$

where Q is the amount of heat determined in the experiment in the bomb with the burning powder cooled down to temperature 15°C (or 288° absolute), whereas $\left(\frac{f}{\theta}\right)$

gives the amount of work produced by gases during their cooling down to 0° (absolute). Hence:

$$E Q = \frac{f}{\theta} \left(1 - \frac{288}{T_1}\right) \sim 0.9 \left(\frac{f}{\theta}\right)$$

If we are given the value of the efficiency it is necessary to know definitely whether this efficiency is determined in respect to $\left(\frac{f\omega}{g}\right)$; then its real value will be smaller or if this value is determined in respect to $E Q$, then the efficiency will be higher.

The efficiency of a unit of the weight of charge ω is

$$\eta_{\omega} = \frac{(mv^2)}{\omega} \cdot \frac{Kg \cdot dm}{Kg}$$

the value of η_{ω} is largely affected by the relative length of the bore, by the size of web of powder and the length ℓ_k of the projectile travel at the moment of the end of burning. For not too lengthy guns of

medium caliber: $\eta_{\omega} = 1200000 - 1400000 \frac{Kg \cdot dm}{Kg}$
 or: $120-140 \frac{cm \cdot m}{Kg}$

while for small arms $\eta_{\omega} = 100-110 \frac{cm \cdot m}{Kg}$

In case of howitzers using full charge $\eta_{\omega} = 150-160 \frac{cm \cdot m}{Kg}$ and is decreased with a decrease of ω .

There is a simple relationship between P_2 and η_{ω} :

$$P_2 = \eta_{\omega} \cdot \frac{g}{f} \quad \text{or:} \quad \frac{P_2}{\eta_{\omega}} = \frac{g}{f}$$

In the practical applications of interior ballistics a ratio η_2 of the average pressure P_{av} taken on the

length of travel l_2 to the maximum pressure p_m is very useful:

$$\eta_2 = \frac{(p_{av})_2}{p_m}$$

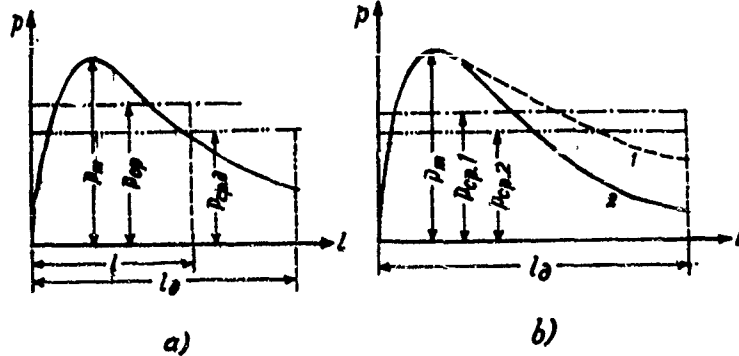


Fig. 88

At left: $(p_{av})_2$ on the length l and $(p_{av})_2$ on the whole length l_2 .

At right: the average pressure $(p_{av})_2$ as a characteristic of the more progressive curve 1 than the curve 2. Thus the coefficient η_2 is a characteristic of the progressiveness of burning within the bore.

$$\text{Since } (p_{av})_2 \cdot S \cdot l_2 = \frac{\gamma m v_2^2}{2}$$

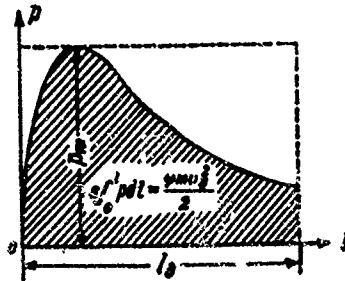
and $S l_2 = W_2$ is a working volume of the gun bore we have:

$$h_2 = \frac{(p_m v_2)}{P_m} = \frac{\varphi_m v_2^2}{2W_2 P_m}$$

and h_2 can be called the coefficient of utilization of the working volume of the bore.

The third interpretation of h_2 can be seen from the following form:

$$h_2 = \frac{\varphi_m v_2^2}{2s l_2 P_m} = \frac{s \int_0^{l_2} p \, dl}{s P_m l_2} = \frac{\int_0^{l_2} p \, dl}{P_m l_2} = \frac{\text{Total area}(p, l)}{\text{Rectangular area}(P_m l_2)}$$



See Fig. 89

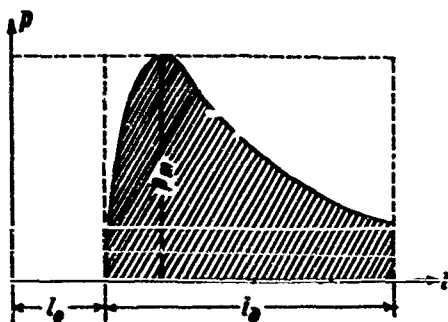
Utilization of the working volume of the gun canal.

Here η_2 may be called the coefficient of the filling up of the indicator diagram (p, l).

Including in the analysis ~~the~~ whole volume of the bore ($S l_2$) with chamber ($S l_0$) or : $S(l_2 + l_0) = W_c$

we may consider the ratio:

$$R_2 = \frac{\frac{4m v_2^2}{2}}{W_c p_m} = \eta_2 \frac{W_2}{W_c} = \eta_2 \frac{l_2}{l_2 + l_0} < \eta_2$$



See Fig. 90

R_2 is the characteristic of the ballistic utilization of the whole volume of the gun canal.

2. The relationship between the gas pressure within bore and the loading conditions

Equation (53):
$$p = \frac{f \frac{\omega}{s} \psi - \frac{q}{s} \cdot \frac{\varphi m v^2}{s}}{l_v + l}$$

differentiating with respect to time we obtain:

$$\frac{dp}{dt} = \frac{1}{l_v + l} \left[f \frac{\omega}{s} \cdot \frac{d\psi}{dt} - \frac{\varphi m}{s} v \cdot \frac{dv}{dt} - p \left(\frac{dl_v}{dt} + \frac{dl}{dt} \right) \right]$$

now, remembering that: $\frac{d\psi}{dt} = \frac{s_i}{\lambda_i} \cdot \frac{s}{s_i} u, p = \frac{\pi}{I_K} \cdot G \cdot p = \Gamma \cdot p$

$$p = \frac{\varphi m}{s} \cdot \frac{dv}{dt}$$

$$\frac{dl_v}{dt} = v; l_v = l_0 \left(1 - \frac{q}{s} \right); \alpha - \frac{1}{s} = \frac{1}{s_i}; a = \frac{\omega}{s} \cdot \frac{1}{s_i}; I_K = \frac{e_i}{u_i}$$

$$l_v = l_0 \left[1 - \frac{q}{s} - \Delta \left(\alpha - \frac{1}{s} \right) \psi \right]$$

we will have:

$$\frac{dp}{dt} = \frac{p}{l_v + l} \left[f \frac{\omega}{s} \cdot \frac{\pi G}{I_K} - \varphi v - \left(v - a \frac{\pi}{I_K} G p \right) \right] = \frac{p}{l_v + l} \left[f \frac{\omega}{s} \cdot \frac{\pi G}{I_K} u_i \left(1 + \frac{1}{s_i} \cdot \frac{p}{f} \right) - v (1 + \varphi) \right]$$

At the beginning when $p = p_0$ ("shot-start" pressure)

$$l = 0; v = 0; l_v = l_{v_0}$$

we have:

$$\left(\frac{dp}{dt} \right)_0 = p_0 \frac{f \omega}{s l_{v_0}} \cdot \frac{\pi G}{I_K} \left(1 + \frac{1}{s_i} \cdot \frac{p_0}{f} \right) = p_0 \frac{f \omega}{s l_{v_0}} \Gamma_0 \left(1 + \frac{1}{s_i} \cdot \frac{p_0}{f} \right) \dots (58)$$

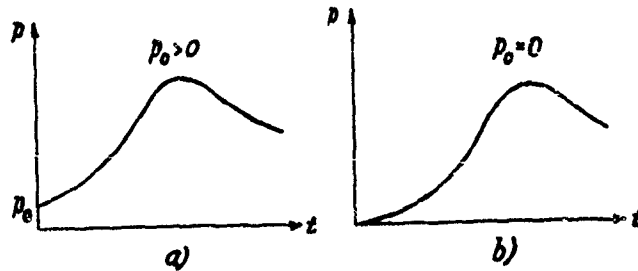


Fig. 91

At left - the curve (p, t) when $p_0 > 0$; $(\frac{dp}{dt})_0 > 0$

At right - the practically unrealizable curve (p, t)
when $p_0 = 0$ and $(\frac{dp}{dt})_0 = 0$

The derivative: $\frac{dp}{dt} = \frac{dp}{dt} \cdot \frac{dt}{dt} = \frac{1}{v} \cdot \frac{dp}{dt} = \frac{p}{\ell_0 + \ell} \left[\frac{f_w x_0}{L} \cdot \frac{6}{v} \left(\frac{p}{p_0} \right) - (1 + \theta) \right] \dots (59)$

See Fig. 92 - at $v=0$ becomes infinity.



The maximum pressure is determined from: $\frac{dp}{dt} = 0$ or $\frac{dp}{dt} = 0$

$$f \frac{\omega}{S} \cdot \frac{x_0}{L_K} \delta_m \left(1 + \frac{1}{\delta} \cdot \frac{p_m}{f} \right) - v_m (1 + \theta) = 0$$

where subscript m denotes values corresponding to p_m

$$\text{or: } f \frac{\omega}{S} \Gamma_m \left(1 + \frac{1}{\delta} \cdot \frac{p_m}{f} \right) = v_m (1 + \theta); \quad \Gamma_m = \frac{x_0}{L_K} \delta_m = \frac{S_1}{\lambda_1} u_1 \delta_m$$

If the rate of burning u_1 or the burning surface δ at a certain interval of time after t_m are increased proportionally to the increase in v or in other words if the rate of inflow of powder gases ($f\omega\Gamma$) increases proportionally to the rate of change of the volume of the bore ($vS = \frac{dV}{dt} = \frac{dW_p}{dt}$) then the maximum pressure p_m will stay constant during this interval of time.

At the end of the first period of burning when $t = t_K$ and $\psi = 1$:

$$\left(\frac{dp}{dt} \right)_K = \frac{p_K}{L_1 + L_K} \left\{ f \frac{\omega}{S} \cdot \frac{x_0}{L_K} \delta_K \left[1 + (\alpha - \frac{1}{f}) \frac{p_K}{f} \right] (1 + \theta) v_K \right\} \dots (52')$$

For the beginning of the second period we have from (53)

$$\rho = \frac{f\omega}{S} \cdot \frac{1 - (\frac{v}{v_{\infty}})^2}{\ell_1 + \ell}$$

Differentiating this ρ with respect to t and ℓ we have:

$$\frac{d\rho}{dt} = -(1+\theta) \frac{v}{\ell_1 + \ell} \rho \quad \text{and} \quad \frac{d\rho}{d\ell} = -(1+\theta) \frac{\rho}{\ell_1 + \ell}$$

and for the beginning of the second period (subscript 0).

We will have: $(\frac{d\rho}{dt})_0 = -\frac{(1+\theta)v_0\rho_0}{\ell_1 + \ell_0}$

and $(\frac{d\rho}{d\ell})_0 = -\frac{(1+\theta)\rho_0}{\ell_1 + \ell_0}$

Comparing these expressions with $(\frac{d\rho}{dt})_K$ and $(\frac{d\rho}{d\ell})_K$ from (58') and (59) we see that at the moment of transition from the end of the 1st period to the beginning of the 2nd period both derivatives $\frac{d\rho}{dt}$ and $\frac{d\rho}{d\ell}$ change abruptly and the corresponding curves (ρ, t) and (ρ, ℓ) have angular points (with two tangents) on account of the disappearance of the term: $\frac{f\omega}{S} \frac{x_0}{I_K} \sigma_K \left[1 + (\alpha - \frac{1}{2}) \cdot \frac{\rho_K}{f} \right]$

and after this moment when $\sigma = 0$ these curves will have their slopes gradually decreased to their final values at $\ell = \ell_2$: $(\frac{d\rho}{dt})_2 = -(1+\theta) \frac{\rho_2 v_2}{\ell_1 + \ell_2}$ and $(\frac{d\rho}{d\ell})_2 = -(1+\theta) \frac{\rho_2}{\ell_1 + \ell_2}$.

3. The influence of the form and dimensions of the powder grains on the curves (ρ/ℓ) and (v/ℓ).

The most effective factor in (57) and (59) is

$$f\omega \frac{\rho}{\ell} \mu, \sigma = f\omega r \quad \text{and in particular } \frac{\rho}{\ell} \sigma = \Sigma = \frac{S_1}{\lambda_1} \sigma_1 \frac{S_2}{\lambda_2} \sigma_2$$

1. The influence of the form at the constant web e , for simplicity's sake assumed equal to 1, i.e. $e_1 = 1$ and

$$\Sigma = \chi \cdot \sigma \quad (\omega \text{ is constant})$$

At the beginning of burning: $\chi = 0$; $\sigma = 1$; $\Sigma = \chi$

At the end of burning: $\chi = 1$; $\Sigma_K = \chi \cdot \sigma_K = \chi (1 - 2\lambda + 3\lambda)$

The following Table 21 was calculated for 5 degressive forms: 1-tube; 2-strip; 3-plate; 4-bar; 5-cube.

Table 21

No.	Form of Grain	$\Sigma_0 = \chi$	σ_K	$\Sigma_K = \chi \sigma_K$	$\Sigma_0 = \chi$	σ_K	$\Sigma_K = \chi \sigma_K$
1	Tube	$1 + \beta$	$\frac{1 - \beta}{1 + \beta}$	$(1 - \beta)$	1.003	0.994	0.937
2	Strip	$1 + \alpha + \beta$	$\frac{(1 - \alpha)(1 - \beta)}{1 + \alpha + \beta}$	$(1 - \alpha)(1 - \beta)$	1.060	0.890	0.973
3	Plate	$1 + 2\beta$	$\frac{(1 - \beta)^2}{1 + 2\beta}$	$(1 - \beta)^2$	1.200	0.675	0.810
4	Bar	$2 + \beta$	0	0	2.0	0	0
5	Cube	3	0	0	3	0	0

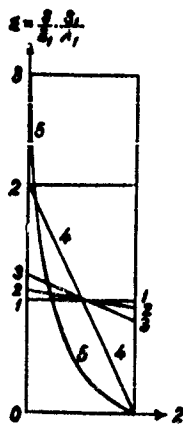
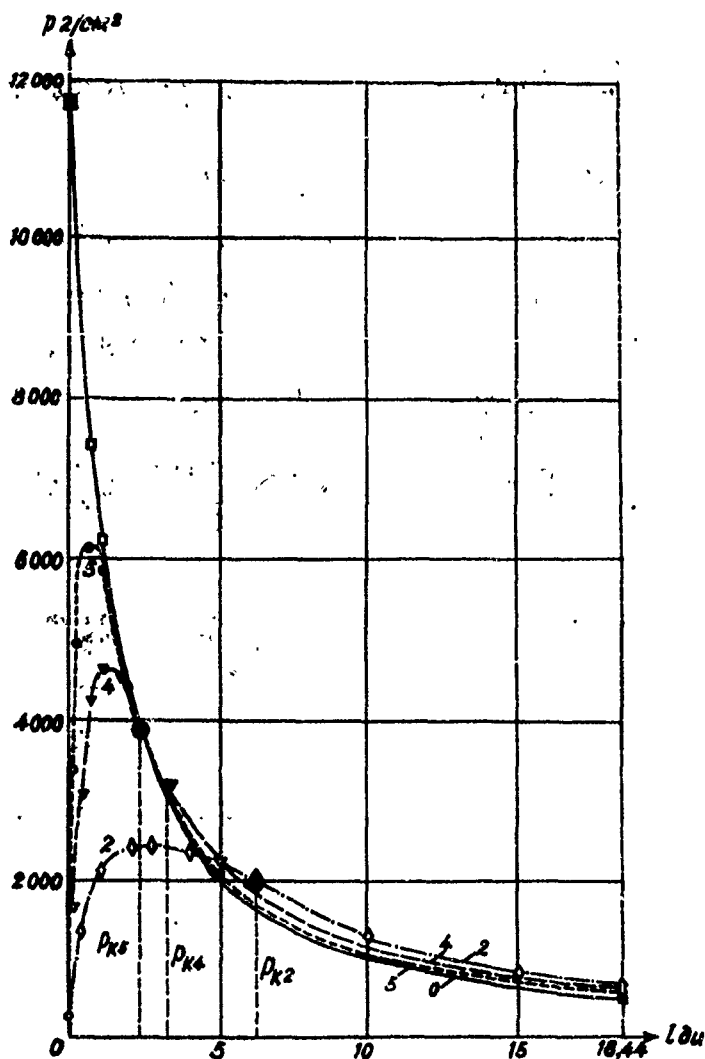


Fig. 93

Shows various curves (1 - 5) of (Σ, λ) for various forms of powder grains given in Table 21.



gives the curves (p, ℓ) calculated for the same ω and various forms and marked by: 0 - instantaneous burning (adiabatic curve) Figure 94 -

2 - for strip; 4 - for bar; 5 - for cube.

Strip powder: $p_m = 2380$; $p_K = 2000$; $\frac{p_K}{p_m} = 0.340$; $v_K = 590$ m/s.

Bar or rod: $p_m = 4600$; $p_K = 3100$; $\frac{p_K}{p_m} = 0.180$; $v_K = 656$ m/s.

260

Cube: $\rho_m = 6200$; $\rho_K = 3800$; $\frac{\rho_K}{\rho_0} = 0.122$; $v_0 = 621 \text{ m/s}$

Adiabatic law: $\rho_m = 11700$; $v_0 = 690 \text{ m/s}$.

2. The influence of the size of web in grains with the same form (strip) on the curves (Σ, λ) and (ρ, ℓ) .

1) $2e_1 = 1.5 \text{ mm}$; 2) $2e_1 = 2.0 \text{ mm}$; 3) $2e_1 = 2.5 \text{ mm}$

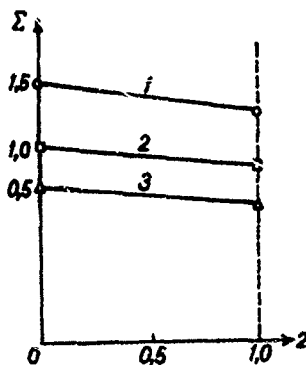
$$\Sigma = \frac{\rho_0}{\rho_1} \sigma_1 ; \Sigma_0 = \frac{\rho_0}{\rho_1} = \frac{106}{\rho_1}$$

$$\sigma_K = 0.889 ; \Sigma_K = \frac{106 \cdot 0.889}{\rho_1} = \frac{0.943}{\rho_1}$$

Table 22

$2e_1$	$\Sigma_0 = \frac{106}{\rho_1}$	$\Sigma_K = \frac{0.943}{\rho_1}$	$\rho_m \text{ g/mm}^3$	$v_0 \text{ m/s}$
1.5	1.414	1.256	3540	632
2.0	1.060	0.973	2070	575
2.5	0.848	0.744	1450	486

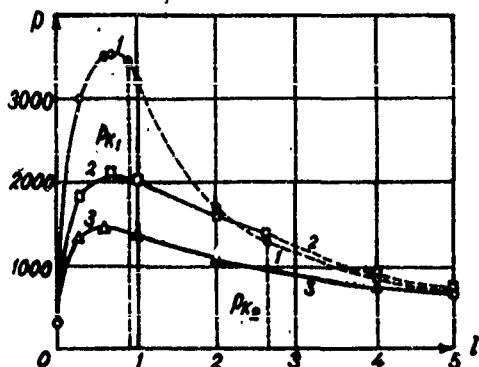
Fig. 95



The intensiveness of burning (Σ, λ) as a function of λ
for: 1-with $2e_1 = 1.5$ 2-with $2e_1 = 2.0$ 3-with $2e_1 = 2.5$

Powder with a smaller web gives a more intensive burning
(see also Fig. 96)

Fig. 98



The curves (P, t) as affected by the size of web:

1-with $2e_1 = 1.5$ 2-with $2e_1 = 2.0$ 3-with $2e_1 = 2.5$

These examples show how by varying web and form of the powder grains it is possible to regulate the process of gas formation in order to have a desired character of variation in the pressure. For example - if we do not want a maximum pressure P_m exceeding a certain prescribed value, then a more advantageous powder is one which is the least degressive. In our case this is a tubular powder, the nearest to the powder with a constant surface of burning. But it is also possible to have a progressive powder which will burn with an increasing burning surface and with a higher work efficiency.

Chapter 4 - Forces acting during the travel of a projectile in a rifled bore.

1. A general description of rifling.

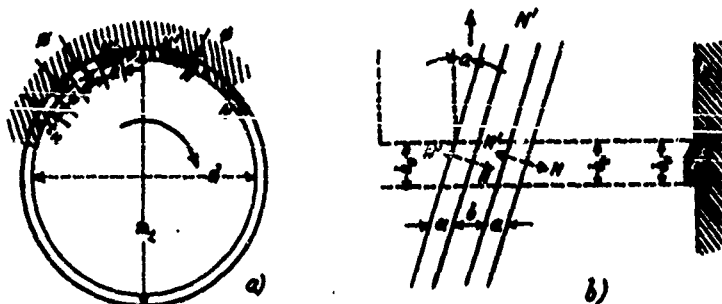


Fig. 97 - Schematic view of rifling.

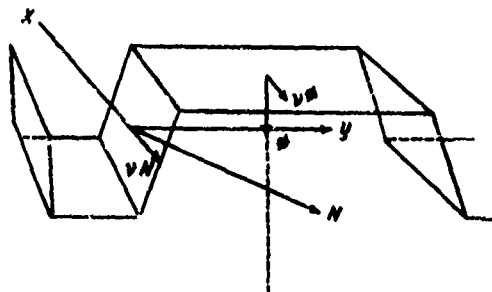


Fig. 98 - Forces acting on rifling:

Rotational force N on the area $b \cdot t_r \cdot \cos \alpha \sim b \cdot t_r$
and reaction N' ;

Radial force φ and frictional force $\nu \varphi$ (negligible)

a - width of a land of rifling; b - width of a bottom of rifling; t_r - depth of rifling. n - number of riflings: $n \approx 3-3.5 d$ or $n = 2d + 8$; d - caliber in cm.

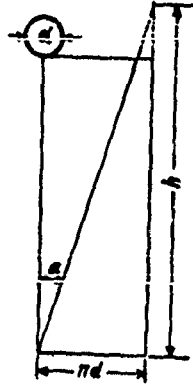


Fig. 99 - rifles of a constant pitch

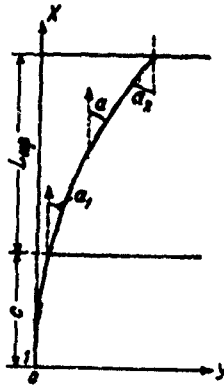


Fig. 100 - a progressive pitch of rifles.

$h = \pi \cdot d \cdot \cot \alpha$; $h = \frac{h}{\alpha} = \frac{\pi}{\tan \alpha}$; $x = ky$; $y = \frac{x^2}{K}$ - the equation of the line of rifling.

With the progressive pitch: $\frac{dy}{dx} = \frac{2x}{K} = \tan \alpha$; $\frac{d(\tan \alpha)}{dx} = \frac{2}{K}$ (constant); α is the angle of rifling.

At the beginning of rifling: $\tan \alpha_0 = \frac{2x_0}{K} = \frac{2c}{K}$

c - is a variable travel of the driving band.

at the muzzle: $\tan \alpha_2 = \frac{2(c+L_r)}{K}$; L_r - is the total length of driving band travel (or length of the rifled part of bore)

hence: $K = \frac{2L_r}{\tan \alpha_2 - \tan \alpha_1}$

then: $C = \frac{K}{2} \cdot \tan \alpha_1 = \frac{\tan \alpha_1}{\tan \alpha_2 - \tan \alpha_1} \cdot L_r$

C is the distance from the beginning of rifling to the point of the full depth of rifling.

Since $x = c + l_c$ then for angle α at any

x we have: $\tan \alpha = \frac{2x}{K} = \frac{2(c+l_c)}{K} = \tan \alpha_1 + (\tan \alpha_2 - \tan \alpha_1) \frac{l_c}{L_r} \dots (62)$

Table 23

$\eta =$	50	40	35	30	25	20
$\alpha =$	3°35'	4°30'	5°07'	5°58'7	7°09'45"	8°56'

2. The resistance of engraving of the driving band and the "shot-start" pressure.

Fig. 101 (p. 201 in book) shows schematically the relative position of the driving band at the beginning, its travel (a \rightarrow b) to the point of the beginning of the full depth of rifling, when the gas pressure reaches the value of "shot-start" pressure: $p_0 = \frac{\pi_0}{S} \frac{Kg}{cm^2}$

At this moment the resistance of engraving is at its maximum; then the deformation of the driving band being

completed, the projectile continues its travel with an abruptly decreased resistance (see Fig. 102, p. 201 in book).

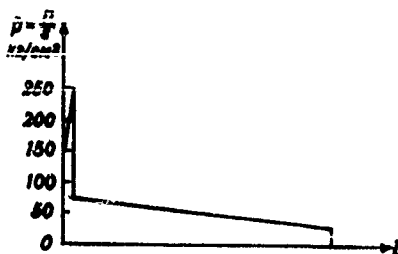


Fig. 102

Variation of the pressure $\frac{F}{S}$ necessary for the engraving of the driving band and moving the projectile along the bore to the muzzle. (76 m/m gun, type of 1902)

curve $(\frac{F}{S}, l)$

Experiments 1898 and 1899 were conducted with the projectile pulled through the bore by mechanical or hydraulic means at ordinary temperature - the obtained values of the resistance were markedly exaggerated in comparison with the actual resistance developed during the firing.

TABLE 24

Constructional Characteristics of Several Guns

Types of Guns	Weight of Recoiling System	Weight of Projectile	Weight of Charge	Muzzle Kinetic Energy $\left(\frac{1}{2} m v^2 \right)$	$\frac{R}{L} = \frac{1}{4}$	α	Angle of Rifling	Depth of Rifling $\frac{m}{m}$	Width of Rifling			Number of Riflings n	Length of the Rifled Part of Bore $\frac{m}{m}$
									Land: $\frac{m}{m}$	Bottom: $\frac{m}{m}$	$\frac{m}{m}$		
76 m/m Mount Artillery 1909	287 Kg.	6.20	0.365	45.85	25	$70^{\circ}45'$	0.76	0.76	3.05	6.94		24	1060
76 m/m Type 1902-1930	570 Kg.	6.20 Kg.	1.080 Kg.	146.10	25	$70^{\circ}45'$	0.76	0.76	2.10	5.38		32	2663
170 m/m Type 1910-1930	1300 Kg.	17.18 Kg.	2.790 Kg.	393.20	25	$70^{\circ}45'$	1.00	1.00	3.00	7.47		32	3419
152 m/m Howitzer 1910-1934	1650 Kg.	43.56 Kg.	7.560 Kg.	952.40	20	$30^{\circ}54'25''$ $80^{\circ}55'37''$	1.50	1.50	3.00	6.97		48	3591
152 m/m Howitzer 1909-1930	1435 Kg.	40. Kg.	2.125 Kg.	311.90	20	$30^{\circ}42'$ $80^{\circ}55'37''$	1.25	1.25	3.81	9.47		36	1809
122 m/m Howitzer 1910-1930	570 Kg.	21.76 Kg.	1.170 Kg.	147.10	20	$30^{\circ}42'$ $80^{\circ}56'$	1.015	1.015	3.04	7.60		36	1260

Special experiments with a shortened 76 m/m gun using small charges in such a way that 50% of projectiles remained in bore after firing and 50% were thrown out of a muzzle at several feet distance. It was observed that at pressure 150 kg/cm. the driving bands were not engraved but had only slight indentations of their front edge. At the pressure 225-275 Kg/cm² some of the projectiles remained in the gun and others were ejected from the gun at a distance of a few feet. The conclusion was that the firing requires a very small surplus pressure for overcoming the resistance due to forces φ and $\nu\varphi$ at the end of the engraving process. Thus the "shot-start" pressure was determined as ~ 250 Kg/cm² which value can vary considerably with changes in rifling or in dimensions of the driving band. Prof. N. F. Drosdov uses $p_0 = 300$ Kg/cm² for his Tables. Granz suggests $p_0 = 270$ Kg/cm² for 76 m/m gun and $p_0 = 550$ Kg/cm² for small arms. Special experiments of P. N. Shkvornikov gave $p_0 = 300-400$ Kg/cm² for small arms.

Gabot gives the following formula for p_0 :

$$p_0 = 4\nu U \frac{H}{d} \cos\alpha \left[1 + \sin\alpha \frac{\sin\alpha + \nu \cos\alpha}{\cos\alpha - \nu \sin\alpha} \right]$$

Here: U - elastic limit for copper = $3000 \left(\frac{\Sigma}{100} \right)^{0.6} + 550$

$$\frac{\Sigma}{100} = 0.1 + 1.1 \frac{D_o - d'}{d' - d_p}$$

H - width of the driving band.

d' - effective caliber; D_o - outer diameter of the driving band.

d_p - diameter of the projectile near to the driving band.

If from the general equation of Pyrostatics we calculate that fraction ψ of the burnt charge, which corresponds to the "forcing pressure" p_o i.e.:

$$\psi_o = \frac{\frac{1}{p} - \frac{1}{p_o}}{\frac{1}{p_o} + \alpha - \frac{1}{p}}$$

then this ψ , as a burnt charge before the projectile starts its travel, will be an indirect evaluation of the significance of the "forcing pressure" p_o . The higher p_o , the larger is $\left(\frac{dp}{dt} \right)$; the steeper is the (p, t) curve in the beginning and the higher will be p_m .

3. Mechanical reactions of the rifling during the projectile travel along the bore.

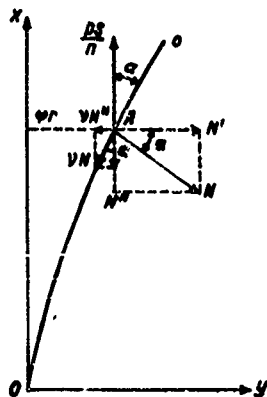


Fig. 104 (p. 205 in book) shows schematically a line of a progressive rifle, point A a center of the area (ρ, t_r) at the distance r from the axis of projectile and α is the angle of rifling; axis x - along the axis of the gun. Acting forces: N , vN and $\frac{p \cdot s}{h}$ where h is a number of riflings; radial forces φ and $v\varphi$ are negligible; (N is a force of reaction of the rifling on the driving band). Equation of the rotational motion of the projectile will be:

$$nrN(\cos\alpha - v\sin\alpha) = I \frac{d\Omega}{dt} \dots (63)$$

here $I = \int r^2 dm = m \rho^2$ - is a moment of inertia

of the projectile, ρ is a radius of inertia; Ω - the angular velocity = $\frac{v \tan\alpha}{r}$;

$$\frac{d\Omega}{dt} = \frac{1}{r} \left(\tan\alpha \frac{dv}{dt} + v^2 \frac{d \tan\alpha}{dx} \right)$$

For the progressive rifling:

$$\frac{d \tan \alpha}{dx} = \frac{\tan \alpha_2 - \tan \alpha_1}{L_r} = K_\alpha \text{ (constant)}$$

For the constant pitch: $K_\alpha = 0$

Then from (63):

$$N = \frac{1}{h} \left(\frac{Q_r}{r} \right)^2 \cdot \frac{\tan \alpha \cdot m \frac{dv}{dt} + K_\alpha m v^2}{\cos \alpha - \gamma \sin \alpha} \dots (64)$$

Equation of the translatory motion:

$$p_{pr} \cdot S - h N (\sin \alpha + \gamma \cos \alpha) = m \frac{dv}{dt} \dots (65)$$

here p_{pr} - gas pressure on the projectile and

$h N (\sin \alpha + \gamma \cos \alpha) = R$ is the force of resistance to the motion over the surface of the contact of the driving band with the riflings.

or:

$$p_{pr} S \left(1 - \frac{R}{p_{pr} S} \right) = m \frac{dv}{dt}; \quad \frac{1}{1 - \frac{R}{p_{pr} S}} \sim 1 + \frac{R}{p_{pr} S} = \varphi_1 > 1$$

(65) will be rewritten: $\frac{p_{pr} S}{\varphi_1} = m \frac{dv}{dt}$

Then (64) will be:

$$N = \frac{1}{h} \left(\frac{p}{r} \right)^2 \cdot \frac{\tan \alpha \cdot S \rho_{pr} + \varphi K_m m v^2}{\varphi_1 (\cos \alpha - \gamma \sin \alpha)}$$

$$\varphi_1 (\cos \alpha - \gamma \sin \alpha) \sim 1$$

Thus the final form for N will be :

$$N = \frac{1}{h} \left(\frac{p}{r} \right)^2 (\tan \alpha \cdot S \rho_{pr} + \varphi K_m m v^2) \dots (66)$$

For the constant pitch of rifling:

$$N = \frac{1}{h} \left(\frac{p}{r} \right)^2 \tan \alpha \cdot S \cdot \rho_{pr} \dots \dots (67)$$

The value $\left(\frac{p}{r} \right)^2$ varies between 0.48 and 0.68 as for example: For a solid bullet 0.48, for a solid cylinder 0.50, Armor-piercing thick walled shell 0.56, a thin-walled explosive shell 0.64 - 0.68.

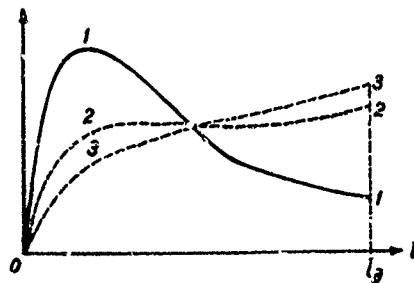


Fig. 105 (p. 207 in book) shows how the force N is affected by the pitch of rifling;

Curve 1 with $\alpha = 10^\circ$ constant

Curve 2 with $\alpha_1 = 5^\circ$ and

$$\alpha_2 = 10^\circ (\text{progressive})$$

Curve 3 with $\alpha_1 = 2^\circ$ and

$$\alpha_2 = 10^\circ (\text{progressive})$$

$$\text{Braking force } R = nN(\sin\alpha + \nu\cos\alpha) = nN\cos\alpha(\tan\alpha + \nu) \dots (68)$$

At the constant pitch ($\cos\alpha \sim 1$):

$$R = \left(\frac{S}{r}\right)^2 (\tan^2\alpha + \nu\tan\alpha) S p_r \dots (69)$$

For the progressive pitch:

$$R = \frac{\lambda}{n} (\tan\alpha S p_r + \varphi_1 K_\alpha m v^2) (\tan\alpha + \nu)$$

For the constant α :

$$\varphi_1 = 1 + \frac{R}{p_r S} = 1 + \left(\frac{S}{r}\right)^2 (\tan^2\alpha + \nu\tan\alpha) \text{ is constant.}$$

Then (65) will be: $S \cdot p_r = \varphi_1 m \frac{dv}{dt}$

thus the resistance of riflings is expressed in terms of an increased mass of projectile. For the progressive

pitch: $\varphi_1 = 1 + \frac{R}{S p_r}$ is not a constant.

4. The amount of work necessary for overcoming the resistance R .

For the constant α : $R = nN\cos\alpha(\tan\alpha + \nu) = \lambda(\tan^2\alpha + \nu\tan\alpha) S p_r$

$$\text{here: } \lambda = \left(\frac{S}{r}\right)^2$$

$$\text{and } \int_0^{\ell} R d\ell = \lambda (\ell g^2 \alpha + v \ell g \alpha) S \int_0^{\ell} \rho_m d\ell = \lambda \ell g^2 \frac{mv^2}{2} + \lambda \ell g \alpha \frac{mv^2}{2}$$

here: $\lambda \ell g^2 \alpha \frac{mv^2}{2} = E_2$ is the work producing the rotational motion of the projectile.

$\lambda v \ell g \alpha \frac{mv^2}{2} = E_3$ is the work producing the translatory motion of the projectile or:

$$E_2 = K_2 \frac{mv^2}{2} \quad \text{and} \quad E_3 = K_3 \frac{mv^2}{2}; \quad K_2 = \lambda \ell g^2 \alpha; \quad K_3 = \lambda v \ell g \alpha$$

Thus we have: $\varphi_1 = 1 + K_2 + K_3$

Chapter 5. Formulae for evaluation of the secondary works.

1. The work producing the rotation of the projectile.
 $E_2 = \frac{I \Omega^2}{2}; \quad I = m \rho^2; \quad \Omega = \frac{v \ell g \alpha}{r}$

Here: Ω - an angular velocity of the projectile.

v - a linear velocity of the projectile.

I - moment of inertia of the projectile.

$$\text{Thus: } E_2 = \frac{m \rho^2 v^2 \ell g^2 \alpha}{2 r^2} = \left(\frac{\rho}{r}\right)^2 \ell g^2 \alpha \cdot \frac{mv^2}{2} = K_2 \left(\frac{mv^2}{2}\right)$$

$$\text{and } K_2 = \left(\frac{\rho}{r}\right)^2 \ell g^2 \alpha.$$

2. The work done in overcoming the friction during the travel.

The force of friction is: $n \gamma N \cos \alpha$.

Hence:

$$E_3 = \int_0^{e_2} n \gamma N \cos \alpha \frac{d\ell}{\cos \alpha} = \left(\frac{Q}{F}\right)^2 \gamma \tan \alpha \int_0^{e_2} p_{pr} d\ell = \left(\frac{Q}{F}\right)^2 \gamma \tan \alpha \left(\frac{m v^2}{2}\right)$$

$$\text{Hence: } K_3 = \left(\frac{Q}{F}\right)^2 \gamma \tan \alpha.$$

3. The work producing the displacement of the powder charge.

The powder gases moving the projectile at the same time also move themselves and the unburned parts of the powder charge - this additional work is performed in a very complicated way which at present is not resolved yet in all its details. We have to resort to certain simplifying assumptions and to a more elementary analysis of the whole process.

In the first place our aim will be to find the expression for the kinetic energy of the parts of the powder charge moving with variable velocities v_w in terms of the kinetic energy of the projectile. We will make the following assumptions:

1. The whole bore including the chamber has a constant (S) cross-sectional area (a varying diameter of the chamber is for the time being neglected).

2. The whole mass of a powder charge $M = \frac{G}{g}$ during the travel of the projectile is uniformly distributed within the volume between the bottom of the chamber and the bottom of the projectile (the length of this volume l_p).

3. The elements of the powder charge are involved only in their transitory motion with their velocities $2v_{co}$ increasing from zero at the bottom of the chamber in proportion to their distances from this bottom (linear law of velocities), being equal to the velocity of the projectile $2v$ at their contact with the bottom of the projectile.

4. The friction between the moving parts of the water charge and the walls of the bore is neglected.

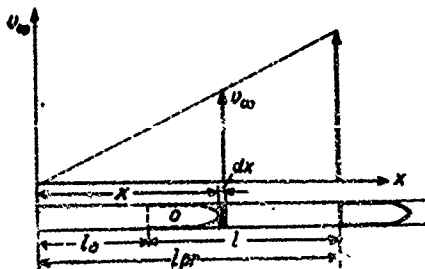


Fig. 106 (p. 212 in book)

Distribution of the velocities v_w of the elements of the powder charge behind the projectile (x - variable distance from the bottom of chamber)

From our assumptions we have: $\frac{d\mu}{\mu} = \frac{dx}{l_{pn}}$ } $d\mu = \mu \cdot \frac{dx}{l_{pn}}$
 and $\frac{v_w}{v} = \frac{x}{l_{pn}}$ } $v_w = v \frac{x}{l_{pn}}$

The kinetic energy of the mass $d\mu$ or: $dE_4 = d\mu \cdot \frac{v_w^2}{2}$

or:

$$dE_4 = \mu \cdot \frac{dx}{l_{pn}} \cdot \frac{x^2}{l_{pn}^2} \cdot \frac{v^2}{2} = \frac{\mu v^2}{2 l_{pn}^3} x^2 dx$$

$$\text{Hence: } E_4 = \frac{\mu v^2}{2 l_{pn}^3} \int_0^{l_{pn}} x^2 dx = \frac{1}{3} \cdot \frac{\mu}{m} \cdot \frac{mv^2}{2} = \frac{1}{3} \cdot \frac{\omega}{q} \cdot \frac{mv^2}{2} = K_4 E,$$

Here the coefficient $K_4 = \frac{1}{3} \cdot \frac{\omega}{q}$ varies between 0.03 to 0.13. Other possible assumptions concerning the distributions of the masses and velocities may result in other values of K_4 as for example: $K_4 = 1/6$ or $1/4$ or $3/11$.

4. Taking into account the widening of the chamber.

(A correction of the first assumption in the previous article 3).

The presence of the different diameters of the chamber and of the bore introduce a very complicated problem in dynamics of the gaseous flow in non-uniform channels. Our basic simplification of this problem consists in the assumption that the whole mass of gases outside the cylinder with the cross-section S is unmovable and not affected at all by the moving mass of gases within the cylinder with its cross-section S . Other assumptions of the previous article ³ concerning the distributions of the mass of gases and their velocities remain the same.

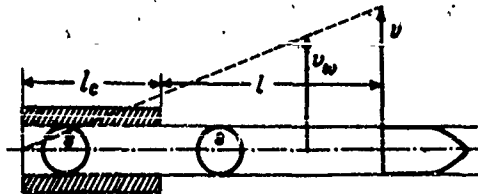


Fig. 107 (p. 213 in book) gives the schematic view of this case - the chamber has its length l_c , its effective length l_0 and its diameter larger than the diameter of the bore. The shaded areas show that volume of gases which does not take part in the movement of gases within the cylinder with the cross-section S .

Then the relative weight $\frac{\omega'}{\omega}$ of moving gases will be :

$$\frac{\omega'}{\omega} = \frac{S(\ell_0 + \ell)}{W_0 + S\ell} = \frac{S(\ell_0 + \ell)}{S(\ell_0 + \ell)} = \frac{1 + \kappa}{1 + \lambda}$$

$$\text{here: } \lambda = \frac{\ell}{\ell_0}, \quad \kappa = \frac{\ell_0}{\ell_c}$$

is the coefficient of the widening of the chamber.

Then: $\omega' = \omega \cdot \frac{1 + \kappa}{1 + \lambda}$

and this mass of gases is moved under the conditions of

the previous case i.e. instead of $K_4 = \frac{1}{3} \cdot \frac{\omega}{\ell}$

we will have: $K_4' = \frac{1}{3} \cdot \frac{\omega'}{\ell} = \frac{1}{3} \left(\frac{1 + \kappa}{1 + \lambda} \right) \frac{\omega}{\ell} = b \frac{\omega}{\ell}$

$$\text{or } b = \frac{1}{3} \left(\frac{1 + \kappa}{1 + \lambda} \right)$$

If $\kappa = 1$, then $K_4' = \frac{1}{3} \cdot \frac{\omega}{\ell}$ and $b = \frac{1}{3}$

Since λ is a variable value $\left(\frac{\ell}{\ell_0} \right)$ we need b taken

at its average value between 0 and $\lambda_2 = \frac{\ell_2}{\ell_0}$ i.e. $b_{av.}$

$$b_{av.} = \frac{1}{3} \left(\frac{1 + \kappa}{1 + \lambda} \right)_{av.} = \frac{1}{3} \cdot \frac{1}{\lambda} \int_0^{\lambda} \frac{1 + \kappa}{1 + \lambda} d\lambda = \frac{1}{3} \left[1 - (1 - \frac{1}{\kappa}) 2.303 \frac{\log(1 + \frac{1}{\kappa})}{\lambda} \right]$$

The following Table 25 (with two entries Λ and \mathcal{N}) gives the average values of ℓ .

Table 25 (p. 214 in book) for ℓ_{av} .

\mathcal{N}	$\Lambda: 0.6$	1.0	2.0	3.0	5.0	7.0	10.0	
1.1	0.309	0.312	0.316	0.319	0.322	0.324	0.326	at $\mathcal{N} = 1$,
1.5	0.246	0.255	0.272	0.292	0.323	0.330	0.336	$\ell = 1/3$
2.0	0.203	0.218	0.242	0.256	0.273	0.284	0.293	which
3.0	0.159	0.179	0.211	0.244	0.255	0.267	0.280	is the
4.0	0.137	0.160	0.180	0.235	0.244	0.259	0.273	limit,
								for ℓ
								with the
								increased
								and de-
								creased \mathcal{N} .

5. The work spent on the recoiling system.

Denoting as Q_0 the weight of the recoiling system,

its mass $M = \frac{Q_0}{g}$ and its velocity V

we have: $E_s = \frac{Q_0}{2g} V^2 = \frac{MV^2}{2}$

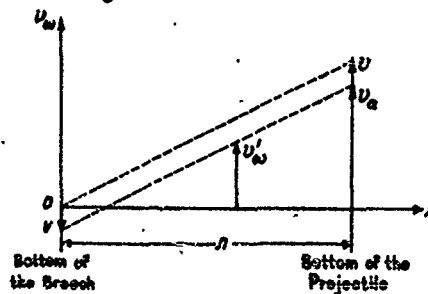


Fig. 108 (p. 215 in book)

Schematic view of the assumed distribution of gas velocities between the bottom of the chamber and the bottom of the projectile within the recoiling gun. The absolute velocity of the projectile: $v_a = v - V$

The absolute velocity of the bottom of the chamber: $-V$

The absolute (average) velocity of the charge:

$$v'_a = \frac{-V + (v - V)}{2} = \frac{v}{2} - V$$

Hence: $-MV + Mv'_a + mv_a = 0$ (equation of the linear momentum)

and: $V = \frac{m + \frac{M}{2}}{M + m + M} \cdot v$

then: $E_s = \frac{M}{2} \left(\frac{m + \frac{M}{2}}{M + m + M} \right)^2 v^2 = \frac{m}{M} \cdot \frac{\left(1 + \frac{1}{2} \frac{M}{m} \right)^2}{\left(1 + \frac{M}{M} + \frac{M}{m} \right)^2} \cdot \frac{mv^2}{2}$

or in terms of weights:

$$E_s = \frac{2}{Q_0} \cdot \frac{\left(1 + \frac{1}{2} \frac{Q_0}{Q_s} \right)^2}{\left(1 + \frac{2}{Q_0} + \frac{Q_0}{Q_s} \right)^2} \cdot \frac{mv^2}{2} = K_s \left(\frac{mv^2}{2} \right)$$

Here: $K_s = \frac{2}{Q_0} \cdot \left(\frac{1 + \frac{1}{2} \frac{Q_0}{Q_s}}{1 + \frac{2}{Q_0} + \frac{Q_0}{Q_s}} \right)^2$

approximately: $K_s \approx \frac{2}{Q_0} \left(1 + \frac{Q_0}{2} \right)$

If the equation of the linear momentum is written in terms of the absolute velocity v_a :

$$\text{then: } -MV + M\left(\frac{v_a - V}{2}\right) + m v_a = 0$$

$$\text{Hence: } V = \frac{2\left(1 + \frac{1}{2} \frac{\omega}{g}\right)}{Q_0\left(1 + \frac{1}{2} \frac{\omega}{Q_0}\right)} v_a$$

K_0 is larger for the howitzers than for the guns because Q_0 for howitzers is always smaller than for the guns.

6. Total sum of the secondary works.

Now we can write a more detailed expression for the coefficient $\varphi = (1 + K_2 + K_3 + K_4 + K_5)$ in the following form: $\varphi = 1 + \left(\frac{Q}{F}\right)^2 \frac{1}{2} \alpha + \left(\frac{Q}{F}\right)^2 \frac{1}{2} \alpha + \frac{1}{2} \frac{\omega}{g} + \frac{Q}{Q_0} \left(1 + \frac{\omega}{g}\right)$
In cases when we do not have sufficient data we may use an approximation for φ given by Prof. V. Sloukhotsky:

$$\varphi \sim K + \frac{1}{3} \frac{\omega}{g} \quad \text{and } K \text{ is varied with the type}$$

of gun, namely: Howitzers: $K = 1.06$

Guns of medium power: $K = 1.04 - 1.05$

Guns with higher power: $K = 1.03$

Small arms: $K = 1.10$

Sugot gives another expression for K :

$$K = 1.05 \left(1 + \frac{1}{4} \frac{\omega}{g}\right)$$

Chapter 6 - Additional questions.

1. The relationship between the gas pressures at the breech p_e and at the base of the projectile p_n . Denoting: m and μ masses of the projectile and of gases (unburned powder included),

j - the acceleration of the projectile

j_w - the average acceleration of the powder charge,

we will have for the base of the projectile:

$$p_n \cdot S = \varphi_1 m j$$

$$\text{For the breech: } p_e = \varphi_1 m j + \mu j_w$$

$$\text{Hence: } p_e = p_n \cdot \left(1 + \frac{\mu j_w}{\varphi_1 m j}\right) = p_n \cdot \left(1 + \frac{j_w \omega}{\varphi_1 j q}\right)$$

The ratio $\left(\frac{j_w}{j}\right)$ is entirely independent on the hypothesis which is assumed in respect to the distribution of the gaseous masses and as well as of their accelerations in various sections of the bore behind the projectile.

At the linear law of the gas velocities we have $\frac{j_w}{j} = 0.5$ which gives:

$$p_e = p_n \cdot \left(1 + \frac{1}{2} \frac{\omega}{q}\right)$$

i.e. Piobert's formula.

During recent years the works of Prof. I. Grave and Docent R. Shkvernikov were published in which this problem has been treated on the basis of the dynamics of gases. Here are given the principal formulae of these

works. With the following denotations:

v_a - absolute velocity of the projectile

v - its relative velocity

V - velocity of the recoiling system

g - weight of the projectile; ω - weight of charge;

Q_0 - weight of the recoiling parts; φ_1 and φ_2 the coefficients taking into account respectively the forces of resistances to the motion of the projectile and to the motion of the recoiling parts.

we will have: $V = i v_a$ and $i = \frac{\varphi_1 g + \frac{1}{2} \omega}{\varphi_2 Q_0 + \frac{1}{2} \omega}$ $V = \frac{i}{1+i} v$
hence: $v_a = v \left(\frac{1}{1+i} \right)$

$$\text{then: } p = p_0 \left[1 + 0.5 \frac{\omega}{\varphi_2} (1-i) \right]$$

The maximum pressure is located not at the breech but at certain distance from it: $x_m = \frac{i}{1+i} l_{pn}$ where the absolute velocity of the powder gases is zero. In the basic equation of pyrodynamics: $p\omega = RT\omega\psi$ we consider p as a certain average pressure existing in the volume behind the projectile.

This pressure p is given now as a function of p_0 and

$$p : p = p_0 \left[1 + \frac{1}{3} \cdot \frac{\omega}{\varphi_2} \left(1 - \frac{i}{2} \right) \right]$$

and:
$$\rho = \rho_0 \left[\frac{1 + \frac{1}{2} \frac{\omega}{\varphi_0} (1 - \frac{z}{2})}{1 + \frac{1}{2} \frac{\omega}{\varphi_0} (1 - z)} \right]$$

When $V = 0$ then $z = 0$ and: $\rho = \rho_0 \left[1 + \frac{1}{2} \frac{\omega}{\varphi_0} \right]$

hence: $\rho \varphi_1 = \rho_0 (\varphi_1 + \frac{1}{2} \frac{\omega}{\varphi_0}) = \rho_0 (1 + K_2 + K_3 + K_4)$

Thus if we disregard the recoil then:

$$\varphi_1 \rho = \varphi \rho_0 \quad \text{or:} \quad \frac{\rho_{pr}}{\varphi_1} = \frac{\rho}{\varphi}, \quad \text{or:} \quad \rho_0 = \rho \frac{\varphi_1}{\varphi}$$

Then our equation of motion of the projectile

$$\rho_{pr} S = \varphi_1 m \frac{dv}{dt}$$

will be: $\frac{\varphi_1}{\varphi} \rho S = \varphi_1 m \frac{dv}{dt} \quad \text{or:} \quad \rho S = \varphi m \frac{dv}{dt}$

This result is very important: It shows that in the basic equation of pyrodynamics: $\rho S (L_v + L) = f \omega \psi - \frac{\varphi m v^2}{2}$

and in the equation of motion of the projectile:

$$\rho S = \varphi m \frac{dv}{dt} \quad \text{or:} \quad \rho S = \varphi m v \frac{dv}{ds}$$

the values of ρ and φ are the same and v (velocity relative with respect to the gun) is the ballistic velocity involved in calculations.

For guns and howitzers $\varphi_1 = 1.02$

For small arms $\varphi_1 = 1.05$

For armor-piercing bullets $\varphi_1 = 1.07$

The coefficient \dot{z} is given by P. Shkvornikov as follows:

Rifles and machine guns	$\dot{z} = 0.0015$
Anti-tank rifles	$\dot{z} = 0.0030$
For guns	$\dot{z} = 0.0200$
For howitzers	$\dot{z} = 0.0350$

2. Heat emitted through the walls of the gun barrel.

In Section II we have seen how the heat emission in case of a constant inner surface (S_0 in the bomb) can be evaluated according to Muraur's theory. Now we will introduce an additional complicating factor - a variable inner surface of the bore (Σ) which varies from the surface of chamber Σ_0 to the surface of the whole gun canal Σ_c from the breech to the muzzle. We will consider only the cooling effect of the walls of the gun on the hot gases neglecting the heating of these walls by mechanical effects of friction and deformations produced by the moving projectile. The basic assumption will remain the same as in the case of the bomb namely - the heat losses are proportional to the number of impacts of hot molecules of gases against the cooling surface, and this number is a function of Σ, ρ, t : viz. $\Sigma \int \rho dt$

The surface of the chamber Σ_0 during the whole process

of firing is affected by the hot gases whereas the surface of the rifled bore is gradually involved in the contact with hot gases. The closer to the muzzle is a part of the bore, the shorter is the time of action of the hot gases, and the smaller is the heat loss. After the moment t_g (when the projectile leaves the muzzle) the process of heat emission is continued over the whole surface of the bore, but since this process does not affect either the pressure or the velocity of the projectile for the time being this phase can be omitted. The whole procedure of the heat loss evaluation is as follows. First of all by preliminary experiments in the bomb the time t_k and the coefficient $C_M\%$ at the density of loading $\Delta = 0.20$ must be determined, then if this powder will burn in the chamber W_0 at the constant density of loading Δ_0 the correction for the heat losses would be:

$$\left(\frac{\Delta T}{T}\%\right) = \frac{C_M}{7774} \cdot \frac{\Sigma_0}{W_0} \cdot \frac{1}{\Delta_0} \dots (70')$$

here: $\frac{\Sigma_0}{W_0} = \frac{4}{D} \div \frac{1}{L_c}$

D - the average diameter of the chamber.

L_c - the length of chamber.

If this powder will burn in the volume of the gun canal

$$W_c = W_0 + s\ell_2 \text{ at the density of loading: } \Delta_c = \frac{\omega}{W_0 + s\ell_2} = \frac{\omega}{W_c}$$

$$\text{then the heat losses will be: } \left(\frac{\Delta T}{T}\right)\% = \frac{C_m}{7.774} \cdot \frac{\Sigma \epsilon}{W_c} \cdot \frac{1}{\Delta_c} \dots (70)$$

The value of the actual losses will be between (70') and (70) and in order to determine this value corresponding to the varying conditions of changes in the pressure and in the cooling surface we must know as functions of time the variations in the pressure and in the surface of the gun canal, where increments are proportional to the projectile travel ℓ . Muracour, using the curves (p, t) , (Σ, t) or (ℓ, t) proceeds as this is shown on the Fig. 109 (p. 221 in book)

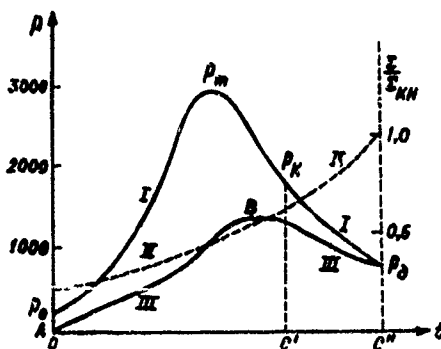


Fig. 109

Muraour's scheme of evaluation of the heat emitted through the walls of the gun. Curve I is (p, t) curve; Curve II is $(\frac{\Sigma}{\Sigma_c}, t)$ curve; the point C' marks

the end of burning $(p = p_n)$. The area $O p_n p_n' O$ is $I_K = \int_0^{t_K} p dt$

The area $C' p_n p_n' C''$ is I_n representing an additional cooling during the second period after the end of burning lasting until the projectile leaves the muzzle (t_n) .

If the cooling surface were constant then the right part of (70) or (70') should be multiplied by the ratio of the areas: $\frac{I_K + I_n}{I_K} > 1$; however the cooling surface

varies from $\frac{\Sigma_0}{\Sigma_c}$ to $\frac{\Sigma_c}{\Sigma_c} = 1$ as is given by the curve II so that our correction will consist of multiplying the ordinates of curves I and II which result is represented by the curve III.

Then the ratio of areas: $\frac{OAB p_n C'' O}{O p_n p_n' C' O} = \frac{\int_0^{t_K} \frac{\Sigma}{\Sigma_c} p dt}{\int_0^{t_K} p dt}$

gives that fraction of the value of the right part of (70) which should be taken as the actual relative lowering of the temperature T . (Muraour found this fraction equal 0.43 - 0.46)

Then we have:

$$\left(\frac{\Delta T}{T}\right) = \frac{C_m}{7.774} \cdot \frac{\Sigma_c}{W_c} \cdot \frac{1}{\Delta_c} \cdot \frac{1}{I_K} \int_0^t \frac{\Sigma}{\Sigma_c} p dt \dots (71)$$

This cooling effect of the walls of the gun canal varies within a wide enough range (from 1% for 152 m/m gun to 15% for small arms).

Prof. M. Serebryakov gave his method for the evaluation

of $\left(\frac{\Delta T}{T}\right)$ without using the curves (p, t) and (c, t) as follows:

Since: $W_c \Delta_c = W_o \Delta_o = \omega$ and $p dt = dI$, then (71) can be rewritten:

$$\left(\frac{\Delta T}{T}\right) = \frac{C_m}{7.774} \cdot \frac{\Sigma_c}{\omega} \cdot \int_0^I \frac{\Sigma}{\Sigma_c} \cdot \frac{dI}{I_K} = \frac{C_m}{7.774} \cdot \frac{\Sigma_c}{\omega} \int_0^I \frac{\Sigma}{\Sigma_c} \cdot \frac{dI}{I_K} \dots (72)$$

but we have: $\varphi m dv = S p dt = S dI$

hence: $dI = \frac{\varphi m}{S} dv$ or: $I_K = \frac{\varphi m}{S} v'_K = \frac{\varphi m}{S} (v'_o + v'_K)$; $v'_K = v'_o + v'_K$

here v'_o is that velocity of the projectile which can be obtained at the moment when $\psi = \psi_o$ provided there was no previous engraving pressure p_o then:

$$v'_o = \frac{S}{\varphi m} I_o = \frac{S}{\varphi m} \int_0^{\psi_o} p dt, \text{ and: } \frac{dI}{I_K} = \frac{dv}{v'_K} = \frac{dv}{v'_o + v'_K}$$

and (72) will be:

$$\left(\frac{\Delta T}{T}\right) = \frac{C_m}{7.774} \cdot \frac{\Sigma_c}{\omega} \int_0^I \frac{\Sigma}{\Sigma_c} \cdot \frac{dv}{v'_o + v'_K} \dots (72')$$

Now from the list of definitions and notations we have:

No. 48. Working surface of the bore Σ_0 at the beginning ($t = t_0$)

No. 49. Final working surface of the bore Σ_c at the moment t_c .

No. 50. Working surface of the bore at any moment t and there are given the values of:

$$\frac{\Sigma}{\Sigma_0} = \frac{L_0 + L}{L_0} = 1 + \frac{L}{L_0}; \quad \frac{\Sigma}{\Sigma_c} = \frac{L_0 + L}{L_0 + L_c}$$

Thus (72') can be rewritten first for the case of heat losses during the travel of the projectile along the bore:

$$\frac{C_M}{7.774} \cdot \frac{\Sigma_0}{\omega} \cdot \int_0^x \frac{\Sigma}{\Sigma_0} \cdot \frac{dI}{I_K} = \frac{C_M}{7.774} \cdot \frac{\Sigma_0}{\omega} \cdot \int_0^v \frac{(L_0 + L) dv}{L_0(v'_0 + v'_K)} \dots (73)$$

and we have to add the heat losses in the chamber during the preliminary period (from $v = 0$ to $v = v'_0$).

$$\frac{C_M}{7.774} \cdot \frac{\Sigma_0}{\omega} \cdot \frac{I_0}{I_K} = \frac{C_M}{7.774} \cdot \frac{\Sigma_0}{\omega} \cdot \frac{L_0 v'_0}{L_0(v'_0 + v'_K)} \dots (74)$$

Summing up (73) and (74) we will have the relative lowering of the temperature through the emission of heat to the walls during the travel of the projectile along the whole gun canal:

$$\left(\frac{\Delta T}{T}\right) = \frac{C_m}{7.774} \cdot \frac{\sum_{\omega} \cdot \frac{\ell_0(v_0 + v) + \int_{v_0}^v \ell dv}{\ell_0(v_0 + v_n)}} = \frac{C_m}{7.774} \cdot \frac{\sum_{\omega} \cdot \eta}{\omega} \quad (75)$$

At the beginning $v=0$ and (75) becomes identical with (70). At the end of the projectile travel $v=v_2$, and (75) will be:

$$\left(\frac{\Delta T}{T}\right) = \frac{C_m}{7.774} \cdot \frac{\sum_{\omega} \cdot \frac{\ell_0(v_0 + v_2) + \int_{v_0}^{v_2} \ell dv}{\ell_0(v_0 + v_n)}} = \frac{C_m}{7.774} \cdot \frac{\sum_{\omega} \cdot \eta_2}{\omega} \quad (76)$$

For the calculation of (76) we need only the curve (v, ℓ)

Fig. 110 (p. 225 in book) shows that η_2 is the ratio of

areas:
$$\eta_2 = \frac{a o e f h d a}{a b c d}$$

The rectangle $aghd a$ represents the heat losses within the chamber, the area $oefgo$ represents the heat losses in the rifled bore, the rectangle $aokda$ represents the heat losses during the preliminary period. The factor η_2 represents the ratio of total losses of heat through the walls of the whole gun canal (taking into account the gradual increase of the cooling surface) to the heat losses within the chamber at the end of burning. The factor η in (75) represents the above-mentioned ratio at any given moment. The Fig. 110 represents the curve (ℓ, v) where ℓ is a function of the independent variable : Fig. 111 represents the curve

(v, ℓ) where v is a function of independent variable ℓ .

Then the ratio h in terms of the curve (v, ℓ) will be

$$h = \frac{\ell_0(v'_0 + v) + v\ell - \int v d\ell}{\ell_0(v'_0 + v_K)} \dots (75')$$

and:

$$h_2 = \frac{\ell_0(v'_0 + v_2) + v_2\ell_2 - \int v d\ell}{\ell_0(v'_0 + v_K)} \dots (76')$$

There are Tables (Chief artillery Board Tables) in

which v_K is given as a function of ℓ in terms of

$\frac{\ell}{\ell_0} = \Lambda$ with $\varphi = 1.05$. Introducing $v_i = v'_0 + v_K = \frac{S I_K}{\varphi m}$;

$$f = 950000; g = 9.81; \sqrt{f \cdot g} = 995$$

Then we will have (75'): $h = \frac{v(1+\Lambda) - \int v d\Lambda}{v_i} = (1+\Lambda) \frac{v}{v_i} - \int \frac{v}{v_i} d\Lambda$

$$\text{now: } \frac{v}{v_i} = \frac{v_{\text{tab}} \cdot \sqrt{\varphi \frac{g}{f}} \cdot \varphi m}{S I_K} = \frac{v_{\text{tab}}}{\sqrt{f \cdot g}} \cdot \frac{1}{\sqrt{B}}, \text{ here } B = \frac{S^2 I_K g}{f \varphi^2 m^2}$$

$$\text{or: } \frac{v}{v_i} = \frac{v_{\text{tab}}}{955 \sqrt{B}}$$

Then (75') will be:
$$\eta = \frac{1}{955\sqrt{B}} \left[(1+\lambda) v_{ke} - \int_0^{\lambda} v_{ke} d\lambda \right]$$

and (76')
$$\eta_a = \frac{1}{955\sqrt{B}} \left[(1+\lambda_a) v_{ke} - \int_0^{\lambda_a} v_{ke} d\lambda \right]$$

Note: in calculations of $\frac{\Sigma_o}{\omega} = \frac{\Sigma_o}{W_o \Delta_o}$ the values of Σ_o and W_o are taken in cm^2 and cm^3 .

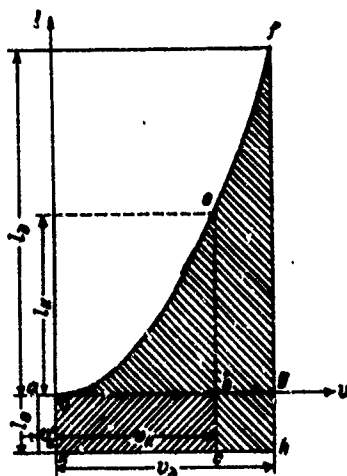


Fig. 110
Scheme of the evaluation of $(\frac{\Delta T}{T})\%$ when l is a function of v .

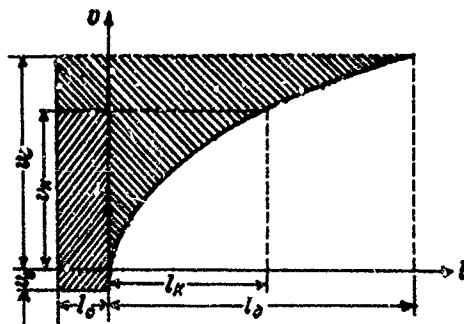


Fig. 111
Scheme of the evaluation of $(\frac{\Delta T}{T})\%$ when v is a function of l .

Table 26 gives the results calculated for the 76 m/m gun type 1900 with the strip powder ($2e_s = 1.03$ m/m) and

$C_M = 4.6\%$ for various ω and Δ .

Factor $\frac{C_M}{7.774} \cdot \frac{\Sigma_0}{W_0} \cdot \frac{1}{\Delta}$ is denoted by K_T

$$\text{then: } \left(\frac{\Delta T}{T}\right)\% = K_T \cdot h_0$$

Table 26

ω	= 1.041	0.892	0.725	0.558
Δ	= 0.613	0.525	0.426	0.328
h_N	= 1.36	1.51	1.75	2.24
h_0	= 3.01	2.83	2.54	2.11
$\left(\frac{\Delta T}{T}\right)_N\%$	= 0.75	0.98	1.39	2.32
$\left(\frac{\Delta T}{T}\right)_0\%$	= 1.67	1.83	2.00	2.18
$(C_N + C_0)$	= 7.79	9.98	14.23	25.05
K_T	= 0.553	0.646	0.795	1.034

Similar calculations for various calibers show that increase in caliber cuts down the heat losses on account of decrease in $\frac{\Sigma_0}{W_0}$. For small arms $\left(\frac{\Delta T}{T}\right)\% \sim 10\%$

and can be reduced by taking smaller $f = R T_i$, i.e. a lower temperature T_i . For guns having caliber from 37 m/m to 76 m/m the heat losses are 2 - 3 % which is

the same amount evaluated in the experiments with the
manometric bomb. This f determined in a bomb

can be applied to a gun without any correction for
the heat losses.

SECTION V - The Outflow of Gases from the Gun

General Remarks

The principal equations of Interior Ballistics make it possible for us to describe the travel of the projectile up to the moment of its leaving the muzzle of a gun.

But the gas action does not cease at the moment of ejection of the projectile. For a certain definite interval of time after that moment the projectile, as well as the gun, are still under the influence of the so called "after-effect" of the powder gases continuing their pressure on the projectile and on the barrel of the gun. During the period when the projectile is within the bore we know how it is possible to establish with some approximation under certain conditions the relationship between the pressure acting on the bottoms of a gun barrel and on the base of the projectile. As soon as the projectile is out of a bore together with certain part of gases the gas action on the projectile becomes abruptly changed because the gases are not any longer within the tube and another part of gases is still within that tube. The gases left in the bore

continue their motion from the bottom of the chamber to the muzzle and, only after passing through the muzzle are they dispersed into the air outside of the bore. As a reaction to this motion of the gaseous mass the mechanical recoiling mass increases its acceleration in opposite direction and the actual maximum of the velocity of a projectile and the velocity of the recoiling system are reached after the time when the projectile leaves the gun.

While almost the whole mass of gases continues its action on the barrel of the gun, only a small central part of the gases continues its action on the base of the projectile with a larger part of gases outrunning the projectile and dispersing in the air around it.

But this comparatively small increase of the actual muzzle velocity is not to be entirely neglected because very delicate mechanisms in time fuses and detonators are beginning their functioning exactly during this period.

But not only for the complete and accurate knowledge of the influence of the "after-effect" on the projectile and recoiling system we need a detailed

study of the gas dynamics. There are several other important practical applications of the theory of gas flow through various orifices:

1. Automatic arms with powder gases deflected from the bore.
2. Guns with a separate burning chamber and separate nozzles. (Gas dynamic or hydrodynamic guns)
3. Recoilless guns.
4. Guns with muzzle-brakes.
5. Mine throwers.
6. Special manometric bombs with nozzles.
7. Chambers for the jet-projectiles or rockets.

In all these cases we have the gas outflow under the high pressure through various orifices and channels. All the sought for relationships are found first for the simplest elementary cases. Only after the introduction of more and more restricting conditions and more experimental corrections we and more accurate, practicable results be obtained.

Chapter 1 - General Information on the Gas Dynamics

1. Velocity of the outflow of gases.

Denoting: U, V, W - projections of the gas velocity on the coordinate axes.

X, Y, Z - projections of the external forces on the same axes.

ρ - density of unit mass of gas

p - the pressure

The basic Euler's equation of the hydrodynamics along the x -axis will be

$$\frac{dU}{dt} = \frac{\partial U}{\partial t} + U \frac{\partial U}{\partial x} + V \frac{\partial U}{\partial y} + W \frac{\partial U}{\partial z} = X - \frac{1}{\rho} \cdot \frac{\partial p}{\partial x} \quad (77)$$

The analogous equations can be written for the other axes.

We will consider one dimensional motion along the x -axis produced by the pressure difference in the absence of the external forces ($X = 0$):

$$\frac{dU}{dt} = \frac{\partial U}{\partial t} + U \frac{\partial U}{\partial x} = - \frac{1}{\rho} \cdot \frac{\partial p}{\partial x} \quad (78)$$

For stationary motion $\frac{\partial U}{\partial t} = 0$; U and p are functions of x only, so:

$$U \cdot \frac{dU}{dx} = - \frac{1}{\rho} \cdot \frac{dp}{dx} \text{ or: } - \frac{dp}{\rho} = U dU = a \left(\frac{U^2}{2} \right)$$

Exchanging the density ρ in terms of weight or

$\rho = \frac{1}{W}$ where W is the specific volume of the gas we

will have:

$$-W dp = d\left(\frac{U^2}{2}\right) \dots (79)$$

Denoting W_1 , velocity U_1 and pressure p_1 of the vessel from which the gas flows out by the subscripts 1 we, after integration of (79), will have:

$$-\int_{p_1}^p W dp = \int_{p_1}^p W dp = \frac{U_1^2 - U^2}{2g} \dots (80)$$

Considering an adiabatic process for which

$$\rho W^\kappa = \rho_1 W_1^\kappa = \text{const.}$$

hence: $W = \frac{1}{\rho^\frac{1}{\kappa}} = W_1 \left(\frac{p_1}{p}\right)^\frac{1}{\kappa}$

Then: $\int_{p_1}^p W dp = W_1 p_1^\frac{1}{\kappa} \int \frac{dp}{p^\frac{\kappa+1}{\kappa}} = \frac{U_1^2 - U^2}{2g}$

or: $W_1 p_1^\frac{1}{\kappa} \cdot \frac{\kappa}{\kappa-1} \left(p_1^\frac{\kappa-1}{\kappa} - p^\frac{\kappa-1}{\kappa} \right) = \frac{\kappa}{\kappa-1} p_1 W_1 \left[1 - \left(\frac{p}{p_1} \right)^\frac{\kappa-1}{\kappa} \right] = \frac{U_1^2 - U^2}{2g}$

This is Saint Venant's formula:

$$U = \sqrt{U_1^2 + \frac{2g\kappa}{\kappa-1} p_1 W_1 \left[1 - \left(\frac{p}{p_1} \right)^\frac{\kappa-1}{\kappa} \right]} \dots (81)$$

If the gas flows out of a large vessel and $U_1 = 0$ then we will have the gas velocity U for the gas flowing

from the vessel at pressure p_i into space at pressure p :

$$U = \sqrt{\frac{2gK}{K-1} \cdot p_i W_i \left[1 - \left(\frac{p}{p_i} \right)^{\frac{K-1}{K}} \right]} \dots \dots (82)$$

If $p = 0$ (the gas flows into a vacuum) then :

$$U_{\max} = \sqrt{\frac{2gK}{K-1} p_i W_i}$$

$$\text{but : } \sqrt{gK p_i W_i} = \sqrt{gK R T_i} = C_i$$

(velocity of sound corresponding to the state of gas with $p_i W_i$ and T_i .)

$$\text{Hence } U_{\max} = \sqrt{\frac{2}{K-1}} \cdot C_i$$

Thus (82) will be:

$$U = C_i \sqrt{\frac{2}{K-1} \left[1 - \left(\frac{p}{p_i} \right)^{\frac{K-1}{K}} \right]}$$

Fig. 112 shows how the velocity U varies as a function

of $\left(\frac{p}{p_i} \right)$; at $p = 0$, $U = U_{\max}$. With the increased $\left(\frac{p}{p_i} \right)$ (the antipressure p working against the gas flow) U is decreasing and at $p = p_i$, $U = 0$. There is a point of inflexion at $x_{cr} = \left(\frac{p}{p_i} \right)_{cr}$ and U_{cr} (critical values).

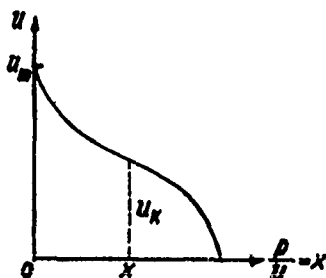


Fig. 112 U as a function of $\frac{p}{p_1} = x$

2. Weight of a discharge of the gas at the unit of time - 1 sec: G_{sec} .

$$G_{sec} = S \rho U = S \rho \sqrt{\frac{2gK}{K-1} \cdot \frac{p_1}{w_1} \left[1 - \left(\frac{p}{p_1} \right)^{\frac{K+1}{K}} \right]} \quad (83)$$

here S is the cross-section of area of the flow, and ρ density of the gas. Inserting $\rho = \frac{1}{w} = \frac{1}{w_1} \left(\frac{p}{p_1} \right)^{\frac{K}{K-1}}$

we will have:

$$G_{sec} = S \sqrt{\frac{2gK}{K-1} \cdot \frac{p_1}{w_1}} \sqrt{\left(\frac{p_1}{p} \right)^{\frac{2}{K}} - \left(\frac{p}{p_1} \right)^{\frac{K+1}{K}}} \quad \dots (84)$$

(Zeiner's formula)

Denoting: $\frac{p_1}{p} = x$ and $\sqrt{\frac{2gK}{K-1} \cdot \frac{p_1}{w_1}} = a$,

we will have : $G_{sec} = a \cdot S \sqrt{x^{\frac{2}{K}} - x^{\frac{K+1}{K}}} = a \cdot S f(x)$

At the steady motion of gas G_{sec} is constant ,

Therefore: $S f(x) = \frac{G}{a_i} = \text{Const.}$

and: $S = \frac{\text{Const}}{f(x)}$

i.e. the cross-section of the flow varies in inverse proportion to $f(x)$. The function $f(x)$ has its maximum at: $x_{cr} = \frac{p_{cr}}{p_i} = \left(\frac{2}{K+1}\right)^{\frac{K}{K+1}}$

then S will be at its minimum and G_{cr} will be at its maximum. This ratio $\left(\frac{p_{cr}}{p_i}\right)$ is called a critical pressures ratio and the corresponding minimum of S_m is called "critical cross-section" of the flow.

The value of x_{cr} is a function of K (see Table 27)

Table 27

$K =$	1.41	1.30	1.25	1.20	1.10
$x_{cr} = \left(\frac{2}{K+1}\right)^{\frac{K}{K+1}} =$	0.527	0.546	0.555	0.565	0.585

Putting $x_{cr} = \left(\frac{2}{K+1}\right)^{\frac{K}{K+1}} = \frac{p_{cr}}{p_i}$ in (82) we will have:

$$U_{cr} = \sqrt{\frac{2gKp_i w_i}{K+1}} = \sqrt{\frac{2}{K+1}} C_i$$

since: $p_i w_i = p_{cr} w_{cr} \cdot \frac{K+1}{2}$

then: $U_{cr} = \sqrt{gKp_{cr} w_{cr}} = C_{cr}$ (Sound velocity at p_{cr}, w_{cr})

Now if we substitute $x_{cr} = \frac{p_{cr}}{p_i} = \left(\frac{2}{K+1}\right)^{\frac{K}{K+1}}$ and $S = S_m$ (minimum) in the formula (84) we will have the following value of the discharge G_{cr} at the critical pressure and critical velocity:

$$G_{cr} = S_m \cdot (x_{cr})^{\frac{1}{K}} \cdot \sqrt{\frac{2gK}{K+1} \cdot \frac{p_i}{w_i} \left[1 - x_{cr}^{\frac{K+1}{K}}\right]} = K_0 S_m \sqrt{\frac{p_i}{w_i}}$$

Here the coefficient $K_0 = \sqrt{\frac{2gK}{K+1}} \left(\frac{2}{K+1}\right)^{\frac{1}{K+1}}$ is almost a constant as it is shown in Table 28.

Table 28

$K = 1.25 \quad 1.20 \quad 1.15 \quad 1.10 \quad 1.41$

$K_0 = 6.518 \quad 6.424 \quad 6.325 \quad 6.224 \quad 6.797$

G_{cr} can be rewritten as: $G_{cr} = \frac{K_0 S_m p_i}{\sqrt{f}}$ because

$$p_i w_i = RT = f \quad \text{or:} \quad G_{cr} = A S_m p_i \dots (85)$$

Here: $\frac{K_0}{\sqrt{f}} = A$ - a constant depending on the nature of powders and their temperatures T_i .

S_m - minimum section of the gas flow.

p_i - the pressure under which the gas is flowing out of a vessel.

The coefficient A is a characteristic of G_{sc} at $S = 1$ and $p_i = 1$ (its dimension is sec.^{-1}).

When the gas is emitted from a vessel the temperature within the vessel T is always lower than T_0 and $p_i W = RT$ where $T < T_0$.

Therefore it will be more correct to write :

$$G_{sc} = \frac{K_0 \cdot S_m}{\sqrt{A W}} p_i = \frac{K_0 S_m p_i}{\sqrt{RT}} = \frac{K_0}{\sqrt{T}} \cdot S_m A = \frac{A}{\sqrt{T}} \cdot S_m \cdot p_i \cdot c \cdot \frac{T}{T_0}$$

Table 29 for $A = \frac{K_0}{\sqrt{T_0}}$

f	$K = 1.1$	1.2	1.5
1,000,000	0.00622	0.00642	0.00661
900,000	0.00656	0.00677	0.00697
850,000	0.00675	0.00695	0.00717
800,000	0.00695	0.00718	0.00739

The coefficient A has been introduced by V.H.Trofimov; for the pyroxilin powders $A = 0.007$ and for the nitro-glycerin powders $A = 0.006$.

3. The total mass expenditure of gases.

The total mass expenditure of gas Y for a time t is:

$$Y = \int_0^t G_{sc} dt$$

Since we have had that: $G_{sc} = A S_m p_i$

here - p is the pressure in the vessel

S_m is the orifice of the outlet.

If we have a bomb with a nozzle and the pressure within the bomb is generated by the burning powder then we can write: $Y = A S_m \int_0^t p dt = A S_m I$, but $I = \frac{G}{u}$,

then: $Y_K = A S_m I_K = A S_m \frac{G}{u}$, at the end of burning.

This formula is very well verified by experiments in a bomb used for burning of powder grains in the form of cylinders with perforations having diameters from 1 m/m to 3 m/m and at the pressures $p_m = 2000-2500 \text{ Kg/cm}^2$.

4. The relationship between the pressure and the cross-section of the gas flow.

When the gases flow out through a conical nozzle, the pressure is decreased in the direction of flow and the velocity of flow is increased

Since $G_{cr} = G_x$ where G_x is the discharge at the cross-section S_x and G_{cr} is discharged at a critical cross-section, then using the equation of continuity we can write: $\frac{S_m u_{cr}}{W_{cr}} = \frac{S_x u_x}{W_x}$

Here S_m - the orifice of the nozzle

S_x - the cross-section where $x = \frac{p}{p_0}$

But: $\frac{S_m U_{en}}{W_{en}} = S_m K_0 \sqrt{\frac{P_1}{W_1}} = S_m \left(\frac{2}{K+1}\right)^{\frac{1}{K+1}} \sqrt{\frac{2gK}{K+1} \cdot \frac{P_1}{W_1}}$

and from (84): $\frac{S_x U_x}{W_x} = S_x \sqrt{\frac{2gK}{K-1} \frac{P_1}{W_1}} \sqrt{x^{\frac{1}{K}} (1-x^{\frac{K+1}{K}})}$

Therefore: $S_x x^{\frac{1}{K}} \sqrt{\frac{1-x^{\frac{K+1}{K}}}{K-1}} = S_m \left(\frac{2}{K+1}\right)^{\frac{1}{K+1}} \sqrt{\frac{1}{K+1}}$

and: $\frac{S_x}{S_m} = \left(\frac{2}{K+1}\right)^{\frac{1}{K+1}} \cdot \frac{\sqrt{\frac{K-1}{K+1}}}{x^{\frac{1}{K}} \sqrt{1-x^{\frac{K+1}{K}}}} \dots (86).$

Here the relative cross-section $\left(\frac{S_x}{S_m}\right)$ is given as a function of the relative pressure $x = \left(\frac{P}{P_1}\right)$ beyond the minimum orifice S_m .

Table 30 for $\left(\frac{S_x}{S_m}\right)$ as a function of x and K .

$\frac{x}{K}$		1/2	1/3	1/4	1/5	1/6	1/10	1/15	1/20
1.1	1.0	1.018	1.180	1.373	1.560	1.762	2.500	3.364	4.180
1.2	1.0	1.010	1.143	1.309	1.477	1.639	2.260	2.967	3.625
1.25	1.0	1.007	1.128	1.282	1.438	1.590	2.162	2.802	3.405
1.3	1.0	1.005	1.115	1.258	1.404	1.545	2.075	2.670	3.214
1.4	1.0	1.002	1.093	1.218	1.346	1.470	1.931	2.440	2.900

5. The reactive force developed in the vessel which is losing gases through the orifice in its wall.

Fig. 113 shows a vessel with gases under a pressure p acting on each element s of the inner surface. The outer pressure p_a of the atmosphere is acting in the opposite direction. If the orifice having its cross-sectional area S is open then the gases begin to flow out of the vessel and the vessel will be under the effects of the two following forces:

1. Force $R' = S(p - p_a)$ which acted before the opening of the orifice; $R' \sim Sp$.
2. Force R'' caused by the outflow of the mass of gases and is determined by the "linear momentum principle":

$$U dm = R'' dt$$

$$\text{or: } U \frac{0}{g} S U dt = R'' dt$$

$$\text{hence: } R'' = \frac{G_{sec}}{g} U.$$

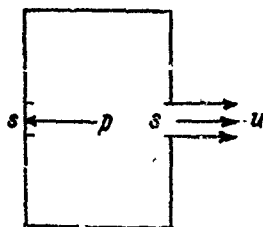


Fig. 113 Schematic view of the outflow of gases from the vessel and the reactive force acting on the vessel.

Thus the total reactive force $R = P' + R'' = p + \frac{G_{sm}}{g} U$

The assumption is made that there is no displacement of gases within the vessel ($U_i = 0$) and if the vessel is sufficiently large then the total momentum of gaseous mass is not changed.

The formula for R being referred to the opening S_a of the expanding nozzle with $p = p_a$ and $U = U_a$ will be:

$$R = \frac{G_{sm}}{g} U_a + S_a p$$

Now G_{sm} , U_a , S_a , p_a should be referred to the minimum cross-section S_m and the inner pressure p_i in formulae (82, and (86). Thus we will have:

$$R = \frac{G_{sm}}{g} U_a + p_a S_a = \frac{S_m}{g} \cdot \sqrt{gK} \left(\frac{2}{K+1} \right)^{\frac{K+1}{2}} \sqrt{\frac{p_i}{\rho_i}} \sqrt{\frac{2gK}{K+1}} \sqrt{\rho_i K} \sqrt{1 - \left(\frac{p_a}{p_i} \right)^{\frac{K+1}{K}}} + \frac{p_a}{p_i} \cdot p_i \cdot \frac{S_a}{S_m} S_m = K x_m \sqrt{\frac{2gK}{K+1}} \sqrt{1 - x_a^{\frac{K+1}{K}}} \left[1 + \frac{K+1}{K} \cdot \frac{x_a^{\frac{K+1}{K}}}{1 - x_a^{\frac{K+1}{K}}} \right] p_i S_m \quad (8)$$

here: $x_a = \frac{p_a}{p_i}$ and $x_m = \left(\frac{2}{K+1} \right)^{\frac{K}{K+1}}$

Here we have K , x_a , p_i , S_m as factors affecting the value of R but only p_i and S_m are involved in a

directly proportional influence on the value of R .

We may rewrite R in this way:

$$R = \gamma \cdot S_m p_1$$

$$\text{here } \gamma = K \left(\frac{2}{K+1} \right)^{\frac{K}{K-1}} \sqrt{\frac{K+1}{K-1}} \sqrt{1 - x_a^{\frac{K}{K-1}}} \left[1 + \frac{K-1}{2K} \cdot \frac{x_a^{\frac{K}{K-1}}}{1 - x_a^{\frac{K}{K-1}}} \right] \quad (88)$$

The coefficient γ for a given nozzle is affected only by the value of K . γ is not affected neither by Δ nor by p . This coefficient is called "a coefficient of the propulsive action" (Langevain). If there is not a special nozzle but an ordinary orifice then at

$$x_a = x_m = \left(\frac{2}{K+1} \right)^{\frac{K}{K-1}}$$

we will have:

$$\gamma_0 = K \left(\frac{2}{K+1} \right)^{\frac{K}{K-1}} \left(1 + \frac{K-1}{2K} \cdot \frac{\frac{2}{K+1}}{\frac{K-1}{K+1}} \right) = \frac{K+1}{2} \left(\frac{2}{K+1} \right)^{\frac{K}{K-1}} = \frac{K+1}{2} x_m \quad (89)$$

If the nozzle is an indefinitely large one and open into vacuum then $x = 0$

and

$$\gamma_{max} = K \sqrt{\frac{K+1}{K-1}} \left(\frac{2}{K+1} \right)^{\frac{K}{K-1}} = K \sqrt{\frac{K+1}{K-1}} \cdot x_m$$

Table 31 gives the values of γ corresponding to various values of $(\frac{S_a}{S_m})$ and $(\frac{d_a}{d_m})$ or ratios of the cross-sectional areas and diameters of the opening of the end of nozzle (a) to the minimum cross-section of the flow (m)

Table 31

$\frac{d_a}{d_m} =$	1	2	3	4	5	6
$\gamma =$	1.24	1.62	1.72	1.80	1.86	1.89
$\frac{S_a}{S_m} =$	1	4	9	16	25	36

From this table we observe that the reactive force R is considerably increased with the enlargement of the end of a nozzle d_a only to a certain degree; for the diameter d_a larger than $5d_m$ R is not any more as responsible as it is for $d_a < 4d_m$. In jet-projectiles $(\frac{d_a}{d_m}) \leq 3$

6. The principal formulas.

The velocity of the outflow:
$$U = \sqrt{\frac{2}{\gamma-1} \cdot p_m \left[1 - \left(\frac{p}{p_m} \right)^{\frac{\gamma-1}{\gamma}} \right]}$$

here p and W , are the pressure and specific volume of gases in the vessel from which the gases are discharged. The discharge in 1 sec. through the cross-section S_m is: $G_{\text{ex.}} = A p S_m$

Here:

$$A = \frac{K_2}{V_f} = F(K, f) \quad \begin{cases} A = 0.007 \text{ for pyroxylin powder} \\ A = 0.006 \text{ for nitroglycerin powder} \end{cases}$$

$$K = \frac{G_p}{G_w} = 1 + \theta$$

The discharge of gases as a function of time t :

$$Y = \int_0^t G_{sm} dt = A \cdot S_m \int_0^t p dt$$

If the gases are formed by the burning powder then:

$$\int_0^t p dt = \frac{p_0}{2} ; Y = A S_m \frac{p_0}{2}$$

$$\text{and } Y_K = A S_m \frac{p_0}{2}, \quad (\text{at the end of burning}).$$

$$\text{The reactive force } R = \frac{G_{sm}}{f} U + S p = 7 S_m p$$

When we have the case of gases discharged from a gun with a moving gaseous mass in the bore, then our assumption as to the constancy of the total momentum of gaseous mass in the vessel is not justified. We have to consider another term which corresponds to the increase of the momentum on account of the presence of $\frac{dI}{dt} = m \frac{U}{t} = \frac{G}{f} \cdot \frac{U}{t}$ which is the increase in the impulse, moving the mass m of the charge with a certain average velocity, say $\frac{U}{2}$ (assuming the linear law of the increase of gas velocities).

$$\text{Then } R = \frac{G_{sm}}{f} U + S p + \frac{dI}{dt}$$

Chapter 2 - The application of the principal formulas concerning the discharge of gases.

1. The discharge of gases from the vessel of a given volume. Suppose we have ω_{g} of gases in the volume W_0 . The initial state of the gases is determined by $p_1, T_1, W_1 = \frac{W_0}{\omega}$. We propose to find how the pressure and temperature will vary as functions of time.

We assume the adiabatic state of gases.

Then: $\left(\frac{p}{p_1}\right)^{\frac{\kappa}{\kappa-1}} = \frac{W_1}{W}$ but $W_1 = \frac{W_0}{\omega}$ and $W = \frac{W_0}{\omega - \int G_{\text{gr}} dt}$

Hence:
$$\left(\frac{p}{p_1}\right)^{\frac{\kappa}{\kappa-1}} = \frac{\omega - \int G_{\text{gr}} dt}{\omega} = 1 - \frac{1}{\omega} \int G_{\text{gr}} dt \dots (90)$$

here: $G_{\text{gr}} = K_0 S \sqrt{p}$

but: $\frac{p}{W} = \frac{p_1}{W_1} \left(\frac{p}{p_1}\right)^{\frac{\kappa+1}{\kappa}}$

then: $G_{\text{gr}} = K_0 S \sqrt{\frac{p_1}{W_1}} \cdot \left(\frac{p}{p_1}\right)^{\frac{\kappa+1}{2\kappa}}$

By differentiating (90), we have:

$$\frac{1}{\kappa} \cdot \frac{p^{\frac{1-\kappa}{\kappa}}}{p^{\frac{1}{\kappa}}} dp = - \frac{G_{\text{gr}}}{\omega} dt = - \frac{SK_0 \sqrt{\frac{p_1}{W_1}}}{\omega} \left(\frac{p}{p_1}\right)^{\frac{\kappa+1}{2\kappa}} dt$$

After separation of the variables:

$$\left(\frac{p}{p_1}\right)^{\frac{1-\kappa}{\kappa}} \cdot \left(\frac{p}{p_1}\right)^{\frac{\kappa+1}{2\kappa}} \frac{dp}{p_1} = - \frac{SK_0 \sqrt{\frac{p_1}{W_1}}}{\omega} dt$$

where we denote:

$$\frac{SK_0 \sqrt{\frac{p_1}{W_1}}}{\omega} = C$$

since $x = \frac{p}{p_1}$ or $dp = p_1 dx$
 then the left part will be: $x^{\frac{1-2K}{2K}}$

$$\text{Or: } \int x^{\frac{1-2K}{2K}} dx = -C \int dt$$

$$\text{Hence: } \frac{2K}{K-1} \left[1 - \frac{1}{x^{\frac{1}{K}}} \right] = -Ct, \text{ or: } t = \frac{1}{B'} \left[\frac{1}{x^{\frac{1}{K}}} - 1 \right]$$

$$\text{Here: } B' = \frac{K-1}{2} S_m \frac{K_0}{\omega} \sqrt{\frac{p_1}{W_1}}; K_0 = \sqrt{\frac{2gK}{K+1}} \left(\frac{2}{K+1} \right)^{\frac{1}{K}}$$

This time is required for discharging the gas out of the W which brings down the pressure from p_1 to p .

This relationship holds true up to the time when the ratio $\left(\frac{p}{p_1}\right)$ becomes "critical". If the discharge is made into the atmosphere, then critical $x_{cr} = \frac{p_{(at)}}{p_{cr}} = \left(\frac{2}{K+1}\right)^{\frac{K}{K-1}}$

$$\text{hence: } p_{cr} = \frac{p_{at}}{2.57} = 1.81 p_{cr}$$

The total time of discharge at x_{cr} will be:

$$t_{cr} = \frac{1}{B'} \left[\frac{1}{(x_{cr})^{\frac{1}{K}}} - 1 \right] \dots (91)$$

For various t we can calculate the values of p and thus the (p,t) curve can be computed.

Solving the formula for t with respect to $x = \frac{p}{p_1}$ we will have:

$$\text{from: } W = W_1 \left(\frac{p}{p_1} \right)^{\frac{K}{K-1}} \text{ and } T = \left(\frac{W_1}{W} \right)^{K-1} \quad p = \frac{p_1}{(1+B't)^{\frac{2K}{K-1}}} \dots (92)$$

$$\text{We have: } W = W_1 (1+B't)^{\frac{K}{K-1}} \dots (93) \text{ and: } T = \frac{T_1}{(1+B't)^{\frac{2K}{K-1}}} \dots (94)$$

From (94) and (92) we see that the decrease in temperature T is not so sharp as the decrease in pressure p .

2. The discharge of gases from the bore after the ejection of the projectile from the gun ($t = t_d$).

We can apply the above relationships to the gases left in the bore when the projectile has passed the muzzle. Within the total volume $(W_0 + s l_d)$ we have

ω of gases, i.e. the specific volume of gases

$$W_g = \frac{W_0 + s l_d}{\omega} = \frac{A_2 + 1}{\Delta}$$

here: $A = \frac{C}{C_0}$; $A_2 = \frac{C_2}{C_0}$; $\Delta = \frac{\omega}{\omega_0}$

At the beginning the gas pressure is p_0 ; temperature T_0 , cross-sectional area of the opening S .

$$\text{Taking } B' = \frac{\kappa-1}{\kappa} K_0 \sqrt{\frac{p_0}{W_0}} \cdot \frac{S}{\omega} = \frac{\kappa-1}{\kappa} K_0 \frac{S}{\omega} \sqrt{\frac{p_0 \Delta}{A_2 + 1}}$$

we can write the following expressions for:

1. Pressure: $p = \frac{p_0}{(1 + B' t)^{\frac{\kappa}{\kappa-1}}}$

2. Temperature: $T = \frac{T_0}{(1 + B' t)^2}$

3. Time of discharge: $t = \frac{1}{B'} \left[\left(\frac{p_0}{p} \right)^{\frac{\kappa-1}{\kappa}} - 1 \right]$

All these formulas are valid up to the moment when

$$x = x(\text{critical}) = 0.565-0.545; \text{ i.e. when } p_{\text{cr}} = 1.8 \frac{\text{atm}}{\text{cm}^2} = \frac{1 \text{ atm}}{0.57}$$

The full time of the discharge: $t_{ac} = \frac{1}{B'} \left[\left(\frac{P_0}{P_2} \right)^{\frac{K_0}{K_0-1}} - 1 \right]$

Example: 76% gun. $S = 0.4693 \text{ dm}^2$; $A_0 = 9.0$; $\omega = 1.080 \text{ kg}$; $\Delta = 0.70$
 $T_0 = 2800$; $p_0 = 600 \text{ kg/cm}^2$; $K = 1.2$; $K_0 = 6.424$; $\frac{P_0}{P_2} = 333.3$; $\frac{K_0}{K_0-1} = \frac{1}{1.2}$
 $B' = \frac{2}{3} (6.424) \frac{0.4693}{7000} \sqrt{\frac{2800 \cdot 0.70}{9.0}} = 18.10$; $t_{ac} = 0.03443$.

The time of discharge till the pressure will be 20 atm.

$$t_{20} = \frac{1}{18.10} \left[\left(\frac{600}{20} \right)^{\frac{1}{1.2}} - 1 \right] = 0.01807$$

$$H T_0 = 0.7 T_0 = 1960 \text{ K}^2$$

$$H_{eff} T_{eff} = \frac{1960}{(1 + 18.10(0.03443))^2} = 744 \text{ K}^2 = 471^\circ \text{C}$$

3. The after-effect of powder gases acting on the recoiling mass.

The reactive force R (87, 88) imparts a velocity V to the recoiling mass Q_0 ; this velocity reaches its maximum V_{max} after the moment t_n when the projectile leaves the muzzle. See Fig. 114.

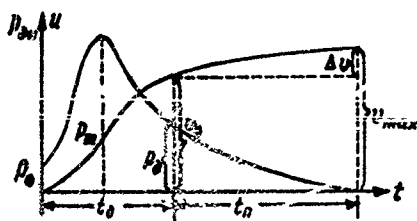


Fig. 114 - The velocity of the recoiling mass as a function of time (t) during the "After-effect" period ($t_n - t_0$.)

During this period of the after-effect ($t_n = t_p$) the velocity of the recoiling mass V is increased from V_p to V_m .

We have already seen that the velocity V of the recoiling mass is given by: $V = \frac{2 + \frac{1}{2}\omega}{Q_0 + \frac{1}{2}\omega} v_a$, where v_a

is the absolute velocity of the projectile.

For the moment when the projectile leaves the muzzle:

$V_p = \frac{2 + \frac{1}{2}\omega}{Q_0} v_a$. ($\frac{1}{2}\omega$ is very small in comparison with Q_0). For the period of time from t_p to t_n the momentum equation will give:

$$\frac{Q_0}{g} V_m - \frac{Q_0}{g} V_p = \int_0^{t_n} R dt \quad \dots (95)$$

If we have to consider the presence of a special braking force F , then:

$$\frac{Q_0}{g} V_m - \frac{Q_0}{g} V_p = \int_0^{t_n} R dt - \int_0^{t_n} F dt \dots (95')$$

The following assumptions can be introduced for the simplification of the problem:

1. The cross-section S of the bore is the "critical" cross-section.
2. The velocity of gases at the moment t_p is the velocity v_a of the projectile.
3. An additional effect (negative) of the decreased average velocity of the gases from $U = \frac{v_a}{2}$ to 0.

$$\text{Thus: } \int_0^{t_n} R dt = \gamma_0 S \int_0^{t_n} \rho dt + \frac{\omega}{g} \int_0^{t_n} \frac{dU}{v_{20}} = \gamma_0 S \int_0^{t_n} \rho dt - \frac{\omega}{g} \cdot \frac{v_{20}}{2}$$

here:

$$\gamma_0 = (\kappa + 1) \chi_{en} \sim 1.22 - 1.24 \dots (69)$$

$$\text{From (92) we have: } \rho = \frac{\rho_0}{(1 + B't)^{\frac{\kappa+1}{\kappa}}}$$

$$\text{here: } B' = \frac{\kappa-1}{2} K_0 \frac{S}{\omega} \sqrt{\frac{\rho_0 \Delta}{\lambda_0 + 1}}$$

$$\text{then: } \int_0^{t_n} R dt = \gamma_0 S \rho_0 \int_0^{t_n} \frac{dt}{(1 + B't)^{\frac{\kappa+1}{\kappa}}} - \frac{\omega}{g} \cdot \frac{v_{20}}{2}$$

$$\text{or: } \int_0^{t_n} R dt = \frac{\gamma_0 S \rho_0}{B'} \cdot \frac{\kappa+1}{\kappa} \left[1 - \frac{1}{(1 + B't)^{\frac{\kappa+1}{\kappa}}} \right] - \frac{\omega}{g} \cdot \frac{v_{20}}{2}$$

Now assuming $\left[1 - \frac{1}{(1 + B't)^{\frac{\kappa+1}{\kappa}}} \right] \sim 1$ and substituting expression

for B'

$$\text{we will have: } \int_0^{t_n} R dt = \frac{\gamma_0 2 \omega \rho_0}{K_0 (\kappa + 1)} \cdot \sqrt{\frac{\lambda_0 + 1}{\rho_0 \Delta}} - \frac{\omega}{g} \cdot \frac{v_{20}}{2}$$

$$\text{Remembering that: } \gamma_0 = (\kappa + 1) \left(\frac{2}{\kappa + 1} \right)^{\frac{\kappa}{\kappa+1}} \text{ and } K_0 = \left(\frac{2}{\kappa + 1} \right)^{\frac{1}{\kappa+1}} \frac{\kappa + 1}{\sqrt{\kappa}}$$

$$\text{and having in view that: } \rho_0 \sqrt{\frac{\lambda_0 + 1}{\rho_0 \Delta}} = \sqrt{\rho_0} \frac{w_c}{\Delta} = \sqrt{\rho_0} w_0$$

$$\text{and } \sqrt{g \kappa \rho_0 w_0} = C_0 \text{ (velocity of sound)}$$

$$\text{We will have: } \int_0^{t_n} R dt = \frac{2}{\kappa} \cdot \left(\frac{2}{\kappa + 1} \right)^{\frac{1}{\kappa}} \frac{\omega}{g} \cdot C_0 - \frac{\omega}{g} \cdot \frac{v_{20}}{2}$$

and now from (95) we have:

here:
$$\frac{Q_0}{\rho} V_m = \frac{Q_0}{\rho} V_d + \frac{2}{K} \left(\frac{2}{K\omega} \right)^{\frac{1}{2}} \frac{\omega}{\rho} C_d - \frac{\omega}{\rho} \frac{V_{da}}{2}$$

$$V_d = \frac{2 + \frac{1}{2}\omega}{Q_0} V_{da}$$

And thus finally:
$$V_m = \frac{2 + \beta\omega}{Q_0} V_{da} + \frac{2}{K} \left(\frac{2}{K\omega} \right)^{\frac{1}{2}} \frac{\omega}{Q_0} C_d - \frac{\omega}{Q_0} \frac{V_{da}}{2}$$

or:
$$V_m = \frac{2 + \beta\omega}{Q_0} V_{da} = \frac{2}{Q_0} (1 + \beta \frac{\omega}{2}) V_{da}$$

where: $\beta = \frac{2}{K} \left(\frac{2}{K\omega} \right)^{\frac{1}{2}} \frac{C_d}{V_{da}^2}$ is the coefficient of the after-effect of gases acting on the recoiling mass.

Since C_d varies within a narrow range we may say that V_{da} or the muzzle velocity of the projectile is a dominating factor in the value of β .

At $K = 1.2$; $\beta = 1.59 \frac{C_d}{V_{da}^2}$ here: $C_d = 10.85 \sqrt{\frac{P_d(A+1)}{\Delta}}$

at $K = 1.25$; $\beta = 1.51 \frac{C_d}{V_{da}^2}$ and $C_d = 11.06 \sqrt{\frac{P_d(A+1)}{\Delta}}$

These values of β are the results of the above shown theoretical approach but there are also empirical values of β :

$$\beta_1 = \frac{1400}{V_{da}^{1/5}} + 0.15 \quad \text{and} \quad \beta_2 = \frac{1200}{V_{da}}$$

Example: 76 mm gun. $\rho_g = 600 \text{ kg/cm}^3$; $A_g + 1 = 10$; $\Delta = 0.70$; $2k = 680 \text{ m/sec}$.

$$V_m = \frac{1}{80} (1 + 2.35 \cdot 0.16) 680 - \frac{1.376}{80} \cdot 680 = 11.7 \text{ m/sec.}$$

$$\beta = 1.59 (10.85) \sqrt{\frac{60000 \cdot (10)}{0.70}} \cdot \frac{1}{6800} = 2.35; Q_0 = 80 \text{ g}; \frac{\omega}{2} = 0.16$$

$$\beta_1 = \frac{1400}{680} + 0.15 = 2.21; \beta_2 = \frac{1300}{680} = 1.912$$

at higher velocity:

$$2k = 1000 \text{ m/sec}; A_g + 1 = 5.0; \Delta = 0.72; \rho_g = 1200$$

$$\beta = 1.59 (10.85) \sqrt{\frac{120000 \cdot (5)}{0.72}} \cdot \frac{1}{10000} = 1.575; Q_0 = 150 \text{ g}; \frac{\omega}{2} = 0.5$$

$$\beta_1 = \frac{1400}{1000} + 0.15 = 1.55; \beta_2 = \frac{1300}{1000} = 1.3; V_m = 11.92.$$

4. The "after-effect" of the powder gases action upon the projectile.

So far we have not yet results of exhaustive experimental investigations of the variations of pressures and velocities within the gas flow ejected from the gun. Results obtained on the basis of gas dynamics present only approximate evaluation of velocity of gases without any accounting for distorting effects caused by the presence of solid particles.

Thus so far we must admit that the problem is still far from a comprehensive solution and that our efforts should be directed to the development of new methods in studying the after-effect period as well as studying and evaluating the error involved in these experimentations. It is not amiss to note that the critical

examination of the experimental results or photographic and cinematographic pictures of the bullets or projectiles not infrequently reveals some contradictions or inconsistencies of these data.

Chapter 3 - Burning of powder in partially closed volume.

1. Gas pressure during the partial escape of the gases through a nozzle.

Such a process takes place in the following cases:

1. Burning of powder in a special manometric bomb having a nozzle constructed for the experimental study of conditions analogous to the actual firing conditions in a gun.
2. Burning of powder in a separate chamber of a gasodynamic gun.
3. Burning of powder in the chamber of a rocket-projectile.

In all these cases the inflow of gases is formed by the burning of powder gases together with the outflow of gases through the nozzle. Hence the pressure can rise as well as fall. The lower the pressure, the easier it is to maintain it at the same level. We will begin with the case of the high pressure when the law

of the rate of burning $u = u, p$ is valid.

Our problem is to derive a formula for the gas pressure within the constant volume W_0 at a given moment of time with the gases escaping through the nozzle.

We denote the discharge of gas up to the given moment (in kg.) Y and the ratio $\frac{Y}{\omega} = \eta$

We have already had the formula for the discharge:

$$Y = \int_0^t G_m dt \quad \text{at the constant pressure } p$$

Here $G_m = A S_m p$; cross-section of the nozzle S_m

A is the coefficient of discharge.

We assume that $G_m = A S_m p$ holds true when p is variable; then: $Y = A S_m \int_0^t p dt = A S_m I$

and for the moment of the "burnt" we have:

$$Y_k = A S_m I_k = A S_m \frac{\varepsilon_1}{u_1}$$

Since I_k depends only on the web $2e$, and rate of burning u , (at the pressure 1) we may say that Y does not depend on the form of powder grain and its progressiveness. For the small enough S_m we may take

$\varphi = \frac{T}{\pi} \omega$. Then (13) will be rewritten for this case.

$$p = \frac{f(\omega\psi - Y)}{W_0 - \alpha(\omega\psi - Y) - \frac{\alpha}{\gamma}(1-\psi)} = \frac{f\omega(\psi - h)}{W_0 - \frac{\gamma}{\gamma-1}(1-\psi) - \alpha\omega(\psi - h)} = \frac{f\Delta(\psi - h)}{1 - \frac{\gamma}{\gamma-1}(1-\psi) - \alpha\Delta(\psi - h)} \quad (96)$$

For a large S_m the ratio $(\frac{T}{T_1})$ is the subject of special discussions.

At the end of burning $\psi = 1$; $h_K = \frac{Y_K}{\omega} = AS_m \cdot \frac{T_K}{\omega}$

$$P_K = \frac{f\omega(1-h_K)}{W_0 - \alpha\omega(1-h_K)} = \frac{f\Delta(1-h_K)}{1 - \alpha\Delta(1-h_K)} \quad \dots (97)$$

If we denote: $\Delta(1-h_K) = \Delta_K$

Then $P_K = \frac{f\Delta_K}{1 - \alpha\Delta_K} \dots (98)$. This is Noble's formula in which Δ_K is that density of loading at which in a closed volume the maximum pressure is $P_m = P_K$.

Hence we have a simple rule for the calculation of powder charge or the density of loading producing at the end of burning at a desired pressure P_K :

Using Noble's formula we calculate

$$\Delta_K = \frac{P_K}{f + \alpha P_K} \quad \text{and} \quad \omega_K = \frac{W_0 P_K}{f + \alpha P_K}$$

Thus from the formula $Y_K = AS_m T_K = AS_m \frac{e_1}{\omega_K}$ we calculate the weight of gas which is lost during the burning time of powder producing an impulse I_K .

Then $(\omega_K + \gamma_K)$ will be the full powder charge which during its burning in the bomb with a nozzle S_K will produce the desired pressure p_K . The value of $I_K = \int p dt$ we can find by the previous experiment in the closed bomb, because I_K for powders of simple form does not depend on Δ or on the mode of variation of p . Suppose we have the pressure in a closed bomb P and in a bomb with the nozzle p : the times are τ and t ; then $de = u, P d\tau$ and $de = u, p dt$ will be the thickness of burned powder. Since the times τ and t are different in inverse proportion to P and p hence:

$$P d\tau = p dt \quad \therefore I_K = \int p dt = \int P d\tau$$

Now knowing I_K and γ_K and having $I = \int p dt$ from the experimental curve, we can find h for every moment and find the corresponding ψ .

$$\text{Thus we will have: } \gamma = h\omega = \gamma_K \cdot \frac{I}{I_K} \quad \text{or: } h = \gamma_K \frac{I}{I_K}$$

Now having solved (96) with respect to ψ we will have:

$$\psi = \frac{p(\frac{1}{\alpha} - \frac{1}{\beta}) \cdot h(f + ap)}{f + p(\alpha - \frac{1}{\beta})} = \frac{\frac{1}{\beta} - \frac{1}{\alpha}}{\frac{f}{p} + \alpha - \frac{1}{\beta}} + \frac{f + ap}{f + (\alpha - \frac{1}{\beta})p} \cdot h$$

The first term in the right part is a regular expression for the part of charge ψ which during its burning in a closed bomb with the same Δ as in a chamber with a nozzle, will produce pressure p . The second term takes into account the effect of the outflowing gases.

The ratio η is a characteristic of the relative intensity of the outflowing gas or of the relative discharge of gases during the time of burning.

The larger S_m and I_K are the smaller ω is, the larger η is, but it is always smaller than 1.

2. Character of the pressure curve in a chamber with a nozzle having a small opening.

We will consider the case of a powder with the constant burning surface ($\alpha = 1.0$; $\lambda = 0$; $\beta = 1$).

Pressure at any moment is:

$$p = \frac{f\omega(\psi - \eta)}{W_0 - \frac{1}{2}(1 - \psi) - \alpha\omega(\psi - \eta)} = \frac{f\omega(\psi - \eta)}{W_\psi + \alpha\omega\eta}$$

Because of the discharge of gases the free volume during the burning is larger than the free volume in the case of a closed vessel and we conclude that the free volume ($W_\psi + \alpha\omega\eta$) varies less than W_ψ and we will take it as a certain average value $\overline{W_{av}}$.

$$\dot{W}_{av} = \dot{W}_{av} + \alpha \omega \frac{1}{\dot{h}_{av}} = \dot{W}_0 - \alpha' \omega + \alpha \omega \frac{h}{x}; \quad \frac{\dot{W}}{W_0} = \frac{1}{x}; \quad \frac{h}{h_0} = \frac{h}{x}$$

Then the pressure $p = \frac{f\omega}{W_{av}} (\psi - h) ; \quad h_{av} = \frac{AS_m I_n}{x\omega}$

Differentiating with respect to t and remembering that: for the powder with a constant burning surface or for strip powder: $x \epsilon_{av} = 1; \quad \frac{d\psi}{dt} = \frac{u}{\epsilon}; \quad p = \frac{p}{I_n}; \quad \frac{dh}{dx} = \frac{AS_m p}{\omega}$

~~We will have:~~ $\frac{dp}{dt} = \frac{f\omega}{W_{av} I_n} \left[\frac{1}{x} - \frac{AS_m}{\omega} \right] p = \frac{f\omega}{W_{av} I_n} (1 - h_n) p = \frac{1}{\epsilon} \cdot p$

Denoting $\frac{f\omega}{W_{av} I_n} (1 - h_n) = \frac{1}{\epsilon}$ (constant) and integrating:

$$\int \frac{dp}{p} = \frac{1}{\epsilon} \int dt$$

we will have: $\log_2 \left(\frac{p}{p_0} \right) = \frac{t}{\epsilon}$

or $p = p_0 e^{\frac{t}{\epsilon}}$ (see formula (41)).

We have the same formula we had before, when we were considering burning within a closed volume, but our present constant ϵ , corresponds not to the burning of ω kg. but of $\omega(1 - h_n) \text{ kg.}$ of powder at a density of loading $\Delta_n = \frac{\omega(1 - h_n)}{W_0}$ but not with $\Delta = \frac{\omega}{W_0}$.

The time of complete burning: $t_n = 2.303 \epsilon, \log \left(\frac{p_n}{p_0} \right)$.

We should also remember that p_0 in this case is not the same p_0 in (41) because now the igniter does not work in a closed volume.

Fig. 122 presents the curve (pt) - in a closed volume (1) and the curve (pt) with the outflow of gases through the nozzle (2).

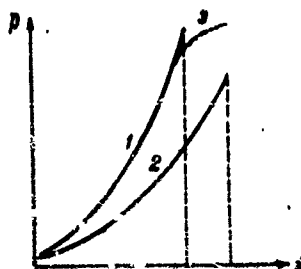


Fig. 122 - Curves (pt): 1 - in the closed volume
2 - in the bomb with a nozzle.

Both curves are theoretical curves, calculated under the assumption that the geometrical law of burning is valid but we know that the character of the pressure curve obtained under actual physical condition will differ - the real curve will have a point of inflection. Therefore the real curve (2) should also be distorted.

A good approximation of the solution of the problem of finding the curve (pt) when the burning of powder is going on along with an outflow of gases through a nozzle can be obtained in the following way.

The inflow per second of gases formed during the burning is given by: $\omega \frac{dV}{dt} = \omega \frac{S_1}{\lambda_1} \cdot \frac{S_2}{S_1} u \cdot p = \omega \Gamma p (K^{2/3} m)$

The discharge per second: $G_{sm} = \frac{dV}{dt} = \omega \cdot \frac{dV}{dt} = AS_m \rho$

If the inflow of gases is larger than the outflow, then the pressure within the chamber having the nozzle will be increased. If the inflow is smaller than the outflow, the pressure in the chamber having the nozzle will be decreased, and the pressure will be at its maximum or constant when the inflow is equal to outflow.

Therefore the character of the variations in the pressure depends on the mutual relationship between $(\frac{dV}{dt})$ and

$(\frac{dV}{dt})$ or (ωV) and (AS_m) . Hence there is a single graphical solution of the problem. We calculate (ωV) as a function of ψ (curves 1-1, 2-2, 3-3 on Fig. 123) and compare these curves with a straight line parallel to ψ -axis drawn at the distance AS_m (line a-a' on Fig. 123).

The line a-a' is everywhere under the curve (1-1) then the inflow of gases is greater than the discharge, then the ordinates of pressure curves (p, ψ) and (p, t) are increased until the end of burning and the maximum pressure will be at the end of burning with the $(\frac{dp}{dt})$ at its maximum (curve 1 on Fig. 124).

If line $a a'$ begins under the $(\omega P, \psi)$ curve (curve 2-2 on Fig. 123) then it intersects with the $(\omega P, \psi)$ curve at the point (ψ_m, P) and goes on above this curve, this means that at the beginning the pressure will be increased to its maximum at ψ_m (see curve 2 on Fig. 124) and afterwards the discharge will prevail ($AS_m > \omega P$). Now if ωP is everywhere lower than AS_m (curve 3-3 on Fig. 123) it means that for all the burning time the inflow never will compensate the discharge of gases and the pressure will be on decline the entire time, and even the extinguishing of the burning may be possible (curve 3 on Fig. 124). All three curves of the Fig. 123 represent powders differing only in the sizes of their webs (the smallest web - curve 1-1); the middle web - curve 2-2 and the largest web - curve 3-3). Thus by varying only the web of the strip powder we can obtain three different (p, t) curves. And inversely too - using the same powder by the varying the size of the nozzle (S_m) or the weight of the charge ω we can get the desired location of the line aa' . Therefore a manometric bomb with a nozzle can be used for the experimental studies of the burning process under conditions approaching the

real firing process in gun i.e. not only the increasing pressures but the decreasing as well.

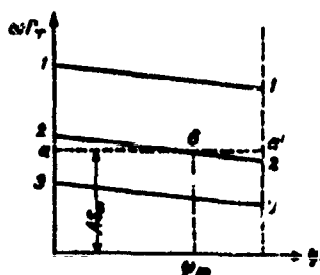


Fig. 123 - Characteristics of the inflow and outflow of gases - $(\omega\Gamma, \psi)$ and (AS_m, ψ) curves (theoretical)

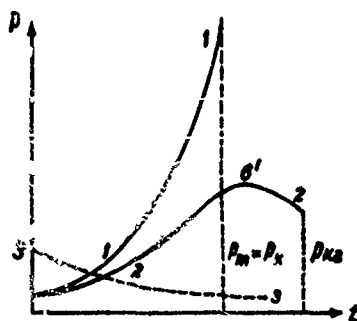


Fig. 124 - Pressure curves (p, t) in a bomb with the nozzle.

All the above presented considerations are based on the analysis of results derived from the geometrical law of burning but the experimental (\bar{r}, ψ) curves differ considerably from the theoretical: in case of the degressive powders this difference is displayed at the beginning and at the end of curves and in case of the progressive powders the curves differ along the whole range of ψ from 0 to 1. Fig. 125 and Fig. 126 present the experimental curves $(\omega/\bar{r}, \psi)$ calculated on the basis of the physical law of burning for strip powder and multiperforated powder respectively.

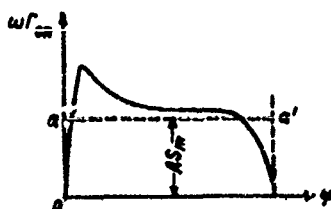


Fig. 125 - Relationship between the inflow and outflow of gases for the strip powder - $(\omega/\bar{r}, \psi)$ and (AS_m) curves.

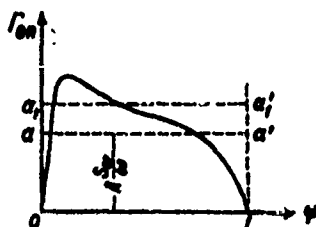


Fig. 123 - Relationship between the inflow and outflow of gases for the multiperforated powder - (ω, ψ) and (AS_m) curves.

The ordinates of the experimental curves (Γ, ψ) always fall before the end of burning. Therefore they always intersect their lines aa' (AS_m) and the maximum pressure is always obtained before the end of burning. But sometimes the whole curve (Γ, ω) can be located below the experimental line aa' (AS_m) as it is in case of the small igniter with the pressure $p_g \sim 50 \frac{\text{kg}}{\text{cm}^2}$.

- then the powder will not burn at all.

Such examples were demonstrated in experimental cases with the pyroxylin igniter, developing $p_g = 50 \frac{\text{kg}}{\text{cm}^2}$.

Very often its gases were discharged through the nozzle and powder was not ignited. The calculations for one

of these cases show that $\frac{AS_m}{\omega} = 0.007 \frac{0.47}{2.002} = 0.098 \frac{\text{cm}^3}{\text{g} \cdot \text{sec}}$
 and for this powder $\Gamma = 20.(0.0075) = 0.150 \frac{\text{g} \cdot \text{m}^3}{\text{kg} \cdot \text{sec}}$.

If the ignition was instantaneous, the powder could not have been extinguished because: $\Gamma > \frac{AS_m}{\omega}$ but since the ignition was not instantaneous, and its actual initial Γ was only 0.040 - 0.050 i.e. considerably lower than 0.098, so the discharge through the nozzle was larger than the inflow of gases and the powder could not burn.

3. Formula for the maximum pressure (P_m).

Having differentiated (96) with respect to t and remembering that:

$$\frac{d\psi}{dt} = \Gamma p \quad \text{and:} \quad \frac{dh}{dt} = A \cdot \frac{S_m}{\omega} p$$

we will have $\frac{dP}{dt} = 0$ in the following form:

$$f \Delta \left(\Gamma_m - A \frac{S_m}{\omega} \right) - p_m \left[\alpha \Delta A \frac{S_m}{\omega} - \Delta \Gamma_m \left(\alpha - \frac{1}{f} \right) \right] = 0$$

or:
$$\Gamma_m \left[1 + \left(\alpha - \frac{1}{f} \right) \frac{P_m}{f} \right] = A \frac{S_m}{\omega} \left(1 + \alpha \frac{P_m}{f} \right)$$

hence:
$$\omega \Gamma_m = AS_m n' \dots (N)$$

here:
$$n' = \frac{1 + \alpha \frac{P_m}{f}}{1 + \left(\alpha - \frac{1}{f} \right) \frac{P_m}{f}} > 1$$

For $f = 200,000$; $\alpha = 1$ and various ρ_m n' will be:

$$n'_{200} = 1.014; \quad n'_{1000} = 1.066; \quad n'_{2000} = 1.126$$

for the rockets ($\rho_m \leq 150$) $n' = 1.0$;

for the bomb with a nozzle $n' = 1.10$

Thus the necessary requirement for the practical realization of ρ_m as it is given by (N) is the same as we

had in the previous discussion, i.e.: $\omega \rho_m > AS_m$.

Having calculated the curves (ψ, I) and (ρ, I) and various values of $\frac{AS_m}{\omega} n'$ for several ω we will have the scheme shown on Fig. 127.

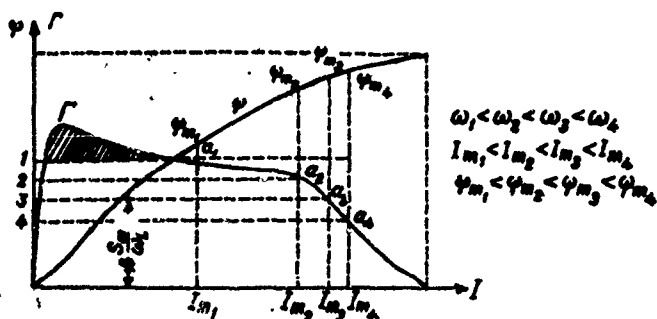


Fig. 127 - Calculating procedure for determining the maximum pressure ρ_m in the manometric bomb with a nozzle.

For any ω_i we find the intersection (point a_i) of the curve (Γ, I) with the horizontal straight line at the distance $\frac{As_m}{\omega}$ from the I-axis. The point a_i gives at once both values of I_{im} and ψ_{im} , thus we have $h_{im} = \frac{As_m}{\omega_i} I_{im}$ and, knowing ψ_{im} and h_{im} , we calculate p_m . Since $\psi = \int_0^I \omega I$ is equal to the area between the curve (Γ, I) and I-axis and the rectangular area $I \cdot \frac{As_m}{\omega} = h$ represents the value of the discharge, we have the difference $(\psi - h)$ in form of the shaded area on the Fig. 127. The larger ω_i , the lower the straight line $\frac{As_m}{\omega}$ is, the larger is p_m and the larger $(\psi - h)$ is, i.e. a larger portion of ω will be burned when p_m is reached.

It is of interest to note, that in a bomb with the nozzle the maximum pressure is not affected by W_0 and Δ but by the relationship between $\omega\Gamma$ and As_m and in case of a gun its maximum pressure is also determined by the relationship between $\omega\Gamma$ and the rate of increase of the volume Sv of the gun canal.

These results are verified in practice in all cases when the burning rate is $u = u/p$ i.e. for the high pressures (higher than $1000 \frac{\text{kg}}{\text{cm}^2}$) or for the powders

with small grains when the burning is very fast. At the low pressures (250 or less) and for powders with a large web the law $u = u, p$ cannot be applied. Since we have not yet definite reliable information as to the effect of the heated mass of powder on its u , it is advisable to make use of the law: $u = u', p^y$ where $u' > u$,

Then the rate of the inflow of gases:

$$\omega \cdot \frac{dV}{dt} = \omega \frac{S_i}{\lambda_i} \cdot \frac{S_i}{S_i} u' p^y = dS u' p^y$$

and the intensity of the discharge: $G_{sm} = \frac{dV}{dt} = A S_m p$.

Representing graphically as functions of p these characteristics of the inflow and outflow of gases

(Fig. 128) we will have them as a parabolic curve for

$(\omega \cdot \frac{dV}{dt})$ and a straight line for $(\frac{dV}{dt})$; at the

point of intersection of these lines - point a - there a constant pressure is reached, and if after this point the pressure begins to grow up then $(\frac{dV}{dt})$ is increased i.e. the discharge will prevail and the pressure must decrease. If after point a the pressure is decreased (to the left of the point a) when the inflow will prevail and the pressure must be increased. Thus in this case when the pressures are low and the rate of burning is $u = u', p^y$ we have the process of keeping the

pressure at the same level as a self-regulating stable process.

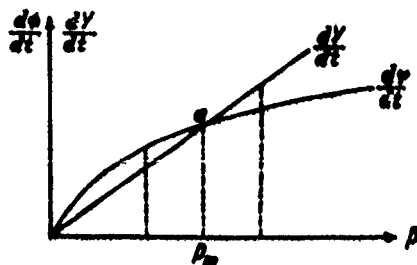


Fig. 128 - Diagram of the rates of the inflow ($\frac{dY}{dt}$) and outflow ($\frac{d\phi}{dt}$) as functions of p (for the low pressures and powders with large webs).

The same trend of the leveling off the pressure can be found in cases of low pressures and small Δ when the integral curves (I, I) vary with the change in Δ in such a way that at the beginning the curves (I, I) with smaller Δ are higher than the curves with larger Δ and at the approaching the end the location of curves is reversed i.e. the curves with the smaller Δ are lower than the curves with the larger Δ . This is shown on Fig. 129.

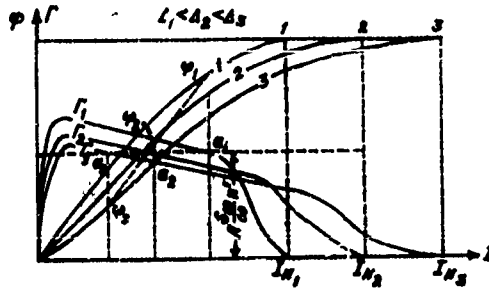


Fig. 129 - Curves (I, I) and (ψ, I) with various Δ .

$$\Delta_1 < \Delta_2 < \Delta_3 \quad \text{and} \quad \psi_3 < \psi_2 < \psi_1.$$

As soon as the equality of I and $\frac{AS_m}{\omega} n'$ is established for instance at the point a_3 , then the curve I_3 begins to run lower than the distance $\frac{AS_m}{\omega} n'$ and the pressure must be decreased but at the lower pressure we must follow the curve I_2 at the point a_2 with the increased ψ_2 and the same transition will be necessary at the point a_1 with its still larger ψ_1 . Thus the pressure will be maintained at its initial level corresponding to the point a_1 . Nothing similar is found at the higher pressures where there is only one curve (I, I) as it was shown on Fig. 127 and the curve (I, I) will stay lower than the horizontal line $(\frac{AS_m}{\omega} n')$

i.e. the discharge will prevail and the pressure will steadily become decreased.

Chapter 4 - Outline of the theory of muzzlebrakes.

1. General information.

The efficiency of a muzzlebrake is the relative decrease of the kinetic energy of the recoiling mass:

$$\eta' = \frac{Q_0 V_{max}^2 - Q_0 V_0^2}{Q_0 V_{max}^2} = \frac{V_{max}^2 - V_0^2}{V_{max}^2}$$

The relative decrease in velocity: $r = \frac{V_{max} - V_0}{V_{max}}$

and $\eta' = r(2-r)$

where Q_0 - weight of the recoiling mass

Q_0 - total weight of Q_0 and of the brake.

V_{max} - maximum velocity of the recoil without the action of brake.

V_0 - maximum velocity of the recoil affected by the action of brake.

There are two types of the muzzlebrakes - active brake working by the direct impact of the ejected gases against a special surface of the recoiling mass and reactive brake in which the gases are ejected from the muzzle along the curved channels of the brake in the opposite direction to the projectile's motion.

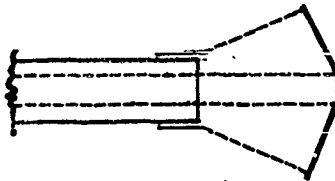


Fig. 130 - The active brake

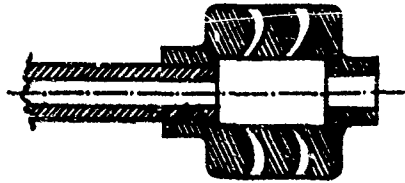


Fig. 131 - The reactive brake.

2. A mechanical reaction of gases on the surface of the curved channels of the muzzlebrake. (From the course of Interior Ballistics by Prof. D. Venzel, 1939).

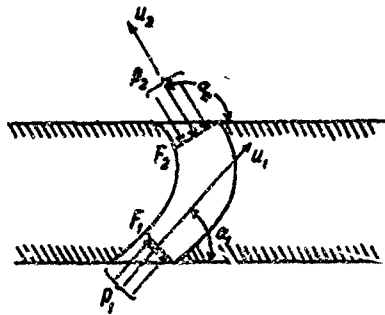


Fig. 132 - Forces acting in the channel of the muzzle-brake.

Forces acting in the channel of the muzzlebrake.

F_1 - a normal cross-section of the inlet opening;
(gas velocity U_1)

$\alpha_1 < \frac{\pi}{2}$ - the angle of the inlet.

F_2 - a normal cross-section of the outlet opening;
(gas velocity U_2)

$\alpha_2 > \frac{\pi}{2}$ - the angle of the outlet.

From the momentum equation written for the mass $\frac{G_0}{g} dt$ of gases within the curved channels of the brake and acting forces (pressures P_1 and P_2 and reaction R_0) along the X -axis (direction of the X -axis with + against the recoil motion) we will have the following expression for $(R_0)_x$:

$$(R_0)_x = \frac{G_0}{g} (U_1 |\cos \alpha_1| + U_2 |\cos \alpha_2|) + F_1 P_1 \cos \alpha_1 + F_2 P_2 \cos \alpha_2 \quad (99)$$

where $|\cos \alpha_i|$ is the absolute value of $\cos \alpha_i$.

Here G_0 , R_0 , F_1 and F_2 refer to the sum of all cross-sections of channel in the brake.

3. The total reaction on the gun produced by gas flow through the muzzlebrake.

The total reaction has the following components:

1. Reaction along the X -axis of gases flowing out of the gun through the muzzle proper taken from (87) and (89):

$$R_x = -(K+1) \left(\frac{2}{K+1} \right)^{\frac{K}{K+1}} S p = -\frac{2}{3} S p.$$

2. Reaction along the x -axis of gases flowing in the opening F_1 :

$$R_{1x} = - \left(\frac{G_1}{g} U_1 + F_1 p_1 \right) \cos \alpha,$$

3. Reaction (99):

$$R_{2x} = \frac{G_2}{g} \left(U_2 |\cos \alpha_2| + U_1 \cos \alpha_1 \right) + F_2 p_2 |\cos \alpha_2| + F_1 p_1 \cos \alpha_1.$$

then a sum:

$$R_{2x} = -\frac{2}{3} S p + \left(\frac{G_2}{g} U_2 + F_2 p_2 \right) |\cos \alpha_2| < 0$$

(acting along the projectile motion.

Prof. D. Ventzel gives the final expression for R_{2x} :

$$R_{2x} = \left\{ 1 - \frac{1}{K+1} \left[\Psi \chi \cdot \frac{2x}{\sqrt{K+1}} \left(\frac{2}{K+1} \right)^{\frac{K}{K+1}} \sqrt{1 - \left(\frac{A}{A_1} \right)^{\frac{K+1}{K}}} + \frac{F_2 A_2}{F_1 p_1} \right] \frac{F_2}{S} |\cos \alpha_2| \right\} \frac{2}{3} S p = \alpha \frac{2}{3} S p$$

here Ψ the coefficient expressed in terms of $\left(\frac{\alpha_1 + \sqrt{K} - \alpha_2}{2} \right)$

and given in a special table.

Table for Ψ

$\frac{\alpha_1 + \beta_1 - \alpha_2}{\beta_1} =$	15°	20°	25°	30°	40°	50°	60°	70°
Ψ	0.725	0.770	0.815	0.845	0.890	0.920	0.940	0.950

χ - the coefficient affected by the curvature of channels (at $\alpha_1 < 30^\circ$ $\chi = 0.75 - 1.0$)
 the ratios $\frac{B}{B_1}$ and $\frac{F_1}{F_2}$ are mutually interdependent and are given in Table 33.

Table 33

$\frac{B}{B_1}$	0.5	0.4	0.3	0.2	0.1	0.05	0.01
$\frac{F_1}{F_2}$	1.01	1.06	1.19	1.46	2.25	3.61	11.80

4. The total impulse of the reaction of gases.

The momentum equation for the "after-effect" period and in the presence of the muzzle brake will be:

$$\frac{Q_0}{g} \cdot (V_3 - V_2) = \int_0^{t_2} R_2 dt - \frac{\omega}{g} \cdot \frac{v_{2a}}{2} = I_2 = \frac{\omega}{g} \cdot \frac{v_{2a}}{2}$$

hence: $V_3 = V_2 + \frac{g}{Q_0} I_2 - \frac{\omega}{Q_0} \cdot \frac{v_{2a}}{2}$, here $R_2 = \alpha_2 \gamma S p$

The pressure p is expressed in the same form as it was given for the after-effect period without the brake

only the coefficient B' should be changed for B_2

$$B_2 = B' \left[1 + \chi \frac{F_1}{S} \left(\frac{2}{K+1} \right)^{\frac{1}{2} \cdot \frac{K+1}{K-1}} \right]$$

and the duration of the after-effect period will be:

$$t_{n\pi} = \frac{1}{B_z} \left[\left(\frac{1}{K\omega} \right)^{\frac{1}{K}} \left(\frac{p_2}{p_a} \right)^{\frac{K}{K-1}} - 1 \right]$$

And the impulse $I_z = \int_0^{t_n} R_z dt$ with $R_z = \alpha_z \cdot \gamma \cdot S \cdot p$

$$\text{will be: } I_z = \alpha_z \gamma S p_2 \int_0^{t_n} \frac{dt}{(1 + \beta_z(t))^{\frac{K}{K-1}}} = \alpha_z (K-1) \left(\frac{1}{K\omega} \right)^{\frac{1}{K-1}} \cdot \frac{S p_2}{B_z} \left[1 - \frac{1}{(1 + \beta_z(t))^{\frac{1}{K-1}}} \right]$$

Remembering that $V_2 = \frac{p_a S \omega}{Q_0} t$ and inserting the value of I_z in the above formula for V_B we will have:

$$V_B = \frac{p_a}{B_z} \left(1 + \frac{1}{K} \right) \frac{\omega}{2} + \alpha_z \frac{1}{K} \left(\frac{1}{K\omega} \right)^{\frac{1}{K}} \frac{\omega}{Q_0} C_2 \cdot \frac{\omega}{2} = \frac{p_a}{Q_0} \left(1 + \beta_z \frac{\omega}{2} \right) \frac{\omega}{2}$$

$$\text{here: } \beta_z = \alpha_z \frac{1}{K} \left(\frac{1}{K\omega} \right)^{\frac{1}{K}} \cdot \frac{C_2}{\frac{\omega}{2}}$$

at $K = 1.2$;

$$\beta_z = 1.589 \alpha_z \frac{Q_0}{\omega^2}; \quad C_2 = 10.85 \sqrt{\frac{p_2 (1 + \beta_z)}{\Delta}}$$

The efficiency of the muzzlebrake = $\eta = \frac{V_{mex}^2 - V_B^2}{V_{mex}^2}$

$$\text{or: } \eta = 1 - \left(\frac{1 + \beta_z \frac{\omega}{2}}{1 + \beta_z \frac{\omega}{2}} \right)^2$$

Practical values of η are 40-50%, in exceptional cases 70% and even 80%.

PART II
THEORY AND PRACTICE
OF THE
SOLUTION OF PROBLEMS
OF
INTERIOR BALLISTICS
(Theoretical and Applied Pyrodynamics)

Introduction.

A general problem of Interior Ballistics consists in finding all regularities and relationships existing between the loading conditions and ballistic elements of the firing which give us means for complete control over the firing process.

Loading conditions are: dimensions of the chamber and gun canal, construction of the rifling, weights of gun, projectile and powder charge, engraving pressure, type and physico-chemical and ballistic characteristics of powder and powder gases.

Ballistic elements of firing are: pressure (p), velocity (v), travel of the projectile (ℓ), temperatures of powder and powder gases, amount of acting gases ($\psi\omega$) at a given moment of time. The first problem of Interior Ballistics consists of finding by calculations how the pressure and velocity of projectile vary as functions of time (t) and travel (ℓ) under given loading conditions. Thus obtained curves (p, t), (p, ℓ), (v, t) and (v, ℓ) give the two most important ballistic characteristics of the gun: the maximum pressure p_m and the maximum-muzzle velocity (v_s). This problem always has one definite solution (p_m and v_s).

By varying the given loading conditions we may find solutions of many partial problems. The second principal problem of Interior Ballistics is the problem of the ballistic design of the gun which consists of determining the constructional data for the gun tube as well as loading conditions for a given projectile (its caliber and weight) in such a way that a given projectile will have the required muzzle velocity (U_0) at the maximum pressure not exceeding a definite limit. The desired muzzle velocity as a rule is predetermined by certain tactical-technical requirements. Having found all the sought for elements we proceed with the calculations of the curves (p, t) , (v, t) , (p, l) , (v, l) . It is obvious that the desired $2k$ and $\frac{h}{m}$ can be obtained for a given projectile in many different ways and thus we may have many variants of the desired artillery system; our problem after all is the problem of making a rational, most appropriate selection of only one variant among many. Hence we have special very important practical cases of finding a most effective system, as a system with the shortest gun, or with a gun having a minimum weight or volume, etc.

All the methods applicable to the solutions of problems in Interior Ballistics can be classified in four groups: 1) Empirical; 2) Analytical; 3) Numerical and 4) Tabular.

Section VI - Analytical methods of Solution of the
Direct Problem of Interior Ballistics.

Basic Assumptions.

1. The burning of powder follows the course prescribed by the geometric law.
2. The process of powder burning proceeds at a certain average pressure.
3. The chemical composition of the products of burning remains the same during the process of burning as well as afterwards during the period of adiabatic expansion of the gases.
4. The rate of burning is assumed to be: $u = u, p$.
5. All the accountable secondary works are taken proportional to the kinetic energy of the projectile and all are included into coefficient φ .
6. The projectile begins its motion at the initial "shot-start" pressure p_0 (engraving pressure). The two preliminary periods of the gradual increase of pressure (static period) and of the gradually increased

resistance to the motion of the projectile are neglected.

7. Neither work spent on engraving nor the increase of the velocity of the projectile during the engraving are accounted for.

8. The expansion of the walls of the bore, leakage of gases through the clearance between the driving band and the surface of rifling and air resistance to the moving projectile within the bore are all neglected.

9. The cooling effect of the walls of the bore can be accounted for indirectly by taking a decreased value of

$$f = RT, \text{ or an increased value of } \theta = \frac{1}{1 + \beta T_{av}}$$

10. The value of θ is considered as a constant average value of $\left(\frac{C_p}{C_v} - 1\right)$ during the whole process of firing.

11. The motion of the projectile is considered until the moment when the base of the projectile leaves the muzzle.

Chapter 1 - The solution of the basic problem using the geometric law of burning and considering the engraving pressure.

The following system of basic equations is taken:

$$\rho s(l_0 + l) = f \omega \psi - \frac{1}{2} \psi m v^2 \dots (1)$$

$$u = \frac{de}{ds} = u_0 \rho \dots (2)$$

$$\psi = \kappa z (1 + \lambda z) \dots (3)$$

$$pS = \varphi m \frac{d\psi}{dz} \quad (4)$$

or:

$$pS = \varphi m \cdot v \frac{d\psi}{dz} \dots (5)$$

To begin with the problem will be solved for the degressive powders ($\kappa > 1$, $\lambda > 0$, $\mu = 0$) and separately for the preliminary period, for the first period (up to the end of burning, at the moment t_k) and for the second period (at the moment t_2 , when the projectile leaves the muzzle).

1. The preliminary period.

During this period we are interested in the following elements: engraving pressure p ; the burned fraction of the charge ψ ; the relative thickness of the burned powder $z = \frac{e}{z_0}$ and the relative burned surface of powder $\sigma = \frac{S}{S_0}$. All these values, being the final values of the preliminary period, are the initial values for the first period.

The igniter will provide its pressure:

$$p = \frac{f_0 \omega_0}{W_0 - \frac{Q}{\lambda} - \alpha_0 \omega_0} \dots (6)$$

here the subscript B refers to the igniter; the product $\alpha_0 \omega_0$ can be neglected. At the pressure p_0 the powder charge ω begins to burn and at the moment when the engraving pressure p_0 will be reached:

$$p_0 = p_B + \frac{f \omega \psi_0}{W_0 - \frac{f}{p_B} - \frac{f}{p_0} \psi_0} \dots (7)$$

here: $\frac{1}{p_0} = \alpha - \frac{1}{p}$

The engraving pressure p_0 is known (normally for the guns between 250 $\frac{\text{kg}}{\text{cm}^2}$ and 400 $\frac{\text{kg}}{\text{cm}^2}$).

From (7) we calculate :

$$\psi_0 \frac{(p_B - p_0) \left(\frac{1}{p_0} - \frac{1}{p} \right)}{f + (p_B - p_0) \left(\alpha - \frac{1}{p} \right)} = \frac{\frac{1}{p_0} - \frac{1}{p}}{\frac{f}{p_B - p_0} + \frac{1}{p}} \quad (8)$$

or approximately:

$$\psi_0 = \frac{\frac{1}{p_0} - \frac{1}{p}}{\frac{f}{p_B} + \frac{1}{p}} \dots (9)$$

ψ_0 is normally between 0.02 and 0.10 and largely depends on Δ . Then: $\sigma_0 = \sqrt{1 + 4 \frac{\Delta}{\psi_0}}$

and from: $\sigma_0 = 1 + 2 \Delta \Delta_0$

we obtain: $Z_0 = \frac{G_0 - 1}{2\lambda} = \frac{G_0^2 - 1}{2\lambda(G_0)} = \frac{2\psi_0}{(G_0 + 1)20}$

Since: $G_0 \sim 1$, then: $Z_0 = \frac{\psi_0}{20}$.

For the further discussion we need the effective length (l_{ψ}) of the free volume of the chamber at the beginning of the motion of the projectile, when ψ_0 is burned. (See No. 55 in the list of terms and notations):

$$l_{\psi} = \frac{W_{\psi}}{S} = \frac{1}{S} \left[W_0 - \frac{\omega}{\lambda} - \frac{\omega \psi_0}{\lambda} \right] = l_{\Delta} \left[\frac{1}{\Delta} - \frac{1}{\lambda} - \frac{\psi_0}{\lambda} \right]$$

here: $l_{\Delta} = \frac{W_0}{S} \cdot \frac{\omega}{W_0} = \frac{\omega}{S}$

3. The first period.

Prof. N. Drosdov's variable: $x = Z - Z_0$ at the beginning of projectile's motion: $x = 0$; $x = Z_0$; at the end of burning: $Z = 1$; $x = 1 - Z_0$. All variables: ψ , ψ' , l and β should be expressed as functions of x .

1. $\psi = f_1(x)$: $\psi = \alpha x + \alpha \lambda x^2 = \alpha x_0^2 + \alpha \lambda x_0^2 + x(1 + 2\lambda Z_0) \cdot \alpha \lambda x^2$

here: $\psi_0 = \alpha x_0^2 + \alpha \lambda x_0^2$ and: $1 + 2\lambda Z_0 = G_0$

Drosdov's notation: $K_1 = \alpha G_0$

Finally we have: $\psi = \psi_0 + K_1 x + \alpha \lambda x^2 \dots (10)$

2. $v = f_2(x)$

From: $S\rho = \varphi m \frac{dv}{dx}$ and: $u = \frac{de}{dx} = u, \rho$
 and remembering that: $x = \frac{S}{\rho}$; $I_N = \frac{e}{u}$,

we have: $dv = \frac{S}{\varphi} \cdot \frac{I_N}{m} \int_{x_0}^x dx$

Having integrated: $\int dv = \frac{S I_N}{\varphi m} \int_{x_0}^x dx$

we obtain: $v = \frac{S I_N}{\varphi m} (x - x_0) = \frac{S I_N}{\varphi m} \cdot x \dots (11)$

For the end of burning:

$$v_k = \frac{S}{\varphi} \cdot \frac{I_N}{m} (1 - x_0) \quad (12)$$

(11) can be rewritten:

$$v^2 = \frac{S^2 I_N^2}{\varphi^2 m^2} x^2 = \frac{S I_N^2 \theta}{2 f_w \varphi m} \cdot \frac{2 f_w}{\varphi m \theta} x^2 = \frac{\theta I_N^2}{2 \varphi m} x^2 \quad (11')$$

or:

$$v = v_{km} \sqrt{\frac{\theta}{2}} \cdot x \dots (11'')$$

Here the ratio $\left(\frac{\theta}{2}\right)$ - the projectile weight per unit of the cross-sectional area (S) is called "a cross-sectional loading of the projectile". Formula (12) however is not sufficient for answering some other important questions in which the variable ℓ is involved

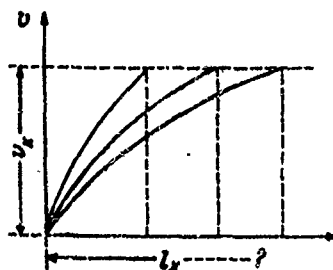


Fig. 133 v_k is determined but l_k is unknown yet.

3. $l = f_2(x)$.

The following two basic equations:

$$ps(l_k + l) = f\omega\psi - \frac{\rho}{2}\varphi_m v^2 = f\omega\left(\psi - \frac{v^2}{v_{lim}^2}\right)$$

$$\text{here : } v_{lim}^2 = \frac{2f\omega}{\rho\varphi_m}$$

$$\text{and: } \int S dl = \varphi_m v dv$$

will give:

$$\frac{dl}{l_k + l} = \frac{\varphi_m}{f\omega} \cdot \frac{v dv}{\psi - \left(\frac{v}{v_{lim}}\right)^2} \dots (13^*)$$

The right part of this equation with v and ψ given in (11) and (10) will be:

$$\frac{\varphi_m}{f\omega} \cdot \frac{\frac{S^2 I_{\pi}^2}{\varphi^2 m^2} \cdot x dx}{\psi_0 + K_1 x + K_2 x^2 - \frac{S^2 I_{\pi}^2 \varphi_m \theta}{\varphi^2 m^2 2 f \omega} \cdot x^2} = \frac{S^2 I_{\pi}^2}{f \omega \varphi_m} \cdot \frac{x dx}{\psi_0 + K_1 x - \left(\frac{S^2 I_{\pi}^2 \theta}{f \omega \varphi_m^2} \cdot x \right) x^2}$$

here:

$$\frac{S^2 I_K^2}{f \omega \psi m} = B$$

is Prof. Drosdov's "parameter of loading conditions"

$$\text{or: } B = \frac{S^2 a_1^2}{a_1^2 f \omega \psi m} ; \frac{e_1^2}{a_1^2} = I_K^2$$

$$\text{Denoting } \frac{B}{2} - K_1 x = B_1,$$

we will have (13°):

$$\frac{dl}{l_0 + l} = \frac{B x dx}{\psi_0 + K_1 x - B_1 x^2} \dots \dots (13)$$

or:

$$\frac{dl}{l_0 + l} = - \frac{B}{B_1} \cdot \frac{x dx}{\xi_1(x)} \dots \dots (13')$$

$$\text{Here: } \xi_1(x) = x^2 - \frac{K_1}{B_1} x - \frac{\psi_0}{B_1}$$

(13') can be rewritten:

$$\frac{dl}{dx} + \frac{B}{B_1} \cdot \frac{x}{\xi_1(x)} \cdot l = - \frac{B}{B_1} \cdot \frac{x}{\xi_1(x)} \cdot l_0$$

or:

$$\frac{dl}{dx} + P_x l = Q_x l$$

here P_x and Q_x are functions of x .

This linear equation of the first order has been integrated without any additional assumptions or simplifications by Prof. Drosdov in 1903 (this rigorous complete

integration will be shown in Chapter 2). Here we will proceed with the simplifying assumption, that the variable l_y is taken at its constant average value l_{avr} .

Here: $l_{avr} = l_0 \left[1 - \frac{\alpha}{2} - \Delta(\alpha - \frac{\alpha}{2}) \psi_{avr} \right]; \psi_{avr} = \frac{\psi_0 + \psi}{2}$

Then having integrated (13') we have:

$$\log_e \left(1 + \frac{l}{l_{avr}} \right) = - \frac{B}{B_0} \log_e Z_x; l Z_x = \int_0^x \frac{x dx}{B(x)}.$$

hence:

$$l = l_{avr} (Z_x^{-\frac{B}{B_0}} - 1) \dots (14)$$

Since from (11) we see that v is proportional to x we may say that (14) shows l as a function of v .

4. $p = f_v(x).$

Basic equation of pyrodynamics gives us:

$$p = \frac{f_0}{S} \frac{\psi - \left(\frac{v}{v_{avr}} \right)^2}{l_y + l} = \frac{f_0}{S} \frac{\psi + K_1 x - B_1 x^2}{l_y + l_{avr} (Z_x^{-\frac{B}{B_0}} - 1)} = \frac{f_0}{S} \frac{\psi - \frac{B_0}{2} x^2}{l_y + l} \quad (15)$$

here l_y can be taken in the form of a function of x . Since we already have ψ , v and l as functions of x , it is not necessary to make use of (15) in its final form.

Determining the form of the function $Z_x = e^{\int \frac{x}{\xi(x)} dx}$

$$\int \frac{x dx}{\xi(x)} = \int \frac{x dx}{x^2 - \frac{K_1}{B_1}x - \frac{B_2}{B_1}} = \frac{B_1+1}{2B_1} \int \frac{dx}{x-x_1} + \frac{B_1-1}{2B_1} \int \frac{dx}{x-x_2} \dots (16)$$

From equation: $x^2 - \frac{K_1}{B_1}x - \frac{B_2}{B_1} = 0$

$$\text{we have: } x = \frac{K_1}{2B_1} (1 \pm \sqrt{1 + 4 \frac{B_2}{K_1^2}}) = \frac{K_1}{2B_1} (1 \pm \ell);$$

$$\ell = \sqrt{1 + 4 \frac{B_2}{K_1^2}} = \sqrt{1 + 4\ell}.$$

$$\text{and: } \xi_1(x) = (x-x_1)(x-x_2); x_1 = \frac{K_1}{2B_1}(1+\ell); x_2 = \frac{K_1}{2B_1}(1-\ell)$$

$$\text{and: } \frac{x}{\xi_1(x)} = \frac{A_1}{x-x_1} + \frac{A_2}{x-x_2}$$

$$\text{hence: } A_1 = -\frac{x_2}{x_2-x_1}; A_2 = \frac{x_1}{x_2-x_1}; x_2-x_1 = -\frac{K_1}{B_1}\ell$$

$$\text{thus we have: } A_1 = \frac{B_1+1}{2B_1} \quad \text{and} \quad A_2 = \frac{B_1-1}{2B_1}$$

Then we have (16);

$$\int \frac{x dx}{\xi_1(x)} = \frac{B_1+1}{2B_1} \int \frac{dx}{x-x_1} + \frac{B_1-1}{2B_1} \int \frac{dx}{x-x_2} = \log_e \left[\left(1 - \frac{x}{x_1}\right)^{\frac{B_1+1}{2B_1}} \left(1 - \frac{x}{x_2}\right)^{\frac{B_1-1}{2B_1}} \right] \log_e Z_x$$

$$\text{hence: } Z_x = \left(1 - \frac{x}{x_1} \cdot \frac{B_1+1}{K_1}\right)^{\frac{B_1+1}{2B_1}} \left(1 + \frac{x}{x_2} \cdot \frac{B_1-1}{K_1}\right)^{\frac{B_1-1}{2B_1}} \dots (17)$$

Thus Z_x is a function of a variable $\beta = \frac{B_1}{K_1} x$

and a constant $\gamma = \frac{B_1}{K_1} \cdot \psi$

Since in (14) we need Z_x the Table is calculated for $\log(Z_x)$ with the two entries: β and γ . This Table is shown on page 290 (in book) with its title: "Table of Log. of Function $Z_{(\beta, \gamma)}$ ".

(16) can be rewritten: $\int \frac{x dx}{Z_x(x)} = \int \frac{\beta d\beta}{\beta - \gamma} = \log Z_x$

3. The evaluations of the maximum pressure p_m . Very often we need p_m without previous calculations of the entire curves (p, ρ) or (p, t). Using the equation (59) for $(\frac{dp}{dx})$ we will have the relationship between p_m and x_m from:

$$\frac{dp}{dx} = \frac{p}{\rho + \epsilon} \left[\frac{f \omega}{s} \cdot \frac{\gamma}{I_K} \cdot \frac{\sigma}{v} \left(1 + \frac{p}{f \rho} \right) - (1 + \theta) \right] = 0$$

with $\sigma = 1 + 2\lambda x = \sigma_0 + 2\lambda x$ and $v = \frac{S I_K}{\varphi_m} x$

as follows: $\frac{f \omega}{s} \cdot \frac{\gamma}{I_K} \cdot \frac{(\sigma_0 + 2\lambda x_m) \varphi_m}{S I_K x_m} \left[1 + \left(\alpha - \frac{1}{f} \right) \frac{p_m}{f} \right] - (1 + \theta) = 0$

hence:

$$x_m = \frac{K_1}{\frac{\beta(1+\theta)}{1 + (\alpha - \frac{1}{f}) \frac{p_m}{f}} - 2\lambda} \dots (18)$$

Table of Integrals of Numerical Values of the Function $\text{Erfi } Z^{-1} (P, Y)$

$P \backslash Y$	0	0.0005	0.001	0.002	0.004	0.006	0.008	0.010
0	0	0	0	0	0	0	0	0
0.020	0.0088	0.0080	0.0075	0.0067	0.0057	0.0049	0.0044	0.0039
0.040	0.0177	0.0168	0.0161	0.0150	0.0134	0.0123	0.0114	0.0106
0.060	0.0269	0.0258	0.0250	0.0238	0.0219	0.0204	0.0192	0.0181
0.080	0.0362	0.0351	0.0342	0.0329	0.0307	0.0290	0.0275	0.0262
0.100	0.0458	0.0446	0.0436	0.0422	0.0398	0.0379	0.0362	0.0347
0.120	0.0555	0.0543	0.0533	0.0517	0.0491	0.0471	0.0452	0.0435
0.140	0.0655	0.0642	0.0632	0.0615	0.0588	0.0565	0.0545	0.0527
0.160	0.0757	0.0744	0.0734	0.0716	0.0687	0.0663	0.0641	0.0622
0.180	0.0862	0.0848	0.0838	0.0819	0.0789	0.0763	0.0740	0.0720
0.200	0.0969	0.0955	0.0944	0.0925	0.0893	0.0867	0.0842	0.0820
0.220	0.1079	0.1065	0.1053	0.1034	0.1001	0.0972	0.0947	0.0924
0.240	0.1192	0.1177	0.1166	0.1145	0.1111	0.1081	0.1055	0.1031
0.260	0.1308	0.1293	0.1281	0.1260	0.1224	0.1194	0.1166	0.1141
0.280	0.1427	0.1411	0.1399	0.1378	0.1341	0.1309	0.1280	0.1254
0.300	0.1549	0.1533	0.1521	0.1499	0.1461	0.1428	0.1398	0.1371
0.320	0.1675	0.1659	0.1646	0.1624	0.1585	0.1551	0.1520	0.1491
0.340	0.1805	0.1783	0.1775	0.1752	0.1712	0.1677	0.1645	0.1615
0.360	0.1938	0.1922	0.1908	0.1884	0.1843	0.1807	0.1774	0.1743
0.380	0.2076	0.2059	0.2046	0.2021	0.1979	0.1941	0.1907	0.1875
0.400	0.2219	0.2201	0.2188	0.2163	0.2119	0.2080	0.2045	0.2012

Table of Logs of Numerical Values of the Function $\text{Im} Z^{-1}(\rho, \gamma)$ (Cont.)

$\rho \backslash \gamma$	0.020	0.040	0.060	0.080	0.100	0.150	0.200
0	0	0	0	0	0	0	0
0.020	0.0023	0.0017	0.0011	0.0009	0.0008	0.0006	0.0004
0.040	0.0079	0.0054	0.0041	0.0033	0.0028	0.0020	0.0015
0.060	0.0144	0.0103	0.0081	0.0067	0.0057	0.0042	0.0033
0.080	0.0215	0.0161	0.0130	0.0109	0.0094	0.0070	0.0056
0.100	0.0292	0.0225	0.0185	0.0157	0.0137	0.0104	0.0084
0.120	0.0373	0.0294	0.0246	0.0211	0.0185	0.0142	0.0116
0.140	0.0458	0.0368	0.0311	0.0269	0.0238	0.0185	0.0152
0.160	0.0546	0.0446	0.0380	0.0332	0.0295	0.0232	0.0191
0.180	0.0637	0.0528	0.0453	0.0399	0.0356	0.0283	0.0234
0.200	0.0732	0.0613	0.0530	0.0469	0.0421	0.0337	0.0281
0.220	0.0830	0.0702	0.0611	0.0543	0.0490	0.0395	0.0381
0.240	0.0932	0.0794	0.0695	0.0621	0.0562	0.0456	0.0384
0.260	0.1037	0.0889	0.0783	0.0702	0.0638	0.0520	0.0440
0.280	0.1145	0.0988	0.0874	0.0787	0.0717	0.0588	0.0499
0.300	0.1256	0.1090	0.0969	0.0875	0.0799	0.0659	0.0561
0.320	0.1371	0.1196	0.1067	0.0967	0.0885	0.0733	0.0626
0.340	0.1490	0.1306	0.1169	0.1062	0.0974	0.0810	0.0694
0.360	0.1613	0.1419	0.1275	0.1161	0.1067	0.0890	0.0766
0.380	0.1740	0.1536	0.1385	0.1263	0.1163	0.0974	0.0840
0.400	0.1871	0.1659	0.1499	0.1370	0.1264	0.1062	0.0917

Table of $\ln g$ s of Numerical Values of the Function $\ln g Z^{-1} (p, \gamma)$ (Cont.)

$p \backslash \gamma$	0	0.0005	0.001	0.002	0.004	0.006	0.008	0.010
0.420	0.2366	0.2238	0.2335	0.2310	0.2264	0.2224	0.2187	0.2154
0.440	0.2518	0.2500	0.2486	0.2461	0.2414	0.2373	0.2335	0.2301
0.460	0.2676	0.2658	0.2643	0.2617	0.2569	0.2527	0.2488	0.2453
0.480	0.2840	0.2822	0.2806	0.2779	0.2730	0.2687	0.2647	0.2610
0.500	0.3010	0.2992	0.2976	0.2948	0.2898	0.2853	0.2812	0.2773
0.520	0.3187	0.3169	0.3153	0.3124	0.3073	0.3026	0.2984	0.2943
0.540	0.3372	0.3353	0.3337	0.3307	0.3255	0.3207	0.3163	0.3121
0.560	0.3565	0.3545	0.3529	0.3498	0.3445	0.3396	0.3350	0.3307
0.580	0.3767	0.3747	0.3730	0.3699	0.3644	0.3593	0.3545	0.3501
0.600	0.3979	0.3959	0.3941	0.3909	0.3852	0.3799	0.3750	0.3704

Table of Logs of Numerical Values of the Function $\text{Erg Z}^{-1}(\beta, \gamma)$ (Cont.)

$\beta \backslash \gamma$	0.020	0.040	0.060	0.080	0.100	0.150	0.200
0.420	0.2007	0.1786	0.1617	0.1481	0.1369	0.1153	0.0998
0.440	0.2148	0.1917	0.1739	0.1596	0.1478	0.1247	0.1082
0.460	0.2294	0.2052	0.1866	0.1715	0.1589	0.1345	0.1169
0.480	0.2446	0.2193	0.1998	0.1839	0.1705	0.1447	0.1260
0.500	0.2604	0.2340	0.2136	0.1968	0.1827	0.1554	0.1354
0.520	0.2768	0.2493	0.2279	0.2102	0.1954	0.1665	0.1452
0.540	0.2939	0.2653	0.2428	0.2242	0.2086	0.1780	0.1555
0.560	0.3117	0.2819	0.2583	0.2388	0.2223	0.1900	0.1662
0.580	0.3304	0.2992	0.2745	0.2540	0.2366	0.2025	0.1773
0.600	0.3500	0.3174	0.2915	0.2699	0.2516	0.2156	0.1889

For powders with a constant surface of burning: $\lambda=0; K_1=0.5; \gamma=1$

we will have:

$$x_m = \frac{1 + (\alpha - \beta) \frac{\rho_m}{f}}{B(1 + \theta)} \quad \dots (19)$$

Now we assume a certain value ρ_m^0 , calculate x_m' from (19) or (18) and for this x_m' we calculate:

$$\begin{aligned} v_m' &= \frac{S I_m}{\rho_m'} x_m' \\ \psi_m' &= \psi_0 + K_1 x_m' + \gamma \lambda (\rho_m')^2 \\ e_m' &= e_{\lambda, \gamma} (Z_{x_m' - 1}) \\ \rho_m' &= \frac{f \omega}{S} \cdot \frac{v_m - (\frac{f \omega}{S})^2}{e_m' + 1} \end{aligned}$$

If ρ_m' differs not more than 10-20 $\frac{\mu}{cm}$ from ρ_m^0 then ρ_m^0 is a desired ρ_m . If ρ_m' is considerably different from the assumed then we take ρ_m' for the calculations of x_m'' as the next approximation for calculation of v_m'', ψ_m'', e_m'' and ρ_m'' . Since all our calculations are of ρ_{max} give results more or less close to the value of ρ_m -- all these approximations are varied within a close range and they all must be lower than ρ_m . Normally a good result is obtained after two successive approximations.

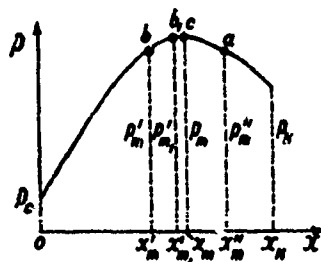


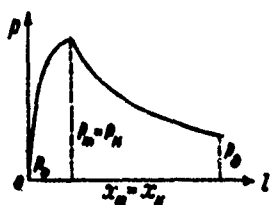
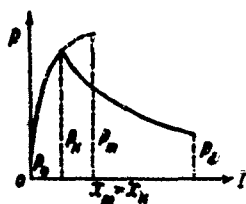
Fig. 134 Curve (p, x) for finding x_m and p_m .

It must be remembered that (18) or (19) are used for the calculation of the approximate values of x_m but not for the evaluation of p_m . Thus the calculated value of x_m may have no physical meaning if $x_m > x_K$. If $x_m < x_K$ we have a normal case when the maximum pressure is obtained somewhere before the end of burning.

If $x_m = x_K$ the maximum pressure corresponds to the end of burning.

If $x_m > x_K$ we have a so-called case of the "unreal maximum"; in this case the powder is burnt on the ascending part of the curve (p, x) and the actual pressure begins to decrease before the analytical maximum is reached.

Fig. 135 ($x_m < x_K$), Fig. 136 ($x_m = x_K$) and Fig. 137 ($x_m > x_K$) present all these three cases.

Fig. 135 ($x_m < x_K$)Fig. 136 ($x_m = x_K$)Fig. 137 ($x_m > x_K$)

Thus for the end of the first period we have:

$$\psi_K = 1; \ell_K = \ell_1 = \ell_0(1 - \alpha \Delta); x_K = 1 - z_0; \ell_K = \ell_{0K} \left(Z_{x_K}^{-\frac{B}{2}} - 1 \right)$$

$$v_K = \frac{S I_K}{\varphi m} x_K; p_K = \frac{f \omega \left(1 - \frac{B}{2} x_K^2 \right)}{S(\ell_1 + \ell_K)}$$

4. The second period (t_2 ; l_2 ; p_2 ; v_2)

This period begins with:

$$\psi = 1; v = v_K; l = l_K; p = p_K; l_0 = l_1; T = T_K.$$

The basic equation for this period:

$$p \cdot S(l_1 + l) = f\omega - \frac{1}{2} \varphi m v^2 = f\omega \left(1 - \frac{v^2}{v_{lim}^2}\right) \quad (20)$$

$$\text{here: } v_{lim}^2 = \frac{2f\omega}{\varphi \theta m}$$

Strictly speaking θ for this period should be taken larger than it was used in the first period but as a rule the majority of authors take θ as a certain average for these both periods.

A. The pressure as a function of l .

From the adiabatic equation:

$$pW^{1+\theta} = p_K W_K^{1+\theta} \quad \dots (21)$$

where W and W_K are the free volumes behind the projectile and remembering that:

$$W = W_0 - \alpha\omega + Sl = S(l_1 + l)$$

$$W_K = W_0 - \alpha\omega + Sl_K = S(l_1 + l_K)$$

we will have:

$$p = p_K \left(\frac{l_1 + l_K}{l_1 + l} \right)^{1+\theta}$$

and:

$$p_2 = p_K \left(\frac{l_1 + l_K}{l_1 + l_2} \right)^{1+\theta} \quad \dots (22)$$

B. The velocity of the projectile as a function of ℓ .

The basic equation of pyrodynamics for any moment and for the beginning of the second period will

be:
$$p s(\ell_1 + \ell) = f \omega \left(1 - \frac{v^2}{v_{lim}^2}\right)$$

and :
$$p_K s(\ell_1 + \ell_K) = f \omega \left(1 - \frac{v_K^2}{v_{lim}^2}\right)$$

hence:

$$v = v_{lim} \sqrt{1 - \left(\frac{\ell_1 + \ell_K}{\ell_1 + \ell}\right)^{\theta} \left(1 - \frac{v_K^2}{v_{lim}^2}\right)} \dots (23)$$

Since:
$$v_K = \frac{S I_K}{\varphi m} (1 - z_0)$$

then:
$$\frac{v_K^2}{v_{lim}^2} = \frac{S^2 I_K^2 (1 - z_0)^2}{\varphi^2 m^2} \cdot \frac{\varphi \theta m}{2 f \omega} = B \frac{\theta}{2} (1 - z_0)^2$$

and (23) will be:

$$v = v_{lim} \sqrt{1 - \left(\frac{\ell_1 + \ell_K}{\ell_1 + \ell}\right)^{\theta} \left[1 - \frac{B \theta}{2} (1 - z_0)^2\right]} \dots (24)$$

for $\ell = \ell_2$.

$$v_2 = \sqrt{\frac{2g}{\varphi} \cdot \frac{f}{\theta} \cdot \frac{\omega}{2} \left\{1 - \left(\frac{\ell_1 + \ell_K}{\ell_1 + \ell_2}\right)^{\theta} \left[1 - \frac{B \theta}{2} (1 - z_0)^2\right]\right\}} \dots (25)$$

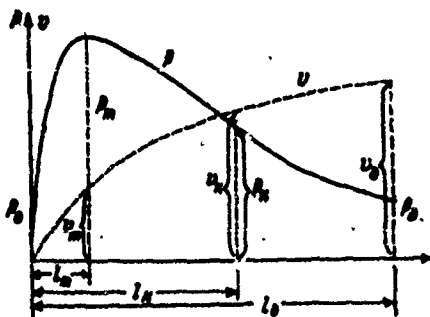


Fig. 138 presents normal curves (p) and (v) calculated for first and second periods.

C. Formulae for temperature of powder gases.

From the equation of the energy balance (52) we have:

$$\frac{RT_1 \omega \psi}{\theta} - \frac{RT_0 \omega \psi}{\theta} = \varphi m \frac{v^2}{2}; \quad RT_1 = f$$

or:
$$f \frac{\omega \psi}{\theta} \left(1 - \frac{T_0}{T_1}\right) = \frac{\varphi m v^2}{2}$$

hence:

$$\frac{T_0}{T_1} = 1 - \frac{\varphi m \theta}{2 f \omega} \cdot \frac{v^2}{\psi} = 1 - \frac{1}{\psi} \cdot \frac{v^2}{v_m^2} \dots (26)$$

Since: $v = \frac{S I \kappa}{\varphi m} x$; $\psi = \psi_0 + \kappa_1 x + \kappa_2 \lambda x^2$

and remembering that: $B = \frac{S^2 I \kappa^2}{f \omega \varphi m}$

we rewrite (26):

$$\frac{T_0}{T_1} = 1 - \frac{B \theta}{2} \cdot \frac{x^2}{\psi} = 1 - \frac{B \theta}{2} \cdot \frac{x^2}{\psi_0 + \kappa_1 x + \kappa_2 \lambda x^2}$$

At the end of burning ($\psi = 1$):

$$\frac{T_2}{T_1} = 1 - \frac{R}{2}(1-x_0)^2 = 1 - \varphi R_2 \dots (27)$$

At the muzzle ($\psi = 1$; ℓ_2 ; T_2 ; v_2):

$$\frac{T_2}{T_1} = 1 - \frac{v_2^2}{2c^2} = 1 - \varphi R_2 \dots (28)$$

Using (24) we may have another form for (28):

$$T_2 = T_1 \left[1 - \frac{R}{2}(1-x_0)^2 \right] \left(\frac{\ell_1 + \ell_2}{\ell_1 + \ell_2} \right)^0$$

D. Formulae for calculation of time (t).

$$\int dt = \int \frac{d\ell}{v} ; t = \int dt = \int \frac{d\ell}{v} = \frac{\ell'}{v_0} + \int \frac{d\ell}{v} ; v_0 = \frac{c + v'}{2} = \frac{v'}{2}$$

$$\ell' = \frac{2\ell'}{v'} ; t = \frac{2\ell'}{v'} + \int \left(\frac{1}{v} \right) d\ell \dots (30)$$

A better approximation for ℓ' can be found by considering a linear law of variations not for the velocity but for the pressure p (from p_0 to p')

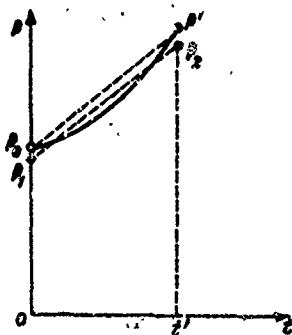


Fig. 139. Curve (p, t) for the initial interval t' .

$$\alpha = \frac{(p+p')t'}{\int p dt}$$

Here:

$$\frac{dv}{dt} = \frac{S}{\varphi_m} \rho = \frac{S}{\varphi_m} \cdot \alpha \left(\rho_0 + \frac{\rho' \rho_0}{t'} \cdot t \right); \quad v = \frac{S\alpha}{\varphi_m} \left(\rho_0 t + \frac{\rho' \rho_0}{2} \cdot \frac{t^2}{t'} \right).$$

$$\text{at } t': v_{t'} = \frac{S\alpha}{\varphi_m} \left(\rho_0 + \frac{\rho'}{2} \right) t'; \quad t' = \frac{\xi'}{v_{t'}}.$$

$$v_{t'}' = \frac{1}{t'} \int_0^{t'} v dt = \frac{1}{t'} \cdot \frac{S\alpha}{\varphi_m} \int_0^{t'} \left(\rho_0 t + \frac{\rho' \rho_0}{2t'} t^2 \right) dt = \frac{S\alpha}{\varphi_m} \cdot \frac{1}{t'} \left(\rho_0 \frac{t'^2}{2} + \frac{\rho' \rho_0}{6} \frac{t'^3}{t'} \right) =$$

$$= \frac{S\alpha}{\varphi_m} \cdot \frac{2\rho_0 + \rho'}{6} t' = \frac{2\rho_0 + \rho'}{3} \frac{v'}{2\rho_0 + \rho'};$$

$$t' = \frac{\xi'}{v_{t'}'} = \frac{3\xi'}{v'} \cdot \frac{\rho_0 + \rho'}{2\rho_0 + \rho'} \dots \dots (31)$$

A still better approximation for t' will be obtained if we use not a linear law for ρ but a parabolic law of 2nd degree. Then we will have:

$$t' = \frac{4\xi'}{v'} \cdot \frac{2\rho_0 + \rho'}{5\rho_0 + \rho'}$$

Prof. E. Bravin gave the following formulas for the calculations of time within the periods:

$$\text{From } 0 \text{ to } t_m: \quad t_m = \frac{3\xi_m}{v_m} \cdot \frac{\rho_0 + \rho_m}{2\rho_0 + \rho_m}$$

$$\text{From } t_m \text{ to } t_n: \quad t_n - t_m = \frac{3(\xi_n - \xi_m)(\rho_m + \rho_n)}{v_m(\rho_m + 2\rho_n) + v_n(2\rho_m + \rho_n)}$$

$$\text{From } t_n \text{ to } t_2: \quad t_2 - t_n = \frac{3(\xi_2 - \xi_n)(\rho_n + \rho_2)}{v_n(\rho_n + 2\rho_2) + v_2(2\rho_n + \rho_2)}$$

Duration of the preliminary period:

$$t_0 = 2.303 \tau_0 \log\left(\frac{\rho_0}{\rho_2}\right); \quad \frac{1}{\tau_0} = \frac{f \Delta \mathcal{K}}{(1 - \frac{A}{\beta}) I_K}$$

Chapter 2 - Prof. N. Drosdov's Rigorous Integration of the Equation (13)

Equation (13), can be rewritten: (l_y is a variable)

$$\frac{dl}{dx} = \frac{B(l_y + l)x}{\psi - \frac{1}{2} \theta x^2} \quad (33)$$

Denoting: $M = \frac{Bx}{\psi - \frac{1}{2} \theta x^2}$ (34)

we have (33):

$$\frac{dl}{dx} - Ml = Ml_y \quad (35)$$

After integration we have:

$$l = e^{\int M dx} \int l_y e^{-\int M dx} M dx \quad (36)$$

We had already:

$$\int M dx = \frac{B}{\beta_1} \int \frac{\rho d\rho}{\rho + \beta - \beta^2} = \log_e Z^{\frac{B}{\beta_1}} \quad (37)$$

the integral:

$$Y = \int l_y e^{\int M dx} M dx = \int l_y d(-e^{\int M dx}) = -l_y e^{\int M dx} + \int e^{\int M dx} dl_y$$

Having in view (37) we will obtain:

$$Y = -l_y Z^{\frac{B}{\beta_1}} + l_{y_0} + \int_{l_{y_0}}^{l_y} Z^{\frac{B}{\beta_1}} dl_y$$

But we know that:

$$\psi = \psi_0 + \kappa_1 x + \alpha \lambda x^2; \ell_\psi = \ell_x a \psi_0; a = \frac{\psi_0}{\lambda} (\alpha - \frac{1}{\lambda})$$

$$\text{and } d\ell_\psi = -a\kappa_1 dx - 2a\alpha\lambda x dx$$

Then:

$$Y = -\ell_\psi Z^{\frac{B}{2}} + \ell_\psi - a\kappa_1 \int Z^{\frac{B}{2}} dx - 2a\alpha\lambda \int Z^{\frac{B}{2}} x dx \dots (38)$$

$$\text{From (34) and (37): } \int \frac{Bx dx}{\psi_0 + \kappa_1 x - \alpha \lambda x^2} = -\frac{B}{B_1} \log_2 Z$$

$$\text{hence: } x dx = (x^2 \frac{\kappa_1}{B_1} x - \frac{\psi_0}{B_1}) \frac{dZ}{Z}$$

Eliminating the second integral in the right part of (38) we will find that this integral is:

$$\int Z^{\frac{B}{2}} x dx = \frac{B}{B_1} \int (x^2 \frac{\kappa_1}{B_1} x - \frac{\psi_0}{B_1}) d(Z^{\frac{B}{2}})$$

Integrating by parts we have:

$$\int Z^{\frac{B}{2}} x dx = \frac{B}{B_1} (x^2 \frac{\kappa_1}{B_1} x - \frac{\psi_0}{B_1}) Z^{\frac{B}{2}} + \frac{B}{B_1} \cdot \frac{\psi_0}{B_1} - \frac{2B}{B_1} \int Z^{\frac{B}{2}} x dx + \frac{\kappa_1}{B_1} \int Z^{\frac{B}{2}} dx$$

Hence:

$$\int Z^{\frac{B}{2}} x dx = \frac{Bx^2 - \kappa_1 x - \psi_0}{B + 2B_1} Z^{\frac{B}{2}} + \frac{\psi_0}{B + 2B_1} + \frac{\kappa_1}{B + 2B_1} \int Z^{\frac{B}{2}} dx$$

Now using the notations:

$$a_1 = -\frac{2B_1}{B + 2B_1}; \ell_1 = \frac{1}{\ell_0} (\ell_{\psi_0} + a a_1 \psi_0); c_1 = \frac{a \kappa_1}{\ell_0} (1 - a_1) \dots (39)$$

and remembering that: $x^2 = \frac{K_1}{B_1} x - \frac{\psi_0}{B_1} = \frac{1}{B_1} (\psi - \frac{B_0}{2} x^2)$

we rewrite (38):

$$Y = -l_p Z^{\frac{B_1}{2}} - a a_1 (\psi - \frac{B_0}{2} x^2) Z^{\frac{B_1}{2}} + l_0 (l_1 - c_1 \int Z^{\frac{B_1}{2}} dx) \quad (38)$$

and then (36) will be:

$$l = Z^{\frac{B_1}{2}} [l_p Z^{\frac{B_1}{2}} - a a_1 (\psi - \frac{B_0}{2} x^2) Z^{\frac{B_1}{2}} + l_0 (l_1 - c_1 \int Z^{\frac{B_1}{2}} dx)] \quad (36)$$

substituting: $\frac{\omega}{S \delta_1} = a$ and $l_p = l_{\Delta} - \frac{\omega \psi}{S \delta_1}$; $\delta_1 = \alpha - \frac{1}{\gamma}$

and having in view that: $\frac{\omega}{l_0} = \frac{\omega}{N_0 \delta_1} = \frac{\Delta}{\delta_1}$

we will have the final formula given by Prof. N. Drosdov:

$$\frac{l}{l_0} + \frac{l_{\Delta}}{l_0} - \frac{\psi \Delta}{\delta_1} = - \frac{a_1 \Delta}{\delta_1} (\psi - \frac{B_0}{2} x^2) + (l_1 - c_1 \int Z^{\frac{B_1}{2}} dx) Z^{\frac{B_1}{2}} \quad (40)$$

Here: $\int Z^{\frac{B_1}{2}} dx = \frac{K_1}{B_1} \int Z^{\frac{B_1}{2}} d\beta$ and special Table for $Z^{\frac{B_1}{2}}$

with 3 entries: β , γ and $\frac{B_1}{B_0}$ for this integral is given by Prof. D. Ventzel (Appendix 4 in book).

The following formulae should be used when Prof.

Drosdov's method is applied:

$$\varphi = K + \frac{1}{3} \frac{\omega}{\delta} ; \quad \varphi_m = \frac{\omega}{\delta} ; \quad I_K = \frac{g_i}{u_i} ; \quad \psi_K = \frac{I_K}{(\varphi_m)} ; \quad \frac{\omega}{\delta} ; \quad \frac{f\omega}{\delta} ; \quad \frac{\rho\omega}{\delta} ; \quad \frac{1}{\delta}$$

$$\delta_i = \alpha - \frac{1}{\delta} ; \quad a = \frac{\omega}{\delta_i} ; \quad \ell_{\psi_0} = \ell_{\Delta} - a\psi_0 ; \quad \ell_0 = \frac{w_0}{\delta}$$

$$B = \frac{I_K^2}{f\psi \cdot \varphi_m} ; \quad B_1 = \frac{B_0}{2} - \kappa\lambda ; \quad C = \frac{B_1}{K_1} ; \quad K_1 = \kappa\delta_0 ; \quad \beta = \frac{B_1}{K_1} x$$

$$f = \frac{C\psi_0}{K_1} = \frac{B_1\psi_0}{K_1} ; \quad a_1 = -\frac{2\kappa\lambda}{B+2B_1} ; \quad b_1 = \frac{1}{\ell_0} (\ell_{\psi_0} + a a_1 \psi_0) ; \quad c_1 = \frac{a K_1}{\ell_0} (1 - a_1)$$

$$\psi = \frac{S I_K}{\varphi_m} x ; \quad \psi = \psi_0 + K_1 x + \kappa\lambda x^2$$

$$p = \frac{f\Delta(\psi - \frac{B_0}{2} x^2)}{\frac{\ell_0}{2} + \frac{\ell_{\Delta}}{2} - \psi \frac{\Delta}{\delta}} ; \quad x_m = \frac{K_1}{B+2B_1} + h$$

$$h = \frac{C_1}{B+2B_1} \cdot \frac{\psi_m - \frac{B_0}{2} x_m^2}{(\ell_0 - c_1 \int_0^{x_m} \psi dx) Z^{-\frac{1}{\delta}}}$$

Table 3 for h with 2 entries: B and Δ is given on page 311 in book.

$\frac{A}{B}$	0.20	0.25	0.30	0.35	0.40	0.45	0.50	0.55	0.60	0.65	0.70	0.75	0.80
1.0	0.025	0.031	0.037	0.044	0.052	0.062	0.075	0.090	0.108	0.123	0.151	0.177	0.208
1.1	0.020	0.025	0.031	0.037	0.044	0.052	0.062	0.074	0.089	0.106	0.125	0.147	0.173
1.2	0.017	0.021	0.026	0.031	0.037	0.044	0.052	0.062	0.073	0.088	0.104	0.122	0.144
1.3	0.014	0.018	0.022	0.027	0.032	0.038	0.045	0.053	0.063	0.075	0.088	0.103	0.122
1.4	0.012	0.015	0.019	0.023	0.027	0.032	0.038	0.046	0.054	0.064	0.075	0.088	0.104
1.5	0.010	0.013	0.016	0.020	0.024	0.028	0.034	0.040	0.047	0.055	0.065	0.076	0.089
1.6	0.009	0.012	0.014	0.017	0.021	0.025	0.030	0.035	0.041	0.048	0.056	0.066	0.077
1.7	0.008	0.010	0.012	0.015	0.018	0.022	0.026	0.031	0.036	0.042	0.049	0.057	0.066
1.8	0.007	0.009	0.011	0.013	0.016	0.019	0.023	0.027	0.032	0.037	0.043	0.050	0.058
1.9	0.006	0.008	0.010	0.012	0.014	0.017	0.020	0.024	0.029	0.033	0.039	0.045	0.051
2.0	0.006	0.007	0.009	0.011	0.013	0.016	0.019	0.022	0.026	0.030	0.035	0.040	0.046
2.2	0.005	0.006	0.008	0.010	0.011	0.013	0.016	0.018	0.021	0.024	0.028	0.032	0.037
2.4	0.004	0.006	0.007	0.008	0.010	0.011	0.013	0.015	0.018	0.021	0.024	0.027	0.030
2.6	0.004	0.005	0.006	0.007	0.008	0.009	0.011	0.013	0.015	0.018	0.020	0.022	0.025
2.8	0.003	0.004	0.005	0.006	0.007	0.008	0.010	0.011	0.013	0.015	0.017	0.019	0.021
3.0	0.0025	0.0035	0.0045	0.0055	0.0065	0.0075	0.009	0.010	0.011	0.0125	0.014	0.0155	0.0175

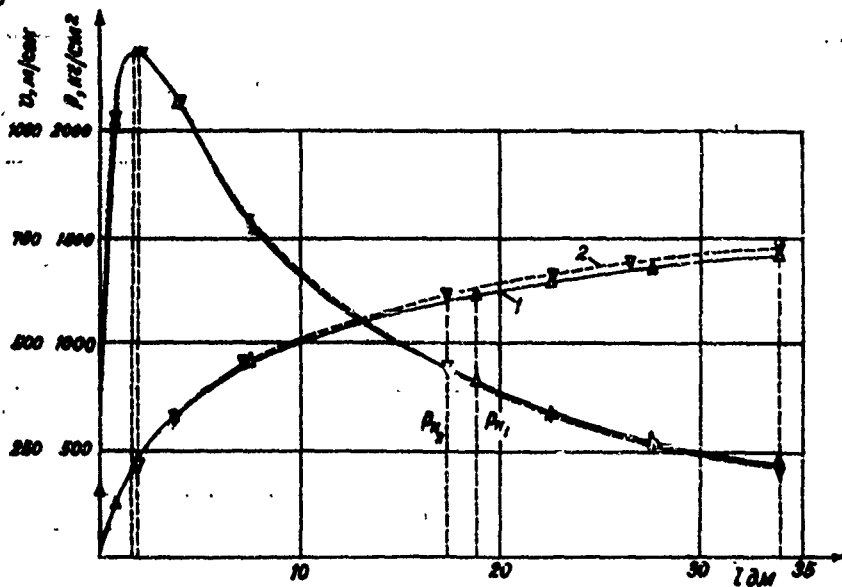


Fig. 140 - curves (p, l) and (v, l) :

1 - exact solution

2 - approximation with

Chapter 3. Solutions of Problems for Simpler Cases.

1. Case of the instantaneous burning.

This case is not a normal one in practice, but has a considerable theoretical interest as an ideal limiting process emphasizing the meaning and significance of the gradual burning of the dimensions and forms of powder grains and its basic curve (p, l) can be called "a directive curve" for all the curves (p, l) of gradual burning.

Using dry pulverized pyroxylin powder or a very fine porous powder at the density of loading $0.50 - 0.75$ we have the starting maximum pressure of $20,000 - 40,000$ Kg./cm². The analytical solution in this case is a simple one. One variable ψ is eliminated, being equal to 1. The initial data: $W_0; S; l_0; \omega; q; f; \alpha; k_1 + 0$ and the coefficient $\varphi = a + b \frac{q}{S}$; the effective length of chamber $l_1 = \frac{W_0 - \alpha \omega}{S}$. The basic equation:

$$p S (l_1 + l) = f \omega - \frac{1}{2} \gamma m v^2 \quad (41)$$

and the equation of the projectile travel:

$$p S dl = \varphi m v dv \quad (42)$$

The maximum pressure:

$$p_1 = \frac{f \omega}{1 - \alpha \Delta} = \frac{f \omega}{W_0 - \alpha \omega} = \frac{f \omega}{S l_1} \quad (43)$$

From (41) and (42) we have:

$$\frac{d\ell}{\ell + \ell} = \frac{\varphi m v \cdot dv}{f\omega - \frac{1}{2}\varphi m v^2} = -\frac{1}{\theta} \frac{d(\frac{\varphi m}{2} v^2)}{f\omega - \frac{1}{2}\varphi m v^2}$$

After the integration we have:

$$\frac{\ell + \ell_1}{\ell_1} = \left(\frac{f\omega - \frac{1}{2}\varphi m v^2}{f\omega} \right)^{-\frac{1}{\theta}} = \left(1 - \frac{v^2}{\frac{2f\omega}{\varphi m}} \right)^{-\frac{1}{\theta}} \quad (44)$$

hence: $v_{\text{lim}}^2 = \frac{2\theta f\omega}{\varphi m}$

Finally we have:

$$v = v_{\text{lim}} \sqrt{1 - \left(\frac{\ell_1}{\ell + \ell_1} \right)^{\theta}} \quad (45)$$

From (44) and (41) we determine ρ as a function of ℓ

$$\rho = \frac{f\omega}{\frac{1}{2}\varphi m} \left(\frac{\ell_1}{\ell + \ell_1} \right)^{\theta} = \rho_1 \left(\frac{\ell_1}{\ell + \ell_1} \right)^{\theta} \quad (46)$$

but: $\frac{\ell_1}{\ell + \ell_1} = \frac{W_1}{W_1 + \Delta W} = \frac{W_0 - \Delta W}{W_0 - \Delta W + \Delta W}$

Thus (46) is the equation of the adiabatic with the initial value of the pressure: $\rho_1 = \frac{f\omega}{1 - \alpha\omega}$

For the adiabatic process the relationship of temperatures between which the work of gases is performed is as follows:

$$\frac{T}{T_1} = \left(\frac{\ell_1}{\ell + \ell_1} \right)^{\theta}$$

Hence (45) will be:

$$v = v_{\text{lim}} \sqrt{1 - \frac{T}{T_1}} \quad (47)$$

A new variable: $y = \frac{\ell}{\ell_1}$ representing the relative travel of the projectile is respect to the effective

length l , is called "the number of free volumes of gas expansion".

Then (45) and (46) will be:

$$v = v_{lim} \sqrt{1 - \frac{1}{(1+y)^2}} \dots (48)$$

and :

$$p = p_i \cdot \frac{1}{(1+y)^{2+2}} \dots (49)$$

Thus practically p and v are functions of one variable y .

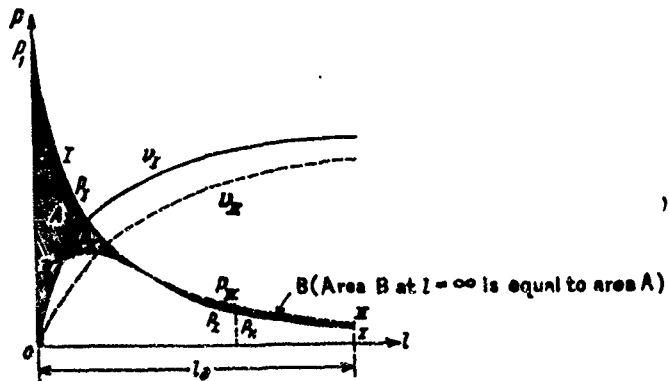


Fig. 141 shows a comparison of the effects produced by the same charge of powder on the projectile when the burning is instantaneous (curves marked I) and where the burning is gradual (curves marked II); curves (p, l) and (v, l) express results of the same final effect produced by the powder - i.e. its maximum possible work

$s \int_0^{\infty} p d\ell = \frac{f w}{g}$ which is the same area of the curves ($p\ell$) having different forms - Curve I and curve II :

Curve II will have the same area as the curve I only at the indefinite length of $\ell(\infty)$ but for all practical lengths ℓ_2 , the area of curve II is distinctly smaller than the corresponding area of the curve I and therefore the velocity of the projectile propelled by the gradual burning will be lower than the velocity of the same projectile propelled by the same charge of powder burned instantaneously. Velocity curves ($v\ell$) marked I and II approach each other to their final concurrence at infinity, v_{II} being consistently lower than v_I .

2. Case of a powder with a constant surface of burning when the engraving pressure is neglected. In case of degressive powder we have no explicit relationships between p , v and ℓ when the engraving pressure p_0 is involved in the equations - as this was shown above we have void an auxiliary variable x . Now we will assume:

1. Powder has characteristics of the constant surface of burning: $x=1; \lambda=0; \psi=x$
(tubular powders with long tubes)

2. The motion of projectile begins at $p = p_0; \psi_0 = 0$ this assumption is equivalent to considering a projectile with its ready made engraving.

3. That $\alpha = \frac{1}{2}$ this assumption simplifies formulas and qualitative evaluations of the loading conditions.

In general the preliminary periods are entirely omitted.

The beginning of the projectile motion is characterized

by: $p_0 = p_2; \psi_0 = 0; \chi_0 = 0; l_0 = 0; v = 0; l_2 = l_\psi = l_0(1 - \alpha\Delta)$ because $\alpha = \frac{1}{2}$

The law of burning has its form: $\psi = \chi = \alpha \dots (50)$

and the independent variable is ψ and the formula determining v is:

$$v = \frac{S I \kappa}{\varphi m} \cdot \psi \dots (51)$$

The basic equation:

$$p s(l_1 + l) = f \omega \psi - \frac{\rho}{2} \varphi m v^2 = f \omega (\psi - \frac{\rho \omega}{2} \psi^2)$$

The elementary work: $p \cdot s dl = \varphi m v dv = \frac{S^2 I \kappa^2}{\varphi m} \psi \cdot d\psi$

Thus the differential equation of the projectile motion is:

$$\frac{dl}{l+l_1} = \frac{B d\psi}{1 - \frac{\rho \omega}{2} \psi} = - \frac{2}{\theta} \cdot \frac{- \frac{\rho \omega}{2} d\psi}{1 - \frac{\rho \omega}{2} \psi}$$

Its integration gives:

$$1 + \frac{l}{l_1} = (1 - \frac{\rho \omega}{2} \psi)^{-\frac{2}{\theta}} \dots (52)$$

and finally:

$$\ell = \ell_1 \left[\frac{1}{(1 - \frac{2}{3} \theta \psi)^{\frac{1}{2}}} - 1 \right] \dots (53)$$

and denoting $\frac{\ell}{\ell_1} = \gamma$ from (52) we have:

$$\psi = \frac{2}{3\theta} \left[1 - \frac{1}{(1+\gamma)^{\frac{1}{2}}} \right] \dots (54)$$

Since: $v = \frac{5 I_{\kappa}}{\phi m} \cdot \psi$

we have: $v = \frac{2 f_{\infty}}{5 I_{\kappa}} \left[1 - \frac{1}{(1+\gamma)^{\frac{1}{2}}} \right] \dots (55)$

Thus we have v and ψ as functions of ℓ or γ .

Remembering that:

$$p_0 = \frac{f_0 \omega_0}{W_0 - \frac{\omega}{\lambda}} \approx \frac{f_0 \omega_0}{W_0 - u \omega} = \frac{f_0 \cdot \Delta_0}{S \ell_1} \dots (56')$$

and taking this pressure of the igniter into consideration we will have the following expression for the pressure p :

$$p = \frac{f_0 \omega_0 + f_0 \psi \cdot \frac{5}{2} \gamma m v^2}{S(\ell + \ell_1)} \dots (56)$$

The relative energy of the igniter: $\chi_{\frac{0}{\beta}} = \frac{f_0 \cdot \omega_0}{f \omega}$

then (56) gives:

$$p = \frac{f_w [\chi_0 + \psi(1 - \frac{1}{2}\psi)]}{sL_1(1+\psi)} = p_1 \frac{\chi_0}{1+\psi} + p_1 \frac{\psi}{(1+\psi)^{3/2}} \dots (57)$$

here $p_1 = \frac{f_w}{sL_1} = \frac{f_{\Delta}}{L_{\Delta}\Delta}$ is the maximum pressure of the whole charge instantaneously burned in the chamber at the density of loading Δ .

Now using (52) and (54) we will have from (57)

$$\text{here: } p = p_1 \cdot \frac{\chi_0}{1+\psi} + p_1 \frac{2}{\pi^2} \left[1 - \frac{1}{(1+\psi)^2} \right] \cdot \frac{1}{(1+\psi)^{3/2}} \dots (58)$$

$$p_1 = \frac{\chi_0}{1+\psi} = \frac{p_1 f_{\Delta} \omega_0}{f_w(1+\psi)} = \frac{p_1 f_{\Delta} \omega_0}{p_1 sL_1(1+\psi)} = p_0$$

is the igniter pressure acting in the bore and rapidly decreasing with the increasing ψ - its value can be neglected in comparison with the pressure developed by the charge. When $\psi = 0$ (at the beginning) we have in (58) only the first term p_0 . With the increased ψ one factor of the second term in (58) $\left[1 - \frac{1}{(1+\psi)^2} \right]$ is increased and another $\frac{1}{(1+\psi)^{3/2}}$ is decreased thus p will reach its maximum value at certain $\psi = \psi_m$. Equalizing the first derivative

of $\left[1 - \frac{1}{(1+\psi)^2} \right] \cdot \frac{1}{(1+\psi)^{3/2}}$ to zero we will determine ψ_m corresponding to the maximum pressure p_m :

$$1 + y_m = \frac{(1 + \theta)^{\frac{1}{2}}}{(1 + \frac{\theta}{2})^{\frac{1}{2}}} = F_1(\theta) \quad (59)$$

at $\theta = 0.2$, $F_1(0.2) = 2.387$

Hence:

$$\frac{L_m}{L_i} = y_m = F_1(\theta) - 1; \quad L_m = L_i(1 - \alpha \Delta) [F_1(\theta) - 1] \dots (60)$$

Inserting (59) in (58), (54) and (55) we will have respectively:

$$\frac{b}{i_m} = \frac{P_i}{B} \cdot \frac{2}{\theta} \left[\frac{\theta}{2(1+\theta)} \right] \left(\frac{1+\frac{\theta}{2}}{1+\theta} \right)^{\frac{2+\theta}{2}} = \frac{P_i}{B} \left(\frac{1}{1+\theta} \right) \left(\frac{1+\frac{\theta}{2}}{1+\theta} \right)^{\frac{2+\theta}{2}} = \frac{P_i}{B} F_2(\theta) \dots (61)$$

at $\theta = 0.2$, $F_2(0.2) = 0.320$

$$\psi_m = \frac{1}{B(1+\theta)} \dots \dots (62)$$

and :

$$v_m = \frac{f\omega}{S I_K} \cdot \frac{1}{1+\theta} \dots (63)$$

At $\theta = 0.2$; $p_m = 0.320 \frac{P_i}{B}$; $L_m = L_i(1 - \alpha \Delta)(1.387)$

For the end of burning $\psi = 1$. Then:

$$v_K = \frac{S I_K}{\phi_m} \dots (64)$$

From (53):

$$1 + y_K = \frac{1}{(1 - \frac{\theta}{2})^{\frac{1}{2}}} \dots \dots (65)$$

$$p_K = \frac{P_i}{(1 + y_K)^{\frac{1}{2} + \frac{\theta}{2}}} = P_i \left(1 - \frac{\theta}{2} \right)^{\frac{2+\theta}{2}} \dots (66)$$

For the second period we will have:

$$\text{For the pressure: } p = p_K \left(\frac{\ell_1 + \ell_K}{\ell_1 + \ell} \right)^{\gamma_0} = p_K \left(\frac{1 + \gamma_K}{1 + \gamma} \right)^{\gamma_0}$$

or:

$$p = \frac{p_1}{\left(1 - \frac{\gamma_0}{2}\right)} \cdot \frac{1}{(1 + \gamma)^{\gamma_0}} \dots (67)$$

This is the equation of the adiabatic with its initial ordinate:

$$\frac{p_1}{1 - \frac{\gamma_0}{2}}$$

For the velocity:

$$v = v_{lim} \sqrt{1 - \left(\frac{1 + \gamma_K}{1 + \gamma}\right)^{\gamma_0} \left(1 - \frac{\gamma_0}{2}\right)} = v_{lim} \sqrt{1 - \frac{1}{\left(1 - \frac{\gamma_0}{2}\right)} \cdot \frac{1}{(1 + \gamma)^{\gamma_0}}} \dots (68)$$

Temperature of gases.

We had for instantaneous burning:

$$\frac{T}{T_1} = \left(\frac{p}{p_1} \right)^{\frac{\gamma_0}{\gamma_0 - 1}} = \frac{1}{(1 + \gamma)^{\gamma_0}} \dots (69)$$

And for gradual burning:

$$\frac{T}{T_1} = 1 - \frac{1}{\psi} \cdot \frac{v^2}{v_{lim}^2} = 1 - \frac{\gamma}{\psi} \cdot \frac{\gamma}{v_{lim}^2}$$

Remembering that $v_{lim}^2 = \frac{2f\omega}{\psi\theta m}$ and taking ψ and v from (51) and (55) we will have:

$$\frac{T}{T_1} = 1 - \frac{SI_K \cdot \psi\theta m \cdot 2f\omega}{2f\omega \cdot \theta SI_K} \left[1 - \frac{1}{(1 + \gamma)^{\gamma_0}} \right]$$

or:

$$\frac{T}{T_1} = \frac{1}{(1 + \gamma)^{\gamma_0}} \dots (70)$$

(69) and (70) show that the cooling with instantaneous burning is almost twice as faster than for gradual burning.

$(\frac{T}{T_i})$ can be written in terms of ψ :

$$\frac{T}{T_i} = 1 - \frac{v_{\infty}^2 \psi^2}{\psi^2 T_i} = 1 - \frac{\beta_0}{2} \psi^2 \dots (71)$$

For the end of burning: $\frac{T}{T_i} = 1 - \frac{\beta_0}{2}$

For the second period ($\psi = 1$): $\frac{T}{T_i} = 1 - (\frac{\beta_0}{2})$

and using (68) for $\frac{v}{v_{\infty}}$ we will have:

$$\frac{T}{T_i} = \frac{1}{(1 - \frac{\beta_0}{2})} \cdot \frac{1}{(1 + \gamma)^0} \dots (72)$$

Chapter 4 - A detailed Analysis of the basic Relationships for the Simplest case ($\mathcal{X} = 1$; $\psi_{\infty} = 0$; $\alpha = \frac{1}{\gamma}$).

2. The basic curves of p, v, T and ψ as functions of y or ℓ ($y = \frac{\ell}{r_i}$).

Immediate inspection of the above discussed equations and curves shows that there are only two types of polytropic curves, and that these in their combinations can produce all varieties of analytical forms involved in that discussion. These basic polytropic curves are shown in Fig. 142.

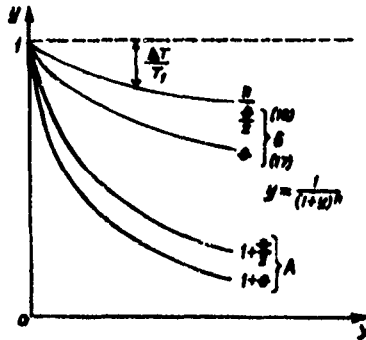


Fig. 142 - The principal types of polytropic curves.
 Two curves with the exponents θ and $\frac{\theta}{2} < 1$
 All curves start at the point $(0, 1)$

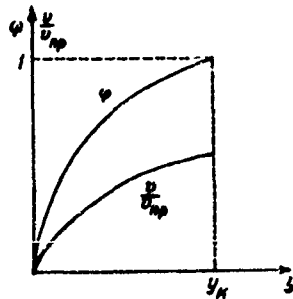


Fig. 143 - Curves: (ψ, y) and $(\frac{\psi}{2}, y)$

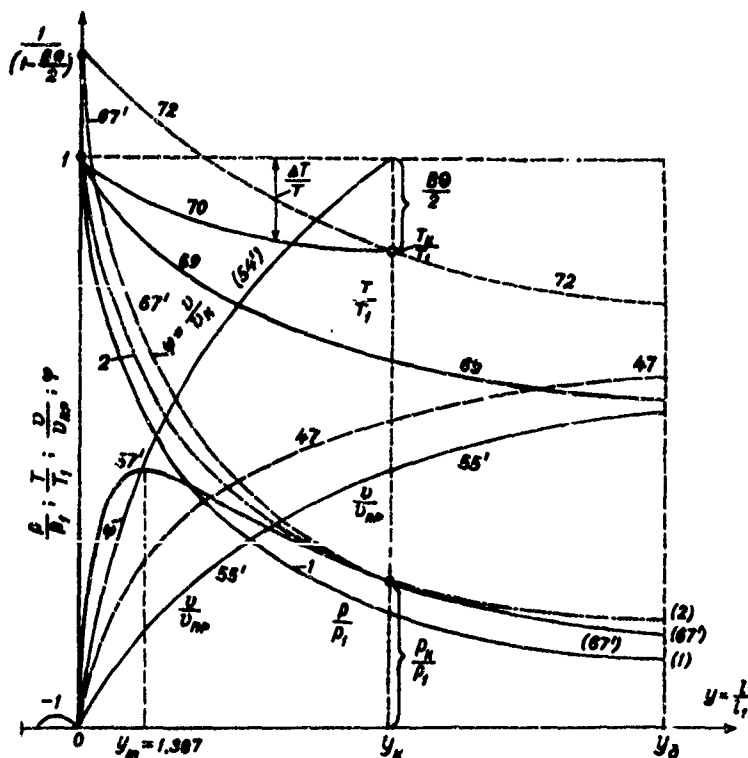


Fig. 144 - Represents ballistic curves of $\frac{p}{p_i}$, $\frac{T}{T_i}$, $\frac{v}{v_{im}}$ and ψ as functions of $y = \frac{c}{c_{im}}$ for both cases - instantaneous burning and gradual burning. All curves are marked by numbers of the corresponding equations as they are given in text.

$$\frac{T}{T_i} = \frac{1}{(1+y)^0} \dots (69) \text{ Instantaneous burning.}$$

$$\frac{T}{T_i} = \frac{1}{(1+y)^{\frac{1}{2}}} \dots (70) \text{ Gradual burning.}$$

$$\psi = \frac{2}{B\theta} \left[1 - \frac{1}{(1+y)^{\frac{1}{2}}} \right] = \frac{2}{B\theta} \left[1 - \frac{T}{T_i} \right] \dots (54')$$

$$\frac{v}{v_m} = \sqrt{\frac{B\theta}{2}} \cdot \psi = \sqrt{\frac{2}{B\theta}} \left[1 - \frac{1}{(1+y)^{\frac{1}{2}}} \right] = \sqrt{\frac{2}{B\theta}} \left[1 - \frac{T}{T_i} \right] \dots (55')$$

$$v = \frac{2f\omega}{\theta S I_N} \left[1 - \frac{1}{(1+y)^{\frac{1}{2}}} \right] \dots (55)$$

$$\frac{p}{p_i} = \frac{\psi}{(1+y)^{\frac{1}{2}}} \dots (57')$$

$$\frac{p_N}{p_i} = \frac{1}{(1+y_N)^{\frac{1}{2}}} \dots (58')$$

For the second period:

$$\frac{p}{p_i} = \frac{1}{1 - \frac{B\theta}{2}} \cdot \frac{1}{(1+y)^{\frac{1}{2}}} \dots (67')$$

$$\frac{T}{T_i} = \frac{1}{1 - \frac{B\theta}{2}} \cdot \frac{1}{(1+y)^{\frac{1}{2}}} \dots (72)$$

$$\frac{v}{v_m} = \sqrt{1 - \frac{T}{T_i}} \dots (68')$$

From (55) we see that v is not affected by the weight of projectile q during the period of burning if we keep the same Δ , the same powder. If we will change only q (parameter B) then p , ψ , p_m and ψ_m will vary but v_m and location of the maximum pressure

$y_m = \frac{L_m}{L_i}$ will stay constant. Hence the practical

conclusion: If keeping the same charge and sort of

powder we decrease q but the muzzle velocity at firing remains the same then we conclude that we have the case of incomplete burning for both projectiles.

2. The conditions necessary for maintaining constant maximum pressure.

In the ballistic design of guns one practical requirement usually insisted upon is - that the maximum pressure should not exceed a given value. Hence it is very important for the designer to know how he can change the loading conditions without affecting the value of the maximum pressure. The above shown relationships permit us to formulate the analytical conditions of maintaining of the value p_m in a given gun at varying ω and Δ .

We had (61):

$$p_m = \frac{p}{B} F_2(\theta) = \frac{f\Delta}{1-\alpha\Delta} \cdot \frac{f\omega^2 q}{g \cdot s^2 I_K^2} F_2(\theta)$$

At the given powder and q the maximum pressure can be changed either by varying Δ or $I_K = \frac{e_i}{u_i}$; hence

the required condition of the constancy of p_m will be:

$$p_m = \frac{F_2(\theta)}{B} \cdot \frac{f\Delta}{1-\alpha\Delta} = \text{Const.} ; B = \frac{s^2 I_K^2}{f\omega^2 q m} = \frac{s^2}{f\omega^2 q m} \cdot \frac{e_i^2}{u_i^2}$$

$$\text{or: } B\left(\frac{1}{\Delta} - \alpha\right) = \frac{f}{p_m} \cdot F_2(\theta) = a_m (\text{Const}) \dots (74)$$

If $\alpha = \frac{1}{\lambda}$ at $\psi = 1$ and $\psi_0 = 0$ we will have $B(\frac{1}{\Delta} - \frac{1}{\lambda}) =$
 $= \text{const.}$ Having a known a_m for any given Δ we find

B and from the value of B we find I_K or $2e$.

The condition (74) shows that if we increase Δ (for preserving constant ρ_m) we will have to increase the web $2e$, so much, that the decrease in B on account of a larger $\Delta(\omega)$ would be overcome by the increased $2e$.

Another important interpretation of (74) follows from rewriting it in another form:

$$\text{or } \frac{S^2 I_K^2 2(1-\alpha\Delta)}{f\omega^2 q \Delta} = \frac{S^2 I_K^2 W_0(1-\alpha\Delta)}{f\omega^2 q m} = \frac{S^2 I_K^2 M}{f\omega^2 q m} = a_m$$

$$\frac{I_K^2 W_1}{\omega^2} = \frac{a_m f q m}{S^2} = \frac{f^2 q m F_2(\theta)}{S^2 \rho_m} = K_m \dots (75)$$

Hence:

$$I_K = \frac{\sqrt{K_m}}{\sqrt{W_0 - \alpha\omega}} \cdot \omega = \frac{e_i}{a_i} \dots (76)$$

This result shows that we have to increase e , not in proportion with the increase in ω in order to keep ρ_m constant.

3. Location of ρ_m in the bore (l_m)

We had in (50):

$$l_m = l_i [F_i(\theta) - i] = l_0 (i - \alpha\Delta) [F_i(\theta) - i]$$

At given Δ and composition of powder ℓ_m is constant and not affected by the thickness of powder $2e$, or by the weight of projectile Q . Only by varying Δ it is possible to remove the section with the maximum pressure closer or farther from the beginning of motion. If Δ is increased with the increasing B and in $2e$, then ℓ_m is decreased and:

$$\psi_m = \frac{1}{B(1+\theta)} \dots (62)$$

will also be decreased i.e. the fraction of the powder charge, burned at the moment of the maximum pressure, will be also decreased.

4. The end of burning and the travel of the projectile along the bore.

From the formula (65) we have:

$$\ell_k = \ell_0(1 - \alpha\Delta) \left[\frac{1}{(1 - \frac{B\theta}{2})^{\frac{1}{2}}} - 1 \right] \left. \vphantom{\frac{1}{(1 - \frac{B\theta}{2})^{\frac{1}{2}}}} \right\} \begin{array}{l} \text{Travel of the} \\ \text{projectile at} \\ \text{the end of} \\ \text{burning.} \end{array}$$

and from (66):

$$p_k = p_1 \frac{1}{(1 + \gamma_k)^{1 + \frac{1}{2}}} \left. \vphantom{\frac{1}{(1 + \gamma_k)^{1 + \frac{1}{2}}}} \right\} \begin{array}{l} \text{Pressure at} \\ \text{the end of} \\ \text{burning.} \end{array}$$

At given Δ , ℓ_K is increased with the increase of B (on account of increase in $2e$). With the decrease of q at the same Δ , ℓ_K is increased.

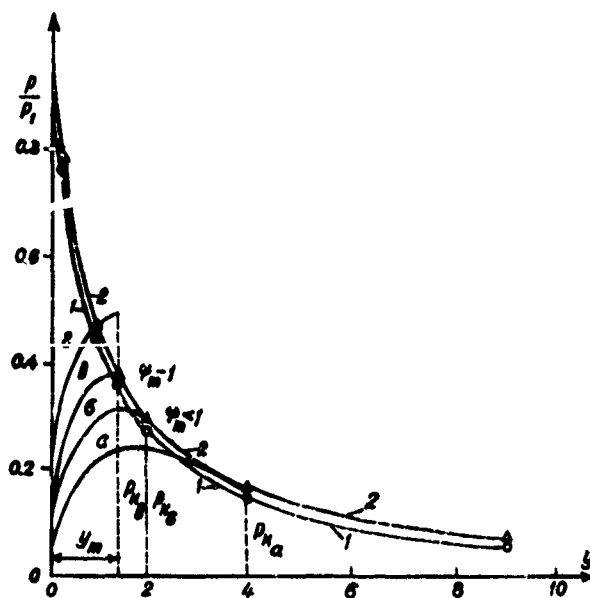


Fig. 145 - Presents a set of curves (p, y) marked:
 a - thick powder; σ - normal powder; ϵ - thin powder;
 \hat{e} - a very fine powder. These curves show the character of variations in the pressure with the change of thickness of powder at the same Δ . All maximum pressures are at the same y_m and the final pressures p_K are located along the curve marked 2 which is calculated from (66) at $\theta = 0.2$; $1 + \frac{\epsilon}{2} = 1.1$. Another curve marked 1 represents an instantaneous burning with its

adiabatic pressure curve $(1 + \theta) = 1.2$. All curves $a - \delta - b - c$ intersect with the curve 1 but their continuations (after p_K) are running between the curves 1 and 2.

Pressure p'' during the second period:

$$p'' = \frac{p_i}{(1 - \frac{\theta}{2})} \cdot \frac{1}{(1 + \theta)^{1.2}}$$

Pressure p' at the instantaneous burning:

$$p' = \frac{p_i}{(1 + \theta)^{1.2}}$$

Hence: $\frac{p''}{p'} = \frac{1}{1 - \frac{\theta}{2}} = \text{Const.}$

All the above shown curves and formulas for the simplest case ($\chi = 1$; $\psi_0 = 0$; $\alpha = \frac{1}{\chi}$) give a general view of the basic relationships between the ballistic elements of the firing process: they show the value and location of the maximum pressure, how p_m is affected by the loading conditions (Δ, B); in the same way are presented p_K and l_K ; conditions necessary for the preservation of desired p_m are analyzed and a very important factor of the interdependence of the curve (v, l) during the 1st period from the weight of projectile is noted and discussed.

For more involved cases ($\chi \neq 1.0$; $\psi_0 \neq 0$; $\alpha \neq \frac{1}{\chi}$) we cannot derive such simple relationships. In these cases we have to analyze the influences of separate

elements considering series of several variants or to make use of data supplied by the ballistic tables.

Chapter 5 - Other Methods of Solution of the Ballistic Problem.

1. Prof. G. Oppokov's method.

For the integration of the basic equation:

$$\frac{d\ell}{\ell_\psi \cdot \ell} = \frac{Bx dx}{\psi_0 + K_1 x - B_1 x^2} \dots \dots (13) \text{ or} \quad (78)$$

Prof. Oppokov introduces a new variable \tilde{z} given by:

$$\ell = \tilde{z} + a \frac{B_0}{2} x^2 - \ell_\Delta \quad (79)$$

here:

$$a = \ell_\Delta - \ell_i = \frac{\omega}{S} \left(\alpha - \frac{1}{\lambda} \right) \dots (80)$$

Then (79) after differentiation will be:

$$\frac{d\ell}{dx} = \frac{d\tilde{z}}{dx} + B_0 a x$$

and:

$$\ell_\psi + \ell = \ell_\Delta - a \psi + \ell = \ell_\Delta - a (\psi_0 + K_1 x + K_2 \lambda x^2) + \ell$$

using ℓ given by (79) we will have:

$$\ell_\psi + \ell = \tilde{z} + a \frac{B_0}{2} x^2 - a (\psi_0 + K_1 x + K_2 \lambda x^2)$$

or:

$$\ell_\psi + \ell = \tilde{z} - a (\psi_0 + K_1 x - B_1 x^2)$$

Then (78) will be rewritten:

$$\frac{dz}{dx} + B\theta ax = \frac{Bx}{\psi_0 + Kx - B_1x^2} \left[z - a(\psi_0 + Kx - B_1x^2) \right]$$

or:

$$\frac{dz}{dx} - \frac{Bx}{\psi_0 + Kx - B_1x^2} \cdot z = -Ba(1+\theta)x$$

The integral of this equation will be:

$$z = e^{\int \frac{Bx dx}{\psi_0 + Kx - B_1x^2}} \left[C_1 - Ba(1+\theta) \int e^{-\int \frac{Bx dx}{\psi_0 + Kx - B_1x^2}} x dx \right] \quad (81)$$

here C_1 is a certain constant.

Taking Prof. Drosdov's function:

$$Z^{-\frac{B}{B_1}} = e^{\int \frac{Bx dx}{\psi_0 + Kx - B_1x^2}}$$

then the partial integral for $\frac{dz}{dx}$ will be:

$$z = Z^{-\frac{B}{B_1}} \left[C_1 - Ba(1+\theta) \int Z^{\frac{B}{B_1}} x dx \right]$$

this z inserted in (79) will give:

$$l = Z^{-\frac{B}{B_1}} \left[C_1 - Ba(1+\theta) \int Z^{\frac{B}{B_1}} x dx \right] + a \frac{B\theta}{2} x^2 = l_\Delta x$$

The initial conditions are: $l=0; x=0; Z^{-\frac{B}{B_1}}=1; \int Z^{\frac{B}{B_1}} x dx=0$

Then from the last equation we will determine C_1 ,

$$0 = 1[C_1 + 0] + 0 - l_\Delta$$

or:

$$C_1 = l_\Delta$$

Thus the final expression for ℓ will be:

$$\ell = Z^{\frac{3}{2}} \left[\ell_{\Delta} - aB(1+\theta) \int Z^{\frac{3}{2}} x dx \right] + a \frac{\beta_0}{2} x^2 - \ell_{\Delta} \quad (82)$$

2. Prof. I. P. Grave's method.

This method was devised by Prof. Grave as an improvement of method used by Bianchi (1910). Bianchi considered $\ell_{\psi_{av}}$ and ψ as related each to other in the following way:

$$\left. \begin{array}{l} \psi_{av} = 0 \\ \ell_{\psi_{av}} = \ell_{\Delta} \end{array} \right\} \psi_{av} = \frac{1}{2} \left\{ \begin{array}{l} \psi_{av} = 1 \\ \ell_{\psi_{av}} = \ell_{\Delta} \frac{3}{2} \end{array} \right\} \left\{ \begin{array}{l} \psi_{av} = 1 \\ \ell_{\psi_{av}} = \ell_1 \end{array} \right\}$$

Under these conditions the curves (ρ, ℓ) and (v, ℓ) have the angular points at the beginnings of the second and third phases. Prof. Grave considers ℓ_{ψ} as a variable determined by the average value of its derivative: $\frac{d\ell_{\psi}}{d\ell} = -K < 0$ because ℓ_{ψ} is a decreasing value during the burning.

Hence we have:

$$\ell_{\psi} = \ell_{\psi_0} - K\ell \quad \dots (83)$$

At $\psi = 1$ (end of burning):

$$\ell_1 = \ell_{\psi_0} - K\ell_K \quad \text{or}$$

$$K = \frac{\ell_{\psi_0} - \ell_1}{\ell_K} = \frac{\left(\frac{\ell_{\psi_0} - \ell_1}{\ell_1}\right)}{\left(\frac{\ell_K}{\ell_1}\right)} \quad \dots (84)$$

Then (78) will be rewritten:

$$\frac{d\ell}{\ell_{\psi_0} + (1-K)\ell} = \frac{\beta x dx}{\psi - \frac{\beta_0}{2} x^2}$$

After the integration we have:

$$\frac{1}{1-K} \cdot \log_2 \left[\frac{e_{\kappa} + (1-K)e}{e_{\psi_0}} \right] = \int_0^x \frac{\beta x dx}{\psi - \frac{\beta^2}{2} x^2} = -\frac{\beta}{\beta_1} \log_2 Z = \log_2 (Z^{-\frac{\beta}{\beta_1}})$$

and finally:

$$e = e_{\psi_0} Z^{-\frac{\beta}{\beta_1}} - e_{\psi} \dots \dots (85)$$

But the constant K involves the ratio $\frac{e_{\kappa}}{e_1}$ and e_{κ} is supposed to be not known yet. Prof. Grave gives a special nomogram which is used for finding $(\frac{e_{\kappa}}{e_1})$ from given loading conditions $(\frac{e_{\psi_0}}{e_1})$ and $(2.303 \frac{\beta}{\beta_1} \log Z^{-1})$. Thus having $\frac{e_{\kappa}}{e_1}$ we find K and can use (85).

Chapter 6 - Prof. M. E. Serebryakov's Method of Solution of the Principal Problem, Based on the Physical Law of Burning.

It has already been shown that real burning for several reasons does not follow the course prescribed by the geometrical law of burning. The analysis made by means of the experimental curves (r, ψ) and (r, t) disclosed that even in cases of powders with the simple forms of their grains their burning always presents certain abnormal features like - non-instantaneous ignition or an accelerated burning of the outer layers (irregular "humpy" curves). For phlegmatized and porous powders the geometrical law cannot be applied at all.

The actual law of burning can be studied and reliably established only by burning powder in the manometric bomb at various densities of loading and by analyzing the curves of pressures and velocities as functions of time. From the analysis of (p, t) curve we obtain the characteristics of the intensity of gas formation Γ and $I = \int p dt$ as functions of ψ and t . Then the curves (p, t) , (Γ, t) , (I, ψ) are used for the evaluation of pressures and velocities at the actual burning in the bore of a gun. Thus the principal problem of interior ballistics is solved. Only by using these curves it is possible in practice to disclose certain individual peculiarities of powders of different brands. Not infrequently the powder lots of the same make which are supposed to be identical in their chemical composition and grain dimensions at the firing tests with the same $\frac{p}{m}$ and $\frac{2\psi}{L}$ required not the same weights of charges but differ as much as 6 - 8%. Experimental tests in the manometric bomb with these powders disclosed that their rates of burning were different to the extent of 15 - 20%. In the same way the principal problem for phlegmatized and porous powders can be solved by the applying the experimental

(physical) law of burning. This law requires the use of the rate of burning expressed in the form $u = u, p$, which is a direct consequence of the observable fact, that the curves (I, ψ) at various Δ are identical. In other words our basic postulate is that in the bomb at various Δ as well as in the gun (when during the firing the density of loading is continually decreased), the impulse or $\int p dt$ is a monotonic function of ψ and is not affected by the value of Δ . This statement was proved by experiments in manometric bombs at various constant densities of loading and its extrapolation is fully justifiable for the cases of much higher densities of loading existing in guns.

1. The principal relationships under the physical law of burning.

Our basic datum is the pressure curve obtained from the experiments in a bomb, and this curve is used for the calculations of the pressure and velocity curves expected to be realized at the firing of a gun. The density of loading in a gun: $\Delta = \frac{w}{W_0 + sP}$ during the firing is the main factor controlling the value of the pressure.

The following notations will be used:

Δ_1 - density of loading in a bomb.

Δ - the initial density of loading in a gun.

P and τ - are the values of pressure and time corresponding to the given ψ and Δ as they are recorded in a bomb as the curve (P, τ)

p and t - are the values of pressure and time corresponding to the same value of ψ at the variable density of loading Δ in a gun.

The corresponding values of the integrals are as follows:

$$\begin{array}{ll} \text{In a bomb: } \int_0^{\psi} P d\tau = I & \text{In a gun: } \int_0^{\psi} p dt = i \\ \int_0^{\psi} P d\tau = I_0 & \int_0^{\psi} p dt = i_0 \\ \int_0^{\psi} P d\tau = I_{\kappa} & \int_0^{\psi} p dt = i_{\kappa} \end{array}$$

From the experiments in a bomb we have tables or curves of the values I, I_0, I_{κ} .

Since the impulse is not affected by the value of Δ

we will have:

$$\int_0^\psi p dt = \int_0^\psi P d\tau \begin{cases} i = I & \text{and after} \\ i_0 = I_0 & \text{differentiating:} \\ i_K = I_K & p dt = P d\tau \end{cases} \quad (87)$$

Here: $d\tau$ is an elementary interval of time during which the burned fraction ψ will have its increment $d\psi$ at the burning of powder in a constant volume at the density of loading Δ . dt is an elementary interval of time during which the same $d\psi$ of the same ψ will be burned at the pressure p , at Δ determined by the current value of ℓ - the projectile travel along the bore of a gun. Here $\Delta = \frac{\omega}{W_0 + s\ell}$ and the independent variable is ψ .

2. Velocity v as a function of ψ .

From: $\varphi m dv = S p dt$

we have: $\varphi m v = S \int_0^\psi p dt = S(i - i_0)$

here: $\psi_0 = \frac{i_0 - i}{i_0 + \alpha - i}$ is a fraction of the charge burned in a gun before the beginning of motion of the projectile.

Thus we have:

$$v = \frac{S}{\varphi_m} (i - i_0) \dots (88)$$

or:

$$v = \frac{S}{\varphi_m} (I - I_0) \dots (89)$$

Here I and I_0 are known for the values of ψ and ψ_0 from the experiments in a bomb and $\frac{S}{\varphi_m}$ is known for a given gun.

Thus v is given by (89) as a function of ψ .

for $\psi = 1$, we have:

$$v_K = \frac{S}{\varphi_m} (I_K - I_0) \dots (90)$$

For the end of burning.

Here I_K is the impulse corresponding not to certain average thickness of powder but to the maximum thickness which may considerably deviate from the average thickness.

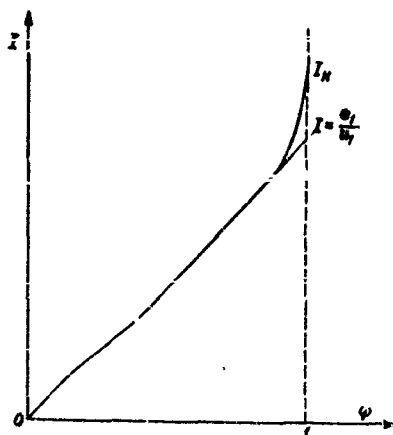


Fig. 146 - Shows the curve (I, ψ) with I_K which corresponds to the maximum thickness and I_0 which corresponds to the average value $\frac{(e_1)_{av}}{u_1} = I_0$; $I_K > I_0$.

Hence we conclude that v_k for the actual burning will be greater than v_k^* , corresponding to the geometrical law of burning and also l_k (physic law) will be larger than l_k^* (geometric law).

3. Travel of the projectile as a function of ψ .

From (88) we have: $dl = \frac{S}{\varphi_m} (i - i_0) dt$

and after the integration:

$$l = \frac{S}{\varphi_m} \int_{i_0}^i (i - i_0) dt \dots (91)$$

Here dt corresponds to the element $d\psi$ and is affected by the pressure p which for the time being is unknown. From the experiments in a bomb we will have the following expression, analogous to (91):

$$L_k^* = \frac{S}{\varphi_m} \int_{i_0}^i (I - I_0) d\tau = \frac{S}{\varphi_m} \int_{i_0}^i \int_{\tau_0}^{\tau} p d\tau d\tau = \frac{S}{\varphi_m} \cdot G \dots (92)$$

Here the value of L is a function of ψ obtained by the second integration with respect to τ along the curve $\int_{\tau_0}^{\tau} p d\tau$ and by multiplication by $(\frac{S}{\varphi_m})$. We know that L is a travel of the projectile corresponding to the burned fraction ψ and we consider the value of L as a travel of the projectile if the pressure behind the projectile were developed according to the same law which is effective in a bomb at the constant Δ , when the same fraction ψ is burned.

This value L can be determined by the experiment in a bomb. We take a bomb with a large volume (300 cu. cm³.) and with the free piston (cross-sectional area 1 cm².) having its stroke about 3 cm.; then the additional volume will be only about 1% and we can consider the travel of such piston under the pressure acting in a constant volume. Our immediate problem is to find the relationship between ℓ and L and since L is a function of ψ we will find ℓ as a function of ψ in the following way:

Differentiating (91) and (92)

we have: $\frac{d\ell}{dL} = \frac{d\ell}{d\psi} \dots (93)$

and from (87) $\frac{d\ell}{d\psi} = \frac{P}{p} \dots (94)$

The ratio $(\frac{P}{p})$ is determined from the expressions for these pressures.

$$P = \frac{RT_1 \alpha_1 \psi}{W_p} = \frac{f \Delta_1 \psi}{1 - \frac{\Delta_1}{\alpha_1} - \Delta_1 (\alpha - \frac{1}{\alpha}) \psi} = \frac{f \psi}{\frac{1}{\alpha_1} - \frac{1}{\alpha} - (\alpha - \frac{1}{\alpha}) \psi}$$

The denominator is a free specific volume of gases

at Δ_1 . Since the last term in the denominator is very small in comparison with the first terms we will consider the average value of W_p at $\psi_{av} = \frac{1}{2}$, then:

$$W_{\psi_{av}} = W_0 \left[1 - \frac{\Delta_1}{\alpha} - \Delta_1 (\alpha - \frac{1}{\alpha}) \psi_{av} \right] = W_0 \left[1 - \frac{\alpha + \frac{1}{\alpha}}{2} \Delta_1 \right] = W_0 (1 - \alpha' \Delta_1)$$

We will have notations: $\frac{1}{2}(\alpha + \beta) = \alpha'$; $\frac{1}{\Delta_1} - \alpha' = a_1$; $\frac{1}{\Delta_0} - \alpha' = a_0$.

Then: $P = \frac{f\omega}{a_1}$

and: $\rho = \frac{RT\omega\psi}{W_{av} + S\ell} = \frac{f\Delta_0\psi}{1 - \alpha'\Delta_0 + \frac{\ell}{\Delta_0}} \cdot \frac{T}{T_1} = \frac{f\omega}{a_1 + \frac{\ell}{\Delta_0}} \cdot \frac{T}{T_1} = \frac{f\omega}{a_1(1 + \frac{\ell}{a_1\Delta_0})} \cdot \frac{T}{T_1}$

Here: $a_0\ell_0\Delta_0 = \ell_0(1 - \alpha'\omega_0) = \ell_{av} = \ell_{av}$.

For the gradual burning:

$$\frac{T}{T_1} = \left(\frac{W_0 - \alpha'\omega}{W_0 - \alpha'\omega + S\ell} \right)^{\frac{Q}{2}} = \left(\frac{a_0}{a_0 + \frac{\ell}{\Delta_0}} \right)^{\frac{Q}{2}} = \left(\frac{1}{1 + \frac{\ell}{a_0\Delta_0}} \right)^{\frac{Q}{2}}$$

Then finally:

$$\frac{P}{\rho} = \frac{a_0}{a_1} \left(1 + \frac{\ell}{\ell_{av}} \right)^{1 + \frac{Q}{2}} \quad (95)$$

Now (93) and (94) will give:

$$d\ell = dL \frac{a_0}{a_1} \left(1 + \frac{\ell}{\ell_{av}} \right)^{K'}; \quad K' = 1 + \frac{Q}{2}$$

After the integration we have:

$$\int_0^{\ell} \frac{d\ell}{\left(1 + \frac{\ell}{\ell_{av}} \right)^{K'}} = \frac{a_0}{a_1} \int_{\psi_0}^{\psi} dL$$

denoting: $1 + \frac{\ell}{\ell_{av}} = x$

Then the left integral will be:

$$\int_0^{\ell} \frac{d\ell}{\left(1 + \frac{\ell}{\ell_{av}} \right)^{K'}} = \frac{2}{Q} \ell_{av} \left(1 - \frac{1}{x^{\frac{Q}{2}}} \right)$$

The right integral:

$$\frac{a_0}{a_1} \int_{\psi_0}^{\psi} dL = \frac{a_0}{a_1} L_{\psi_0}^{\psi}$$

Thus we have:

$$1 - \frac{1}{x^2} = \frac{\theta}{2} \frac{a_0}{a_1 l_{av}} \cdot L_{\psi}^{\psi} = B' L_{\psi}^{\psi} \dots (96)$$

$$\text{Here: } B' = \frac{\theta}{2} \cdot \frac{a_0}{a_1 l_{av}} = \frac{\theta}{2} \cdot \frac{\Delta_0 - \alpha'}{\Delta_1 - \alpha'} \cdot \frac{1}{l_0(1 - \alpha' \Delta_0)} = \frac{\theta}{2} \cdot \frac{1}{\Delta_0 l_0} \cdot \frac{1}{\Delta_1 - \alpha'}$$

$$\text{but } \Delta_0 l_0 = \frac{\omega}{2}$$

$$\text{So: } B' = \frac{\theta}{2} \cdot \frac{2}{\omega} \cdot \frac{1}{\Delta_1 - \alpha'} \dots (97)$$

And finally from (96) solving it for ℓ :

We have:

$$\ell = l_{av} \left[\frac{1}{(1 - B' L_{\psi}^{\psi})^{\frac{2}{\theta}}} - 1 \right] \dots (98)$$

We had an approximate solution with l_{av} in this form:

$$\ell = l_{av} \left[Z_x^{\frac{\theta}{2}} - 1 \right] \dots (14)$$

If we have $\chi = 1$ and $\lambda = 0$ then $\frac{B}{B_0} = \frac{2}{\theta}$

and then: (98) will be:

$$\ell = l_{av} \left[(1 - B' L_{\psi}^{\psi})^{-\frac{2}{\theta}} - 1 \right] \dots (99)$$

and (14) will be:

$$\ell = l_{av} \left[Z_x^{\frac{\theta}{2}} - 1 \right]$$

which shows that the function $(1 - B' L_{\psi}^{\psi})$ applied with the physical law of burning is a counter part of the function Z_x used with the geometrical law of

burning. Thus (89) and (98) will give v as a function of ℓ . Instead of ℓ_{av} considered on the whole range of firing process we may use:

$$\ell_{\psi_{av}} = \ell_0 \left[1 - \frac{\Delta}{\rho} - \Delta \left(\alpha - \frac{1}{\rho} \right) \left(\frac{\psi_0 + \psi}{2} \right) \right] \dots (100)$$

which is ℓ taken for a current value of the average ψ . This auxiliary function ℓ_{ψ_0} being determined for a definite density of loading Δ , in a bomb is a true expression of the physical law of burning controlling the actual process of firing. The pressure is found from the basic equation of pyrodynamics:

$$p = \frac{f\omega\psi - \frac{1}{2}\varphi_m v^2}{S(\ell_{\psi} + e)} \dots (101) \text{ or } (53) \text{ in Part I.}$$

here all variables are known as functions of ψ .

Differentiating with respect to ℓ as was shown in (59), Part I, we have:

$$\frac{dp}{d\ell} = \frac{p}{\ell_{\psi} + e} \left\{ \frac{f\omega}{S} \Gamma \left[1 + \left(\alpha - \frac{1}{\rho} \right) \frac{p}{f} \right] - (1 + \theta)v \right\}$$

here: $v = \frac{S}{\varphi_m} (I - I_0)$ and Γ are known as functions of ψ .

Making $\frac{dp}{d\ell} = 0$ we will have:

$$\text{or: } \frac{f\omega}{S} \Gamma_m \left[1 + \left(\alpha - \frac{1}{\rho} \right) \frac{p_m}{f} \right] - (1 + \theta) \frac{S}{\varphi_m} (I_m - I_0)$$

$$I_m - I_0 = \frac{f\omega\varphi_m}{S(1+\theta)} \left[1 + \left(\alpha - \frac{1}{\rho} \right) \frac{p_m}{f} \right] \Gamma_m \dots (102)$$

Denoting:
$$\frac{f\omega \varphi m}{S^2(1+\theta)} \left[1 + (\alpha - \frac{1}{\beta}) \frac{p_m}{f} \right] = D$$

we have finally:
$$I_m - I_0 = D \cdot \Gamma_m$$

Considering $I - I_0 = f_1(\psi)$ and $D \cdot \Gamma = f_2(\psi)$
 we will find $(I_m - I_0)$, ψ_m and Γ_m determined by
 the point of intersection of two curves $f_1(\psi)$ and $f_2(\psi)$
 , which is shown on Fig. 147.

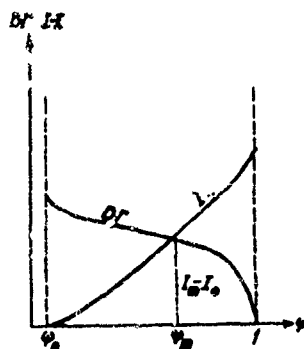


Fig. 147 Curves $I - I_0 = f_1(\psi)$ and $D \cdot \Gamma = f_2(\psi)$

At $\psi = 1$ (the end of burning) we have:

$$\psi_K = \frac{S}{\omega m} (I_K - I_0)$$

$$l_K = l_{av} \left[(1 - B' \frac{\psi_K}{\psi_0})^{\frac{1}{\beta}} - 1 \right]$$

$$p_K = \frac{f\omega}{S} \cdot \frac{1 - (\frac{\psi_K}{\psi_m})^2}{l_1 + l_K}$$

For the second period formulas are as we had them before:

$$\rho = \rho_n \left(\frac{e_i + e_n}{e_i + e} \right)^{1+\theta} \quad (103)$$

$$v = v_{\text{lim}} \sqrt{1 - \left(\frac{e_i + e_n}{e_i + e} \right)^{\theta} \left(1 - \frac{v_n^2}{v_{\text{lim}}^2} \right)} \dots (104)$$

4. Graphical interpretation of the solution based on the physical law of burning.

When applying the physical law of burning the first step consists of the ballistic analysis of a given powder: for two densities of loading Δ , and Δ_n in a bomb must be determined - f , covolume α , the experimental characteristic of the intensity of gas formation $\Gamma(\psi)$ and the impulse $I = \int_0^{\psi} p d\psi$ as this is shown on Fig. 148.

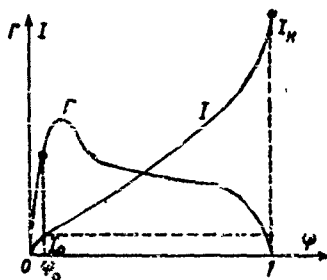


Fig. 148 - Basic curves (Γ, ω) and (I, ψ) .

From given loading conditions we calculate ψ_0

$$\psi_0 = \frac{\frac{1}{\Delta_0} - \frac{1}{\Delta}}{\frac{1}{\rho_0} + \alpha - \frac{1}{\Delta}}$$

and on the curve (I, ψ)

I_0 is determined. Subtracting this I_0 from all I'_s we will determine another curve $(I - I_0)$ as a function of ψ and of τ as it is shown on Fig. 149.

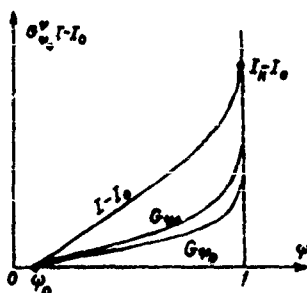


Fig. 149 - The auxiliary curves determining the elements of firing.

Numerical integration along the curve $(I - I_0)$ as a function of τ will give us $\int_{\psi_0}^{\tau} (I - I_0) d\tau$ as a function of ψ .

Let us denote: $G_{\psi_0}^{\psi} = \int_{\psi_0}^{\psi} \int_{\psi_0}^{\tau} P d\tau d\tau = \int_{\psi_0}^{\psi} (I - I_0) d\tau$;

multiplying $(I - I_0)$ and $G_{\psi_0}^{\psi}$ on $(\frac{\Sigma}{\psi_m})$ we have:

$$v = \frac{\Sigma}{\psi_m} (I - I_0) \dots (89)$$

and:
$$L_y^* = \frac{\bar{S}}{\bar{\phi}_m} \cdot G_y^* = \frac{\bar{S}}{\bar{\phi}_m} \int_{\psi_0}^{\psi} (\bar{I} - I_0) d\tau \quad \dots (92)$$

Velocity v_y^* is a function of ψ not affected by Δ .

Function L_y^* as a function of ψ is affected by Δ , because the time element $d\tau$ corresponding to $d\psi$ is decreased when Δ is increased as this can be seen

from the following:
$$\Gamma = \frac{d\psi}{d\tau} \cdot \frac{1}{\beta}$$

or:
$$d\tau = d\psi \cdot \frac{1}{\Gamma\beta}$$

and:
$$P = \frac{f_{\Delta, \psi}}{1 - \frac{\Delta}{\beta} - \Delta \cdot (\alpha - \frac{1}{\beta}) \psi} \sim \frac{f_{\Delta, \psi}}{1 - \alpha' \Delta}$$

Therefore $d\tau$ will be decreased when Δ , will be increased. As a result of this the curves G_y^* and L_y^* as functions of ψ will run higher for smaller Δ .

From (89) and (92) we can determine \bar{v} as function of L or ℓ , for various Δ (Δ_1, Δ_2 and Δ_0 which is the initial density of loading in gun) which is shown on Fig. 150.

gases used for separate locations of the projectile in the bore. No assumptions different from those which are normally used in practice are involved. The basis of this method is the pressure curve (P, ℓ) obtainable in a bomb as a characteristic of the real law of burning with its all deviations from the geometrical law.

The analogous result can be obtained by the numerical integration of Taylor's series or finite differences.

If we admit the use of the geometrical law, the present method can be used if we take:

$$\sqrt{r} = \frac{x_0}{\bar{x}_K} \delta = \frac{x_0}{\bar{x}_K} \sqrt{1 + 4 \frac{\lambda}{x_0^2} \psi} = \frac{1}{\bar{x}_K} \sqrt{x_0^2 + 4 \lambda \psi}$$

This means that this method is more general and more flexible than other methods based on the geometrical law of burning.

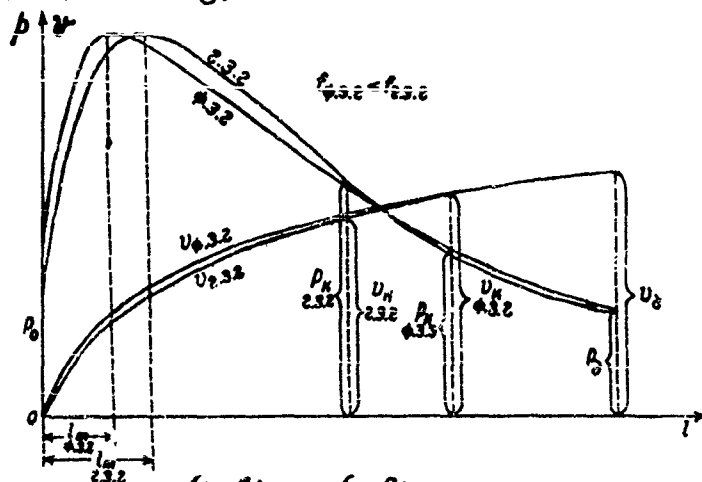


Fig. 151 - Curves (p, ℓ) and (v, ℓ) obtained by 2 methods. Solid lines - physical law of burning. Dotted lines - geometrical law of burning.

Resume: 1. Maximum pressure is obtained earlier:

$(l_m)_{phys.} < (l_m)_{geom.}$ when calculated, applying the physical law.

2. Velocity curve is higher before the end of burning when calculated applying the physical law.

3. The same value p_m is obtained at the lower value of f , when calculated applying the physical law.

4. The end of burning (l_k) and v_k are greater and p_k is smaller when calculated applying the physical law.

5. The muzzle velocity v_2 and the pressure p_2 are the same when calculated by both methods.

Note: "Physical Law of burning in Interior Ballistics" by Prof. M. E. Serebryakov, published in Moscow, 1940 is translated into English by V. A. Nekrassoff as a very helpful supplement to the course in Interior Ballistics of the same author. The results obtained by Prof. Serebryakov are original, new and important for the practical applications of Interior Ballistics to the design of artillery systems.

Section VII - Numerical MethodsChapter 1 - Numerical integration in finite differences.

1. Application to the determination of a function.
 1. Tabular determination of a function.
 2. Finite differences of various orders.
 3. General properties of finite differences.
 4. Evaluation of the coefficients of a function.
 5. Practical uses of the finite differences.
 - a. Interpolation of a function.
 - b. Interpolation of an argument (inverse interpolating).
 - c. Evaluation of definite integrals.
2. Numerical integration of the differential equations.
 - a. Numerical integration of equations of the first order.

Example 1: Integration of equation:

$$\frac{dy}{dx} = x - y.$$

Example 2: Integration of equation:

$$\frac{dl}{dv} = \frac{1}{2\frac{v}{l}} \cdot \frac{2v}{\frac{v}{l}} (l_v + l)$$

- b. Numerical integration of equations of the second order.

Example: Integration of: $\psi m \frac{dv}{dt} = Sp$

$$\text{or: } \frac{d^2 l}{dt^2} = \frac{Sp}{\varphi m}$$

$$\text{having in view that: } p = \frac{f a \psi}{s} \cdot \frac{\psi - \frac{\bar{v}}{2a}}{l_p + l}; \quad l_n = l_a \cdot l_u \psi$$

$$l_a = \frac{\omega}{s} \left(\frac{1}{\alpha} - \frac{1}{\beta} \right)$$

$$l_u = \frac{\omega}{s} \left(\alpha - \frac{1}{\beta} \right)$$

Chapter 2 - Solution by Development in Taylor Series.

$$\text{Equations: } p s (l_p + l) = f a \psi - \frac{1}{2} m \varphi v^2$$

$$\psi = \alpha z (1 + \lambda z)$$

$$\frac{dl}{dt} = u = u, p$$

$$\frac{d\psi}{dt} = \frac{S_1}{\lambda_1} \cdot \sigma u, p = \frac{\gamma_1}{\epsilon_1} \sigma u, p$$

$$p s = \varphi m \frac{dv}{dt} = \varphi m \frac{d^2 l}{dt^2}$$

$$v = \frac{S I_{\lambda}}{\varphi m} (z - z_0); \quad z = z_0 + \frac{\varphi m}{S I_{\lambda}} v = z_0 + \frac{\varphi m}{S I_{\lambda}} \cdot \frac{dl}{dt}$$

All variables are expressible in terms of l and of its derivatives. Thus if we take t as the independent variable then l will be that function which we have to develop in Taylor's series and, having value of l_n at the moment t_n we will evaluate l_{n+1} and its derivatives for $t_{n+1} = t_n + \Delta t$. Hence we will find z , ψ , v , p and \dot{l} i.e. all the elements of the firing.

Section VIII - Empirical Methods of Solution.Chapter 1 - Monomial and Differential Formulas.

1. Monomial empirical formulas.

Prof. N. Zaboudsky's formulas 1894 and 1914

For 3" field artillery gun: $v_s = H_1 \frac{\omega^{3/4}}{d^{1/2} \ell^{1/4} q^{3/4}}$

$$p_m = K_1 \frac{\omega^2 q^{3/4}}{d^2 \ell_0}$$

For 3", 4.2" and 6" guns:

$$v_s = H \frac{\Delta^{1/4} \omega^{3/4}}{(2e)^{1/4} q^{1/4}} ; p_m = K \frac{\Delta^{2/5} \omega^{3/5} q^{4/5}}{(2e)^{4/5}}$$

Here H , K , H_1 and K_1 empirical coefficients for given loading conditions.

2. Empirical differential formulas.

Formulae obtained by the Testing Commission of the

Okhta Powder Plant (1895-1910). Here: $\Delta t\%$ - percent of weight lost.

$$\frac{\Delta p_m}{p_m} = 2 \frac{\Delta \omega}{\omega} - \frac{1}{3} \frac{\Delta e}{e} - \frac{1}{3} \frac{\Delta W_0}{W_0} + \frac{1}{4} \frac{\Delta q}{q} - 0.15(\Delta H\%) + 0.0036(\Delta t^\circ)$$

$$\frac{\Delta v_s}{v_s} = \frac{3}{4} \frac{\Delta \omega}{\omega} - \frac{1}{2} \frac{\Delta e}{e} - \frac{1}{3} \frac{\Delta W_0}{W_0} - \frac{2}{3} \frac{\Delta q}{q} - 0.04(\Delta H\%) + 0.0011(\Delta t^\circ)$$

3. Prof. V. E. Sloukhotzky's corrective formulae and tables.

Corrective formulas for p_m and v_s or $\frac{\Delta p_m}{p_m}$ and $\frac{\Delta v_s}{v_s}$ as they are affected by the variations in parameters X .

(I_x, ω, f, q and W_0) are given in terms of coefficients m for ρ_m and ℓ for v_b .

For every parameter X we have: $\frac{\Delta \rho_m}{\rho_m} = m_x \cdot \frac{\Delta X}{X}$

$$\text{and } \frac{\Delta v_b}{v_b} = \ell_x \cdot \frac{\Delta X}{X}.$$

Coefficients m are affected by the values of ρ_m and Δ

Coefficients ℓ are affected by the values of ρ_m, Δ and $\lambda = \frac{q}{2}$. (Tables are given here--see the next 2 pages).

4. Formulae and tables given by G. Kisnensky.

Since in empirical formulae in majority of cases the weight of powder charge ω or the thickness of grains ($2e$) are not taken into account, Kisnensky worked out his empirical formulas among which here are given the following:

$$v_b = h (\omega - \omega_0)^{\frac{1}{2}} - \text{here } \omega_0 \text{ is that}$$

part of the powder charge which is spent during the firing on the secondary works and is given by:

$$\omega_0 = 0.001 (sl, q)^{\frac{1}{2}} (2e)^{\frac{1}{2}} = \omega - (W_0 + sl, q) \cdot \frac{\rho_b}{f + \alpha \rho_b}$$

here subscript v_b refers to the moment when the projectile leaves the muzzle.

Table for m_x (I_k, ω, f, q, w_0)

$\frac{\Delta}{p_m}$	m_{I_k}				m_{ω}				m_f			
	0.5	0.6	0.7	0.8	0.5	0.6	0.7	0.8	0.5	0.6	0.7	0.8
2000	1.49	1.40	1.32	1.24	2.04	2.17	2.29	2.38	1.80	1.78	1.72	1.64
2500	1.50	1.46	1.40	1.33	2.14	2.28	2.43	2.57	1.81	1.81	1.76	1.67
3000	1.50	1.50	1.46	1.40	2.22	2.39	2.56	2.74	1.78	1.81	1.78	1.69
3500	1.45	1.51	1.50	1.44	2.30	2.49	2.69	2.90	1.73	1.78	1.78	1.70
4000	1.36	1.48	1.50	1.46	2.38	2.59	2.82	3.05	1.66	1.73	1.76	1.71
4500	1.24	1.42	1.48	1.47	2.45	2.69	2.94	3.19	1.58	1.68	1.74	1.71
	m_q				m_{w_0}				l_{w_0}			
	0.69	0.73	0.76	0.78	1.36	1.45	1.52	1.59	4	6	8	10
2000	0.69	0.73	0.76	0.78	1.36	1.45	1.52	1.59	0.34	0.23	0.16	0.14
2500	0.72	0.78	0.81	0.83	1.48	1.58	1.67	1.74				
3000	0.72	0.80	0.84	0.86	1.57	1.68	1.78	1.86				
3500	0.70	0.80	0.86	0.88	1.63	1.75	1.86	1.96				
4000	0.66	0.79	0.87	0.89	1.66	1.80	1.92	2.03				
4500	0.59	0.76	0.86	0.89	1.68	1.83	1.96	2.08				

Table for l_x (I_{ϕ} , f , q)

$\Delta\delta$	4					6					8					10				
	$\frac{\Delta}{P_m}$	0.5	0.6	0.7	0.8	0.5	0.6	0.7	0.8	0.5	0.6	0.7	0.8	0.5	0.6	0.7	0.8			
l_{x_1}	2000	0.38	0.55	-	-	0.30	0.45	0.49	-	0.25	0.38	0.46	-	0.22	0.33	0.46	-			
	2500	0.24	0.39	0.53	-	0.18	0.29	0.44	0.48	0.16	0.26	0.37	0.46	0.14	0.22	0.32	0.45			
	3000	0.17	0.28	0.41	0.50	0.12	0.21	0.32	0.46	0.10	0.17	0.27	0.39	0.09	0.15	0.23	0.34			
	3500	0.12	0.20	0.31	0.43	0.09	0.15	0.23	0.35	0.07	0.12	0.19	0.29	0.07	0.11	0.17	0.26			
	4000	0.09	0.15	0.23	0.33	0.07	0.11	0.17	0.25	0.06	0.09	0.14	0.21	0.05	0.08	0.13	0.19			
4500	0.07	0.12	0.18	0.26	0.05	0.09	0.13	0.18	0.05	0.08	0.11	0.15	0.04	0.07	0.10	0.14				
l_{x_2}	2000	0.86	0.97	-	-	0.76	0.87	0.95	-	0.73	0.83	0.92	-	0.72	0.80	0.89	0.93			
	2500	0.76	0.86	0.97	-	0.68	0.77	0.86	0.92	0.66	0.73	0.81	0.88	0.65	0.71	0.77	0.84			
	3000	0.68	0.77	0.86	0.94	0.63	0.69	0.75	0.82	0.61	0.66	0.71	0.77	0.60	0.65	0.69	0.74			
	3500	0.63	0.70	0.77	0.84	0.59	0.63	0.68	0.73	0.58	0.61	0.65	0.69	0.56	0.60	0.63	0.67			
	4000	0.60	0.65	0.71	0.76	0.56	0.59	0.63	0.66	0.55	0.58	0.60	0.62	0.54	0.56	0.58	0.61			
4500	0.58	0.62	0.67	0.71	0.54	0.56	0.59	0.62	0.53	0.55	0.57	0.58	0.52	0.54	0.55	0.57				
l_y	2000	0.69	0.77	-	-	0.66	0.72	0.73	-	0.63	0.69	0.72	-	0.62	0.67	0.72	0.69			
	2500	0.63	0.69	0.75	-	0.61	0.66	0.71	0.72	0.59	0.64	0.69	0.71	0.57	0.62	0.66	0.71			
	3000	0.59	0.64	0.69	0.72	0.57	0.61	0.66	0.71	0.56	0.60	0.64	0.68	0.54	0.57	0.61	0.66			
	3500	0.57	0.60	0.64	0.69	0.55	0.58	0.62	0.66	0.54	0.57	0.60	0.64	0.53	0.55	0.58	0.62			
	4000	0.55	0.58	0.61	0.64	0.54	0.56	0.59	0.62	0.53	0.55	0.57	0.60	0.52	0.54	0.56	0.59			
4500	0.54	0.56	0.59	0.62	0.53	0.55	0.57	0.59	0.52	0.54	0.56	0.57	0.52	0.53	0.55	0.57				

Table for l_x (I_x, w, f, q) (Cont.)

λ	4					6				8				10			
	p_q	0.5	0.6	0.7	0.8	0.5	0.6	0.7	0.8	0.5	0.6	0.7	0.8	0.5	0.6	0.7	0.8
l_q	2000	0.28	0.18	-	-	0.32	0.26	0.19	-	0.34	0.29	0.21	-	0.36	0.31	0.26	0.21
	2500	0.34	0.29	0.20	-	0.37	0.32	0.27	0.22	0.39	0.34	0.29	0.23	0.40	0.36	0.31	0.26
	3000	0.38	0.33	0.28	0.22	0.40	0.36	0.32	0.27	0.42	0.38	0.34	0.29	0.43	0.39	0.35	0.30
	3500	0.41	0.37	0.33	0.28	0.42	0.39	0.35	0.32	0.44	0.41	0.37	0.33	0.44	0.41	0.38	0.34
	4000	0.43	0.39	0.36	0.32	0.44	0.41	0.38	0.35	0.45	0.43	0.40	0.37	0.45	0.43	0.40	0.37
	4500	0.44	0.41	0.38	0.35	0.45	0.43	0.40	0.33	0.46	0.44	0.42	0.40	0.46	0.44	0.42	0.40

Chapter 2 - Empirical Formulae and Tables.

1. Leduc's formulae.

$$v = \frac{a\ell}{b+\ell}; \quad v_2 = \frac{a\ell_2}{b+\ell_2}; \quad \rho = \frac{\varphi_m a^2 b}{5} \cdot \frac{\ell}{(b+\ell)^3}; \quad \ell_m = \frac{b}{2}$$

$$\rho_m = \frac{4}{27} \cdot \frac{\varphi_m a^3}{5 \cdot b}; \quad v_m = \frac{a}{3}; \quad v = \frac{d\ell}{dt}; \quad dt = \frac{b+\ell}{a\ell} \cdot d\ell$$

$$t = t_1 + \frac{1}{a} \left[b \log \left(\frac{b}{\ell_1} + \ell - \ell_1 \right) \right]; \quad \ell_1 = \ell_m = \frac{b}{2}$$

$$t = \frac{b}{a} \left[3.174 + \frac{\ell}{b} + 2.303 \log \frac{2\ell}{b} \right]$$

from v_2 and ρ_m we will have:

$$a = \frac{27 \rho_m S \ell_2}{8 \varphi_m v_2} \cdot \left(1 - \sqrt{1 - \frac{16 m \varphi v_2^2}{27 \rho_m S \ell_2}} \right) = \frac{27}{16 \eta} \left(1 - \sqrt{1 - \frac{23}{27} h} \right) \frac{23}{27}$$

$$\text{here: } h_2 = \frac{\rho_m v_2}{\rho_m} = \frac{\varphi_m v_2^2}{2 \rho_m S \ell_2}$$

When a is determined then: $b = \left(\frac{a}{v_2} - 1 \right) \ell_2$.

Since a and b are found from the values of v_2 and ρ_m

Leduc gave the empirical formulae for a and b in terms of the loading conditions and characteristics of powder:

$$a = \alpha \left(\frac{w}{q} \right)^{1/2} \Delta^{1/2}; \quad b = \beta \left(\frac{w_0}{q} \right)^{3/2} \left(1 - \frac{3}{4} \Delta \right)$$

Here α is a characteristic of the potential of a powder and varies only slightly, and β is a characteristic of the rate of burning, largely depends on Δ , and varies within a very wide range (from 2 to 65).

For pyroxylin powders: $\alpha \sim 2080$

$$\text{then: } a = 2080 \left(\frac{w}{q} \right)^{\frac{1}{2}} \Delta^{\frac{1}{2}} \text{ and } b = \left(\frac{a}{2\ell_0} - 1 \right) \ell_0.$$

Prof. Serabryakov gives empirical values of β as a function of $I = \int p dt$ from the experiments in the manometric bomb. For the powder with seven perforations:

$$\beta = 4.25 \int_{v=0.05}^{v=0.85} p dt$$

For the powder with one perforation: $\beta = 2.15 \int_{v=0.05}^{v=0.95} p dt$

He also gives the following simplified formulas for a and b :

$$a = 0.16 \sqrt{2.5 \frac{a}{q}} ; b = 2\ell_0 \Delta$$

2. Heidenreich's Tables (1900)

Heidenreich's Table 8

$\eta = \frac{\rho_{cp}}{\rho_m}$	$\Sigma(\eta) = \frac{l_m}{l_x}$	$\Pi(\eta) = \frac{\rho_x}{\rho_{cp}}$	$\Phi(\eta) = \frac{v_m}{v_x}$	$\Theta(\eta) = \frac{t_m}{t_{cp}}$	$T(\eta) = \frac{t_x}{t_p}$
0	0	--	--	0	--
0.05	0.0046	--	--	0.033	--
0.10	0.0104	0.200	0.288	0.069	0.646
0.15	0.0177	0.240	0.306	0.108	0.695
0.20	0.0262	0.274	0.322	0.150	0.744
0.25	0.0360	0.306	0.337	0.196	0.792
0.30	0.0471	0.338	0.352	0.246	0.842
0.35	0.0597	0.368	0.367	0.300	0.893
0.40	0.0740	0.400	0.383	0.358	0.946
0.45	0.0903	0.432	0.399	0.420	1.000
0.50	0.1090	0.465	0.416	0.487	1.056
0.55	0.132	0.501	0.435	0.560	1.116
0.60	0.160	0.541	0.457	0.642	1.180
0.65	0.192	0.585	0.482	0.734	1.249
0.70	0.231	0.635	0.511	0.835	1.322
0.75	0.283	0.697	0.546	0.958	1.406
0.80	0.360	0.779	0.592	1.115	1.507
0.825	0.422	0.838	0.636	1.225	1.575
0.85	0.605	1.000	0.747	1.485	1.715
0.825	0.855	1.181	0.908	1.735	1.815
0.80	0.980	1.254	0.987	1.835	1.845
0.79	1.000	1.266	1.000	1.850	1.850

Heidenreich's Table 9

$\lambda = \frac{i}{i_m}$	$H(\lambda) = \eta$	$\Psi(\lambda) = \frac{p}{p_m}$	$\Omega(\lambda) = \frac{v}{v_m}$	$Z(\lambda) = \frac{t}{t_m}$
0.25	0.445	0.690	0.375	0.689
0.50	0.615	0.890	0.624	0.830
0.75	0.723	0.970	0.828	0.924
1.00	0.790	1.000	1.000	1.000
1.25	0.833	0.966	1.145	1.063
1.50	0.848	0.893	1.268	1.119
1.75	0.849	0.828	1.372	1.170
2.00	0.843	0.769	1.460	1.218
2.5	0.818	0.668	1.609	1.306
3.0	0.786	0.590	1.726	1.387
3.5	0.753	0.527	1.824	1.463
4.0	0.721	0.475	1.909	1.536
4.5	0.691	0.433	1.981	1.606
5.0	0.663	0.397	2.046	1.672
6	0.614	0.340	2.158	1.801
7	0.572	0.297	2.250	1.923
8	0.536	0.263	2.328	2.042
9	0.504	0.236	2.395	2.156
10	0.476	0.214	2.453	2.267
11	0.451	0.195	2.504	2.376
12	0.429	0.179	2.551	2.483
13	0.409	0.166	2.592	2.588
14	0.391	0.154	2.630	2.692
15	0.375	0.144	2.665	2.794
16	0.360	0.135	2.698	2.895
17	0.347	0.127	2.730	2.994
18	0.335	0.120	2.760	3.092
19	0.323	0.114	2.787	3.189
20	0.312	0.108	2.812	3.286
25	0.270	0.086	2.921	3.758
30	0.238	0.071	3.004	4.214
35	0.213	0.060	3.070	4.659
40	0.194	0.052	3.132	5.095
50	0.164	0.041	3.220	5.946
75	0.120	0.027	3.373	7.995
100	0.096	0.020	3.480	9.966

Section IX - Tabular Methods of Solving the Problems of
Interior Ballistics.

Chapter 1 - The Importance of Tabular Methods for
Artillery Practice.

In 1910 Prof. N. Drosdov designed his tables in which P_m , 2ϵ and $(\frac{L_K}{L_0})$ were given. This was an important step in the progress of Interior Ballistics. Not only did the direct problem receive a simpler and shorter solution but inverse problems involved in the designing of guns received their simpler solutions: the evaluation of L_K assuring the desired 2ϵ at given Δ with the complete burning within the bore ($L_K < L_0$); the determining of the web of powder assuring the desired P_m ; the comparison of several variants with changeable ω and 2ϵ , but with constant P_m etc. These tables were immediately admitted in practice, expanded, supplemented and in 1933 republished and used as the basis for other tables published by the chair of Interior Ballistics of the Artillery Academy for powders with constant surface of burning. In 1933 were also published the tables of the Artillery Scientific Research Institute (Russian abbreviated title - А.И.И.) in which for given loading conditions can be found not

only ρ_m, l_m, l_n, v_0 but also velocities and times as functions of L .

Thus such empirical sources as Ledue's formulas or Heidenreich's tables became obsolete mainly because of their uselessness when evaluations of the powder charge or of the size of powder grain were necessary. In 1942 Tables of the Chief Artillery Board (Г.А.В.) were published under the supervision of Prof. V. Sloukhotzky in three parts and with the Special Fourth part for the use in the ballistic design of guns.

A general outline of the procedure of tabulation.

In order to have tables applicable to guns of all calibers the initial equations used for calculations are written in relative terms i.e. Δ is used instead of ω , the relative travel $\Lambda = \frac{L}{L_0}$ which is the number of volumes of gas expansions ($\frac{L}{L_0} = \frac{V}{V_0}$); $\frac{p}{p_0}$ or $\frac{p}{p_0}$ are used instead of p . The constants are selected in dimensionless form as for example:

$$B = \frac{S^2 I_K^2}{f \omega \varphi m} \quad - \text{ (Drosdov's parameter)}$$

$$H = \frac{2 f \omega \varphi m}{S^2 I_K^2} = \frac{2}{B} \quad (\text{Bianchi - Grave})$$

$$C = \frac{\theta}{H} = \frac{B \theta}{2} \quad (\text{at } \mathcal{X} = 1)$$

In general there are 3 parameters, involved in the equations containing ballistic variables - ρ , v and $\Lambda = \frac{L}{x_0}$ and one independent variable (argument) x .

Parameters are: f, α, δ - characteristics of powder

$\theta = \frac{C_p}{C_w} - 1$ - characteristic of gases

κ - characteristic of the form of powder grain.

ρ_0 - characteristic of the riflings and driving band

B and Δ - characteristics of the loading conditions

A natural way for reducing number of parameters is to consider several of them as constants; for instance: if $f, \alpha, \delta, \kappa, \rho_0$ and θ are constant then ρ, v and Λ will be functions of only 2 parameters B and Δ and tables will be with two entries.

There is another way of reducing number of parameters: it is possible to select more complex variables and more complex parameters but then the use of tables becomes more complicated.

Chapter 2 - Tables for Determining the Principal
Elements of a Firing (p_m, ℓ_m, ℓ_n, V_2)

1. Prof. N. Drosdov's Tables.

These tables are constructed for the strip powders with the average values of $\mathcal{N} = 1.06$ and $\mathcal{N}\lambda = -0.06$. The constant characteristics are:

$$f = 950000 \frac{\text{cm}}{\text{kg}}; \alpha = 0.98 \frac{\text{cm}^2}{\text{kg}}; \beta = 1.6 \frac{\text{cm}^2}{\text{kg}}; \phi = 1.05$$

$$\rho = 300 \frac{\text{kg}}{\text{cm}^3}; K = 1 + 0 = 1.2; g = 981 \frac{\text{cm}}{\text{sec}^2}; \alpha - \frac{1}{\beta} = \frac{1}{\beta} = 0.355 = \frac{1}{2.82}$$

Entries in tables are: Δ and $B = \frac{S^2 \ell^2}{u^2} \cdot \frac{1}{f \omega \phi m} = \frac{S^2 I_n^2}{f \omega \phi m}$

These tables are given at the end of book (Appendix 2)

in four parts: Part I for ρ ; Part II for $\frac{\ell_n}{\ell_m}$; Part III- $\frac{\ell_m}{\ell_n}$ and Part IV for $\log \left[1 - \frac{2\phi}{\beta} (1 - \lambda)^2 \right]$

These tables are constructed for $\mathcal{N} = 1.06$ and $\mathcal{N}\lambda = -0.06$

For the strip powder having $f = 950,000$. But practice shows that the 7 perforation powder produces the same pressures and velocities which can be obtained at the same values of powder charges using the strip powder, if their webs $(2e)_{7p.}$ and $(2e)_{st.}$ will be taken related each to the other as follows:

$$(2e)_{st.} = \frac{10}{7} (2e)_{7p.} \quad \text{or:} \quad (2e)_{7p.} = \frac{7}{10} (2e)_{st.}$$

If we apply these tables when the actual value of f is not 950,000 but f_i , then the entry B is taken as $(\frac{f_i}{950000} \cdot B)$ for finding p_m ; and for finding v_2 we multiply its tabular value by $\sqrt{\frac{f_i}{950000}}$. If φ_i is not 1.05 then the correction for v_2 will be a factor

$$(v_2)_{\text{tab}} \cdot \sqrt{\frac{1.05}{\varphi_i}}$$

2. Tables of the Chair of Interior Ballistics of the Artillery Academy (C. I. B.).

These tables calculated under the supervision of Prof. I. Grave in 1933 for any values of f and φ for powder having the constant burning surface (long tubular powder). The calculations were based on formulas given by Bianchi and improved and developed by Prof. Grave. As constant parameters were taken:

$$\alpha = 0.98; \delta = 1.6; \gamma = 1.0; \lambda = 0; \theta = 0.2; \frac{R}{f} = 0.035$$

The entries are: Δ and the parameter of loading conditions :

$$H = \frac{2f\omega\varphi m}{S^2 I_k^2} = \frac{2}{B} \text{ or } C = \frac{B}{H}; \text{ at } \theta = 0.2; C = 0.1B$$

H is given from 2 to 0.5 or C from 0.10 to 0.40 in steps 0.01 and Δ from 0.10 to 0.90 in steps of 0.01. These tables give p_m and v_2 slightly lower than they are obtained from Drosdov's tables. Differences which are about 10% for p_m and 2% for v_2 can be explained

as results of difference in the values of γ : In Drosdov's tables $\gamma = 1.06$, and in Tables (C.I.B.)

$\gamma = 1.0$. Yet this difference in γ accounts for only about 6% out of the total 10% difference in p_m . The remaining 4% also have their explanation in that approximation introduced by Prof. Grave into the integration of the equation giving l as a function of x . This approximation results in the higher values of l and lower values of p_m as compared with l and p_m in Drosdov's Tables.

Chapter 3 - Detailed Tables for the Curves of Pressures and Velocities.

1. Tables of the Artillery Scientific Research Institute (ASRI) (in Russian *A.H.H.H.*) 1933.

Tables of Drosdov and Grave give p_m, l_m, p_x and l_x ; for v_1 we have to make additional calculations because we need l_2 , which is not given in Tables.

There also are not given the intermediate values of $p,$

v, l and values of the time, t . The ASRI tables are the next step in the progress of table construction.

They are based on the same constants used by Prof.

Drosdov and on Drosdov's formulae and they furnish all necessary data for the construction of curves (p, l).

(v, ℓ) and (t, ℓ). They have three entries: for every Δ varying in steps of 0.01 from 0.05 to 0.95 there are 2 entries of B and $\Lambda = \frac{\ell}{\ell_0}$. Parameter B varies from 0.7 to 3 and for $\Delta > 0.8$ B varies from 1.2 to 1.4; parameter Λ varies from 0 to 15. Velocities and times are given in provisory units. Hence tabulated values v_{ℓ} and t_{ℓ} should be converted into actual values v and t by the following multiplications:

$$v = v_{\ell} \sqrt{\frac{\omega}{g}} \quad \text{and} \quad t = t_{\ell} \ell_0 \sqrt{\frac{g}{\omega}} \cdot 10^{-6}$$

(here ℓ_0 in dm.).

These tables are used for the strip powder having its $\chi = 1.06$ and $\chi\lambda = -0.06$, but the same conversion factor 0.7 can be used in order to make these tables calculated for strip powder with its web $(2\ell)_{st}$ applicable to 7 perforation powder with its web $(2\ell)_{7p}$ if we will take $(2\ell)_{7p} = 7/10 (2\ell)_{st}$.

One important defect in these tables was found and corrected by Prof. Bravin in 1935: calculations of time for the first interval of Λ from 0 to 0.1 were all wrong almost to the extent of 100% on account of the erroneous (not sufficiently accurate) evaluation of the initial interval of time $t' = \frac{2\ell'}{v'}$. Prof. Bravin gave the formula: $t' = \frac{2\ell'}{v'} \cdot \frac{\rho_0 + \rho}{2\rho_0 + \rho}$,

2. Tables of the Chief Artillery Board (in Russian Г.А.У). These tables were published in 1942. Being similar to Tables (А.Н.М.М) they are more convenient and accurate and have a larger range of variations of parameter B (from 0 to 4). They have 4 parts:

Part I - tables for pressures; Part II - tables of tabulated velocities $2v_{rel} = v \cdot \sqrt{\frac{g}{g_0}}$

Part III- tables of tabulated times: $t_{rel} = t \cdot \frac{1}{g_0} \sqrt{\frac{g}{g_0}} \cdot 10^6$

$$\text{or : } t = t_{rel} \cdot g_0 \cdot 10^{-6} \sqrt{\frac{g}{g_0}}$$

Parameter Δ varies in steps of 0.01 from 0.05 to 0.95

Tables are calculated for: $f = 950,000 \frac{\text{kg} \cdot \text{cm}}{\text{kg}}$; $\alpha = 1$

$\delta = 1.6 \frac{\text{kg}}{\text{cm}^2}$; $\rho = 300 \frac{\text{kg}}{\text{cm}^3}$; $\theta = 0.2$;

$\chi = 1.06$; $\chi\lambda = -0.06$; $\varphi = 1$.

Part IV - Special tables for the ballistic design of guns.

Chapter 4 - Tables Based on the Generalized Formulae with the Reduced Number of Parameters of with the Relative Variables.

1. Formulae and Tables due to Prof. B. Okunev.

This work of Prof. Okunev is one among several similar works of Russian ballisticians published in 1939-1941 in which in order to reduce a large number of parameters

and to avoid dealing with the absolute values of the principal elements of firing, the authors (Profs. Drosdov, Okounev, Gorokhov, Oppokov) introduced grouping parameters and relative variables. Prof. Okounev's method has the following relative variables:

$$\rho = \frac{p}{p_1} \cdot (p_1 = \frac{f_{\Delta}}{1-\alpha_{\Delta}}); \nu = \frac{v}{v_{\Delta}}; C = \frac{c}{c_1}; T = \frac{q \cdot q_1}{g \cdot s} \cdot \frac{v_{\Delta}}{p_1}; X = \frac{\Lambda}{1-\alpha_{\Delta}} = \frac{c}{c_1},$$

and generalized parameters: $R = \sqrt{\frac{2}{B\theta}} = \sqrt{\frac{H}{\theta}}$, and $\Lambda = \frac{1-\frac{\Delta}{\theta}}{1-\alpha_{\Delta}} = \frac{c_{\Delta}}{c_1}$, here: $\Lambda_{\Delta} = \frac{1}{\theta}$ and θ is a parameter used in Pyrostatics for calculation of ψ (Part I, Section II).

From:

$$\rho = \frac{f_{\Delta}}{1-\alpha_{\Delta}} \cdot \frac{\psi - \frac{B\theta}{2} x^2}{\Lambda_{\psi} + \Lambda}, \text{ here } \Lambda_{\psi} = 1 - \frac{\Delta}{\theta} - (\alpha - \frac{1}{\theta})\psi$$

we have:
$$\rho = \frac{f_{\Delta}}{1-\alpha_{\Delta}} \cdot \frac{\psi - \frac{B\theta}{2} x^2}{\frac{\Lambda_{\psi}}{1-\alpha_{\Delta}} + \frac{\Lambda}{1-\alpha_{\Delta}}}$$

or:
$$\frac{\rho}{p_1} = \rho_{rel} = \frac{\psi - \frac{B\theta}{2} x^2}{X_{\psi} + X}$$

The basic equation:

$$\frac{d\rho}{dx} + \frac{B}{\theta} \cdot \frac{x}{\theta(\alpha)} \rho = -\frac{B}{\theta} \cdot \frac{x}{\theta(\alpha)} \frac{c}{c_1} = -\frac{B}{\theta} (\alpha - 1) (K_1 - 2x\lambda x)$$

will be rewritten:
$$\frac{d(X_{\psi} + X)}{dx} + \frac{B}{\theta} \cdot \frac{x}{\theta(\alpha)} (X_{\psi} + X) = -(\Lambda_{\Delta} - 1) (K_1 - 2x\lambda x)$$

Hence we see that $\rho = \frac{p}{p_1}$ and X are functions of the argument and 5 parameters $\theta, \alpha, Z_0, \Lambda_{\Delta}, B$ but not of 8 parameters as we had before. Prof. Okounev gave tables

for calculations of ρ_{ad} , X , $y = \frac{v}{v_{ad}}$ and $c = \frac{c}{T}$ as functions of Λ_a , $R = \sqrt{\frac{2}{\beta}}$ and z_0 and tables for ρ_{ad} , X and c as functions of parameters Λ_a , R , z_0 and an argument y .

2. Prof. N. Drosdov's method (1941).

As the relative variable $\Pi = \frac{p}{p_0}$ is taken. Instead of

the parameter Λ_a another: $\xi = 1 - \frac{1}{\Lambda_a} = 1 - \delta$ is used.

Besides this Prof. Drosdov selects two more parameters:

$$R = \frac{R(\alpha - \delta)}{f} = \frac{p_0}{f \delta}, \quad \text{and} \quad R_1 = \frac{R}{1+R} = \frac{1}{f \frac{p_0}{p_0} + 1}$$

which are functions of f , α , δ and p_0

Normal values of these parameters are: $R = 0.01121$

and: $R_1 = 0.01108$

The relative maximum pressure $\Pi_m = \frac{p_m}{p_0}$ and the velocity v^* (during the first period) are given in the following expressions:

$$\Pi_m = \frac{\frac{(1 + \beta_m - \beta_m^2)}{\gamma} \cdot z_m^{\frac{\beta}{\gamma}}}{1 - R \frac{S'_m}{\gamma}}$$

here: β , γ , B and β , are the same as we had them before and:

$$\beta_m = \frac{1}{\frac{\beta}{\gamma} + 2} (1 + \Pi_m R) = \frac{\theta}{2(1+\theta)} (1 + \Pi_m R)$$

$$S'_m = \int_0^{\beta_m} z^{\frac{\beta}{\gamma}} d\beta \quad \text{for } \beta = \beta_m$$

Then:

$$v = \beta \sqrt{\frac{\beta}{\beta_1} \cdot \frac{R'}{R} - \frac{\beta_0 s \ell_0 (1 - \frac{\alpha}{\beta})}{\gamma \varphi m}}$$

The results obtained by Prof. Drosdov from the use of these parameters and variables were applied by him for various investigations of the comparative significance in varying certain factors affecting the value of β_m ; for instance he gave tables showing how $\Delta \beta_0, \Delta \alpha, \Delta \chi, \Delta f$ and $\Delta \theta$ are related to the corresponding value of $\Delta \beta_m$ (these tables are partly shown in book - p. 442-444).

3. Formulas and tables obtained by Mr. Gorokhov and Mrs. Sviridov (1940).

Using parameters and variables involved in Prof.

Drosdov's solution and introducing a new parameter D_1 ,

$$D_1 = D \frac{n(1+\theta)}{2+n}; D = \frac{\alpha - \frac{\chi}{\beta}}{\frac{\chi}{\beta} - \frac{\chi}{\beta_1}} \cdot \frac{\chi_1^2}{\beta_1^2}; \ell_1 = \ell_0 (1 - \frac{\alpha}{\beta})$$

the authors gave the following expression for the trav-

el of the projectile: $\ell = N(\gamma, \beta, n) [1 - D_1 L(\gamma, \beta, n)] + \varphi$

Here: $\varphi = \frac{\theta}{2} D n \beta^2$; $K_1 = \chi^2 - 4 \chi \lambda \psi$; $B_1 = \chi \lambda + \frac{\beta \theta}{2}$; $n = \frac{\beta}{\beta_1}$,

$$N(\gamma, \beta, n) = \bar{Z}^n(\gamma, \beta)$$

$$L(\gamma, \beta, n) = \gamma + \int_0^{\beta} \frac{\alpha \beta}{N(\gamma, \beta, n)} - \frac{\gamma + \beta - \beta^2}{N(\gamma, \beta, n)}.$$

For $\log Z'(\gamma, \beta)$ and $L(\gamma, \beta, n)$ are given tables in which: $0 < \gamma < 0.13$; $0 < \beta < 0.70$; $3 \leq n < 14$.

Formula for the pressure:
$$P = \frac{\alpha \cdot \beta}{f} \cdot p = \frac{D \cdot (\beta + \gamma - \beta^2)}{\theta - \gamma - D \cdot (\beta + \gamma \beta^n)}$$

For the maximum pressure $\beta = \beta_m$ determined by the formula:
$$\beta_m - \frac{1}{2+n} = D \cdot \left\{ \left(\gamma + \int_{N(\gamma, \beta, n)}^{\beta_m} \frac{d\beta}{N(\gamma, \beta, n)} \right) \left(\beta_m - \frac{1}{2+n} \right) + \frac{\gamma + \beta_m - \beta_m^2}{(2+n) N(\gamma, \beta, n)} \right\}$$

for $(\beta_m - \frac{1}{2+n})$ special table is given.

These formulae are used in cases when conventional constants $(\alpha, \delta, f, f_0, \theta, \gamma)$ are somewhat deviated from their normal values, and in cases of composite charges or when the burning out of slivers of the progressive powder should be considered.

Chapter 5 - General Information on the Theory of Similarity.

1. Theoretical fundamentals.

Guns are ballistically similar when their curves (p, ℓ) and (v, ℓ) are similar - i.e. can be made identical by the appropriate selection of scales. Algebraical expressions of this requirement are as follows:

$$F_1(p, \ell) \equiv F_2(\alpha, p; \alpha_1 \ell) \text{ - for pressure curves.}$$

$$Q_1(v, \ell) \equiv Q_2(\beta, v; \beta_1 \ell) \text{ - for velocity curves.}$$

When Δ is not the same in both guns then this requirement results in the necessity that $\alpha = \frac{1}{f}$, which cannot be realized in practice; this is the reason for considering in a similarity discussion only cases when Δ is the same in both guns. The following relative variables and parameters are considered in theory of similarity:

$$\frac{\rho}{f} = \Delta \cdot \frac{\psi - \frac{\Delta \theta}{2} x^2}{\Lambda_\psi + \Lambda}; \quad \Lambda = \Lambda_{av\psi}(\bar{Z}_x^{-\frac{\Delta}{2}}); \quad \bar{Z}_x = \frac{v}{v_{ac}} = \frac{v}{\sqrt{f g B}} = \frac{\Delta - f}{\frac{f}{\rho} + \alpha - \frac{1}{f}}; \quad Z_0 = \frac{2\psi_0}{\pi(\theta + 1)} \sim \frac{\psi_0}{\pi}$$

$$\psi = \psi_0 + \pi \sigma_0 x + \pi \lambda x^2; \quad \psi_0 = \frac{\Delta - f}{\frac{f}{\rho} + \alpha - \frac{1}{f}}; \quad \Lambda_\psi = 1 - \frac{\Delta}{f} - \Delta(\alpha - \frac{1}{f})\psi; \quad B = \frac{5^2 I_{K^2}^2}{f \omega \varphi g}; \quad B_1 = \frac{B_0}{2} - \eta \lambda$$

For two guns with the same Δ their (ρ, ℓ) curves and (v, ℓ) curve will be similar if for the same value of x the values of ρ, v, Λ will be the same, and this result can be realized only under conditions that:

1. The nature of the powder (f, α, θ) is the same.
2. The form of the powder (λ, λ) is the same.
3. $\frac{B_0}{f}$ or ψ_0 is the same.
4. Parameter B is the same.

Then the following elements will be identical:

$$B; \psi_0; \psi; \Lambda_\psi; \Lambda_{av\psi}; \bar{Z}_{ac}; \delta = \frac{B_1 \psi_0}{K_1^2}; \beta = \frac{B_1}{K_1} x; \log \bar{Z}_x; \Lambda; \rho.$$

and the curves (p, λ) and (v, λ) will be identical, hence the curves (p, ℓ) and (v, ℓ) will be similar,

for these 2 guns, during the whole first period.

For the end of burning ($\psi = 1$) we will have the same values $v_K, p_K, \lambda_K, \lambda_i$ for both guns.

For the same period:

$$p = p_K \left(\frac{\lambda_K + 1 - \alpha \Delta}{\lambda + 1 - \alpha \Delta} \right)^{1+\theta}$$

$$\left(v \sqrt{\frac{\varphi \ell}{\omega}} \right)^2 = v_{K\ell}^2 = \frac{2g}{\theta} \left\{ 1 - \left(\frac{\lambda_K + 1 - \alpha \Delta}{\lambda + 1 - \alpha \Delta} \right)^\theta \left[1 - \frac{\theta \theta}{2} (1 - \lambda_K)^2 \right] \right\}$$

Thus the above shown results are only expression of the fact that all the calculated tables are nothing but the practical application of the theory of similarity.

2. Some theorems of the theory of similarity.

Definitions:

1. Geometrically similar gun barrels are such which have their linear dimensions proportional to their calibers, their cross-sectional areas proportional to the squares of the calibers and their volumes of chambers and canals proportional to the cubes of calibers.

2. Two guns having their weights of powder charges and projectiles proportional to the cubes of their calibers are called similarly charged guns.

Theorem 1. For geometrically similar and similarly charged guns their curves (p, ℓ) and (p', ℓ') will be similar if the webs of powders or the impulses I_K for these guns are proportional to their calibers. This result is obtainable from the equality of the parameters B for these guns.

Theorem 2. In similar and similarly charged guns the equal relative travels Δ correspond to the equal pressures and equal velocities of projectiles. This result in respect to pressures is obtainable from the similarity of pressure curves at the same Δ and equal B . For similarly charged guns $\frac{\omega'}{\varphi' \ell'} = \frac{\omega''}{\varphi'' \ell''}$ and $v_{A\ell}' = v_{A\ell}''$, and hence $v' = v''$.

Theorem 3. At firings from the same gun at the same powder charge and at the same p_m the obtained muzzle velocities v_5' and v_5'' will be related as:

$$\frac{v_5'}{v_5''} = \sqrt{\frac{\varphi' \ell'}{\varphi'' \ell''}}$$

This result is obtainable from $v_{A\ell}' = v_{A\ell}''$ as it follows from given conditions at given B, Δ and p_m .

From $p_m = \text{const.}$ and $B' = B''$ we will have:

$$\frac{I_K'}{\varphi' \ell'} = \frac{I_K''}{\varphi'' \ell''} \text{ or: } \frac{I_K'}{I_K''} = \sqrt{\frac{\varphi'' \ell''}{\varphi' \ell'}}$$

i.e. the impulses I_K' and I_K'' will be proportional to

the square roots of φ_2'' and φ_2'' .

But it should be remembered that at every change from one gun to another with another caliber the web of powder, the nature of the powder, ρ and the heat losses are all changed also and this fact leads to the conclusion that the theorems of the theory of similarity can be admitted only as certain approximations of the real relationships.

Section I - Ballistic Design of the Guns.

General Remarks.

The most important basic problem of ballistic design is to find all the constructional data and loading conditions at which a given projectile will be propelled with a desired muzzle velocity at the maximum pressure not exceeding a given limit. The constructional data consists of: Chamber volume W_0 ; cross-section of bore S ; length of travel along the bore ℓ_1 ; length of chamber ℓ_2 (considering its widening χ); the number of volumes of expansion: $\Lambda_0 = \frac{\ell_2}{\ell_0}$; the total length of canal L_c , and the volume of the canal: $W_c = W_0 + S\ell_2 = S(\ell_0 + \ell_2)$. The loading conditions are: the relative weight of charge $\frac{w}{q}$ of a given sort of powder (f, u, δ, θ); density of loading Δ ; dimensions and form of powder grains; the impulse $I_K = \frac{e_i}{u_i}$. The curves (p, ℓ) , (v, ℓ) , (p, t) and (v, t) present the initial basic material for the further calculations of designers: the mechanical designer, the ammunition designer, powder engineer and technologists all start their work with these basic curves. Thus the rational ballistic design of the gun barrel is the true basis of the design of the whole artillery system, and the degree of

446

"rationality" of the ballistic design is conditioned by the completeness of studying of all the relationships between the pressure, velocity and travel of the projectile. The problem of ballistic design always has a plurality of solutions or determinations of constructional details which may be used for producing a desired muzzle velocity for a given projectile. Also the rational method of design is supposed to give the maximum number of variants with the proper criteria of their appraisals. It should be remembered, however, that not only ballistic factors and relationships are to be taken into consideration; there are other additional criteria derived from the technico-tactical requirements closely connected with every given type of a designed gun. Very often there are also additional requirements concerning the weight of a gun or weight of the whole system, the total length of a gun, or the maximum of energy delivered $\left(\frac{cm^2 s^{-2}}{s^2}\right)$ i.e. the gun power. The effective skill of the artillery constructor is displayed in his ability to produce a design which is rational from the ballistic viewpoint and satisfies at the same time the technico-tactical requirements. The rational methods of ballistic design must show the shortest way to the proper

selection of one variant among all investigated variants of the desired system. General trends of varying parameters must be well known and clearly understood. The qualitative evaluations of the service effectiveness and expediency of a designed system are supplemented by the quantitative relationships specified by the calculations.

The principal relationships between the constructional data of a gun and the loading conditions are the subject of the "Theoretical Fundamentals of the Ballistic Design of the Gun".

The establishment of such general relationships necessary for ballistic design involves the construction of certain auxiliary tables and the use of several functions which can be derived from the basic tables given by Prof. N. F. Drosdov as well as of tables of ASRI and Chief Artillery Board. Such tables can be used not only for strip powders with $f = 950,000 \text{ kg}\cdot\text{dm/kg}$ but also for other powders and even for composite charges of the two different types. All the principal assumptions of Pyrodynamics (geometric law of burning), the law of the rate of burning ($u = u, p$), the average pressure behind the projectile, etc. are taken into account in all

theoretical discussions of ballistic design. Here is presented a list of several authors and their work in this field.

Prof. N. Drosdov (1910-1948) has paved the way for ballistic design and has laid the foundation for the Russian School principally in the direction of the search for the optimum gun which produces the maximum $\left(\frac{m\psi^2}{2}\right)$ at a given length of a gun and a maximum pressure. The French school defines the optimum gun as a gun with the maximum total work: $\left(\frac{m\psi^2}{2}\right)$ at its maximum.

Prof. J. Grave (1934-1937) in his course on Pyrodynamics gave a very complete exposition of the theory of ballistic design with his own original researches in this field.

Prof. V. Sloukhotzky (1934-1942) has made for the first time an investigation of the problem of the life of a gun bore. Under his supervision have been published the Tables of the Chief Artillery Board (CAB) Tables, with his own Tables of ballistic design.

Prof. B. Okounov (1939) has made an analysis of the comparative effects of various parameters on the "productivity" of an artillery system, constructed series

of special tables and gave general principles for a rational selection of the best ballistic design.

Prof. D. Ventzel (1939-1946) gave the theory of the ballistic design of small arms with special tables.

Docent M. Gorokhov (1940-1945) has published several special researches with tables and diagrams on the general theory of ballistic design.

Prof. E. M. Serebryakov in 1940 has proposed a general concept of "the economic loading conditions" and gave a theory of "the gun with its minimum volume" which has marked advantages in comparison with the French "gun of maximum power". A more general approach is given in a special "Directive Diagram" which is used for the selection of the required variant. (See Section X, Chapter 3).

Chapter 1 - Initial data.

1. Ballistic Characteristics of a Gun.

There are 3 groups of ballistic characteristics of a gun:

1. Construction characteristics of the gun canal.
2. Characteristics of the loading conditions and
3. Energetic characteristics of the firing.

4. Constructional Characteristics of the Canal.

1. Chamber volume per unit of weight of the projectile $\left(\frac{W_0}{q}\right)$ is a very important factor affecting v_b . The range of variation of $\left(\frac{W_0}{q}\right)$ is from 0.1 to 2.0. Sometime another ratio $\left(\frac{W_0}{d^3}\right)$ varying from 1.6 to 33.0 is also used.

2. Lengths of the barrel and of the canal expressed in calibers $\left(\frac{L}{d}\right)$ and $\left(\frac{L_c}{d}\right)$. For high muzzle velocity ($v_b = 1500 \text{ m/s}$) these relative lengths can be as high as 150 or still higher.

3. The number of the expansion volumes $\Lambda_2 = \frac{L_2}{L_c} = \frac{W_2}{W_0}$ or the relative travel of a projectile in terms of the effective length of the chamber L_c . This characteristic is most important determining the very type of a gun. In moder guns Λ_2 varies from 3.0 to 10; in very powerful guns $\Lambda_2 \sim 3-4$; in automatic guns with small chambers $\Lambda_2 \sim 8-10$.

4. The characteristic of the depth of rifling n_s is determined from: $S = n_s d^2$; at $t_n = 0.01 d$, $n_s = 0.80$
 at $t_n = 0.02 d$, $n_s = 0.83$

(t_n is the depth of rifling)

5. The coefficient of the widening (or of the bottleness) of chamber is $\chi = \frac{L_c}{L} > 1$. This coefficient in

guns varies from 1.05 to 3.0; in small arms χ may be as high as 1.0.

B. Characteristics of the Loading Conditions.

6. The density of loading $\Delta = \frac{w}{W_0}$ varies within a very wide range. In small arms $\Delta = 0.80-0.95$; in very powerful guns $\Delta = 0.65-0.78$, in ordinary guns $\Delta = 0.55-0.70$; in howitzers (full charge) $\Delta = 0.45-0.60$, in howitzers (reduced charges) $\Delta = 0.10-0.35$; in minethrowers $\Delta = 0.03-0.12$. As a rule Δ is increased with increases in p_m and v_s .

7. The relative weight of a charge $\left(\frac{w}{q}\right)$ largely affecting the velocity of a projectile as well as the work producing the movement of the charge gases, varies from 0.01 to 1.5.

8. The coefficient of the weight of a projectile $C_q = \left(\frac{q}{d^3}\right)$ primarily affects the velocity of a projectile. At a given velocity the values $\left(\frac{L_0}{d}\right)$, $\left(\frac{L_2}{d}\right)$, $\left(\frac{L_c}{d}\right)$ and $\left(\frac{I_{cr}}{d}\right)$ are all proportional to C_q ; the smaller C_q the smaller is the web of a powder at the same maximum pressure p_m .

For armor-piercing shells: $C_q = 16-18 \frac{\text{kg}}{\text{dm}^3}$

For high-explosive shells: $C_q = 12-16 \frac{\text{kg}}{\text{dm}^3}$

For armor-piercing shells with core: $C_q = 10-16 \frac{\text{kg}}{\text{dm}^3}$

For bullets (light): $C_2 = 20-25 \text{ kg/dm}^3$

For bullets (heavy with core): $C_2 = 25-30 \text{ kg/dm}^3$

9. The relative impulse (in calibers) $(\frac{I_N}{d})$ is characteristic of the gun power and of the conformity of the web of powder with the caliber ($\frac{I_N}{d} = \frac{e_i}{d}$, here $2e_i$ is a web.)
At $v_b \sim 350-700 \text{ m/s}$, $\frac{I_N}{d} = 500-1000 (\frac{\text{kg/dm}}{\text{sec}})$

In small arms at $v_b = 870 \text{ m/s}$, $\frac{I_N}{d} = 3000$ in the anti-tank rifles $\frac{I_N}{d} = 5000$

10. The loading parameter $B = \frac{S^2 I_N^2}{f \omega \varphi q}$ is a combination of $\frac{\omega}{q}$, C_2 and $\frac{I_N}{d}$ and is the basic characteristic affecting the value of ρ_m and ℓ_N . The normal range of variation for B is from 1.9-2.0. It is very convenient to write

B in such a way that will show the relative (not absolute) values of the separate factors of loading conditions, for example:

$$B = \frac{n_s^2 d^4 I_N^2 q}{f \omega \varphi q^2} = \frac{g n_s^2 (\frac{I_N}{d})^2}{f (\frac{\omega}{q}) \varphi C_2^2}$$

here $\varphi = a + b(\frac{\omega}{q})$ is a function of $(\frac{\omega}{q})$

Here $(\frac{I_N}{d})$ affects the value of ρ_m and ℓ_N without a marked change in v_b . The ratios $(\frac{\omega}{q})$ and C_2 affect largely v_b and their influence on ρ_m can be compensated by the corresponding change in $(\frac{I_N}{d})$.

C. The Energetic Characteristics

11. The coefficient of the gun power: $C_g = \frac{E_d}{d^2} = C_g \cdot \frac{v_d^2}{2g}$

Normally C_g varies between 100 to 1700 $\left(\frac{\text{tons-met.}^2}{\text{dm}^2}\right)$

12. The coefficient of the utilization of the unit of the weight of charge:

$$h_w = \frac{E_d}{w} = \frac{g v_d^2}{2g w} = \frac{\left(\frac{v_d^2}{g}\right)}{\left(\frac{w}{g}\right)} \left(\frac{\text{ton-met.}}{kg}\right)$$

For guns of medium power: $h_w = 120-140$

For very high v_d : $h_w = 20-80$

For small arms: $h_w = 100-110$

For howitzers (full charge): $h_w = 140-160$

13. The efficiency of the power charge: $\eta_2 = \frac{0.45}{f w} = h_w \cdot \frac{0}{f}$
varies from 0.20 to 0.30.

14. The characteristic of the location of projectile at the end of burning: $h_K = \frac{C_K}{C_d} = \frac{1_K}{1_d}$

For guns: $h_K = 0.50-0.70$

For howitzers: $h_K = 0.25-0.30$ (full charges)

15. The characteristic of the utilization of the working volume (bore) of the gun canal W_e :

$$h_b = \frac{R_{av}}{P_m} = \frac{\varphi m v_d^2}{2 S l_d P_m} = \frac{\varphi m v_d^2}{2 P_m W_e}$$

here: $W_e = S l_d = W_0 \Lambda_d$

With the increased Λ_d from 3 to 10, h_b normally is decreased from 0.70 to 0.40.

p_0 - engraving pressure. The values of D_0 and d are in m/m ; $p_0 (\frac{kg}{cm^2})$; v m/sec ; K_1 is given as a function of the caliber d :

d : 50; 100; 150; 200; 250; 300; $K_1=1.0$; $K_2=1.0$
 $K_1 \cdot 10^6$: 15.80 7.10; 3.40; 2.00; 1.96; 1.93;

$\frac{d}{L} \cdot 10^3$ is 1.28 for guns; and 1.40 for small arms.

The ratio $(\frac{v_1}{v_2})^2$ is too small in comparison with $\Lambda_2 (\frac{v_1}{v_2})^2$

The ratio $(\frac{v_1}{v_2})^2$ is given in the following table as a function of Λ_2 and χ_H and $\chi_H = \frac{L_2}{\lambda_H}$

here: $\lambda_H = L_c + 0.75d$

hence: $\chi_H = \frac{1}{(\frac{L_2}{L_c} + 0.75 \frac{d}{L_c})} = \frac{1}{\frac{L_2}{L_c} + 0.75 \frac{d}{L_c}}$

2. Collection and Calculation of the Preliminary Data

Having as given caliber d , weight of projectile q and v_2 , the preliminary data are collected from the information related to the similar guns: d ; w_0 ; S ; L_c ;

L_2 ; L_{2H} ; $\frac{L_c}{L_2}$; $\frac{L_c}{L_{2H}}$; q ; $C_2 = \frac{q}{d^3}$

characteristics of powder ($f, \alpha, \delta, \theta$) its dimensions and form; ω ; $I = \frac{q}{u_i}$; P_m ; v_2 .

In tables usually is given L_{2H} - the length of the rifled bore, then: $L_2 = L_{2H} + (0.5 \text{ to } 1.0)d$; 0.5 - for the old projectiles, 1.0 for the new projectiles.

Table for $\frac{v_1}{v_2}$

$\frac{\Delta b}{x_H}$	3	4	5	6	7	8	9	10
0.6	0.270	0.256	0.243	0.233	0.223	0.215	0.211	0.208
0.8	0.237	0.222	0.209	0.199	0.189	0.180	0.174	0.168
1.0	0.213	0.197	0.184	0.174	0.165	0.157	0.150	0.143
1.2	0.196	0.180	0.167	0.157	0.149	0.141	0.134	0.128
1.4	0.183	0.166	0.153	0.143	0.135	0.128	0.121	0.115
1.6	0.171	0.154	0.141	0.131	0.124	0.116	0.111	0.105
1.8	0.161	0.144	0.131	0.122	0.115	0.109	0.103	0.098
2.0	0.152	0.135	0.123	0.114	0.107	0.101	0.096	0.092
3.0	0.120	0.105	0.095	0.088	0.083	0.078	0.074	0.070

Using these data by calculations the following characteristics are found: Δ ; $\frac{\omega}{q}$; $(\frac{I_K}{\alpha})$; $h_\omega = \frac{E_2}{\omega} = \frac{x_2^2}{(\frac{q}{\alpha})}$; $r = \varphi R_2$.

$$h_\omega = \frac{E_2 \theta}{f \omega} = h_\omega \frac{\theta}{f}; C_2 = \frac{E_2}{\alpha^2} = C_2 \cdot \frac{x_2^2}{\alpha^2}; h_2 = \frac{R_2}{\rho_m} = \frac{\varphi m x_2^2}{25 \ell_2 \rho_m} = h_\omega \frac{\varphi \Delta}{\Lambda_2 \rho_m}$$

$$R_2 = \frac{\varphi m x_2^2}{25(\ell_2 + \ell_2) \rho_m} = h_2 \cdot \frac{\Lambda_2}{\Lambda_2 + 1}$$

3. Selection of the Ballistic Criteria for the Comparative Evaluation of Variants.

From given data we know only C_1 and C_2 ; the rest of characteristics will be found in the calculation of variants. The most important characteristics are the

following: $\Lambda_2 = \frac{W_2}{W_0} = \frac{\ell_2}{\ell_0}$; $\frac{\ell_2}{\alpha}$; $\frac{W_2}{q} = \frac{W_0}{q} (\Lambda_2 + 1)$; $\frac{\omega}{q}$; $h = \frac{\Lambda_K}{\Lambda_2}$.

$$h_2 = \frac{R_2}{\rho_m}; h_\omega = \frac{E_2}{\omega}; N$$

When selecting variants it is advisable to take those, which have the largest possible h_2 , R_2 with h_ω and h_K within 0.60 - 0.70; such a choice leads to more economical utilization of the charge with the smaller $(\frac{\omega}{q})$ and with the greater Λ_2 (for increasing N). But larger h_2 and R_2 result in getting smaller h_ω . There are several approaches for finding certain compromises, conciliating this contradiction. For example, Prof. B. Okounev (1939) suggested taking the value of $H = \sqrt{r \cdot h_2}$ as the characteristic of an advantageous variant.

Here $r' = \frac{0.20 v_{\omega}^2}{2.57 \omega} = k_{\omega} \frac{v_{\omega}^2}{\omega}$, this r' being not affected by β_m has its maximum value at $\nu = \frac{v_{\omega}}{v_{\omega m}} = 0.52$. Prof. Okounov suggests for small arms $\nu > 0.52$ (0.55-0.56) and for guns of high power: $\nu < 0.52$ (0.48-0.50). Prof. I. Grave as a further development of Prof. Okounov's idea recommends: $H' = \sqrt[m+n]{(r')^m (k_{\omega})^n}$ (without giving values of m and n)

Prof. M. Serebryakov found that $H'' = \sqrt[n]{R_2 (k_{\omega})^n}$ gives better results with γ varying from 0 to 1.5. The exponent γ or H'' somehow depends on the type of a gun and thus reflects to a certain extent the influence of technico-tactical requirements. Prof. Sloukhotzky found that very good results are obtained using as the criterion for the usefulness of a selected variant the value of: $Z = k_{\omega} \cdot k_{\omega} \sqrt[4]{N}$

This criterion takes into account not only the ballistic requirements but constructional and economical ones as well. The constructional factor is: $k_{\omega} = \frac{g v_{\omega}^2}{L_{\omega}}$ (L_{ω} is the length of the whole barrel of a gun). The economical factor is: N . But it should be admitted that this question of the most reliable combined criterion still is in the phase of a preliminary accumulation of

experimental data and numerous researches. The very selection of the initial variants is usually made by using special graphs or Tables. One of the most usable graphs is given in the Fig. 157.

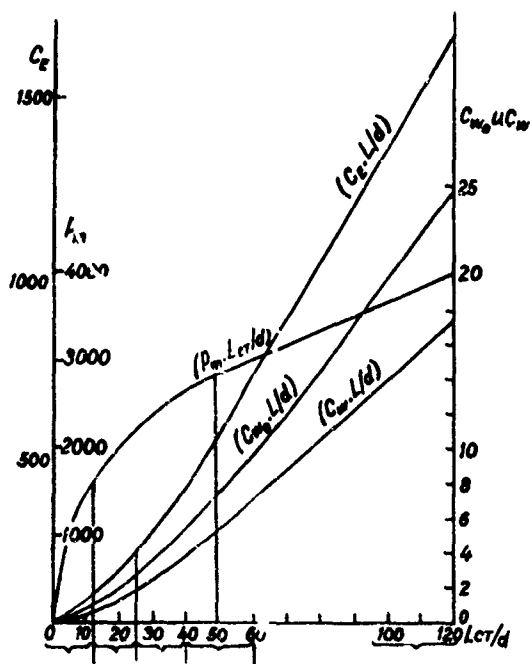


Fig. 157 - The principal ballistic characteristics.

The following characteristics are given in Fig. 157 as functions of the relative length of the whole barrel ($\frac{L_e}{d}$): The coefficients: $C_f = \frac{E}{d^3}$; $C_{w_0} = \frac{W_0}{d^3}$; $C_w = \frac{w}{d^3}$ and ρ_m . The coefficient of the utilization of the charge $\eta_w = \frac{Q}{C_w}$. A marked advantage of this graph is in its independence of gun calibers. The horizontal ($\frac{L_e}{d}$) - axis is marked in accordance with the corresponding lengths of various types of guns:

$\frac{L_e}{d} \leq 10$ - mortars.

$\frac{L_e}{d} \geq 10$
 $\frac{L_e}{d} \leq 25$ - howitzers.

$\frac{L_e}{d} \geq 25$
 $\frac{L_e}{d} \leq 40$ - field guns.

$\frac{L_e}{d} \geq 40$
 $\frac{L_e}{d} \leq 60$ - naval guns.

$\frac{L_e}{d} \geq 60$
 $\frac{L_e}{d} \leq 120$ - long distance guns.

This graph was devised by the engineer N. Oupornikov for guns manufactured by the Schneider Creuzot C^o (1930)

Prof. Sloukhotzky (1934) gave the following Table

in which the characteristics $\eta_w; \rho_m; \Delta; \chi = \frac{Q}{C_f}; (\frac{L_e}{d})$ are presented as functions of $C_f = \frac{E}{d^3}$. The Table presented here is a considerably improved and enlarged variant of the original Table of 1934.

Prof. Sloukhotzky's Table

C_2 $\frac{\text{ton-inch}}{\text{dm}^3}$	η_w $\frac{\text{ton-in.}}{\text{Kg.}}$	P_m $\frac{\text{Kg.}}{\text{cm}^2}$	Δ $\frac{\text{Kg.}}{\text{dm}^3}$	$\gamma \frac{L}{e}$	$(\frac{L}{d})$
100	124	1700	0.50	1.02	14
200	120	1950	0.55	1.09	23
300	117	2200	0.59	1.18	31
400	114	2400	0.62	1.28	38
500	112	2600	0.64	1.39	44
600	110	2800	0.66	1.50	51
700	108	2950	0.67	1.61	57
800	107	3100	0.68	1.73	64
900	106	3250	0.69	1.85	71
1000	105	3350	0.69	1.98	78
1100	104	3450	0.70	2.11	85
1200	104	3550	0.71	2.25	91
1300	103	3650	0.71	2.40	98
1400	103	3750	0.72	2.57	105
1500	102	3900	0.73	2.75	112
1600	102	4000	0.74	2.95	119

Chapter 2 - Theoretical Fundamentals of Ballistic

Design (1941)

1. The most advantageous and economical densities of loading at a given maximum pressure p_m .

At a given $\lambda_0 = \frac{L_0}{L}$ and p_m the weight of charge ω and the web ($2e_1$) can be varied with p_m preserving its given value; then the muzzle velocity v_0 will also vary and a systematical tracing of these variations of

v_0 reveals some important relationships between λ_0 ,

v_0 , L_0 and Δ . The minimum of $\Delta = \Delta_1$, at which we may obtain a given p_m will be at the instantaneous burning of powder in the chamber before the beginning of the projectile's travel, then:

$$p_m = \frac{f \Delta_1}{1 - \alpha \Delta_1} \quad \text{or} \quad \Delta_1 = \frac{1}{\left(\frac{f}{p_m}\right) + \alpha} \quad \text{and} \quad \omega_1 = W_0 \Delta_1$$

$$\text{or:} \quad \omega_1 = \frac{W_0}{\left(\frac{f}{p_m}\right) + \alpha}$$

Now keeping p_m constant we will increase ω and the parameter $B = \frac{S^2 I_K^2}{f \omega \psi m}$ having $B = \frac{a_m \Delta}{1 - \alpha \Delta}$

where $a_m = \frac{f F_2(\theta)}{p_m}$ (see formula 74): $B\left(\frac{1}{\Delta} - \alpha\right) = a_m (\text{const.})$
 At $\theta = 0.2$, $a_m = 0.32 \cdot \left(\frac{f}{p_m}\right)$

then we will have:

$$I_K = \frac{\sqrt{K_m} \cdot \omega}{\sqrt{W_0 - \alpha \omega}} = \frac{2}{u}, \quad \dots \quad (76)$$

here $K_m = \frac{f^2 F_2(\theta) \varphi m}{S^2 \rho_m} = \frac{a_m f \varphi m}{S^2}$

I_K is increased when ω is increased, hence e , must be increased. With these increases in ω and e , the value (see (60)) $l_m = l_0(1 - \alpha \Delta) [F_1(\theta) - 1]$ will be decreased (ρ_m will be closer to the beginning of motion) and the end of burning (l_K) will approach the muzzle, and at certain value of Δ_i , l_K will be equal to l_0 (the end of burning will be exactly at the muzzle). On further increases in Δ and I_K we will have incomplete burning and v_2 will be decreased. The experiments and calculations show that at this increase in Δ from Δ_1 to Δ_2 the muzzle velocity v_2 will pass through its maximum v_{2m} (as is shown in Fig. 158).

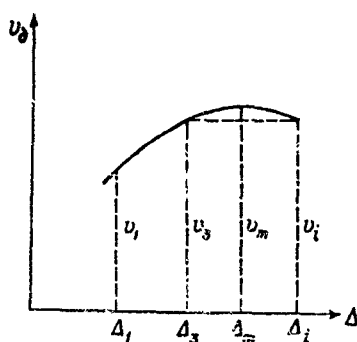


Fig. 158 v_2 as a function of Δ at the constant ρ_m

Thus at Δ_i , $v_{2i} < v_{2m}$ and $\Delta_m < \Delta_i$ and Δ_m is such density of loading at which for a given powder, at given ρ_m the muzzle velocity will be at its maximum. This density of loading Δ_m is called the most advantageous density of loading. The difference $(v_{2m} - v_{2i})$ is small enough (0.5-2%) and the French School of ballisticians for a long time considered v_2 as the maximum when the end of burning was reached at the muzzle. Therefore v_{2m} and Δ_m are located between (v_i, Δ_i) and a certain pair (v_e, Δ_e) which has $v_e = v_i$ and

$\Delta_e < \Delta_i$ can be determined. This density of loading Δ_e is called the economical density of loading. The end of burning with Δ_e will be earlier than at Δ_m or Δ_i . Δ_e is considerably (5% or 10%) smaller than Δ_i . In the following Table 16 calculated for

$A_2 = 6.0$ and $\rho_m = 2500$ we find the characteristics

$$h_K = \frac{L_K}{L_i}; v_2; h_w = \frac{E_2}{\omega}; h_2 = \frac{P_{2m}}{\rho_m}$$

calculated for various Δ among which are taken Δ_e , Δ_m and Δ_i .

Table 16

$\Lambda_2 = 6.0$

$\rho_m = 2500$

Δ_1 0.21	Δ_2 0.55	Δ_e 0.65	Δ_m 0.70	Δ_i 0.75
$\eta_K = \frac{E_K}{E_0} = 0$ $\eta_2 = 425$	0.30 613	0.55 644	0.72 648	1.00 644
$\eta_\omega = \frac{E_\omega}{E_0} = 178$	130	121	114	105
$\eta_2 = \frac{\rho_2}{\rho_m} = 0.277$	0.582	0.643	0.650	0.643

Practically the economical density of loading Δ_e should be considered as the most advantageous density of loading. The densities Δ_m , Δ_e and Δ_i are functions of Λ_2 and ρ_m for a given form of powder. The following Tables 17, 18, 19 show how Δ_e , Δ_i and parameter B are all increased with Λ_2 and ρ_m .

These Tables are calculated for the following character-

istics. $\chi = 1.06$; $\chi\lambda = -0.06$; $\varphi = 1.05$;

$f = 950,000 \frac{\text{kg. dm.}}{\text{kg.}}$; $\alpha = 0.98$; $\sigma = 1.6$;

$\theta = 0.2$; $\rho_0 = 300 \frac{\text{kg}}{\text{cm}^2}$

Table 17

 Δ_i (Burning Ends at the Muzzle)

$\frac{p_m}{\Delta_B}$	1800	2000	2200	2400	2600	2800	3000	3200	3400	3600
2	0.437	0.475	0.511	0.547	0.581	0.615	0.649	0.681	0.712	0.740
3	0.501	0.554	0.588	0.619	0.655	0.689	0.721	0.751	0.777	0.802
4	0.541	0.588	0.631	0.672	0.709	0.741	0.771	0.798	0.823	0.846
5	0.577	0.625	0.668	0.709	0.745	0.776	0.805	0.832	0.851	0.879
6	0.603	0.652	0.695	0.733	0.767	0.798	0.827	0.854	0.878	0.900
7	0.622	0.672	0.715	0.753	0.788	0.819	0.848	0.874	0.898	0.900
8	0.634	0.686	0.730	0.768	0.803	0.836	0.864	0.889	0.900	0.900
9	0.644	0.696	0.741	0.780	0.815	0.847	0.875	0.900	0.900	0.900
10	0.653	0.705	0.749	0.788	0.822	0.854	0.883	0.900	0.900	0.900

Table 18

Economical Densities of Loading Δ_0

1-instantaneous burning; -the most advantageous density of loading (minimum of W_0).

Δ_0	1800	2000	2200	2400	2600	2800	3000	3200	3400	3600
2	0.41	0.44	0.48	0.52	0.55	0.58	0.62	0.65	0.68	0.71
3	0.46	0.51	0.55	0.58	0.62	0.65	0.68	0.71	0.74	0.76
4	0.50	0.54	0.59	0.63	0.66	0.70	0.73	0.75	0.78	0.80
5	0.52	0.57	0.61	0.65	0.69	0.72	0.75	0.78	0.80	0.82
6	0.54	0.59	0.63	0.67	0.70	0.73	0.76	0.79	0.81	0.84
7	0.55	0.60	0.64	0.68	0.72	0.75	0.78	0.80	0.83	0.86
8	0.56	0.61	0.66	0.70	0.73	0.76	0.79	0.82	0.84	0.87
9	0.58	0.63	0.68	0.72	0.75	0.79	0.81	0.84	0.86	0.88
10	0.60	0.65	0.70	0.74	0.77	0.80	0.83	0.86	0.88	0.90
1	0.360	0.375	0.385	0.395	0.410	0.425	0.440	0.455	0.465	0.476
2	0.432	0.452	0.468	0.480	0.495	0.510	0.525	0.540	0.555	0.562

Table 19

Parameter B_0 at the Economical Loading Conditions

Δ_0	1800	2000	2200	2400	2600	2800	3000	3200	3400	3600
2	1.45	1.47	1.48	1.49	1.50	1.51	1.56	1.60	1.64	1.68
3	1.74	1.76	1.78	1.80	1.83	1.84	1.85	1.87	1.89	1.90
4	1.94	1.96	2.00	2.03	2.05	2.06	2.07	2.08	2.10	2.10
5	2.07	2.10	2.12	2.14	2.15	2.17	2.19	2.21	2.24	2.27
6	2.20	2.22	2.24	2.24	2.24	2.25	2.26	2.30	2.32	2.41
7	2.28	2.30	2.30	2.31	2.33	2.35	2.37	2.39	2.48	2.56
8	2.34	2.36	2.40	2.42	2.44	2.46	2.48	2.52	2.55	2.61
9	2.47	2.50	2.54	2.57	2.60	2.62	2.64	2.66	2.69	2.71
10	2.58	2.61	2.68	2.70	2.72	2.74	2.80	2.82	2.85	2.85

Table 20Characteristics η_k and η_b at the Economical Loading Conditions

Λ_b	2	3	4	5	6	7	8	9	10
$\eta_k = \frac{I_k}{I_b}$ for all pressures	0.82	0.75	0.70	0.66	0.63	0.60	0.57	0.59	0.63
$\eta_b = \frac{P_{ave}}{P_m}$ at $P_m = 1800$	0.85	0.80	0.75	0.70	0.65	0.60	0.55	0.52	0.50
at $P_m = 3600$	0.79	0.73	0.66	0.60	0.55	0.50	0.45	0.42	0.40

2. The Principal Relationships and Graphs for the Constructional Elements of the Gun Canal

The initial formula is the formula for velocity during the second period because it was already shown that the best utilization of the volume of canal (W_c) and of the weight of the charge is obtained when the burning of powder is ended within the bore i.e. when $\frac{L_K}{L_0} \sim 0.5 - 0.7$.

From (24) (See Part II) we have:

$$v_2^2 = v_{lim}^2 \left\{ 1 - \left(\frac{\Lambda_{K+1} - \alpha \Delta}{\Lambda_{K+1}} \right)^{\theta} \left[1 - \frac{\beta \theta}{2} (1 - z_0)^2 \right] \right\} \dots (119)$$

Here: $v_{lim}^2 = \frac{2gfw}{\varphi \theta q}$; $\Lambda_K = \frac{L_K}{L_0}$; $\Lambda_2 = \frac{L_2}{L_0}$; $\Lambda_{K+1} = \frac{L_{K+1}}{L_0} = \frac{W_c}{W_0}$; $\varphi = \alpha - \frac{\beta \theta}{2}$

Denoting: $\frac{v_2^2}{v_{lim}^2} = \varphi r = r'$; $\frac{v_K^2}{v_{lim}^2} = \frac{\beta \theta}{2} (1 - z_0)^2 = r_K$; $K = (\Lambda_{K+1} - \alpha \Delta) \left[1 - \frac{\beta \theta}{2} (1 - z_0)^2 \right]$

and solving (119) with respect to $\Lambda_{K+1} = \frac{W_c}{W_0}$ we will have:

$$W_c = W_0 \left[\frac{K}{(1 - r')^{\frac{1}{\theta}}} + \alpha \Delta \right] \dots (120)$$

For the volume W_c

or: $L_2 = L_0 \left[\frac{K}{(1 - r')^{\frac{1}{\theta}}} + \alpha \Delta - 1 \right] \dots (121)$

For the total length of travel of the projectile.

From Prof. Drosdov's Tables we have that A_K and B are affected only by Δ and ρ_m , hence: $K = F(\rho_m, \Delta)$

$$\text{Now } \gamma' = \frac{v_2^2 \cdot 4g \cdot \theta}{2g \omega f} = \frac{\theta}{f} \cdot \frac{v_2^2}{2g} \cdot \frac{(a + b \frac{\omega}{2})}{(\frac{\omega}{2})}$$

is a function only of $(\frac{\omega}{2})$ and $\frac{\theta}{f} \cdot \frac{v_2^2}{2g} = K_v$ (constant at given v_2)

$$\text{At } f = 950,000; \quad \theta = 0.2; \quad g = 98.1 \frac{\text{dm.}}{\text{sec}^2}$$

$$K_v = \frac{v_2^2 (\frac{dm}{sec})}{952,106}, \text{ and } \gamma' = K_v \cdot \frac{a + b \frac{\omega}{2}}{a} = f_2(\frac{\omega}{2})$$

$$W_0 = \frac{\omega}{\Delta}; \quad \frac{W_0}{2} = \frac{1}{\Delta} \cdot \frac{\omega}{2} = f_3(\frac{\omega}{2}, \Delta)$$

$$\text{Then (120) will be: } \frac{W_0}{2} = \frac{W_0}{2} \left[\frac{K(\rho_m, \Delta)}{(1-\gamma')^2} + \alpha \Delta \right] \dots (122)$$

At given ρ_m, v_2, d, g the volume $(\frac{W_0}{2})$ is also a function only of two variables Δ and $\frac{\omega}{2}$. Now instead of $(\frac{W_0}{2})$ and $(\frac{W_0}{2})$ we can insert the relative lengths of the whole canal $(\frac{L_c}{\alpha})$ and of the length of the chamber $(\frac{L_0}{\alpha})$ in calibers. The effective length of canal $L'_c = L_0 + L_2$ and $W_c = S L'_c; W_0 = S L_0$.

$$\text{Then (122) will be: } \frac{L'_c}{\alpha} = \frac{L_0}{\alpha} \left[\frac{K(\rho_m, \Delta)}{(1-\gamma')^2} + \alpha \Delta \right] \dots (123)$$

$$\text{Here: } \frac{L_0}{\alpha} = \frac{W_0}{S \alpha} = \frac{W_0}{\pi_3 \alpha^3 \alpha} = \frac{1}{\pi_3} \cdot \frac{W_0}{2} \cdot \frac{2}{\alpha^3} = \frac{C_2}{\pi_3} \cdot \frac{1}{\Delta} \cdot \frac{\omega}{2}$$

is a function of Δ and $(\frac{\omega}{2})$.

$$\text{The factual length of the canal: } L_c = L'_c + L_2 = \frac{L_0}{\gamma} + L_2$$

denoting: $n' = 1 - \frac{1}{\alpha} = 1 - \frac{\ell_c}{\ell_0} = \frac{\ell_0 - \ell_c}{\ell_0}$

hence: $L_c = \frac{\ell_0}{\alpha} + \ell_2 + \ell_0 - \ell_0 = \ell_0 + \ell_2 - (\ell_0 - \frac{\ell_0}{\alpha}) = L_c' - \ell_0(1 - \frac{1}{\alpha})$

Then (123) will be: $\frac{L_c}{\alpha} = \frac{\ell_0}{\alpha} \left[\frac{K(R_m, \Delta)}{(1-r')^{\frac{1}{2}}} + \alpha \Delta - n' \right] \dots (124)$

and

$$\frac{\ell_2}{\alpha} = \frac{\ell_0}{\alpha} \left[\frac{K(R_m, \Delta)}{(1-r')^{\frac{1}{2}}} + \alpha \Delta - 1 \right] \dots (125)$$

Now a general conclusion is, that at given α, q, v_j, ρ_m (as always is in the case of ballistic design) all the constructional elements of the gun canal, namely - the whole volume W_c , its working part $W_2 = S\ell_2$, chamber volume W_0 and actual canal length L_c (considering the widening of a chamber) - all these elements are functions only of 2 variables (loading conditions): Δ and $(\frac{\omega}{q})$. This result means, that if we will consider three coordinates Z, Δ and $\frac{\omega}{q}$, then the coordinate $Z = f(\Delta, \frac{\omega}{q})$ can be assigned as one of the following variables: $(\frac{W_c}{q}); (\frac{W_2}{q}); (\frac{W_0}{q}); (\frac{S\ell_2}{q}); (\frac{L_c}{\alpha}); (\frac{\ell_2}{\alpha}); (\frac{\ell_0}{\alpha}); (\frac{L_c}{\alpha})$

and in each case we will have an equation of a certain surface. The analyses of all these cases shows that at given v_j and ρ_m all these surfaces, except in case of the surface $\frac{W_0}{q} = f(\Delta, \frac{\omega}{q})$ are asymmetric surfaces (hammocks) having their convexities turned down.

(see Fig. 159). Their lowest points correspond to the minimum values of W_c , L_c , ℓ_s , W_s , mentioning only the most important elements of the rational design of a gun. The simplest surface is: $\frac{W_o}{q} = \frac{1}{\Delta} \cdot \left(\frac{\omega}{q}\right)$

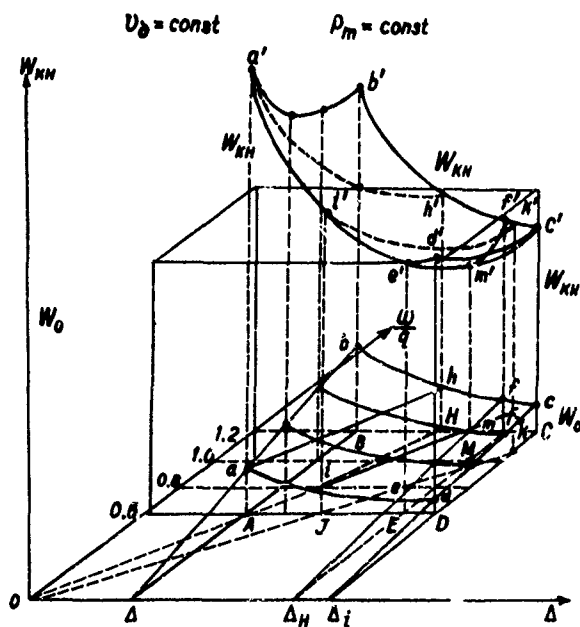


Figure 159

a'b'c'd' - surface: $\frac{W_KH}{q} = F\left(\Delta, \frac{\omega}{q}\right)$. . . hammock

a b c d - surface: $\frac{W_o}{q} = \frac{1}{\Delta} \cdot \left(\frac{\omega}{q}\right)$ an asymmetric
hyperbolic chute

Coordinate Δ varies from Δ_1 (instantaneous burning) to Δ_2 (the burning at the muzzle); coordinate $(\frac{w}{2})$ is shown at 0.6; 0.8; 1.0; 1.2.

Purely geometrical interpretations of the results of intersections of the surfaces: $\frac{W_0}{2} = \Delta \left(\frac{w}{2} \right)$ and $\frac{W_c}{2} = F(\Delta, \frac{w}{2})$ with the planes parallel to the plane $(\Delta, \frac{w}{2})$ or parallel to the plane $(Z, \frac{w}{2})$ - being translated into terms of volumes W_0 and W_c , density of loading Δ , and relative weight $(\frac{w}{2})$ will contain important information concerning the relationships between these elements, especially when there are involved particular cases of determining the minimums of W_0 or of W_c or cases requiring the preservation of the constant values of W_0 or W_c . Schematically these details are shown in Fig. 159 and Fig. 160 (case of $W_c = \text{constant}$)

3. Determining Loading conditions (Δ and $\frac{\omega}{q}$) for a Gun of Minimum Volume - $(W_c)_{min.}$

A. Determining $\Delta_{min.}$ at which W_c is minimum (at the constant $\frac{\omega}{q}$ or r').

Formula (120) being written in its complete form is:

$$\frac{W_c}{q} = \frac{\omega}{q} \cdot \frac{1}{\Delta} \left\{ \frac{(1 + \alpha \Delta) \left[1 - \frac{B\theta}{2} (-2\gamma)^{\frac{1}{2}} \right]^{\frac{1}{2}}}{(1 - r')^{\frac{1}{2}}} + \alpha \Delta \right\} \dots (126)$$

To find the minimum W_c (we do not know the analytical expressions of Λ_K and B in terms of Δ) we should take a certain constant $(\frac{\omega}{q})$ and a series of various Δ (planes parallel to the plane $(Z, \frac{\omega}{q})$ and thus consider the obtained sections of the surface W_c . Then we take a constant Δ and a series of various $\frac{\omega}{q}$ (planes parallel to the plane (Z, Δ)). The analytical solution is possible for the case $\frac{\omega}{q} = \text{Const.}$ and $\psi_0 = 0$

(a powder with constant surface of burning) then (126) will be:

$$\frac{W_c}{q} = \frac{\omega}{q} \cdot \frac{1}{\Delta} \left[\frac{1 - \alpha \Delta}{(1 - \frac{B\theta}{2})^{\frac{1}{2}}} \cdot \frac{1}{(1 - r')^{\frac{1}{2}}} + \alpha \Delta \right] \dots (127)$$

At the constant $p_m : B = \frac{a_m \Delta}{1 - \alpha \Delta} = \frac{a_m}{\frac{1}{\Delta} - \alpha}$;

$$\text{here: } a_m = \frac{f F_2(\theta)}{p_m} \quad \text{at } \theta = 0.2$$

$$F_2(\theta) = 0.32$$

Introducing a new variable: $y = \frac{1}{\Delta} - \alpha$ and denoting $\frac{a''}{2} \theta = \alpha''$ we will have:

$$\frac{W_c}{2} = \frac{\omega}{2} \cdot \frac{1}{(1-r')^2} \left[\frac{y}{(1-\frac{a''}{2})^2} + \alpha(1-r')^2 \right] \dots (128)$$

Since $r' = \frac{F_1 \theta}{f \omega} \varphi$ is independent of Δ and y we can now differentiate $(\frac{W_c}{2})$ with respect to y and make this derivative equal to zero:

$$1 - \frac{1}{\theta} \cdot \frac{a''}{y_{ma}} \cdot \frac{1}{(1-\frac{a''}{2})^2} = 0$$

here: y_{ma} corresponds to - the most advantageous density of loading.

Hence:

$$y_{ma} = \frac{1}{\Delta_{ma}} - \alpha = \frac{1+\theta}{\theta} a'' = \frac{1+\theta}{2} \cdot a'' = \frac{1+\theta}{2} F_2(\theta) \frac{f}{P_m} \dots (129)$$

and: $\Delta_{ma} = \frac{1}{\alpha + \frac{(1+\theta)F_2(\theta)f}{P_m}}$; denoting: $\frac{(1+\theta)F_2(\theta)}{2} = \frac{1}{2} \left(\frac{1+\theta}{1+\theta} \right) = F_3(\theta)$
at $\theta = 0.2$ $F_3(\theta) = 0.192$

We have finally:

$$\Delta_{ma} \text{ (the most advantageous } \Delta) = \frac{1}{\alpha + F_3(\theta) \frac{f}{P_m}} = \frac{1}{\alpha + 0.192 \frac{f}{P_m}}$$

We see that Δ_{ma} is independent of $\frac{\omega}{2}$ and is increased when we take a higher P_m ; this Δ_{ma} corresponds to the minimum of W_c at any value of $\frac{\omega}{2}$ - we call this Δ_{ma} - the most advantageous density of loading.

The following table shows how Δ_{ma} is affected by the value of p_m

$$p_m = 2000; 2400; 2800; 3200; 3600; 4000 \quad \text{for } \chi = 1.06$$

$$\Delta_{ma} = 0.53; 0.60; 0.66; 0.71; 0.76; 0.81$$

At $\chi = 1.00$ the above values of Δ_{ma} will be increased at 0.02. There is also an empirical formula for Δ_{ma} :

$$\Delta_{ma} = \sqrt{\frac{p_m - 300}{5700}}; \quad p_m \left(\frac{\text{kg}}{\text{cm}^2} \right)$$

If $\gamma_{ma} = \frac{1+\theta}{2} a_m$ is inserted into $B = \frac{a_m}{\frac{1}{2} - \alpha} = \frac{2}{1+\theta} = \text{Const.}$ Therefore the minimum of W_c at any given p_m and corresponding value of Δ_{ma} is always obtained at the same constant value of B which at $\theta = 0.2$ and

$$\psi_0 = 0 \text{ will be: } B_{ma} = 1.667$$

In Prof. Drosdov's Tables at $p_0 = 300 \frac{\text{kg}}{\text{cm}^2}$ $B_{ma} = 1.91-1.93$

B. The Most Efficient Relative Charge $\left(\frac{\omega}{q}\right)$ at which the Canal Volume W_c is Minimum ($\Delta = \text{Constant}$)

If we take a series of constant values of Δ (planes parallel to the plan $\left(\frac{W_c}{q}, \frac{\omega}{q}\right)$ we can find the conditions and value of $\left(\frac{\omega}{q}\right)$ at which W_c will be a minimum. Now in (126) we have $\Delta = \text{constant}$ and :

$$K = (\Lambda_k + 1 - \alpha \Delta) \left[1 - \frac{B\theta}{2} (1 - \alpha) \right]^{\frac{1}{\theta}} = f(p_m, \Delta) = \text{Const.}$$

Instead of $\left(\frac{\omega}{2}\right)$ a new variable is taken:

$$r' = \varphi r_0 = \frac{a + b\left(\frac{\omega}{2}\right)}{\left(\frac{\omega}{2}\right)} \cdot \frac{\theta v_0^2}{2gf} = K_v \cdot \frac{a + b\left(\frac{\omega}{2}\right)}{\left(\frac{\omega}{2}\right)}; K_v = \frac{\theta v_0^2}{2gf}$$

Hence:
$$\frac{\omega}{2} = \frac{a K_v}{r' - b K_v}$$

then (126) will be

$$\frac{W_c}{2} = \frac{1}{\Delta} \cdot \frac{a K_v}{r' - b K_v} \left[\frac{K}{(1-r')^{\frac{1}{2}}} + \alpha \Delta \right] \dots (126')$$

Differentiating with respect to r' and equating to

zero we have:
$$\frac{1}{(1-r')^{\frac{1}{2}}} - \frac{1}{\theta} \cdot \frac{r' - b K_v}{(1-r')^{\frac{3}{2}}} + \frac{\alpha \Delta}{K} = 0$$

or for minimum of W_c :

$$\frac{1}{\theta} \cdot \frac{r' - b K_v}{(1-r')^{\frac{3}{2}}} - \frac{1}{(1-r')^{\frac{1}{2}}} = \frac{\alpha \Delta}{K} = f(P_m, \Delta) \dots (127)$$

The left part is a function of r' and velocity v_0 (given value). The right part $\frac{\alpha \Delta}{K}$ is given (Δ -const.,

P_m is given) thus the equation has a certain solution

r' , at which $\left(\frac{W_c}{2}\right)$ will be at its minimum. Exactly in the same way we will find the following equations for r' producing the minimum of L_c and the minimum of

l_2 . - Thus we will have the following two equations:

$$(L_c)_{\min}: \frac{1}{\theta} \cdot \frac{r' - b K_v}{(1-r')^{\frac{3}{2}}} - \frac{1}{(1-r')^{\frac{1}{2}}} = \frac{\alpha \Delta - n'}{K} \dots (128)$$

$$(l_2)_{\min}: \frac{1}{\theta} \cdot \frac{r' - b K_v}{(1-r')^{\frac{3}{2}}} - \frac{1}{(1-r')^{\frac{1}{2}}} = \frac{\alpha \Delta - 1}{K} \dots (129)$$

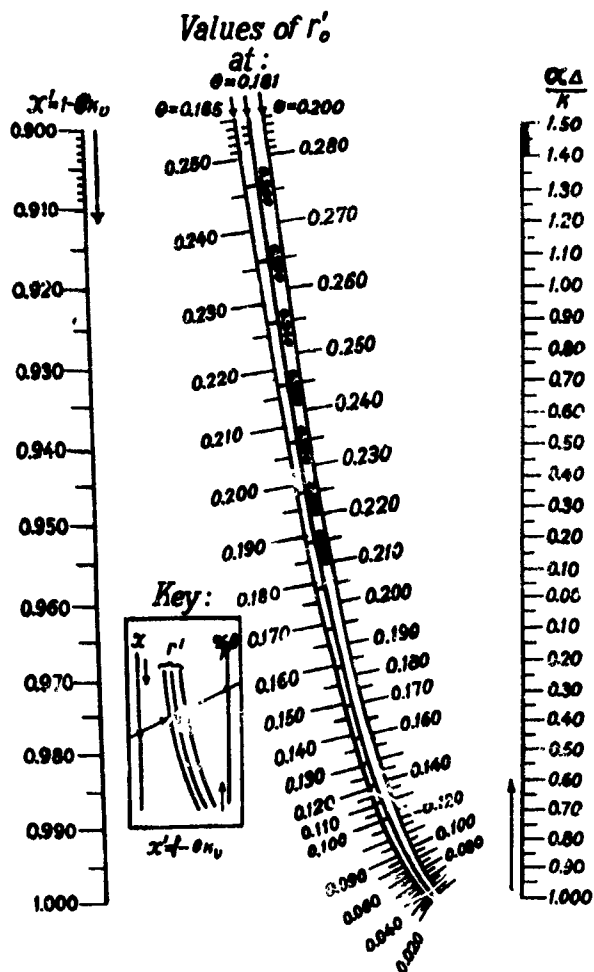


Fig. 161 Nomogram for an optimal value of r'

A special nomogram (Fig. 161) gives solutions of equations (127), (128) and (129) for the known values of $\frac{\alpha \Delta}{K}$, $\frac{\alpha \Delta - h'}{K}$ and $\frac{\alpha \Delta - 1}{K}$ (read on the right scale) and of $x' = 1 - bK_v = 1 - b \frac{\theta}{f} \cdot \frac{24^2}{x_g^2}$ (read on the left scale) and the sought for r' (read on the middle curvilinear scale at the intersection with the straight line passing through x' and reading on the right scale). Scales for r' are given for the three values of θ : $\theta = 0.165$, $\theta = 0.181$ and $\theta = 0.200$. The reading of r' will be the highest on its scale for (127) next lower r' will be for (128) and the lowest r' will be for (129) - which means that $\frac{\omega}{q} = \frac{a}{K - b}$ and $\frac{W_0}{q} = \frac{\omega}{q} \cdot \frac{1}{\Delta}$ will be increased with the decreases in r' .

Thus the gun with the minimum L_c will have a larger W_0 and larger $(\frac{\omega}{q})$ than the gun with the minimum W_c and the gun with the minimum ℓ_0 will have still larger values of W_0 and $\frac{\omega}{q}$ than the gun with the minimum W_c . The conclusion is that the gun with the minimum W_c , having a desired \mathcal{V}_0 and given β_m , has a smaller W_0 and a smaller $\frac{\omega}{q}$ than the gun with the minimum L_c and minimum ℓ_0 . This is the reason for calling such gun "the optimum gun". There are also given special Tables: for $(\frac{\alpha \Delta}{K})$ with the entries Δ and β_m and for $\frac{1}{(1-r')^2}$ at $\theta = 0.2$.

Table $\frac{\alpha \Delta}{\lambda}$ (C.A.B. tables) ($\alpha = 1$)

$\frac{\rho_m}{\Delta}$	1600	1800	2000	2200	2400	2600	2800	3000
0.40	0.342	0.376	0.404	0.424	0.442	0.458	0.473	0.486
0.42	0.345	0.384	0.415	0.440	0.460	0.478	0.493	0.507
0.44	0.348	0.389	0.424	0.453	0.477	0.497	0.516	0.530
0.46	0.350	0.392	0.430	0.465	0.492	0.514	0.534	0.552
0.48	0.348	0.394	0.436	0.474	0.505	0.530	0.553	0.572
0.50	0.345	0.396	0.440	0.481	0.515	0.546	0.570	0.594
0.52	0.339	0.395	0.441	0.486	0.524	0.558	0.589	0.612
0.54	0.331	0.394	0.445	0.489	0.530	0.568	0.600	0.628
0.56	0.320	0.388	0.444	0.490	0.535	0.575	0.610	0.641
0.58	0.304	0.378	0.437	0.491	0.538	0.581	0.619	0.653
0.60	0.290	0.367	0.433	0.490	0.540	0.585	0.627	0.665
0.62	0.269	0.349	0.421	0.486	0.539	0.588	0.633	0.674
0.64	0.256	0.335	0.422	0.487	0.537	0.589	0.637	0.682
0.66	-	0.319	0.398	0.469	0.533	0.588	0.638	0.687
0.68	-	0.297	0.381	0.456	0.526	0.585	0.638	0.691
0.70	-	0.282	0.362	0.440	0.513	0.578	0.637	0.691
0.72	-	-	0.339	0.420	0.496	0.566	0.632	0.689
0.74	-	-	0.317	0.402	0.475	0.550	0.622	0.684
0.76	-	-	-	0.377	0.459	0.531	0.605	0.674
0.78	-	-	-	0.351	0.433	0.512	0.585	0.657

Table $\frac{\alpha \Delta}{K}$ (C.A.B. tables) ($\alpha = 1$) (Cont.)

$\frac{p_n}{\Delta}$	3200	3600	4000	4400	4800	5200	5600	6000
0.40	0.500	0.525	0.549	0.574	0.596	0.617	0.635	0.653
0.42	0.521	0.547	0.570	0.597	0.622	0.645	0.666	0.682
0.44	0.545	0.569	0.596	0.622	0.648	0.674	0.698	0.720
0.46	0.568	0.595	0.622	0.649	0.676	0.702	0.727	0.750
0.48	0.592	0.622	0.650	0.676	0.704	0.729	0.754	0.778
0.50	0.614	0.648	0.678	0.705	0.732	0.760	0.786	0.811
0.52	0.634	0.673	0.706	0.734	0.761	0.789	0.817	0.839
0.54	0.652	0.697	0.733	0.763	0.791	0.819	0.845	0.875
0.56	0.669	0.719	0.760	0.793	0.822	0.851	0.881	0.910
0.58	0.685	0.740	0.785	0.823	0.855	0.885	0.915	0.946
0.60	0.700	0.761	0.812	0.854	0.890	0.920	0.952	0.985
0.62	0.713	0.780	0.836	0.885	0.924	0.959	0.991	1.023
0.64	0.724	0.797	0.858	0.910	0.955	0.995	1.029	1.060
0.66	0.731	0.812	0.878	0.934	0.986	1.030	1.069	1.105
0.68	0.736	0.823	0.896	0.958	1.016	1.063	1.105	1.149
0.70	0.739	0.832	0.912	0.980	1.043	1.095	1.145	1.186
0.72	0.738	0.838	0.926	1.001	1.068	1.127	1.180	1.228
0.74	0.735	0.842	0.938	1.021	1.091	1.156	1.212	1.269
0.76	0.730	0.844	0.946	1.036	1.113	1.184	1.245	1.300
0.78	0.722	0.842	0.951	1.047	1.130	1.208	1.280	1.344

Table $\frac{Q_A}{K}$ (3.A.B. tables) ($\alpha = 1$) (Cont.)

$\frac{p_m}{\Delta}$	1600	1800	2000	2200	2400	2600	2800	3000
0.80	-	-	-	-	0.410	0.490	0.567	0.641
0.82	-	-	-	-	0.381	0.464	0.542	0.619
0.84	-	-	-	-	-	0.453	0.535	0.592
0.86	-	-	-	-	-	0.402	0.486	0.565
0.88	-	-	-	-	-	-	0.450	0.533
0.90	-	-	-	-	-	-	0.414	0.498
0.92	-	-	-	-	-	-	-	0.463
0.94	-	-	-	-	-	-	-	-
0.95	-	-	-	-	-	-	-	-

Table $\frac{\alpha \Delta}{K}$ (C.A.B. tables) ($\alpha = 1$) (Cont.)

$\frac{p_m}{\Delta}$	3200	3600	4000	4400	4800	5200	5600	6000
0.80	0.711	0.839	0.953	1.054	1.144	1.231	1.308	1.380
0.82	0.696	0.834	0.952	1.057	1.153	1.250	1.332	1.409
0.84	0.673	0.823	0.949	1.058	1.161	1.262	1.354	1.441
0.86	0.644	0.803	0.942	1.057	1.166	1.269	1.374	1.464
0.88	0.612	0.773	0.930	1.054	1.169	1.276	1.382	1.482
0.90	0.580	0.739	0.908	1.046	1.172	1.281	1.390	1.495
0.92	0.545	0.702	0.871	1.032	1.171	1.290	1.395	1.503
0.94	0.501	0.665	0.831	1.003	1.169	1.298	1.408	1.511
0.95	-	0.644	0.807	0.986	1.162	1.306	1.421	1.526

Table of Function $a_2 = \frac{1}{(1-r')^{1/2}} ; 0 = 0.2$

r'	0	1	2	3	4	5	6	7	8	9
0.17	2.538	2.553	2.569	2.584	2.600	2.615	2.631	2.648	2.665	2.681
0.18	2.698	2.715	2.731	2.748	2.764	2.780	2.797	2.814	2.832	2.850
0.19	2.867	2.885	2.903	2.921	2.939	2.958	2.976	2.995	3.014	3.033
0.20	3.052	3.071	3.090	3.109	3.128	3.148	3.169	3.188	3.209	3.230
0.21	3.241	3.271	3.291	3.312	3.333	3.354	3.375	3.397	3.419	3.441
0.22	3.463	3.485	3.508	3.531	3.554	3.577	3.600	3.623	3.646	3.670
0.23	3.691	3.718	3.742	3.766	3.790	3.815	3.841	3.867	3.893	3.919
0.24	3.945	3.971	3.998	4.025	4.052	4.079	4.105	4.131	4.158	4.185
0.25	4.212	4.240	4.268	4.297	4.326	4.355	4.385	4.415	4.446	4.477
0.26	4.508	4.538	4.568	4.598	4.630	4.661	4.693	4.746	4.759	4.792
0.27	4.825	4.859	4.893	4.927	4.961	4.995	5.030	5.065	5.100	5.135
0.28	5.170	5.206	5.242	5.278	5.315	5.352	5.389	5.426	5.464	5.502
0.29	5.540	5.580	5.620	5.660	5.700	5.741	5.784	5.827	5.870	5.913
0.30	5.957	5.998	6.040	6.082	6.124	6.166	6.212	6.258	6.304	6.350
0.31	6.397	6.443	6.489	6.536	6.583	6.630	6.679	6.729	6.779	6.829
0.32	6.879	6.930	6.981	7.033	7.085	7.137	7.190	7.243	7.296	7.351
0.33	7.404	7.461	7.518	7.575	7.633	7.691	7.750	7.809	7.869	7.929
0.34	7.989	8.051	8.113	8.175	8.237	8.299	8.363	8.427	8.491	8.555
0.35	8.620	8.686	8.753	8.820	8.887	8.954	9.025	9.096	9.167	9.239

As a general conclusion we may state that from general considerations of the relationships given in Interior Ballistics we obtain also general regularities showing how the constructional elements of the gun canal are affected by the loading conditions at given d, q, v_2 and p_m . Furthermore, we have methods for determining those loading conditions for a gun with the minimum W_c or an optimum gun. It was also shown that a desired v_2 at given p_m , can be obtained at different combinations of the constructional elements or loading conditions: we may have this v_2 at the longer or shorter gun canals at the larger or smaller W_0 , at the higher and lower Δ and ω .

Chapter 3. Applications of the Obtained Relationships to the Practical Design of Guns.

1. The "Directive Diagram" its construction and analysis. A special graph is shown in Fig. 163 which has been devised as a reliable tool for making a rational and effective selection of the most appropriate variant among several others, which all satisfy the imperative requirements (ballistic, technical, tactical, economic) of a considered project of gun design.

This graph is called "the Directive Diagram" because it provides a rational direction for making a difficult decision. This graph should be constructed for a given set of initial data: q , ψ and ρ_m . The general idea of this diagram is the practical use of projections on the plane $(\frac{\omega}{q}, \Delta)$ of various plane sections of the surfaces $(\frac{W_p}{q}, \Delta, \frac{\omega}{q})$ and $(\frac{W_c}{q}, \Delta, \frac{\omega}{q})$, which were shown in Fig. 159 and Fig. 160. All these plane sections are obtained by the planes parallel to the

$(\frac{\omega}{q}, \Delta)$ plane. Thus it can be said that the surfaces $(\frac{W_p}{q}, \Delta, \frac{\omega}{q})$ and $(\frac{W_c}{q}, \Delta, \frac{\omega}{q})$ are analyzed as by means of their topographical maps made on the plane $(\frac{\omega}{q}, \Delta)$ in form of the concentric contours for W_c (located around certain middle point which is the projection on the plane $(\frac{\omega}{q}, \Delta)$ of the lowest point of the surface $(\frac{W_c}{q}, \Delta, \frac{\omega}{q})$, which is the point M_0 on Fig. 163. The sections of the surface $(\frac{W_p}{q}, \Delta, \frac{\omega}{q})$ are projected as straight lines all issued from the origin point 0 making various angles with Δ - axis.

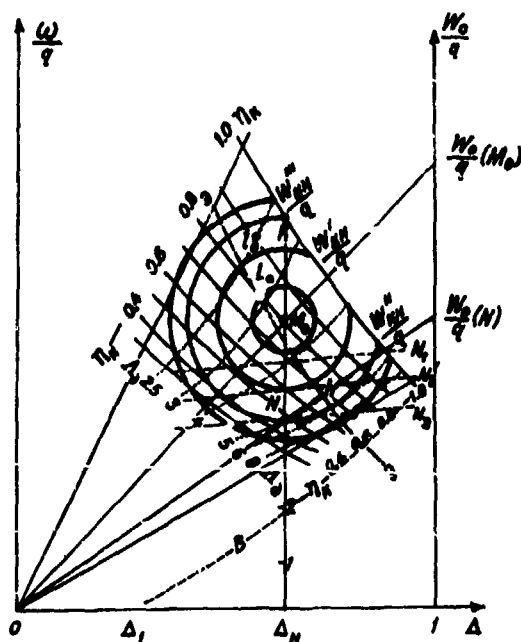


Fig. 163 - The directive diagram for a selection of needed variants.

1. The principal point is M_0 representing the gun with minimum W_c ; the coordinates of M_0 are: Δ_{M_0} (the most advantageous Δ) and $(\frac{\omega}{q})$ (the optimal charge at given q, v_a and ρ_m).
2. The oval counters around M_0 are the lines of equal canal volumes $\frac{W'_c}{q}, \frac{W''_c}{q}, \frac{W'''_c}{q}$ (isochore lines of canal) obtained from the plane sections of the "hammock surface" parallel to the plane $(\frac{\omega}{q}, \Delta)$

3. The straight lines issuing from the origin 0 in the plane $(\frac{\omega}{q}, \Delta)$ have their angle α with the Δ -axis determined by:

$$\tan \alpha = \frac{(\frac{\omega}{q})}{\Delta} = \frac{W_0}{W_c}$$

which means that everyone of these straight lines represents the line of equal volumes $(\frac{W_0}{q})$. These volumes are increased with the angle α . The straight line OM_0 represents the volume $(\frac{W_0}{q})$ corresponding to the gun with the minimum $(\frac{W_c}{q})$. Two straight lines which are tangents to the same oval $(\frac{W_c}{q})$ represent the maximum and minimum of W_0 corresponding to the same W_c - these extreme values of W_0 are determined by the coordinates $\frac{\omega}{q}$ and Δ - i.e. definite loading conditions for $(W_0)_{max.}$ and $(W_0)_{min.}$.

4. As soon as we know for any point of the plane $(\frac{\omega}{q}, \Delta)$ corresponding values of $\frac{W_c}{q}$ and $\frac{W_0}{q}$ we immediately can find $\Lambda_s = \frac{W_c - W_0}{W_0} = \frac{W_c}{W_0}$ i. e. the number of volumes of expansion which is one of the most important characteristics of a gun. The lines of equal Λ_s can be traced on the plane $(\frac{\omega}{q}, \Delta)$ as is shown in dotted lines marked by numbers from 2.5 to 8 on Fig. 133.

5. In the same way the curves of equal $\eta_K = \frac{e_K}{e_s}$ as functions of $(\frac{\omega}{q})$ and (Δ) are represented on the diagram and marked by $\eta_K = 0.3, \eta_K = 0.4 \dots$ up to $\eta_K = 1.0$.

The line $\eta_K = 1$ represents the case in which the burning is ended when the projectile is at the muzzle ($\ell_K = \ell_s$)

6. Parameter of loading B at given p_m is an increasing function of Δ and this curve (B, Δ) is also shown on Fig. 163. This curve begins at the point $\Delta = \Delta_0$, and

$B = 0$; at Δ_{ma} (marked Δ_K) $B \approx 1.91$ or 1.93 .

7. The lines of equal N (number of firings not dangerous for a gun) are represented by lines marked N_1, N_2, N_3 almost parallel to the Δ - axis; the larger N is closer to Δ - axis ($N_3 > N_2 > N_1$) - thus it is advisable to take smaller $\frac{\omega}{q}$, larger Δ and smaller W_0 (smaller $\Delta q \propto \frac{W_0}{q}$).

8. The dot-dash line named by the Russian letter $\mathfrak{D}-\mathfrak{D}$ represents the variation of the economic loading conditions $\frac{\omega}{q}$ and Δ_0 ; this line passes a little lower than the point M_0 at the ordinate corresponding to Δ_{ma} - the most advantageous density of loading.

9. The characteristic $\eta_\omega = \frac{2 \cdot V_0^2}{\omega \cdot L_g} = \frac{(\frac{V_0^2}{L_g})}{(\frac{\omega}{2})}$ can be represented by straight lines parallel to Δ - axis marked by the various values of $(\frac{\omega}{q})$.

10. Functional variations of $\eta_0 = \frac{R_v}{R_m} = \frac{2 \cdot V_0^2}{2g W_0 R_m}$ can be traced along the straight lines representing equal volumes $\frac{W_0}{q}$; in both points of intersections of this straight line with the counter corresponding to a

constant ($\frac{W_c}{q}$) we will have also equal $W_d = W_c - W_0$ or equal λ_d . If we draw a perpendicular from the point M_0 on the straight line of equal W_0 we will mark there a point (k on the Fig. 163) which will represent the minimum W_c with the minimum W_d and the maximum of λ_d . It can be admitted as a general rule that within the region to the right and down from the straight line OM_0 any point which is moved closer to the point M_0 will have a smaller $\frac{W_c}{q}$, a larger $\frac{W_0}{q}$ and a larger ratio $\frac{E_d}{P_d W_d}$.

2. A General Outline of the Practical use of the Directive Diagram.

It is obvious that at the very beginning of the application of the directive diagram we should entirely eliminate its zone to the right and above the line $\lambda_K = 0.80$, because $\lambda_K = 0.80$ means that the powder burning very likely will not be ended inside the bore. Next, the entire zone to the left of and above the straight line OM_0 should be also rejected as impracticable because this zone refers to very large W_0 and very small λ_d . Thus the only practical zone for our exploration is a sector with its apex at the point O and enclosed between the straight line OM_0 and the line $\lambda_K = 0.8$. Even

within this sector it is more advisable to stay within the part to the right from the ordinate $\Delta_N = 0.62 - 0.71$ for pressures $p_m \sim 2500-3200 \text{ kg/cm}^2$. For the tubular powders $\Delta \geq 0.75$ is practically the limit of usable densities of loading. For 7 - perforation grain powder and for small arms it is possible to use $\Delta \sim 0.80-0.90$. At the higher $p_m > 3500$, the most advantageous Δ_N is still higher than 0.75 which is unattainable for the tubular powders and then it is necessary to move from the above outlined zone into the sector to the left from the ordinate Δ_N using lower densities of loading and larger W_0 , smaller B and shorter time of the burning of the powder; here Δ_N may be as low as 0.40. This zone can be used for the design of howitzers, when the full charge produces $\Delta_N \sim 0.25-0.30$ and even at the small charges the complete burning within the bore will be assured.

The following thirteen pages (pp. 487-500) in the book describe in detail several practical examples of the use of the directive diagram and calculations of several variants of the same gun design.

Chapter IV. Additional Information.

1. How the Variations of the Maximum Pressure p_m Affect the Constructional Data of the Gun and the Loading Conditions.

From:
$$v_2 = \sqrt{\frac{2s}{\varphi m} \int p d\ell}$$

we may say that the same v_2 (the same area $\int p d\ell$) can be obtained at the higher p_m and shorter travel ℓ i.e. in a shorter gun. Therefore if we are interested in having a shorter gun with the same muzzle velocity v_2 we have to increase p_m , and with the increased p_m all densities of loading Δ , Δ_c , Δ_{ma} , Δ_v will also be increased. Fig. 164 shows how W_c and W_o vary as functions of Δ at given v_2 and with varying p_m .

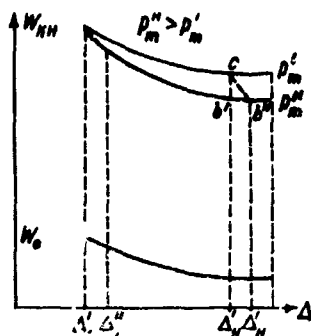


Fig. 164 W_c and W_o as functions of Δ at various p_m ($p_m^H > p_m^N$)

At the increased ρ_m the ordinates of curves W_c and W_e are decreased. The following conclusions can be drawn from Fig. 164:

1. The increase of ρ_m at the same value Δ (point C' moves into point C'') will affect (decrease) the volume W_e (its length too) not as much as the increase of ρ_m made with the increased Δ (point C' moves into point C'').
2. The increase of ρ_m will decrease not only the length of the canal but also the value of A_2 i.e. the relative volume of chamber will be increased.
3. The product $\rho_m W_c$ remains nearly a constant; therefore we may write: $\frac{W_c''}{W_c'} = \frac{A_1'}{A_2'}$ and: $\frac{L_c''}{L_c'} = \frac{\rho_m'}{\rho_m''}$ and also $\frac{C_2''}{C_2'} = \frac{\Delta'}{\Delta''}$ which are relationships very helpful for the ballistic design. If on designing the gun with the minimum volume, the obtained length is larger than a given length - then the only means to secure a desired length will be the increase in ρ_m .

2. How the Characteristics of the Powder Affect the Loading Conditions and the Constructional Data of a Designed gun.

The nitroglycerine powders, being more powerful than the pyroxylin powders, have a higher temperature of burning

which fact largely affects "the life" of a gun. Special "cold powders" (nitroguanidine) have been designed which have lower temperature of burning and smaller f . All the tables are constructed for the pyroxylin powders and it is sometimes highly desirable to evaluate a possible deviation from the tabulated data if other kinds of powders are used. The following characteristics of powders are taken into consideration: f, α, θ . The rate of burning u , is included in the value of $I_{\alpha} = \frac{c}{u}$. Only four types of powders are compared, and the pyroxylin powder is taken as the standard type.

Comparative Table of Powders

No	Powder	$f \frac{Cons}{mg.}$	α	θ	$\frac{f}{f_s} \%$
1	Nitroguanidine	86.5	1.10	0.220	91%
2	Pyroxylin	95	1.00	0.200	100%
3	Nitroglycerine (medium)	105	0.905	0.181	110.5%
4	Nitroglycerine (powerful)	115	0.825	0.165	121.0%

Table of Comparative Values of Ballistic Characteristics Obtainable with Four Types of Powders for the Gun of the Minimum Volume.

№	Characteristics	Powders			
		1	2	3	4
1	"Force" f	31	100	110.5	121.0
2	Temperature of Burning \bar{T}_1	65	100	122	146
3	Parameter of loading B	98.3	100	101.6	103
4	The most advantageous density of loading Δ_{ma}	97	100	102.2	103.7
5	Optimum efficiency η'_0	111.2	100	89.2	80.6
6	Optimum relative charge ($\frac{G}{L}$)	110.7	100	90.1	81.3
7	Chamber volume W_0	114.1	100	88.2	78.4
8	Number of volumes of expansion Λ_2	91.8	100	108.3	117.4
9	Length of travel ℓ_2	104.7	100	95.2	92.0
10	Canal volume W_c	107	100	93.3	88.6
11	Travel at the end of burning ℓ_K	99.5	100	101.5	101.0
12	Impulse of pressure I_K	100.6	100	99.6	99.2
13	$\eta_K = \frac{\Lambda_K}{\Lambda_2} = \frac{\ell_K}{\ell_2}$	94.8	100	105.8	109.8
14	Pressure at the muzzle p_2	93.4	100	107.4	112.4
15	Coefficient of the utilization of the unit of charge η_w	90.8	100	110.7	122.7
16	Coefficient φ	102	100	98.1	96.4
17	Temperature of gases at the muzzle	79	100	126	155
18	$\eta = \frac{p_{ex}}{p_m}$	97.5	100	102.9	104.7
19	Safe number of firings N	209	100	37.8	12.6

Since the ballistic design usually begins with the calculations of the gun with the minimum volume (the initial point N_0 at the directive diagram), all the above shown deviations were calculated for the gun of minimum volume. But it is important to remember that the gun with minimum volume can be recommended only for cases of high muzzle velocity (1500 $\frac{\text{m}}{\text{sec}}$). In cases of lower muzzle velocities we should consider guns with the smaller ω and smaller W_0 i.e. to explore that sector of the directive diagram which is to the right and down from the central point N_0 (minimum volume gun). But even in these cases the above Table still can be used when a considered powder is different from the powder taken in CAB Tables and when the analyzed variant of a gun has not minimum volume. (CAB means Chief Artillery Board)

3. The Relationship Between the Weight of the Barrel of Gun and its Constructional Details at a given V_0 and ρ_m .

In some cases the weight of the barrel Q_b may serve as a criterion in selecting the proper variant. Hence it is desirable to know how Q_b is affected by the variations of the constructional elements of a gun or by the loading conditions. Fig. 165 shows 3 guns differing by their N_0 at the same V_0 and ρ_m . Our problem is to

find how Q_c will vary with Λ_2 . Fig. 166 gives a schematic view of a gun barrel (axial section).

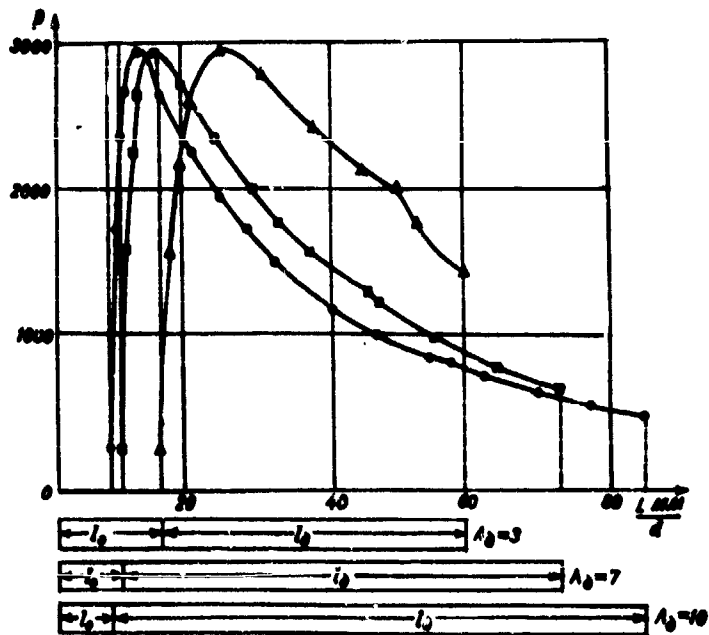


Fig. 165 Three ϵ is differing by their Λ_2 , at the same U_2 and p_m .

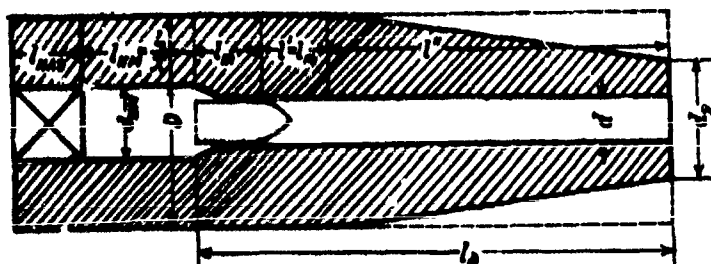


Fig. 156 Schematic view of a gun barrel (axial section)

Here we have: D - the outer diameter of the cylindrical breech part.

d_2 - the outer diameter of the muzzle

d - caliber of bore

d_c - the average diameter of chamber

$l_{br} = l_{br}$ - the length of breech part;

$l_{ch} = l_c$ - the length of chamber, ($l_c = \frac{l_c}{2}$,
 l_c - effective length of chamber)

l_m - travel of the projectile to the moment of p

l' - a margin for a possible shift of p toward the muzzle ($l' \approx 0.5 l_c$)

l'' - length of the conical part of barrel; $l'' = l_c - (l' + l_m) \approx l_c - 1.2 l_c$

ρ' - density of steel = 7.85 kg/dm^3 .

The weight of the barrel will be:

$$Q_b = \delta \left\{ \frac{\pi}{4} D^2 (l_1 + l_2 + l_3 + l_4) + \frac{1}{8} \cdot \frac{\pi}{4} (D_1^2 D d_1 + d_1^2) l_2 - \frac{\pi}{4} d^2 (l_1 + l_2) \right\}$$

Denoting $Q_{b_1} = \frac{\pi}{4} D^2 l_1 \delta$ - the weight of the breech part;

$A = \frac{D}{d}$ and $a_1 = \frac{d_1}{d}$ and dividing by d^3 we will have:

$$\frac{Q_b}{d^3} = \frac{Q_{b_1}}{d^3} + \delta \frac{\pi}{4} \frac{l_2}{d^3} \left\{ \left(\frac{1}{2} + 1 \right) A^2 + \frac{1}{8} (A^2 A a_1 + a_1^2) (A_2 - 1) - (1 + A_2) \right\}$$

dividing by $C_1 = \frac{\pi}{4}$ we have:

$$\frac{Q_b}{d^3} = \frac{Q_{b_1}}{d^3} + \delta \frac{\pi}{4} \frac{l_2}{d^3} \left\{ \left(\frac{1}{2} + 1 \right) A^2 + \frac{1}{8} \left(1 + \frac{a_1}{A} + \frac{a_1^2}{A^2} \right) A^2 (A_2 - 1) - (1 + A_2) \right\} \quad (127)$$

Here: $A = \frac{D}{d}$ is a function of R_m .

$a_1 = \frac{d_1}{d}$ is a function of R_m which in its turn is a function of R_m and A_2 .

In the following three tables we have $\left(\frac{R_m}{R} \right)$, $\left(\frac{a_1}{A} \right)$ and A as functions of R_m and A_2 . We assume the coefficient of safety 1.33 and the elastic stress $\sigma_e = 6000$ kg./cm².

Since $l_1 = 1.5d$ then: $Q_{b_1} = \frac{\pi}{4} D^2 (1.5d) \delta$

and: $\frac{Q_{b_1}}{d^3} \approx 10A^2$

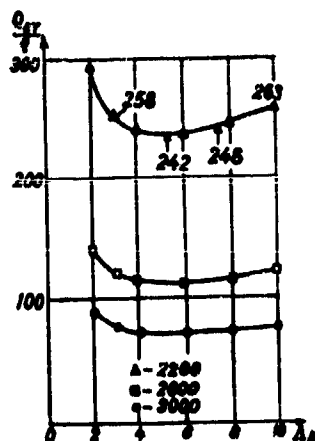


Fig. 167 Curves $(\frac{Q}{q}, \Lambda_2)$ at various P_m
 The upper curve - $P_m = 2200$; the middle curve $P_m = 2600$
 The lower curve - $P_m = 3000$. All curves have the
 minimum at $\Lambda_2 \approx 5 - 6$.

In (127) the relative weight of barrel $(\frac{Q}{q})$ is expressed in terms of the ballistic characteristics $\frac{W}{q}$, Λ_2 , χ , A and $\frac{a_i}{A}$ which are functions of P_m , Λ_2 and Λ_1 . The calculated results from this formula for the pressures P_m taken for 2200, 2600 and 3000 kg/cm² show in Fig. 167 how $(\frac{Q}{q})$ varies with Λ_2 with the pronounced minimum for all three curves at $\Lambda_2 \approx 5 - 6$.

This means that $\Lambda_2 = 5 - 6$ should be selected for the design of the barrel with the minimum weight.

500

Table for $A = \frac{D}{L} = f(\rho_m)$

ρ_m	1800	2200	2600	3000	3600
A	1.68	2.00	2.56	3.79	5.10

Table for $\frac{A}{L} = f_2(\rho_m, A_2)$
at the Economic Loading Conditions.

A_m	$A_2 = 3$	4	6	8	10
1800	0.543	0.451	0.323	0.244	0.208
2200	0.545	0.445	0.305	0.237	0.198
2600	0.521	0.430	0.290	0.220	0.185
3000	0.500	0.405	0.271	0.207	0.172
3600	0.465	0.373	0.250	0.189	0.154

Table for $\frac{A}{L} = \frac{A_2}{D} = f_2(\rho_m, A_2)$

ρ_m	$A_2 = 3$	4	6	8	10
1800	0.774	0.738	0.696	0.667	0.660
2200	0.690	0.650	0.600	0.570	0.560
2600	0.563	0.539	0.477	0.463	0.442
3000	0.396	0.368	0.328	0.312	0.301
3600	0.314	0.285	0.249	0.236	0.228

4. On the Use of Various Ballistic Tables

We have five types of ballistic tables which can be used in the calculating procedure of the ballistic design:

- 1) Tables of Prof. Drosdov for the strip powders ($\lambda=1.06$) and "normal" constants (DRO)
- 2) Tables of the Artillery Scientific Research Institute with the same constants (ASRI)
- 3) Tables of the Chief Artillery Board (CAB) with $\lambda = 1$, $\varphi = 1$.
- 4) Tables of the Chair of Interior Ballistics (CIB) for the powders with constant surface of burning ($\lambda = 1$); ($\lambda \neq 0$) for any f and φ .
- 5) Tables of M. G. Gorokhov [17] for $\lambda = 1.06$ and $\lambda = 1.00$ with "normal" constants (GOR)

The most suitable tables for ballistic design are Tables (CAB) and (GOR). The practical use of any kind of table begins with the selection of the proper coefficient of conformity between the calculated results and experimental data. This can be done by the calculation of the results of firing tests made with the types of gun similar to the designed systems and already used in field service.

Such work has been done with the ten different types of our guns firing with the small relative charges ($\frac{w}{Q} < 0.20$) and the results show that a good conformity with the experimental v_s and ρ_m can be obtained with the use of the (ASRI) Tables with $\varphi = 1.05$. With the use of $\varphi = 1.03 + \frac{1}{3} \cdot \frac{w}{Q}$ with due corrections at given ρ_m all the calculated v_s are 3% lower than experimental.

Thus despite that fact that (ASRI) Tables are constructed for the strip powders ($\chi = 1.06$) and the tested systems all have used the tubular powders or 7-perforation grain powders, which are much more progressive than the tubular powders - still our assumption for $\frac{w}{Q} \leq 0.2$, that the coefficient $\varphi = 1.05$ which is smaller than the actual φ , has compensated the depressiveness of the strip powders and the obtained calculated results of v_s turned out to be close enough to the experimental values (Only 3% less).

Note. If using (ASRI) Tables at $\frac{w}{Q} \leq 0.2$ we take the theoretical value $\varphi = a \cdot \frac{1}{3} \cdot \frac{w}{Q}$ where $a = 1.03 - 1.06$, and $v_s = v_{s, \text{calc}} \sqrt{\frac{w}{Q} \cdot \frac{1.05}{\varphi}}$ then at v_s calculated and equal to its experimental value we will have ρ_m calculated about 10% higher than its experimental value. Only for $\frac{w}{Q} > 0.2$

when $\varphi = 1.05$ markedly deviates from $\varphi = a + \frac{1}{3} \frac{\omega}{q}$ do we have to use corrections for φ , and in this case the differences in powders, calling for some compensation by lowering the value of φ , will make the reduction in the coefficient b necessary by taking it smaller than $1/3$. In the constructional bureaus formula $\varphi = 1.05 (1 + \frac{1}{4} \cdot \frac{\omega}{q})$ is used which at larger $\frac{\omega}{q}$ gives φ , which is smaller than $(1.03 + \frac{1}{3} \frac{\omega}{q})$. It should be remembered that the numerical value of φ affects the constructional elements of the barrel--its length and length of travel of projectile (L_c and l_2).

A general comparison of the four tables (DRO), (ASRI), (CAB) and (GOR) shows that at given Δ and β_m the calculated B and Λ_k are all different:

$$B(\text{DRO}) < B(\text{ASRI}) < B(\text{GOR}) < B(\text{CAB}) \text{ and}$$

$$\Lambda_k(\text{DRO}) < \Lambda_k(\text{GOR}) < \Lambda_k(\text{CAB}) < \Lambda_k(\text{ASRI}).$$

The practical result of this divergency is that, at given U_2 and at equal φ or b we will have different values for l_2 and L_c and the higher is U_2 the greater are these differences. We will have the minimum values of l_2 and L_c with tables (DRO); the maximum values of l_2 and L_c with tables (ASRI). At $U_2 = 1000$ m/s the difference will be about 2% but at $U_2 = 1500$ m/sec the difference will be 7-8%.

At equal Δ or equal B the (CAB) tables give larger values ρ_m than the tables (DRO) and this difference is increased with Δ . For example: at $\Delta = 0.50$ and at equal B we have ρ_m (CAB) - ρ_m (DRO) = 2%; at $\Delta = 0.60$ this difference is 2-1/2 - 3%; at $\Delta = 0.70$ this difference 4 - 5% and at $\Delta = 0.80$, this difference is 5 - 6%. Such a divergency is markedly too large to be explained by the difference in assumed values of α : - in (CAB) tables $\alpha = 1.0$; in (DRO) tables $\alpha = 0.98$. The (ASRI) tables give ρ_m very close to ρ_m of (DRO) tables and the (GOR) tables have ρ_m about 1 - 2% lower than ρ_m in (CAB) tables.

From the (GOR) tables calculated for $\mathcal{N} = 1.06$ and $\mathcal{N} = 1.0$ we may observe that with the change of \mathcal{N} from 1.06 to 1.00 at given Δ and B , the pressure ρ_m is decreased at about 4 - 6% and the larger are Δ and B , the larger is this difference in ρ_m .

At any rate it should be remembered that any tables calculated even on the basis of the mathematically rigorous method are always in some disagreement with the experimental results simply because a theoretical approach to the solution cannot take into account all the details of the process of firing. Every purely

mathematical solution is nothing but an approximation to reality which of course is always more complex than any assumed scheme as a description of the phenomenon under observation. Hence there is the necessity for a proper selection of a certain conversion factor, "a coefficient of conformity" between the theory and experiment. This coefficient can be found by the comparing the calculated results of the firing tests made with guns akin to the prospective designed gun with results obtainable from tables or a table applied to guns which are already in the field service. Then the calculated deviations are likely to be observed in the case of the designed gun.

For pyroxylin powders the best conformity with the experiments can be realized by the proper adjustment of the coefficient b in the formula: $\varphi = a + b \cdot \frac{u}{l}$

We have seen above that at equal φ and b for a given P_m and $U_s = 1500$ m/sec. the (ASRI) Tables give l_2 larger than l_2 found in (DRO) tables and this deviation is about 7 - 8%.

But it is possible to obtain the equal l_2 from both these tables by the adjustment of the coefficient φ or b , and this adjustment may be different for different

cases; i.e. if in one case for tables (DRO) $b = 1/3$ and in another case $b = 1/5$, then in the (ASRI) tables for the first case $b = 1/4$ and for the second case $b = 1/6$.

Now it will be shown how to find the coefficient b from Tables.

5. The Calculation of the Coefficient b from the Tables.

The coefficient a in the formula $\varphi = a + b \frac{\omega}{q}$ is assumed to be 1.03 for the powerful guns, 1.04 - 1.05 for the guns of medium power, 1.06 - 1.05 for howitzers and 1.10 for small arms. The coefficient b should be evaluated from the experimental data.

From (CAB) Tables we have: $(v_{\lambda})_{exp.} = (v_{\lambda})_{calc.} \sqrt{\frac{c\omega}{q\varphi_{exp.}}}$

From (ASRI) Tables we have: $(v_{\lambda})_{exp.} = (v_{\lambda})_{calc.} \sqrt{\frac{\varphi}{q} \cdot \frac{1.05}{\varphi}}$

Hence: From (CAB) Tables: $\varphi_{exp.} = \frac{(v_{\lambda})_{calc.}^2}{(v_{\lambda})_{exp.}^2}$

From (ASRI) Tables: $\varphi_{exp.} = 1.05 \frac{(v_{\lambda})_{calc.}^2}{(v_{\lambda})_{exp.}^2}$

Because: $(v_{\lambda})_{calc.} = (v_{\lambda})_{calc.} \sqrt{\frac{\omega}{q}}$ and: $(v_{\lambda})_{calc.} = (v_{\lambda})_{calc.} \sqrt{\frac{q}{\omega}}$

Knowing $\varphi_{exp.}$ we will have: $b_{exp.} = \frac{\varphi_{exp.} - a}{(\frac{\omega}{q})}$

6. How the Calculated Λ_2 and ϵ_2 are Affected by the Variations in φ and ϵ ?

From (119) we have (remembering that $r' = \frac{v_2^2}{2f} = \varphi \cdot r_2$):

$$(\Lambda_2 + 1 - \alpha \Delta) = \frac{(\Lambda_2 + 1 - \alpha \Delta) [1 - \frac{Q^2}{2} (1 - \alpha \Delta)]^{\frac{1}{2}}}{(1 - r')^{\frac{1}{2}}} = \frac{K}{(1 - r')^{\frac{1}{2}}} = \frac{K}{(1 - \varphi r_2)^{\frac{1}{2}}}$$

Here K = Constant at given Δ and $\frac{Q^2}{2}$.

Differentiating this equation with respect to φ :

we have:

$$d\Lambda_2 = \frac{K}{\theta} \cdot \frac{r'}{(1 - r')^{\frac{3}{2}}} \cdot \frac{d\varphi}{\varphi} \dots (129)$$

Now:
$$\frac{d\Lambda_2}{\Lambda_2 + 1 - \alpha \Delta} = \frac{1}{\theta} \cdot \frac{r'}{(1 - r')^{\frac{3}{2}}} \cdot \frac{d\varphi}{\varphi} \dots (130)$$

From $\epsilon = \frac{\varphi - a}{(\frac{Q^2}{2})}$ we have:
$$\frac{d\epsilon}{\epsilon} = \frac{d\varphi}{\varphi} \dots (131)$$

Hence:
$$\frac{d\varphi}{\varphi} = \frac{\varphi - a}{\varphi} \cdot \frac{d\epsilon}{\epsilon} \dots (132)$$

Now from (130):
$$\frac{d\Lambda_2}{\Lambda_2 + 1 - \alpha \Delta} = \frac{1}{\theta} \cdot \frac{r'}{1 - r'} \cdot \frac{a}{\epsilon} \cdot \frac{d\epsilon}{\epsilon}$$

Here: $r' = \frac{K_v \varphi}{(\frac{Q^2}{2})}$; $K_v = \frac{\theta}{f} \cdot \frac{v_2^2}{\lambda_g}$

and finally:
$$\frac{d\Lambda_2}{\Lambda_2 + 1 - \alpha \Delta} = \frac{K_v}{\theta} \cdot \frac{d\epsilon}{1 - r'} = \frac{v_2^2}{2gf} \cdot \frac{d\epsilon}{(1 - r')}$$

Thus the influence of δ is increased with u .

All the above shown relationships only confirm the necessity of a better adjustment of the coefficient ϵ_n by means of firing tests from guns which are similar in type, constructional details and in their service with the designed gun. This requirement becomes particularly important when higher velocities u are involved. Only by following this method in the design of a new gun can we expect results which will be in good agreement with the practice of the artillery service.

PART III - Solution of the More Involved Problems of Interior Ballistics

Section XI - Solution for Composite Powder Charges

1. General Information

It happens very often in artillery practice that a powder charge must be composed of two different sorts (physically as well as chemically) of powder. Such cases can be found in firing practice from howitzers or at the proving ground when such a combination of ρ and ρ_n is desired which cannot be realized by using ordinary charges.

The ballistic design is usually made for the maximum U_0 and for the full charge (N^0Q) and for the lowest U_n and its charge ($N^n n$). This number of velocities or charges is determined by special requirements largely of a tactical character. The minimum ρ_n for the smallest charge is determined from the technical conditions of a dependable action of the mechanisms of the detonators or time-fuses. All the densities of loading are taken within the range from $\Delta = 0.10 - 0.15$ to $\Delta = 0.40 - 0.60$. Interior ballistics provides the relative weights of components for every charge.

2. Characteristics of the Composite Charges.

Suppose we have a charge ω_{α_1} of α_1' of a powder with a small web $2e'$, and ω_{α_2} of a powder with a larger web $2e''$. Then we may write: $\omega' + \omega'' = \omega$

$$\frac{\omega'}{\omega} = \alpha' ; \frac{\omega''}{\omega} = \alpha'' ; \alpha' + \alpha'' = 1$$

The characteristics of these powders are as follows:

thin powder: $\omega' ; \alpha' ; 2e' ; u' ; \frac{E'}{u'} = I_{\alpha}' ; x' ; \lambda' ; f'$

thick powder: $\omega'' ; \alpha'' ; 2e'' ; u'' ; \frac{E''}{u''} = I_{\alpha}'' ; x'' ; \lambda'' ; f''$

As the first approximation f for a composite charge can be taken: $f = \alpha' f' + \alpha'' f'' \dots (1)$

A more accurate value will be: $f = \alpha' f' \psi + \alpha'' f'' \psi'' \dots (1')$

in which the amounts of the burned powders (varying composition of gases) is considered. For pyroxylin powders

f' and f'' are always very close each to other and formula (1) can be used. For every powder during their compatible burning we have: $de' = \rho dt u' ; de'' = \rho dt u''$

and $\int \rho dt$ is the same for both powders.

Hence: $\frac{E'}{u'} = \frac{E''}{u''} = I$ will be taken as an independent variable.

During the burning ψ a burned fraction of the whole charge ω will be: $\psi = \frac{\omega' f' + \omega'' f''}{\omega} = \alpha' \psi' + \alpha'' \psi'' \dots (2)$

A general expression for $\psi = \kappa Z + \kappa \lambda Z^2$ can be rewritten if instead of Z we use $Z = \frac{I}{I_K}$

$$\frac{\kappa}{I_K} = \kappa \quad \text{and} \quad \frac{\lambda}{I_K} = \mathcal{N}$$

Then:

$$\psi = \frac{\kappa}{I_K} I + \frac{\kappa}{I_K} \cdot \frac{\lambda}{I_K} I^2 = \kappa I + \kappa \mathcal{N} I^2 \dots (3)$$

For the component ω' : $\psi' = \kappa' I + \kappa' \mathcal{N}' I^2 \dots (3')$

$$\text{here: } \kappa' = \frac{\kappa'}{I_K'} ; \mathcal{N}' = \frac{\lambda'}{I_K'}$$

For the component ω'' :

$$\psi = \kappa'' I + \kappa'' \mathcal{N}'' I^2 \dots (3'')$$

$$\text{here: } \kappa'' = \frac{\kappa''}{I_K''} ; \mathcal{N}'' = \frac{\lambda''}{I_K''}$$

Now (2) will be: $\kappa I + \kappa \mathcal{N} I^2 = \alpha' (\kappa' I + \kappa' \mathcal{N}' I^2) + \alpha'' (\kappa'' I + \kappa'' \mathcal{N}'' I^2)$

$$\text{or: } \kappa I + \kappa \mathcal{N} I^2 = (\alpha' \kappa' + \alpha'' \kappa'') I + (\alpha' \kappa' \mathcal{N}' + \alpha'' \kappa'' \mathcal{N}'') I^2$$

Hence:

$$\kappa = \alpha' \kappa' + \alpha'' \kappa'' \dots (4)$$

$$\kappa \mathcal{N} = \alpha' \kappa' \mathcal{N}' + \alpha'' \kappa'' \mathcal{N}'' \dots (5)$$

Therefore the values of f , ψ , κ and $\kappa \mathcal{N}$ for the composite charge are obtained by applying an ordinary rule of evaluation of characteristics of any mixture of the two components.

From (2) by differentiating we have:

$$\frac{d\psi}{dI} = \alpha' \frac{d\psi'}{dI} + \alpha'' \frac{d\psi''}{dI} ; \frac{d\psi}{dI} = \frac{d\psi}{pdc} = f'$$

Hence:

$$P = \alpha' P' + \alpha'' P'' \quad (6)$$

but: $P' = \frac{x'}{I_K} \sigma'$; $P'' = \frac{x''}{I_K} \sigma''$; $P = \frac{x}{I_K} \sigma$

and for our composite charge finally we have:

$$\frac{x}{I_K} \sigma = \alpha' \frac{x'}{I_K} \sigma' + \alpha'' \frac{x''}{I_K} \sigma'' \dots (7)$$

For the beginning of burning: $\sigma' = \sigma'' = \sigma = 1$

For the powders with the same form of grain: $x' = x''$

Then (7) will be: $\frac{x}{I_K} = \alpha' \frac{x'}{I_K} + \alpha'' \frac{x'}{I_K}$

or: $x(\frac{1}{I_K}) = x'(\frac{1}{I_K} \alpha' + \frac{1}{I_K} \alpha'')$

At $x = x'$ we will have:

$$\frac{1}{I_K} = \frac{\alpha'}{I_K'} + \frac{\alpha''}{I_K''} \dots (8)$$

$$\text{and } I_K = \frac{I_K' I_K''}{\alpha' I_K'' + \alpha'' I_K'} = \frac{I_K'}{\alpha' + \alpha'' \frac{I_K'}{I_K''}} = \frac{I_K''}{\frac{\alpha'}{I_K'} + \alpha''} = \frac{I_K''}{\frac{1}{I_K}}$$

which means that the impulse I_K in this case is evaluated not from an ordinary formula for the mixture of

I_K' and I_K''

$$I_K = \alpha' I_K' + \alpha'' I_K'' \dots (9)$$

but as if the mixture were made of $(\frac{1}{I_K'})$ and $(\frac{1}{I_K''})$

I_K calculated from (9) will give a higher ρ_m than

calculated from (8), and formula (9) for a long time was used in practice.

3. Graphical Interpretation of the Curve (ψ, I) in Case of Composite Charges.

In the coordinates ψ and I , the function Γ is a tangent of the angle γ of the slope of the curve (ψ, I) to the I -axis. For the powders with the constant surface of burning this angle γ is constant:

$$\tan \gamma = \frac{1}{I_K}$$

For the composite charges:

we had:
$$\frac{1}{I_K} = \alpha' \left(\frac{1}{I_K'} \right) + \alpha'' \left(\frac{1}{I_K''} \right) \dots \dots (8)$$

and I_K should be determined from:
$$I_K = \frac{I_K' I_K''}{\alpha' I_K'' + \alpha'' I_K'}$$

geometrically (8) is represented by:

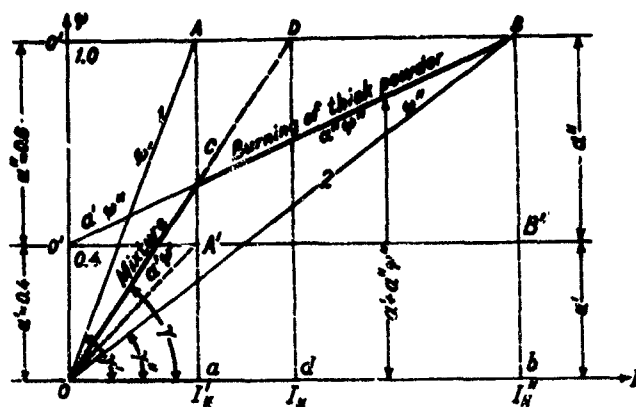


Fig. 168 Shows the burning of a composite charge (two powders of different thicknesses).

Line OC-burning of the mixture: Line CB-burning out of the thicker powder. A straight line 1 (angle γ') represents the burning ψ' of 0.4ω of the powder with a smaller web and impulse I_K' . Another straight line 2 (angle γ'') represents the burning ψ'' of 0.6ω of the powder with a larger web and impulse I_K'' . The height OO'' of the diagram is subdivided at point O' in the two parts: $OO' = 0.4(OO'')$ and $O'O'' = 0.6(OO'')$. $\alpha' = 0.4$;

$\alpha'' = 0.6$; $\alpha' + \alpha'' = 1$. Then the straight line OA' gives the first part of the sum $\psi = \alpha'\psi' + \alpha''\psi''$ namely $\alpha'\psi'$ and the straight line $O'B$ (ordinates measured from the straight line $O'B'$) gives the item $\alpha''\psi''$. Thus the sum $\psi = \alpha'\psi' + \alpha''\psi''$ is obtained by the straight line OC representing the summary burning of both parts of a charge $\omega = \alpha'\omega + \alpha''\omega$. The

point C is the end of burning of $\alpha'\omega$; $OC = I_K'$

$$\alpha C = \alpha' + \alpha'' \frac{I_K''}{I_K'} = I_K' \left(\frac{\alpha'}{I_K'} + \frac{\alpha''}{I_K''} \right) = \frac{I_K'}{I_K'} = \psi_K'$$

We have: $\frac{\alpha C}{Oa} = \frac{OA'}{Oa} + \frac{A'C}{Oa} = \frac{\alpha'}{I_K'} + \frac{\alpha''}{I_K''}$; $\tan \gamma = \frac{\alpha C}{Ja} = \frac{1}{I_K} = \frac{\alpha'}{I_K'} + \frac{\alpha''}{I_K''}$

$$\frac{\psi_K'}{I_K'} = \frac{1}{I_K'} ; \frac{\alpha C}{Oa} = \frac{\psi_K'}{I_K'} = \frac{1}{I_K}$$

After point C the burning proceeds along CB' for which

$$\gamma = \alpha' + \alpha'' \gamma'' \quad \text{At the point B we have:}$$

$$OB = I_K''$$

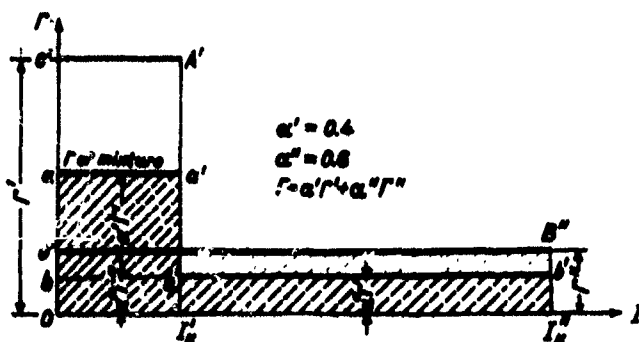


Fig. 139 Graphical representation of (Γ, I) for a mixture of 2 powders: $\alpha' = 0.4$; $\alpha'' = 0.6$; $\Gamma = \alpha'\Gamma' + \alpha''\Gamma''$

Here Γ' is represented by the ordinates of $O'A'$ and

Γ'' by the ordinates of $O''B''$ and $\int_0^{I_N} \Gamma dI = 1$

Since $\Gamma = \text{Const.}$ we have: $\Gamma' I_N' = 1$ and $\Gamma'' I_N'' = 1$

Area $Oaa'a''b''I_N''$ (the intensity of burning for the composite charge) is equal to \int as in the case of burning of an ordinary charge.

According to the formula (6): $\Gamma = \alpha'\Gamma' + \alpha''\Gamma''$

this is the straight line aa' on the Fig. 139. At the point $I = I_N'$ the line aa' is replaced by the line $b'b''$ representing the intensity of gas formation of the remaining part of the thick powder.

4. Analytical solution. (Prof. G. Oppokov)

The simplest case of the two degressive powders of the same chemical composition will be considered. The first phase (as long as the whole charge of the powder with the smaller web is burned out) is characterized by the equation: $\psi = \chi Z'' + \chi \lambda Z''^2$

1. The characteristics χ and $\chi \lambda$ are determined by:

$$\chi = \alpha' \frac{Z'_N}{Z'_N} + \alpha'' \chi''; \quad \chi \lambda = \frac{\chi' \lambda'}{Z'_N} \alpha' + \chi'' \lambda'' \alpha''$$

here: $Z'_N = \frac{I'_N}{I'_N}; \quad \alpha' = \frac{\psi'}{\psi}; \quad \alpha'' = \frac{\psi''}{\psi}$

2. The values of Z_0 and I_N are replaced by Z_0'' and I_N''

here: $Z_0'' = \frac{\psi_0}{\chi} = \frac{\psi_0}{\chi' \left(\frac{Z'_N}{Z'_N} + \alpha'' \right)}$

3. $X = Z'' - Z_0''; \quad X_{N'} = Z_{N'}'' - Z_0'' = Z_{N'}' - Z_0''$

4. At the end of the first phase: $Z_{N'}'' = \frac{Z'_N}{Z'_N}; \quad X_{N'} = Z_{N'}'' - Z_0''$

$$\psi_{N'}' = \frac{3I_{N'}''}{\varphi m} \cdot X_{N'} = \psi_{N_0} X_{N'}$$

The second phase (the burning out of the remaining part of the thick powder)

The same differential equation:

$$\frac{d\ell}{dx} = \frac{Bx(\ell_p + \ell)}{\psi - \frac{3I}{\varphi} x^2} \dots (10)$$

and $\psi = \psi_{0N} X$ are valid

and the equation of the gas formation will be:

$$\psi = \frac{\omega''}{\omega} + \frac{\omega''}{\omega} x'' z'' (1 + \lambda'' z''); \text{ at } x'' = z_0'' + x$$

we will have: $\psi = \psi_0 + K_{12} x + \left(\frac{\omega''}{\omega} x'' \lambda''\right) x^2$

where: $\psi_0 = \frac{\omega''}{\omega} + \left(\frac{\omega''}{\omega} x''\right) z_0'' + \left(\frac{\omega''}{\omega} x'' \lambda''\right) z_0''^2$

and: $K_{12} = \frac{\omega''}{\omega} x'' + 2 \left(\frac{\omega''}{\omega} x'' \lambda''\right) z_0'' = \frac{\omega''}{\omega} x'' (1 + 2 \lambda'' z_0'') = \frac{\omega''}{\omega} x'' Q''$

Thus we see that the law of the gas formation is analogous to the same law used for the first phase which means that for the second phase instead of B we will have $B_2 = \frac{BQ}{2} - \frac{\omega''}{\omega} x'' \lambda''$ and $C_2 = \frac{B}{K_{12}}$ instead of C .

Then the tabular parameters will be: $\beta = C_2 x$

and $\gamma = \frac{C_2 \psi_0}{K_{12}}$

The differential equation: $\frac{d\ell}{dx} = \frac{Bx(\ell_0 + \ell)}{\psi_0 + K_{12}x - B_2x^2} \dots (11)$

and here for the beginning of the second phase $\ell = \ell_{K1}$
and the initial $\beta_0 = C_2 x_{K1}$

Thus after integration we will have:

$$\log \left(\frac{\ell_{K1} + \ell}{\ell_{K1} + \ell_0} \right) = \int_{x_{K1}}^x \frac{Bx dx}{\psi_0 + K_{12}x - B_2x^2} = \frac{B}{B_2} \int_{\beta_0}^{\beta} \frac{\beta d\beta}{\gamma + \beta - \beta^2} \dots (12)$$

Here: $l_{av.} = l_{\Delta} - a \psi_{\Delta}$ and $\psi_{av.} = \frac{\psi_{K_1} + \psi}{2}$

and $\psi_{K_1} = \chi Z_{K_1}'' + \chi \lambda Z_{K_1}''^2 = \psi_0 + K_1 x_{K_1} + \chi \lambda x_{K_1}^2$

The integral in the right part of (12) will be:

$$\frac{B}{B_2} \int_{\beta_{K_1}}^{\beta} \frac{\beta d\beta}{\beta + \beta - \beta^2} = \log_e \left(\bar{Z}^{\frac{B}{B_2}} Z_{0.1}^{\frac{B}{B_2}} \right)$$

Thus finally:

$$\log_e \left(\frac{l_{K_1} + l}{l_{av.} + l_{K_1}} \right) = \log_e \left(\bar{Z}^{\frac{B}{B_2}} Z_{0.1}^{\frac{B}{B_2}} \right)$$

or: $l = (l_{K_1} + l_{av.}) \bar{Z}^{\frac{B}{B_2}} Z_{0.1}^{\frac{B}{B_2}} - l_{av.}$

which is a modification of (14) given in Section VI:

$$l = l_{av.} (\bar{Z}^{\frac{B}{B_2}} - 1)$$

5. Application of (CAB) or (ASRI) Tables for the Problem of the Composite Charges.

These tables are constructed for the ordinary powder charges of a certain sort of powder ($\chi = 1.06$), web $2e$, and U_1). The above shown formula for the impulse

I_K of a mixture can be applied with a good approximation for calculation of I_K and $B = \frac{s^2 I_K^2}{f \omega \phi m}$ as an entry (and Δ) into Tables. If the powders of a mixture have different forms of grains, for example: one part is a degressive powder and another progressive

(7 perforation grain) then for degressive powder we take

$\alpha = 1.06$ and for a progressive we take its equivalent strip powder with $(2e)_{\text{strip}} = \frac{e}{\alpha} (2e)_{\text{perf.}}$.

Thus having determined I'_N and I''_N we find I_N and B .

But this procedure still does not produce the actual location of a projectile ℓ''_N at the end of burning.

That value of $I_N = \frac{I'_N I''_N}{\alpha I'_N + I''_N}$

was determined under the assumption that the character-

istic α of a mixture is equal to α' and α''

i.e. under condition of the burning of mixture of both powders (until point C of the Fig. 168). Such I_N is called "the conditioned I_N ". The actual end of burning must be determined on the (v, ℓ) curve by the ordinate v''_N corresponding to the end of burning of the thick powder (ℓ''_N) :

$$v''_N = \frac{S I''_N}{\varphi m} (1 - \alpha_0) \dots (13)$$

$$\text{Here: } \alpha_0 = \frac{\psi_0}{\psi_0} ; \psi_0 = \frac{\frac{1}{\alpha} - \frac{1}{\alpha'}}{(\frac{1}{\alpha}) + \alpha - \frac{1}{\alpha'}}$$

In the same way we determine ℓ'_N the end of burning of the mixture (when the thin powder is burned out):

$$v'_N = \frac{S I'_N}{\varphi m} (1 - \alpha_0)$$

Having $I_N = \frac{1}{5} \sqrt{B_0 f_{av} m}$ of the mixture and I'_N and I''_N as the characteristics of the components of this mixture we can evaluate from (8) and $\alpha' + \alpha'' = 1$.

$$\text{the percentage: } \alpha' = \frac{\frac{I'_N}{I_N} - 1}{\frac{I'_N}{I_N} - 1} \quad (14) \quad \text{and} \quad \begin{matrix} \omega' = \alpha' \omega \\ \omega'' = (1 - \alpha') \omega \end{matrix}$$

6. Specific details of the Ballistic Design of Howitzers and Calculations of their Charges.

The ballistic design of the howitzers is made for the maximum v_2 corresponding to the full charge (N^0) and maximum pressure P_m . The following data are determined: $\omega_0; W_0; \Lambda_2; L = l_c + l_a; W_c = W_0 (\Lambda_2 + 1)$

From B_0 we find the conditioned impulse I_{N_0} of the mixture for the charge N^0 . The characteristic of powder f_0 is usually taken 90-93 $\frac{\text{g. m.}}{\text{kg}}$. The characteristic h_N is taken 0.30-0.25. Starting from the point

M_0 on the "directive diagram" we explore the sector to the left and down from M_0 where we have smaller Δ , smaller h_N and larger Λ_2 . The characteristic $h_2 = \frac{P_{av}}{P_m}$ will be lower than for guns.

For the minimum charge N^n for v_{2n} and P_{2n} we find

$\Delta_n (0.10-0.15)$, ω_n , B_n , I'_K for the thin powder;

$$f_n \sim 80-82 \frac{B_n \cdot \Delta_n}{W_n}; \quad \omega_n = W_n \Delta_n; \quad \varphi_n = (1.05-1.06) + \frac{1}{5} \frac{\omega_n}{\varphi_n} \frac{v_{d,n}}{v_{d,n}} = \frac{v_{d,n}}{v_{d,n}}$$

$$n_f = \sqrt{\frac{B_n \cdot f_n}{\varphi_n}}$$

and from B_n we find: $I'_K = \sqrt{B_n f_n \omega_n \varphi_n m}$ and $(p_m)_{rel}$.

and finally: $p_{mf} = (p_m)_{rel} \cdot \frac{f}{f_n}$

If $p_{mf} < p_m$ then we change Δ until we have a desired p_m . Thus determined I'_K will be the characteristic of the thin powder used in composite charges.

Knowing ω_0 and ω_n we calculate α'_0 for the charge

$$M^0: \alpha'_0 = \frac{\omega_n}{\omega_0}; \quad \alpha''_0 = 1 - \alpha'_0$$

Knowing I_K and I'_K we find I''_K from: $I''_K = I_{K0} \frac{\alpha'_0}{1 - \alpha'_0 \frac{I_{K0}}{I'_K}}$

$$\text{or: } \frac{1}{I_{K0}} = \frac{\alpha'_0}{I'_K} + \frac{\alpha''_0}{I''_K}$$

In the same way f'' is found from: $f_0 = \alpha'_0 f' + \alpha''_0 f''$

$$\text{or: } f'' = \frac{f_0 - \alpha'_0 f'}{\alpha''_0}$$

Knowing the ranges $(v_{d,0} - v_{d,n})$ and $(\omega_0 - \omega_n)$

we find any intermediate charge: $\omega_i = \omega_n + \frac{\omega_0 - \omega_n}{v_{d,0} - v_{d,n}} (v_{d,i} - v_{d,n})$

Hence: $\Delta_i = W_0 \omega_i$; $\alpha'_i = \frac{\omega_n}{\omega_i}$; $\alpha''_i = 1 - \alpha'_i$; $f_i = \alpha'_i f' + \alpha''_i f''$

Then: $n_{fi} = \sqrt{\frac{\omega_i}{\varphi_i} \cdot \frac{1}{\varphi_i} \cdot \frac{f_i}{f_n}}$; $v_{d,rel} = \frac{v_{d,i}}{v_{d,n}}$; B_i ; p_{mf} and $p = p_{mf} \cdot \frac{f}{f_n}$.

Chapter 2. Solution which takes into Account the
Gradual Engraving of the Driving Band by Riflings of
the Bore.

The preliminary period is subdivided into the two phases: the initial phase and the enforcing phase. The initial phase is described in terms of p_i , ψ_i , K_i , Z_i , which are taken as p_0 , ψ_0 , K_0 , Z_0 in the preliminary period.

In enforcing phase we have the basic equation:

$$\varphi m \cdot \frac{dv}{dt} = (p - \Pi) S, \text{ where } \Pi \text{ is the resistance of the driving band to the engraving related to the unit of } S$$

The pressure p is determined by the equation:

$$p = \frac{f \omega \psi - \theta A}{S(Z_0 + l)} \quad \text{where } A \text{ the total work of the gases}$$

is taken as: $A = \frac{\varphi m v^2}{2} + A_n$ where A_n is the work of Π . The values of Π and A_n are determined

from the experiments; gas formation is determined by:

$$\frac{d\psi}{dt} = \frac{p}{I_k} \sqrt{x^2 + 4x\lambda\psi} \quad (\text{geometric law of burning})$$

We have to proceed with the numerical integration of the following equations: $\frac{d\psi}{dt} = \frac{p}{I_k} \sqrt{x^2 + 4x\lambda\psi}$; $\frac{dv}{dt} = \frac{p - \Pi}{(\frac{\varphi m}{S})}$

$$\frac{dl}{dt} = u \dots (15)$$

$$p = f \frac{\omega}{S} \cdot \frac{\psi - \frac{\theta}{2} x^2 - \frac{\theta}{f \omega} A_n}{Z_0 + l} \dots (16)$$

The following facilitating assumptions are introduced:

1. The variations in ψ are neglected:

then the first equation of (15) will be:

$$\frac{d\rho}{dt} = \frac{x_0}{I_x} \cdot \rho \quad (17)$$

2. The smaller terms in the numerator of ρ (16) are neglected and $(l_p + l)$ is taken as $(l_c + l_a)$, i.e.:

$$l + l_p = l_c + l_a \dots (18)$$

Here: $l_a = \frac{U}{S} \cdot \frac{1}{\alpha} ; \frac{1}{\alpha} = \frac{U}{\omega} - \frac{1}{\beta} ; l_c = l_a - l_a \psi_m ; l_a = \frac{U}{S} \cdot \frac{1}{\beta} ; \frac{1}{\beta} \propto \frac{1}{f}$

3. The force Π has the following expression:

$$\Pi = \Pi_c + \Pi_m \cdot \frac{t}{t_0} \dots (19)$$

where l , is the travel at the end of the phase.

Then (16) will be: $\rho = f \frac{U}{S} \cdot \frac{1}{l_c + l_a}$

Hence: $\frac{d\rho}{dt} = \frac{f \frac{U}{S}}{l_c + l_a} \cdot \frac{d\rho}{dt}$

or remembering (17): $\frac{d\rho}{dt} = \frac{f \frac{U}{S}}{l_c + l_a} \cdot \frac{x_0}{I_x} \cdot \rho$

denoting $t_m = \frac{I_x}{x_0} (l_a + l_c) \cdot \frac{1}{f \frac{U}{S}}$

we will have: $\frac{d\rho}{\rho} = \frac{dt}{t_m} \dots (20)$

Hence: $\rho = \rho_i e^{\frac{t}{t_m}} \dots (21)$

Then the second equation of (15), rewritten having in view (19) and (21), will be:

$$\frac{d^2 l}{dt^2} = \frac{S}{\varphi_m} \left(\rho_i e^{\frac{t}{t_m}} - \rho_i - \Pi_m \frac{t}{t_0} \right) \dots (22)$$

denoting: $\tau^2 = \frac{\varphi_m}{S} \cdot \frac{\ell_i}{\pi_{an}}$; $K^2 = \frac{c_{av}^2}{\tau^2}$; $L = \frac{S \rho_i}{\varphi_m} \cdot c_{av}^2 \dots (23)$

and integrating (22) we will have:

$$\left. \begin{aligned} \frac{\ell}{L} &= \frac{e^{\frac{\ell}{\tau}}}{1+K^2} - \frac{1}{K^2} + \frac{1}{K\sqrt{1+K^2}} \cos\left(\arctg K + K \frac{\ell}{c_{av}}\right) \\ c_{av} \cdot \frac{\nu}{\ell} &= \frac{e^{\frac{\ell}{\tau}}}{1+K^2} - \frac{1}{K\sqrt{1+K^2}} \sin\left(\arctg K + K \frac{\ell}{c_{av}}\right) \end{aligned} \right\} (24)$$

t is measured from the beginning of the phase.

Special Tables for $\frac{\rho}{\rho_i} = e^{\frac{\ell}{\tau}}$ and for $\left(\frac{c_{av} \nu}{L}\right)$
are calculated with the two entries: $\frac{\ell}{L}$ and K^2

Table 1 for	$\left(e^{\frac{\ell}{\tau}}\right)$: -p. 542 - p. 543	} in book
Table 2 for	$\left(\frac{c_{av} \nu}{L}\right)$: -p. 544 - p. 545	

Chapter 3. Solution of the Problem of Interior Ballistics for the Minethrowers.

1. General Information.

The firing of minethrowers has a series of special features making this firing distinct from the ordinary firing of guns. Some of these peculiar characteristics are the results of certain simplifications specifically adopted for minethrowers; others on the contrary, make

this type of firing more difficult for the scientific treatment, because of the lack of definite and reliable knowledge of all the details of this type of firing.

The main charge of the minetrigger (see Fig. 171 - p. 548 in book) is placed within a cardboard case (cartridge case) in the tube of the stabilizer (1) of the mine.

This tube has 4 or 6 round orifices (2) for the discharge of gases out of the cartridge case. The mine slides freely to the bottom of the barrel expelling the air through the clearance (3), and the primer at the end of the mine strikes against the firing pin (4) producing ignition of the primer and powder charge in the cartridge case. At the beginning the powder (at the high density of loading 0.50-0.60) is burning in the closed volume of the cartridge case; finally the gases explode the cardboard walls of the case and through the orifices (2) fill the chamber W.

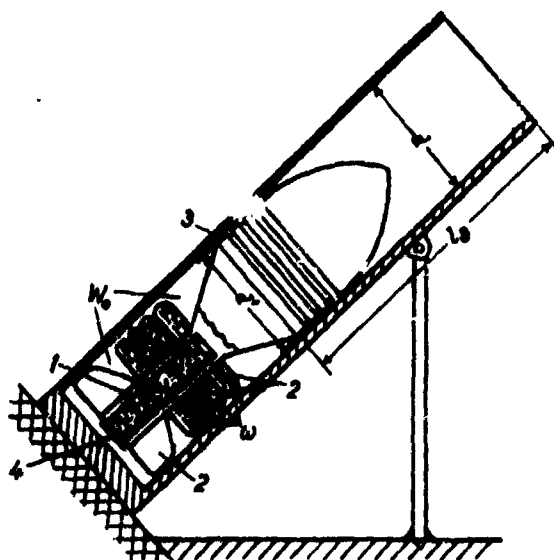


Fig. 171- A schematic view of the minethrower.

Under conditions of a very rapid burning of a fine powder within the tube of the stabilizer, the maximum pressure is very sensitive to every resistance or retardation caused by such an uncertain envelope as the cardboard walls or the thin metallic walls of the stabilizer. As a result of a very small casual difference in the pressures which are high enough to puncture the cardboard walls of a case a very wide dispersion of the maximum pressures within the stabilizer tube can occur. Thus in the case of minethrower the construction, impulse and weight of the igniter, and its rate of burning are

much more significant than they are in the case of ordinary guns. The larger the impulse of the igniter, the more uniform the burning of the charge will be.

The next peculiarity concerns the abrupt expansion and cooling of gases which begin burning within the stabilizer at the high Δ of 0.50-0.80 finally are emitted into the large volume of the chamber behind the mine. Since the surfaces of the wings of the stabilizer and of the bottom part of the mine are large and the density of loading within the volume W_0 is only about 0.01, the heat losses are great and become still greater on account of the slow motion of the mine and the longer duration of contact between the gases and the walls of the barrel.

If there are additional powder charges ω , their powder is ignited by the burning gases of the main charge; thus the mine is propelled by the net action of the main and additional charges. Since the clearance (3) between the surface of the mine and the walls of the bore is large enough, a sizable portion of the gases is lost at the very beginning of the motion of the mine. This is the third specific feature of minethrower firing - the amount of gases lost through the clearance between the mine and the walls of its canal is about 10-15%, whereas the corresponding loss in guns is almost negligible.

The fourth characteristic point about a minethrower is that there is no forcing pressure of the engraving, and there is no problem of the evaluation of work spent on the rotational motion of the mine. Thus the absence of the engraving of the driving band and of certain other secondary resistances makes the problem somewhat easier; on the other hand, the necessity of taking into account large losses of gases and heat involves the application of many complicated inferences and derivations of gas dynamics. Since there is no recoil at all and the relative charge is small (0.01-0.02), the coefficient $\varphi = 1.0$.

In the following analytical solution of the problem of firing minethrowers all notations of parameters and functions are the same as were used previously.

2. Analytical Solution of the Principal Problem of the Smooth Bore Minethrowers. (The Simplified Method of Professor M. Serebryakov).

The following assumptions are made for the analytical solution of this problem:

- 1) There is no forcing initial pressure. The mine moves freely with a clearance between its surface and the smooth walls of the bore.

- 2) Burning of the main charge in the stabilizer tube is not considered. All the gases of the main charge emitted into the volume behind the mine produce there a pressure p and are considered as the igniter for all the additional charges.
- 3) The ignition of all the additional charges is assumed to be instantaneous for all grains and at all points of the grain-surfaces.
- 4) The burning of the additional charges occurs in parallel layers in accordance with the geometric law as is given by the formulas: $\psi = \lambda z + \lambda \lambda z^2$; $\sigma = 1 + 2\lambda z$
- 5) The rate of burning: $u = \frac{dz}{dt} = u, p$
- 6) The mine starts its motion at pressure p_0 at the beginning of the burning of the additional charges at $p = p_0$

7) At the same moment the emission of gases through the clearance begins.

8) The total impulse of the pressure $\int_0^{t_k} p dt = \frac{Q_1}{\alpha_1}$, is not affected by the density of loading Δ and by p_0

9) The emission of gases through the clearance S_{ex} is proportional to the impulse:

$$Y = \omega h = \gamma' A S_{ex} \int_0^t p dt = \gamma' A S_{ex} \cdot I$$

Here: γ part of the gases emitted through the clearance.

The coefficient $A = \left(\frac{2}{\pi W}\right)^{\frac{1}{\pi}} \sqrt{\frac{2\pi K}{K+1} \cdot \frac{1}{f}}$

γ' the coefficient is a characteristic of the clearance S_{cl} (shape, size, dimension)

S_{cl} is the cross-sectional area of the clearance.

10) The heat losses are evaluated by the special experiment which produces burning of the main charge under the same conditions as in the minethrower. During this experiment (within the constant volume) the maximum pressure P_{m_0} of the main charge is observed and the force of the powder of the main charge is determined, taking into consideration: 1) the cooling of gases caused by their expansion from the tube of the stabilizer into the volume behind the mine; 2) the heating of the wall of the stabilizer and 3) the heating of the wings of the stabilizer.

Thus, we calculate: $f_0 = P_{m_0} \left(\frac{1}{\Delta_0} - \alpha_0 \right)$

here: Δ is density of loading of the main charge related to the whole volume W_0 behind the mine (chamber). This value f_0 is considerably lower than f - the force of the additional charges of the same powder which is to be determined by the regular experimental procedure in the manometric bomb. All the rest of the heat loss

is negligible and since there is no work spent on the rotational motion, on the recoil and on the friction, and since the relative weight of the charge ($\frac{w}{W}$) is about 1%, we are justified in assuming that the coefficient $\varphi = 1.0$.

The process of firing is considered during the following three periods:

- 1) The burning of the main charge until the orifices in the walls of the cardboard case are punctured and gases begin their flow into the chamber (period analogous to the preliminary period in guns).
- 2) The first period of the burning of the additional charges with the emission of gases through the clearance (ℓ is varied from 0 to ℓ_n).
- 3) The second period - the expansion of accumulated gases and their emission through S_{cl} .

The motion of the mine and the emission of gases through the clearance S_{cl} begin at the pressure p_0 of the main charge which is determined by the experiment.

The initial pressure p_0 can be experimentally verified and calculated from:

$$p_0 = \frac{f \omega_0}{W_0 - \frac{W_0}{f} - \alpha \omega_0} = \frac{f \Delta_0}{1 - \frac{f}{A} - \alpha \Delta_0}; \quad \Delta = \frac{\omega}{W_0}; \quad \Delta_0 = \frac{\omega_0}{W_0}$$

Denoting: S - the cross-sectional area of the bore of the minethrower: $S = \frac{\pi}{4} d^2$

S' - cross-sectional area of the mine at the diameter of its bourrelet: $S_x = S - S'$

The velocity of the mine is determined from the equation of motion: $\varphi m dv = S' \rho dt$

$$v = \frac{S'}{\varphi m} \int \rho dt = \frac{S'}{\varphi m} \cdot I = \frac{S'}{\varphi m} \cdot I_N \cdot \alpha; \alpha = \frac{S'}{S} = \frac{I_N}{I_N}$$

For the solution we have the following system of equations:

- 1) the basic equation of Pyrodynamics taking into account the loss of gases and of heat:

$$Sp(\ell'_1 + \ell) = f_0 \omega_0 + f \omega \psi - f' \gamma - \frac{Q}{2} \varphi m v^2$$

Herc: f' - the force of the mixture of the main and additional charges, its value varies from f_0 to $\frac{f_0 \omega_0 + f \omega}{\omega_0 + \omega}$ having the intermediate value of $f' = \frac{f_0 \omega_0 + f \omega \psi}{\omega_0 + \omega \psi}$

In order to compensate our omission of the heat losses to the walls of barrel during the first period (assumption 10) we may take instead of the value f' the larger value of f (the force of the additional charges). Then our equation will be rewritten:

$$Sp(\ell'_\psi + \ell) = f_0 \omega_0 + f(\omega\psi - \gamma) - \frac{\rho}{2} \varphi m v^2 \dots (26)$$

$$\text{here: } \ell'_\psi = \frac{1}{f} [w_0 - \frac{\rho}{2}(1-\psi) - \alpha(\omega\psi - \gamma) - \alpha_0 \omega_0]$$

is taking into account the losses of gases through $(S-S')$.

2) The equation for the motion of the mine:

$$S' p a \ell = \varphi m v dv \dots (27)$$

3) The geometric law of burning for the fine strip powder's:

$$\psi = \chi z + \chi \lambda z^2 \dots (28)$$

and for the flat disc grains: $\psi = \chi$

4) Formula for the velocity:

$$v^2 = \frac{S' I_K}{\varphi m} \cdot z \quad (29)$$

5) The relative discharge of gases:

$$h = \frac{Y}{\omega} = \frac{\bar{z}' A S_{cl} I_K}{\omega} \cdot z = h_K z \dots (30)$$

$$\text{where: } h_K = \frac{\bar{z}' A S_{cl} I_K}{\omega} = \frac{\bar{z}' A S_{cl}}{\omega} \cdot \frac{e_1}{a_1} \dots (31)$$

\bar{z}' - the coefficient of the form of the orifices.

h_K - the relative discharge of gases at the end of burning of powder.

$$\text{Let us denote: } B' = \frac{S'^2 I_K^2}{f \omega \varphi m} = \left(\frac{S'}{S}\right)^2 \cdot \frac{S'^2 I_K^2}{f \omega \varphi m} = \left(\frac{S'}{S}\right)^2 B$$

$$\text{and } \chi_0 = \frac{f_0 \omega_0}{f \omega}$$

which is the relative energy of the main

charge.

Now in the basic equation (26) the variables ψ, v, Y and h can be expressed in terms of Z and then (26) will be:

$$Sp(\ell'_p + \ell) = f\omega \left[\chi_0 + \kappa z + \kappa \lambda z^2 - \kappa_1 z - \frac{B'_1}{2} \theta z^2 \right] = f\omega \left[\chi_0 + (\kappa - \kappa_1)z - \left(\frac{B'_1}{2} - \kappa \lambda \right) z^2 \right]$$

From (27) we have:

$$3'p d\ell = \frac{S'^2 I_n^2}{\varphi m} Z dx \dots (33)$$

Dividing (33) on (32) we will have:

$$\frac{g'}{3} \cdot \frac{d\ell}{\ell'_p + \ell} = B' \frac{Z dx}{\chi_0 + \kappa_1 Z - B'_1 Z^2} = - \frac{B'_1}{B'_1} \frac{Z dx}{Z^2 - \frac{\chi_0}{B'_1} Z + \frac{\kappa_1}{B'_1}} = - \frac{B'_1}{B'_1} d(\ell_2 Z)$$

Here: Z is Drosdov's function, $\kappa_1 = (\kappa - \kappa_1)$ and $B'_1 = \frac{B'_1}{2} - \kappa \lambda$; $A_3 = \frac{5}{3} \cdot \frac{B'_1}{B'_1}$

and finally:

$$\frac{d\ell}{\ell'_p + \ell} = - A_3 d(\ell_2 Z) \dots (34)$$

The equation (34) can be solved rigorously using the same method given by Prof. Drosdov, but having in view that Δ for minethrowers is small ($\Delta < 0.15$) which means that ℓ'_p varies very slightly we can take $\ell'_p = (\ell'_p)_{av.} = \text{constant}$. Then the integration of (34) will give:

$$\ell = (\ell'_p)_{av.} [Z^{-A_3} - 1]$$

Here: $\log Z^{-1}$ is given in Drosdov's tables by the two entries (parameters): $\gamma = \frac{B'_1 \chi_0}{\kappa_1^2}$ and $\beta = \frac{B'_1}{\kappa_1} Z$
Thus, the solution for the first period for the minethrower differs from the solution for the ordinary gun

only by 1) the presence of the coefficient $K' = \kappa \cdot \eta_\kappa$ instead of $K_1 = \kappa \delta_0$ at the variable z ; 2) instead of ψ_0 we have $\tilde{\chi}_0 = \frac{f_0 \omega_0}{f \omega}$ and 3) instead of B we have $B' = B \left(\frac{S}{S'}\right)^2$. All these changes, as the results of certain peculiarities of firing a minethrower come to be specific forms of the entries in Drosdov's tables: $\delta' = \frac{B' \tilde{\chi}_0}{K_1^2}$ and $\beta = \frac{B'}{K_1} z$

which means that z' and ℓ are larger and the pressure p is smaller in comparison with the case of the ordinary guns, where there is no such great discharge of gases. The pressure p is determined from (26):

$$p = \frac{f \omega}{S} \cdot \frac{\tilde{\chi}_0 + \psi - \frac{\rho}{2} \frac{v_{mv}^2}{f \omega} - \delta'}{\ell'_p + \ell} = \frac{f \omega}{S} \cdot \frac{\tilde{\chi}_0 + K_1' z - B' z^2}{\ell'_p + \ell} \dots (35)$$

For finding z_m corresponding to the maximum pressure

p_m we differentiate (35) with respect to z and a few algebraical manipulations will give us:

$$z_m = \frac{\tilde{\chi}_0 \left(1 + \frac{p_m}{f \delta_1}\right) - \eta_\kappa \left(1 + \frac{\alpha p_m}{f}\right)}{B_1' \left(\frac{S}{S'} + \theta\right) - 2 \kappa \lambda \left(1 + \frac{p_m}{f \delta_1}\right)} = \frac{\tilde{\chi}_0 - \eta_\kappa \left(\frac{1 + \frac{\alpha p_m}{f}}{1 + \frac{p_m}{f \delta_1}}\right)}{\frac{B_1' \left(\frac{S}{S'} + \theta\right)}{1 + \frac{p_m}{f \delta_1}} - 2 \kappa \lambda} \dots (36)$$

$$\text{here: } \frac{1}{\delta_1} = \alpha - \frac{1}{\delta}$$

when $q_k = 0$ and $S = S'$ we have the ordinary formula for

x_m . If $x_m < 1$ we will have the real maximum pressure; if $x_m > 1$ the maximum is not a real one, the factual maximum will be at the end of burning - the pressure p_k

$$p_k = \frac{f\omega}{S} \cdot \frac{1 + x_m - q_k - \frac{q_k^2}{x}}{c'_1 + c_k}$$

$$\text{here: } c'_1 = c_0 [1 - \alpha \Delta (1 - q_k)] \quad \text{and: } \Delta = \Delta (1 - q_k) = \frac{c_0}{p_k} (1 - q_k)$$

Other elements of the end of the first period will be:

$$x_k = \frac{S' x_k}{S k}; \quad c_k = (c'_1)_{\text{max}} (x_k^{-1}); \quad p_k = \frac{S'}{k};$$

For the solution of the problem during the second period we will have the following equations:

$$Sp(c'_1 + c) = f_0 \omega_0 + f\omega (1 - q_k x') - \frac{R}{2} \varphi m v^2 \dots (37)$$

$$S' p dc = \varphi m v dv \dots (33)$$

$$\text{here: } x' = \frac{I}{x_k} = \frac{\int p dt}{\int p_k dt} = \frac{v}{v_k} > 1$$

The value of $q_k x'$ is taking into account the continued emission of gases through the clearance. As during the first period the total discharge of gases is proportional to the impulse of the pressure, i.e. proportional to the velocity of the mine.

Solution of the equations (37) and (33) is as follows:

(37) can be rewritten:

$$sp(l+l) = f\omega \left[\chi_0 + 1 - \frac{h_N}{\chi_0} v - \frac{v^2}{\chi_0^2} \right] \dots (38)$$

$$\text{here: } h_N = \frac{2' A S_{\omega} I_N}{\omega}; v_N = \frac{S' I_N}{\varphi m}; v_{\omega} = \frac{2 f \omega}{\varphi \omega m}; \frac{h_N}{v_N} = 2' A \frac{S}{\varphi} \cdot \frac{S'}{S} = h_N'$$

Having divided (35) by (38):

$$\frac{d^2 l}{dl^2} = \frac{S}{S'} \cdot \frac{v m}{f \omega} \cdot \frac{v dv}{1 + \chi_0 - \frac{h_N}{\chi_0} v - \frac{v^2}{\chi_0^2}} = \frac{S}{S'} \cdot \frac{2}{\omega} \cdot \frac{v dv}{v^2 + h_N' v - (h_N')^2}$$

or:

$$\int \frac{dl}{l^2 + l} = - \frac{S}{S'} \cdot \frac{2}{\omega} \int \frac{v dv}{v^2 + h_N' v - h_N'^2} \dots (39)$$

here:

$$h_N' = h_N' v_{\omega}^2 = \frac{h_N}{v_N} \cdot v_{\omega}^2; h_N' = (h_N' v_{\omega})^2 = (v_{\omega}')^2$$

$$\text{Denoting } \xi(v) = v^2 + h_N' v - h_N'$$

we find the roots of $\xi(v) = 0$

$$v_1 = -\frac{h_N'}{2} (1+b) \text{ and } v_2 = -\frac{h_N'}{2} (1-b) = \frac{h_N'}{2} (b-1); b = \sqrt{1 + 4 \frac{h_N'}{h_N'^2}} = \sqrt{1 + 4}$$

$$\text{Then: } \frac{v}{\xi(v)} = \frac{A_1}{v - v_1} + \frac{A_2}{v - v_2}; A_1 = \frac{v_2}{v_2 - v_1}; A_2 = \frac{v_1}{v_1 - v_2}$$

$$\text{and } \int \frac{v dv}{\xi(v)} = \log \left(\frac{v - v_1}{v_2 - v_1} \right)^{\frac{v_2}{h_N'}} \left(\frac{v - v_2}{v_1 - v_2} \right)^{\frac{v_1}{h_N'}} = \log \left(\frac{Z_v'}{Z_{v_0}'} \right)$$

Having integrated (39) we have:

$$- \frac{S'}{2S} \log \left(\frac{l' + l}{l' + l_N} \right) = \log \left(\frac{Z_v'}{Z_{v_0}'} \right)$$

or:
$$\left(\frac{\ell'_1 + \ell_\pi}{\ell'_1 + \ell}\right)^{\frac{f_1 \cdot f}{2}} = \left(\frac{v - v_1}{v_\pi - v_1}\right)^{\frac{a_1}{2}} \left(\frac{v - v_\pi}{v_\pi - v_1}\right)^{\frac{\ell_1}{2}}$$

and finally:
$$\ell = \ell'_1 \left[\left(1 + \frac{\ell_\pi}{\ell'_1}\right) \left(\frac{v - v_\pi}{v_\pi - v_1}\right)^{-\frac{f_1 \cdot f}{2}} - 1 \right]$$

Thus for every value $v > v_\pi$ we will find ℓ

Formula for the pressure:

$$p = \frac{f \omega}{s} \cdot \frac{1 + \kappa_0 \frac{f_1 v - v_\pi}{\ell'_1 + \ell}}{\ell'_1 + \ell}$$

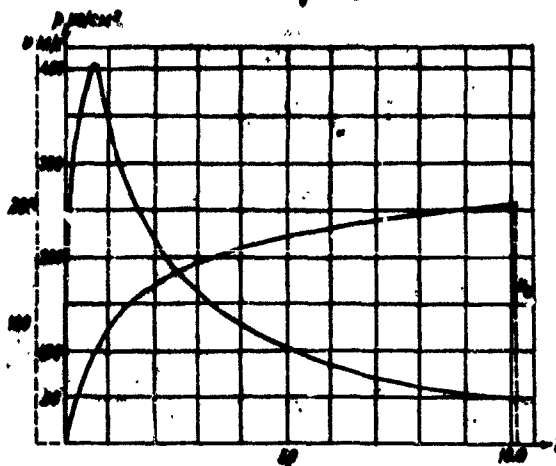


Fig. 172

Curves (p, ℓ) and (v, ℓ) for 82 m/m pinethrower.

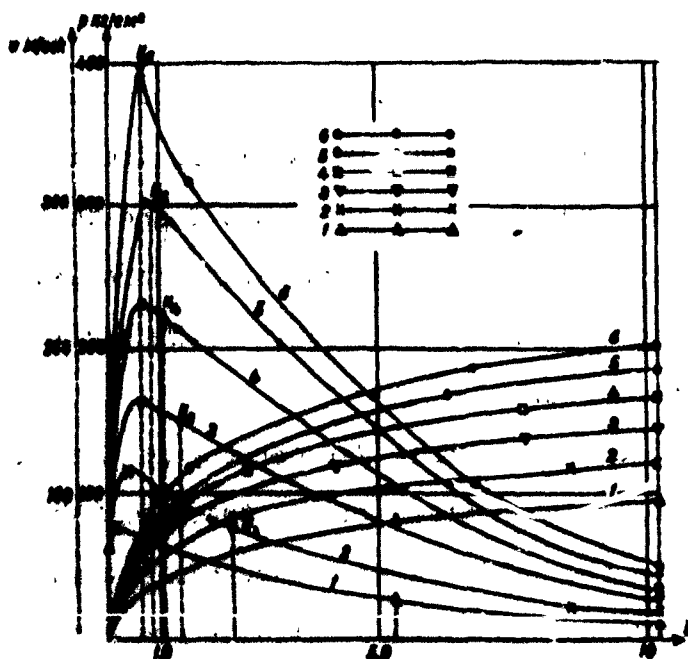


Fig. 172.a

Curves (P, t) and (v, t) for various charges from No. 1 to No. 6 in the 82 m/m minethrower.

Section XII - Guns with Tapered Bores. (Conic Guns)Introduction

As far back as the 1870's conic guns had been suggested and constructed for experimental purposes only. Soon after the First World War German Engineer Gerlich experimented with the conic rifle and found that the maximum velocity of a bullet was markedly increased and the armor-piercing effect was considerably higher than with the ordinary rifle.

During the Second World War conic guns were used in the German Army as antitank guns: there was the antitank gun with the calibers 28 m/m-30 m/m and muzzle velocity 1400 m/sec. and another antitank gun with the calibers 42-28 m/m and the cylindro-conic gun 75-55 m/m. The later model consisted of an ordinary 75 m/m cylindrical rifled bore, with the continued smooth tapered bore from 75 m/m to 55 m/m and with smooth cylindrical bore of 55 m/m to the muzzle of gun. The projectile had two bands: immediately after the bourrelet there was a directing band having a light profile ("skirt") and the other driving band of a more massive form was at its usual place close to the bottom of the projectile. (See Fig. 173.)

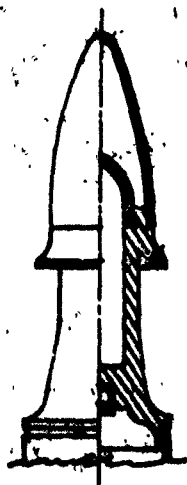


Fig. 175 - An armor piercing shell of the 75/55 m/m tapered gun.

In order to clarify the idea of using the tapered conic gun let us analyze the possibility of having a higher muzzle velocity of a projectile with a smaller weight at the same maximum pressure. Our problem can be stated in this way: we have an ordinary projectile with its weight q' and its muzzle velocity, v' , the impulse of the pressure I_K' the web of powder $2c = I_K' 2u'$.

A new projectile has a weight $q'' < q'$. It is required to find a new velocity v'' , if the maximum pressure p_m and the density of loading A (or weight of charge ω) are unchanged.

From the formula for the second period we have:

$$\frac{Q_2 \theta v_2^2}{2gfw} = 1 - \frac{(\Lambda_K + 1 - \alpha \Delta)^0}{(\Lambda_K + 1 - \alpha \Delta)^0} \left[1 - \frac{K^0}{K^0} (1 - \alpha \Delta) \right] = 1 - \frac{K^0}{(\Lambda_K + 1 - \alpha \Delta)^0} \dots (43)$$

$$\text{where: } K = (\Lambda_K + 1 - \alpha \Delta) \left[1 - \frac{Q_2 \theta v_2^2}{2gfw} \right]; \frac{Q_2 \theta v_2^2}{2gfw} = \frac{Q_2 \theta v_2^2}{2gfw} = \tau_2'$$

At the condition of constancy of p , Δ and ω we have B , K and Λ_K also constant. Therefore the left part of (43) is also constant, hence:

$$Q_2 \theta v_2^2 = (a + b \frac{Q}{Q'}) Q_2 v_2^2 = \text{Const.} \dots (44)$$

$$\text{Therefore: } \left(\frac{Q_2 \theta v_2^2}{Q_2 v_2^2} \right)^2 = \frac{Q' Q'}{Q_2^2 Q'} = \frac{Q'}{Q_2^2} \cdot \frac{a + b \cdot \frac{Q}{Q'}}{a + b \cdot \frac{Q}{Q'}} \dots (45)$$

$$\text{If } \omega \text{ is constant then: } \frac{Q_2 \theta v_2^2}{2gfw} = \eta_{\omega} = \text{Const.}$$

and since at the decrease of weight Q the value of

$Q = a + b \left(\frac{Q}{Q'} \right)$ is increased, therefore η_{ω} must be decreased, i.e., with a lighter projectile the coefficient of the utilization of the charge η_{ω} will be smaller than with a heavier one.

$$\text{So we have: } \eta_{\omega}'' = \eta_{\omega}' \frac{Q'}{Q''}; v_2'' = v_2' \sqrt{\frac{Q'}{Q''} \cdot \frac{Q'}{Q'}} \dots (46)$$

and since B is constant we have one more condition:

$$\text{or: } I_K'' = I_K' \sqrt{\frac{Q'}{Q''} \cdot \frac{Q'}{Q'}} \quad \frac{I_K''}{I_K'} = \text{Const.} \quad (47)$$

and therefore:

$$I'' v_2'' = I' v_2' = \text{Const.}$$

This formula makes it possible to select the weight of a new projectile which will have the desired muzzle velocity in a given gun.

Remembering that the maximum velocity of the recoiling system V_{\max} and the muzzle velocity v_2 of the projectile are in a definite relationship:

$$V_{\max} = \beta \cdot \frac{C \cdot \rho \cdot F}{1.15} v_2$$

where $\beta = \frac{C}{\frac{G}{v_2}} = \frac{C v_2}{G}$ is the coefficient of the "after-effect" of gases.

When we change Q' into Q'' preserving the same ω

$$\text{then: } \frac{G'}{v_2'} = \sqrt{\frac{F'}{F}} \cdot \frac{G}{v_2}; \quad \beta \frac{G'}{v_2'} = \frac{C}{v_2'} \cdot \frac{G'}{v_2'}$$

and

$$\frac{V_{\max}'}{V_{\max}} = \frac{G'}{G} \cdot \frac{v_2}{v_2'} \cdot \frac{1 + \frac{C \omega}{G v_2'}}{1 + \frac{C \omega}{G' v_2'}} = \frac{\sqrt{\frac{F'}{F}} \cdot \frac{G}{v_2} \cdot \frac{v_2}{v_2'}}{1 + \frac{C \omega}{G' v_2'}} \cdot \frac{1 + \frac{C \omega}{G v_2'}}{1 + \beta \frac{G'}{v_2'}}$$

since $\varphi' Q'' < \varphi' Q'$

$$\text{we have } \frac{V_{\max}'}{V_{\max}} < 1$$

Which means that by taking a lighter projectile at the same charge ω we have a higher muzzle velocity but still the maximum velocity of the recoil is decreased, i.e., the stress affecting the mount of the gun will be reduced.

Suppose a projectile with the coefficient of weight $C_2 = 15.0$ has its muzzle velocity $v_2' = 1000$ m/sec.

and $\frac{\omega}{Q} = 0.45$; $\varphi' = 1.03 + \frac{1}{3} \cdot \frac{Q'}{Q} = 1.18$

a lighter projectile with $C_p'' = 7.5 = \frac{C_p'}{2}$ will have:

$$\frac{\omega}{Q''} = 0.90 \quad ; \quad \varphi'' = 1.03 + \frac{1}{3}(0.90) = 1.33$$

Then: $v_2'' = 1000 \sqrt{\frac{H^2}{1.33} \cdot \frac{Q''}{Q'}} = 1330 \text{ m/sec.}$

If $h_w' = 130$, then $h_w'' = 130 \cdot \frac{H^2}{1.33} = 1153$; $I_N'' = I_N' \cdot \frac{1}{1.33} = 0.75 I_N'$

The weight Q'' can be calculated from the equation

$$(45): \quad \left(\frac{v_2''}{v_2'}\right)^2 = \frac{Q'}{Q''} \cdot \frac{a + b \frac{Q'}{Q}}{a + b \frac{Q''}{Q}} = \frac{a Q' + b \omega}{a Q'' + b \omega}$$

$$Q'' = \frac{Q'}{a} \left[\varphi' \left(\frac{v_2''}{v_2'} \right)^2 - b \frac{\omega}{Q'} \right] \dots (48)$$

Chapter 1 -

1.1 Specific Features and Ballistic Properties of a Gun with the Tapered Bore.

The projectile is expected to be as "heavy" as possible in order to lose its velocity as slowly as possible when moving in the air along its trajectory - this property is characterized by the "sectional density" of the projectile $\left(\frac{Q}{A}\right)$ or by its "coefficient of weight" $\left(\frac{Q}{A^2}\right)$; both of these characteristics must be as large as possible. On the other hand, the projectile is expected to be as "light" as possible in order to acquire its prescribed velocity as soon as possible at the shortest

travel along the bore, which means that its $C_2 = \frac{g}{d_1}$ must be as small as possible. The tapered gun with its conic bore is designed to reconcile these two contradictory requirements.

Let us denote d_0 the initial caliber of the conic bore and d_1 the final caliber at the muzzle and $d_1 < d_0$. In such a bore the projectile with its coefficient of weight $C_2 = \frac{g}{d_1} < \frac{g}{d_0}$ has the advantage if compared with the projectile having its $C_2 = \frac{g}{d_0}$ that it acquires a higher velocity at the shorter travel along the conic bore than the velocity of the projectile travelling in a cylindrical bore of caliber d_1 . And at the muzzle our projectile will have its $C_2 = \frac{g}{d_1}$, which will be more advantageous during its travel in the air than with its previous smaller value $C_2 = \frac{g}{d_0}$.

The problem of analysis of the principal properties of the tapered bore is reducible to the comparative analysis of firings of cylindrical guns with various calibers using a projectile of the same weight. We know from the theory of the ballistic design that at the unchangeable Δ , $\frac{g}{d_0}$, ρ_m , v_0 , the lengths of the canal L , and of the chamber C , and webs of powders all expressed in terms of caliber are all proportional

to the coefficients $C_g = \frac{g}{\alpha^3}$ and their absolute values are proportional to $(\frac{g}{\alpha})$ (sectional density).

For the cylindrical canals we have:

$$\text{For the total volume of canal: } \frac{W_0}{\alpha} = \frac{W_0}{\alpha} \left\{ \frac{K(R, \Delta)}{(1-r')^3} + \alpha \Delta \right\}$$

$$\text{And for the reduced length of } W_c: \frac{L'_c}{\alpha} = \frac{\ell_0}{\alpha} \left\{ \frac{K(R, \Delta)}{(1-r')^3} + \alpha \Delta \right\}$$

$$\text{Here: } W_c = S L'_c; L'_c = \ell_0 + \ell_2; W_c = W_0 (\Lambda_2 + 1)$$

$$\text{Therefore: } \left\{ \frac{K(R, \Delta)}{(1-r')^3} + \alpha \Delta \right\} = (\Lambda_2 + 1)$$

$$\text{and since } \frac{L'_c}{\alpha} = \frac{\ell_0}{\alpha} (\Lambda_2 + 1)$$

$$\text{or } \frac{\ell_0 + \ell_2}{\alpha} = \frac{\ell_0}{\alpha} (\Lambda_2 + 1) \text{ i.e.: } \frac{\ell_2}{\alpha} = \Lambda_2 \cdot \frac{\ell_0}{\alpha}$$

$$\text{and } \frac{\ell_2}{\alpha} = \frac{W_0}{S \alpha} = \frac{W_0}{n_s \alpha^3} = \frac{g}{\alpha} \cdot \frac{1}{n_s \Delta} \cdot \frac{g}{\alpha^3} = \frac{g}{\alpha} \cdot \frac{C_2}{n_s \Delta}$$

At given $\rho_m, v_2, \frac{g}{\alpha}, \Delta$ the value of $(\Lambda_2 + 1)$ is constant, $\frac{\ell_0}{\alpha}$ is proportional to C_2 , therefore $\frac{\ell'_c}{\alpha}$ and $\frac{\ell_2}{\alpha}$ are also proportional to $C_2 = \frac{g}{\alpha^3}$ and the absolute values of ℓ_0, ℓ_2, L'_c are proportional to $\frac{g}{\alpha^3}$.

$$\text{Since: } \frac{L'_c}{\alpha} = \sqrt{\frac{f}{g}} \cdot \frac{C_2}{n_s} \sqrt{2\psi} \frac{g}{\alpha}$$

and at given $\rho_m, v_0, \frac{w}{2}, A, B$
 the coefficient φ is constant then $\frac{I^N}{\alpha}$ is also
 proportional to C_2 . The larger is the caliber at
 given q the smaller $\frac{I^N}{\alpha}$ is and the smaller is the
 web of the powder producing the same ρ_m at the same w .

Now from: $C_2 = \frac{q}{\alpha_2^2}$ and $C_2 = \frac{q}{\alpha_1^2}$ we have: $C_2 = (\frac{\alpha_2}{\alpha_1})^2$

and from: $\frac{q}{S_0} = \frac{q}{K\alpha_1^2}$ and $\frac{q}{S_0} = \frac{q}{K\alpha_2^2}$

we have: $\frac{q}{S_0} = \frac{q}{S_0} (\frac{\alpha_2}{\alpha_1})^2$

A practicable ratio $\frac{\alpha_2}{\alpha_1} = \sim 1.46 - 1.85$

Hence: $(\frac{\alpha_2}{\alpha_1})^2 \sim 2.75 - 3.46$; $(\frac{\alpha_2}{\alpha_1})^3 \sim 0.343 - 0.587$

$(\frac{\alpha_1}{\alpha_2})^2 \sim 1.96 - 1.82$; $(\frac{\alpha_1}{\alpha_2})^3 \sim 0.51 - 0.55$

Then: $\frac{q}{S_0} = \frac{q}{S_0} (0.51 - 0.55)$ and since ℓ_2 or L_2 are varied
 in proportion to $\frac{q}{S_0}$ we will conclude that the pro-
 jectile of a given weight in the gun with the caliber

$\alpha_0 = 1.41 \alpha_2$ will have the same v_0 as the pro-
 jectile of the same weight has with gun with the caliber

α_2 but at the travel $\ell_2 = (0.51 - 0.55)\ell_0$ i.e.
 only at one-half of travel ℓ_0 in the gun with the cal-
 iber α_0 . At given W_0 we will have the same values

of W_c and Λ_2 . At given ρ_m the curves (ρ, Λ) and (v, Λ) will be identical. Now if preserving q, W_0 and W_c and $\Lambda_2 = \frac{W_c}{W_0}$ as constants we will change the caliber of a cylindrical gun from the larger to the smaller then we will have ℓ_c, \angle_c and C_g increased. But since $\Delta, q, \frac{W_c}{W_0}, \rho_m$ and v_2 are unchangeable we will have the same curves (v, Λ) and (v, W) for all these cylindrical guns on the whole range between the extreme values of calibers and C_g . Such is a basic property of the ballistically similar guns of various calibers. From this particular property we can derive a comprehensive picture of the meaning and practical value of the whole concept of the "tapered guns".

The conic bore with the constant volumes W_c and W_0 (I.e. $\Lambda_2 = \frac{W_c}{W_0}$) can be considered as the result of the continued transition of the cylindrical bore with the initial caliber α_0 and $C_g = \frac{q}{\alpha_0^2}$ to the cylindrical bore with its caliber α_2 and $C_g = \frac{q}{\alpha_2^2}$. Since it has been shown above that all the curves of velocities as functions of $\Lambda = \frac{W}{W_0}$ are identical for the cylindrical canals with the decreasing calibers we may be justified in the assumption that at a given q the curve of (v, Λ) for the conic bore at the same $\Delta, \frac{W_c}{W_0}, \rho_m$

will also be identical with the same curves of the cylindrical bores of the same volume for various calibers.

Such is a basic assumption concerning the ballistic properties of the conic guns. At the same volumes of the whole conic bore and its working part its length is smaller than the length of the cylindrical bore with the caliber d_2 and is larger than the length of the cylindrical bore with the caliber d_0 . This is schematically shown on Fig. 174.

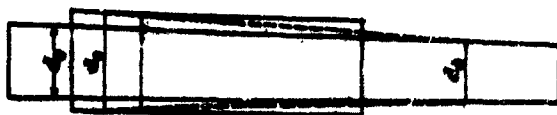


Fig. 174 A comparison of conic and cylindrical bores.

The curve of pressures in functions of $\lambda = \frac{w}{w_0}$ (for the conic canal) will be different from the curve of pressures for the cylindrical bores and after its maximum

it is running higher than these curves (β, Λ) and the end of burning at the same R_m for conic canal comes earlier than for the cylindrical bore, i.e. $(\Lambda_K)_{con.} < (\Lambda_K)_{cyl.}$

1. Notations and geometric characteristics of the conic bore.

Inlet caliber: d_0 ; area S_0

Outlet caliber: d_1

Angle of the cone: β

The length of projectile travel: l_0

The length of the whole cone: $h_K = l_0 \cdot \frac{d_0}{d_1 d_2} = \frac{d_0}{2} \cot \beta$

Total volume of cone: $W_K = \frac{S_0 h_K}{3} = \frac{S_0}{3} \cdot \frac{d_0}{2} \cot \beta$

Volume of the working part of canal W_2 } $W_0 = W_2 + W_K$

Volume of the chamber: W_0

The relative volume of the cone $\Lambda_K = \frac{W_K}{W_0}$

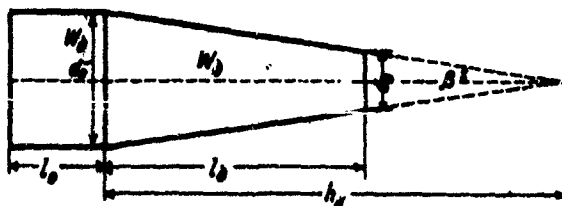


Fig. 175 - Geometric data of the conic bore.

We will consider a relative diameter $y = \frac{d}{d_0} = \frac{h_N \ell}{h_N} = 1 - \frac{e}{h_N}$

Hence: $\ell = h_N(1-y)$; $\ell_2 = h_N(1-y_2)$

$$\frac{S}{S_0} = \left(\frac{d}{d_0}\right)^2 = y^2; \quad \frac{S_{\text{aver}}}{S_0} = \frac{1+y+y^2}{3} \sim y$$

$$W = S_0 \left(\frac{1+y+y^2}{3}\right) \ell = \frac{S_0}{3} h_N (1+y+y^2)(1-y) = \frac{S_0}{3} h_N (1-y^2) = W_N (1-y^2)$$

$$\Lambda_2 = \frac{W_2}{W_0} = \frac{S_0 h_N}{\sqrt{3} S_0 \ell_0} (1-y_2^2) = \frac{h_N}{\sqrt{3} \ell_0} (1-y_2^2)$$

The independent variable is: $\Lambda = \frac{W}{W_0}$; $\Lambda_N = \frac{W_N}{W_0}$

$$y = \sqrt[3]{1 - \frac{W}{W_N}} = \sqrt[3]{1 - \frac{\Lambda}{\Lambda_N}}$$

$$S = S_0 y^2; \quad S_{\text{aver}} = S_0 \frac{1+y+y^2}{3}$$

$$\ell = h_N (1-y)$$

The equations for the conic bore are no different in their appearance from the equations of the cylindrical bore, but it should be noted that now the cross-sectional area S is a variable and not a constant, this is a serious complication for the analytical procedure, but our assumption of the identity of the curves (ψ, Λ) for cylindrical and conic bores makes it possible to consider a certain constant average value of S (provided that the conicity is not very pronounced). For the comparison, we will have in view the cylindrical bore with its characteristics: $d_0; W_0; W_2; q; \frac{\omega}{2}; \Delta; \varphi; I_A; f; \alpha; \delta; \theta; \rho$.

The principal relationships are:

$$S \rho dt = \varphi m dv \dots (1)$$

$$de = u, \rho dt \dots (2)$$

$$\rho(W_p + W) = f \omega \psi - \frac{1}{2} \varphi m v^2 \dots (3)$$

From (3) we have:

$$\rho = f \omega \cdot \frac{\psi - \frac{1}{2} \frac{v^2}{W_p + W}}{W_p + W} = f \Delta \frac{\psi - \left(\frac{v}{\lambda_p + \lambda}\right)^2}{\lambda_p + \lambda} \dots (49)$$

Here: $\lambda_p = 1 - \frac{A}{x} - (\alpha - \frac{1}{x}) \Delta \psi$; $\frac{S}{S_0} = \left(1 - \frac{W_p}{W}\right)^2 = \left(1 - \frac{A}{\lambda_p}\right)^2$, which is the relationship between the relative cross-sectional area of the bore and the relative volume of the bore

$$W_p = \frac{S_0 A}{S} = \frac{S_0}{S} \cdot \frac{A}{x} \cdot G \alpha \beta$$

$$\psi = \psi_0 + \kappa \frac{A}{x} + \kappa \lambda x^2$$

From (1) and (2) we have: $S de = u, \varphi m dv$

$$\text{or: } dv = \frac{S}{\varphi m} \cdot \frac{e}{u} dx = \frac{S I_N}{\varphi m} dx \dots (50)$$

S in (50) has not the immediate connection neither with x nor with v but from the curve (ψ, A) for the cylindrical canal we may establish the relationship between s and v for the conic bore. Thus we will find a constant average S_{av} for the integration of (50).

After integration we will have:

$$v = \frac{S}{\varphi} \cdot \frac{I_N}{m} \cdot \frac{S_{av}}{S} x \dots (51)$$

For the cylindrical bore with the same S_0

$$\text{we have: } v' = \frac{S_0 I_N}{\varphi m} \cdot x'$$

Since for a given λ we have: $v = v'$

$$\text{then: } x' = \frac{S_{ax}}{S_0} \cdot x$$

$$\text{or: } x = \frac{x'}{\left(\frac{S_{ax}}{S_0}\right)} > x' \dots (52)$$

This inequality shows that at the same values of v , ψ and I_N the relative value of the burned thickness of the grain of powder x in the conic bore is larger than the corresponding burned thickness of x' with cylindrical bore. Then writing the expressions for the pressures p (in the conic bore) and p' (in cylindrical bore) we will have

$$p = f \Delta \cdot \frac{\psi - \left(\frac{x}{I_N}\right)^2}{\lambda_\psi + \lambda}$$

$$p' = f \Delta \cdot \frac{\psi' - \left(\frac{x'}{I_N}\right)^2}{\lambda_{\psi'} + \lambda'}$$

From (52) we see that: $x > x'$; $\psi = \frac{1}{2} \cdot x \cdot \lambda x^2 > \psi' = \frac{1}{2} \cdot x' \cdot \lambda x'^2$

$$\lambda_\psi > \lambda_{\psi'}; \lambda_\psi = A - B\psi$$

$$\lambda_{\psi'} = A - B\psi'$$

The conclusion is that $p > p'$ i.e. the basic result of the comparison of the ballistic properties of the conic and cylindrical bores is that at the same loading conditions $(W_0, \frac{W}{x}, \Delta, I_N)$ at the same W and v the burned part ψ of powder charge and the pressure p in the conic bore are larger than the corresponding values in the cylindrical bore, and the more pronounced the conicity is the larger are these differences.

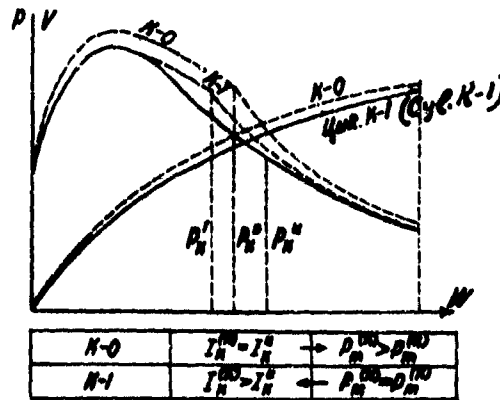


Fig. 176 - Curves (p, W) and (V, W) for the conic gun (in dotted lines) and for the cylindrical gun (in solid lines)

Therefore the pressure curve in the conic bore (see Fig. 176 - p and v for conic bore are shown as dotted lines) constructed as the function of W has a shape of a more progressive character than the same curve for the cylindrical bore and also has its end of burning (points with the subscript K) at the smaller W with the smaller A_K than is observed in the curves for the cylindrical bore.

1.2. On the Relationship Between the Thicknesses of
Powders producing the same Maximum Pressures (P_m)
in the Conic and Cylindrical bores.

Since the comparison of the ballistic properties of the cylindrical and conic bores is always made at the equal P_m we will show how this equality can be obtained by the appropriate change in I_K (which after all means a change in the thickness of the powder).

For the cylindrical bores of different calibers (d_0 and d_1) at given q , P_m and Δ we have $B_0 = B_1$, this means that: $S_0 I_{K_0} = S_1 I_{K_1}$

$$\text{or: } \frac{I_{K_0}}{I_{K_1}} = \frac{S_1}{S_0} = y^2; I_{K_1} = I_{K_0} \cdot \frac{S_0}{S_1} = I_{K_0} \cdot \frac{1}{y^2}$$

For the cylindrical bore we have:

$$x' = \frac{q m}{S_1 I_{K_0}} v$$

For the conic bore we have:

$$x = \frac{q m}{S_0 I_{K_1}} \cdot \frac{v}{\left(\frac{d_0}{d_1}\right)^2} > x'$$

and the difference $(x - x')$ at the increased v and decreased $\left(\frac{S_{av}}{S_0}\right)$ is continually increased.

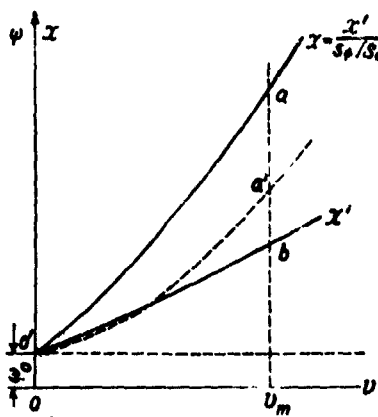


Fig. 177 - Curves (x, v) for the cylindrical bore

(x') and for the conic bore $x = \frac{x'}{(\frac{S_0}{S})}$

Fig. 177 shows how x and x' (or ψ) are varied with v :

x' is represented by the straight line $O'x'$ and x by the curve $O'ax$ tangent to the straight line $O'x'$. At the given v_m and equal Λ'_m we have $x_m > x'_m$ also $\psi_m > \psi'_m$ and $\rho_m > \rho'_m$. If we would like to have $\rho'_m = \rho_m$ then by changing I_x we may bring down the curve $O'ax$ in order to have the equal intensities of the gas formation along the interval of Ov_m for both canals. Suppose we have the powder with the constant surface of

burning: $\psi = \psi_0 + x$

$$\text{we have: } \frac{dx}{dv} = \frac{d\psi}{dv} = \frac{d\psi}{dt} \cdot \frac{dt}{dv}; \quad \text{but } \frac{dv}{dt} = \frac{S\rho}{\varphi m}$$

$$\text{hence: } \frac{dx}{dv} = \frac{dv}{dt} \cdot \frac{\varphi m}{Sp} = \frac{\varphi m}{S} \Gamma$$

$$\text{here } \Gamma = \frac{1}{\rho} \cdot \frac{dp}{dv} = \frac{p}{I_K} \cdot \sigma$$

For the powder with the constant surface of burning:

$$\Gamma = \frac{1}{I_K} \text{ and } \frac{dx}{dv} = \frac{\varphi m}{S} \cdot \frac{1}{I_K}$$

For the conic bore S is decreased and $\frac{dx}{dv}$ is increased. Suppose there is a special requirement to make an average value of $\left(\frac{dx}{dv}\right)$ along the interval of v from 0 to v_m equal to $\frac{dx'}{dv} = \frac{\varphi m}{S_0 I_{K0}}$

$$\text{Then: } \text{aver.} \left(\frac{\varphi m}{S I_K} \right)_m = \frac{\varphi m}{S_0 I_{K0}} \text{ or: } \frac{\varphi m}{S_{av} I_K} = \frac{\varphi m}{S_0 I_{K0}}$$

$$\text{Hence: } I_K = I_{K0} \cdot \frac{S_0}{(S_{av})_m}$$

where $(S_{av})_m$ is an average value of the conical cross-section between the beginning of the bore and its cross-section where the velocity is v_m and the pressure is

p_m . Since Λ'_m is known from the curve (v, Λ') of the cylindrical bore we may find: $\frac{S_{av}}{S_0} = y_m = \sqrt[3]{1 - \frac{\Lambda'_m}{\Lambda_K}}$

$$\text{Thus we have: } I_K = \frac{I_{K0}}{y_m} = I_{K0} \cdot \frac{S_0}{S_{av}} = I_{K0} \cdot \left(\frac{S_0}{S_2} \right) \cdot \left(\frac{S_2}{S_{av}} \right)$$

$$\text{For } \Lambda_K = 6.0 ; \Lambda'_m = 0.6 ; y_m = 0.97, \text{ at } \frac{d_2}{d_1} = 1.4$$

$$\frac{S_2}{S_0} = 1.96 ; I_K = I_{K0} \cdot 0.97 = 1.03 I_{K0} = 1.03 \cdot \frac{1}{1.96} I_{K0} = 0.527 I_{K0}$$

$$\text{at } \Lambda_K = 10.0. \quad y_m = 0.983$$

Thus we see that in order to have the same P_m in the conic bore ($d_2 = 1.4d_1$) the thickness of powder must be about 3% ($I_K = 1.03 I_{K_0}$) in excess over the thickness of powder in the cylindrical bore with the caliber d_0 .

And this thickness must be only 0.527 ($I_K = 0.527 I_{K_2}$) of the thickness of powder in the cylindrical bore with the caliber d_2 . It is not amiss to note that not infrequently the error is made when the cylindrical and conic bores are compared at the same thickness of powders: The maximum pressure for the conic bore will be obtained in such case so much lower that the powder even will fail to burn.

1.3. On the Comparative Lengths of the Barrels with Conic and Cylindrical Bores.

Since the projectile leaves the muzzle of the conic bore of caliber d_2 with its C_2 necessary for producing its desired kinetic energy we must compare the ballistic characteristics of the conic bore of caliber d_2 with the ballistic characteristics of the cylindrical bore having its caliber d_1 . At the same $W_0, \Delta, \frac{W}{Z}, \frac{P}{m}, \frac{V_0}{2}$ these two bores will have the same working volumes W_0 , i.e:

$$\text{Cylindrical volume: } S_0 (l_0)_c = \text{Conical volume } \frac{S_2}{3} (1 + y_2 + y_2^2) (l_2)_c$$

$$\text{or: } (l_0)_c = (l_2)_c \cdot \frac{S_2}{S_0} \cdot \frac{3}{1 + y_2 + y_2^2} = (l_2)_c \cdot \frac{3y_2^2}{1 + y_2 + y_2^2}$$

The relative decrease in the length of the conic bore
(in respect to length of the cylindrical bore $(l_2)_c$)

$$\frac{(l_2)_c - (l_2)_w}{(l_2)_c} = \frac{\delta(l_2)_c}{(l_2)_c} = \frac{1 + y_2 - 2y_2^2}{1 + y_2 + y_2^2}$$

If we have: $\frac{d_2}{d_0} = \frac{28}{20} = 1.4$; $y_2 = 0.715$; $y_2^2 = 0.511$; $\frac{(\delta l_2)_c}{(l_2)_c} = 0.311$

If we have: $\frac{d_2}{d_0} = \frac{26}{20} = 1.362$; $y_2 = 0.734$; $y_2^2 = 0.539$; $\frac{(\delta l_2)_c}{(l_2)_c} = 0.289$

If we consider the relative decrease in respect to $(l_2)_{co}$ of the conic bore then we will have:

$$\text{For } \frac{d_2}{d_0} = 1.4; \frac{(\delta l_2)_c}{(l_2)_c} = 0.452$$

$$\text{For } \frac{d_2}{d_0} = 1.362; \frac{(\delta l_2)_c}{(l_2)_c} = 0.405$$

The conclusion is: at the same $w_0, w_2, w_c, \epsilon, \omega, \Delta, \frac{w_2}{2}$
the conic barrel with $\frac{d_2}{d_0} = 1.4$ gives the same muzzle

velocity v_2 and the same R_m as the cylindrical
barrel with d_2 at the decreased travel of the projec-
tile $(l_2)_{co} = 0.30(l_2)_c$ and at the thickness of powder de-
creased in ratio $(\frac{d_2}{d_0})^2 = \frac{S_2}{S_0}$. This is the main advan-
tage of the conic guns - they provide the desired kinetic
energy of the projectile at a shorter length of the
barrel than do the cylindrical guns. Modern artillery
requiring higher muzzle velocities, came to the use of
guns as long as 150 calibers - which brings in many ser-
ious difficulties in transportation and service (deflec-
tion of the long axes of guns and vibration of the walls
of the long barrels).

1.4. Taking into Account the Secondary Works in the Conic Bore.

All the above given results have been obtained under the assumption of the equality of the coefficient φ in both types of guns. But in reality the guns with conic bores have not a few specific factors affecting the amounts of losses of energy as well as the very forms of the processes creating these losses. For example: a) The motions of gases and unburned particles of the charge go on in the canal which has its cross-section continually decreased along the direction of this motion. b) The mechanical deformation of the guiding and driving bands of the projectile generates an increased resistance to the motion of the projectile within the bore along the whole length of its travel to the muzzle.

We will assume the same form for the coefficient

$$\varphi = \alpha_c + \beta_c \cdot \frac{\omega}{\omega_0}$$

The motion of gases will affect the coefficient β_c especially at the higher velocities and at the larger

when the conic bores are particularly applicable in practice. The component α_c is affected by the forces of resistance and friction of the bands, which are continually increasing and obstruct the motion of

the projectile. This reaction in the conic bores is much greater than it is in the cylindrical bores and it

could be noted also that in conic bores the entire surface of bands subjected to friction is continually increased as a surface of a contact between the bore and the projectile.

In the ordinary guns a is ≈ 1.03 in small arms $a = 1.10$ (almost the whole surface of a bullet is engraved in the rifling), and in conic bores $a > 1.10$.

For the cylindrical bore (omitting the widening of the chamber) $\beta = \frac{1}{3}$; if the widening of chamber is $\lambda = \frac{c_0}{c_1}$ then $\beta = \frac{1}{3} \cdot \frac{\lambda + 1}{\lambda}$ where λ is the current number of the volume of expansion: at $\lambda = 0$

$$\beta_0 = \frac{1}{3} \cdot \frac{1}{\lambda} ; \text{ at } \lambda_1 : \beta_1 = \frac{1}{3} \cdot \frac{\lambda_1 + 1}{1 + \lambda_1}$$

with the increased λ β approaches $\frac{1}{3}$ and $\beta_0 < \beta < \beta_1$

For deriving the analogous formula for b in case of the conic bore accounting for the widening of the chamber we have to make certain additional assumptions:

1. Gas velocity is in various sections of the bore varied as a linear function from the breech to the base of projectile.
2. The gaseous mass is distributed uniformly but in state of motion is only that mass which has the section S equal to the current section of the conic bore.

3. The inner friction in gases and the friction between gases and walls of canal are considered as negligible.

We have our chamber in the conic gun with its widening $X = \frac{L}{L_0}$ and the conic canal has $\frac{d^2}{dx^2} = y$ at the muzzle and at the current position of the projectile

$\frac{d^2}{dx^2} = y$ at its travel l . The relative weight of the moving gas is $\frac{\omega_{mv}}{\omega}$; the necessary work for this motion is $L_0 \cdot \frac{\omega_{mv}}{2}$; the total weight of charge ω .

$$\frac{\omega_{mv}}{\omega} = \frac{S(l+L)}{V_0+W} = \frac{\frac{S_0}{S_0} + \frac{S_{mv}}{S_0} \cdot \frac{L}{L_0}}{1+\Lambda} = \frac{\frac{S_0}{S_0} \cdot \frac{1}{\Lambda} + \frac{S_{mv}}{S_0} \cdot \frac{L}{L_0}}{1+\Lambda} = \frac{\frac{S_0}{S_0} (\frac{1}{\Lambda} + \frac{S_{mv}}{S_0} \Lambda)}{1+\Lambda}$$

$$\text{here } \Lambda = \frac{W}{V_0}$$

$$\text{Since } \frac{S_{mv}}{S_0} = y^2; \quad \frac{S_{mv}}{S_0} = \frac{1+y+y^2}{3} \approx y$$

$$\text{Then: } \omega_{mv} = \omega y^2 \frac{1 + \frac{1}{y}}{1+y} = \omega y \frac{1 + \frac{1}{y}}{1+y}$$

The whole work for moving a cylindrical volume of gases

with cross-section S and weight ω_{mv} is $\frac{1}{3} \cdot \frac{\omega_{mv}}{2} = \frac{1}{3} \cdot \frac{\omega}{2} \cdot \frac{\omega_{mv}}{\omega}$

Putting in here the above shown expression for ω_{mv}

$$\text{we will have: } L_c = \frac{1}{3} y \cdot \frac{1 + \frac{1}{y}}{1+y}$$

$$\text{For the cylindrical bore we have: } y=1 \text{ and } L_c = \frac{1}{3} \cdot \frac{1 + \frac{1}{y}}{1+y}$$

$$\text{and since: } y < 1 \text{ then } L_c < L$$

Thus we see that the work required for the moving parts of the charge in the conic bore at the equal Λ, ω and X is smaller than in the cylindrical bore and the difference between these amounts of work is increased

during the motion of the projectile (because with the increase of Λ y is decreased) i.e., the value of b_c is decreased at $\chi = 1$; $\Lambda = 0$; $y = 1$; $b_c = 1/3$, and with the increased Λ and decreasing y the value of b_c is decreased.

At $\chi > 1$ b_c starts from $b_{c0} = \frac{1}{3}\chi$ and with the increased Λ b_c is increased, goes through its maximum and then falls down.

Here is the Table for b_c and $(b_c)_{av.}$ for the conic bore at $\frac{W_{bo}}{W_0} = 6$ and $\chi = 1.8$

Λ	0	0.2	0.4	0.6	0.8	1.0	2.0	3.0	4.0
b_c	0.185	0.205	0.219	0.228	0.235	0.238	0.241	0.227	0.203
$(b_c)_{av.}$	0.185	0.195	0.203	0.210	0.216	0.220	0.231	0.232	0.230

The curves (b_c, Λ) and (b_{av}, Λ) at various χ are shown on Figure 178 for conic bore (in dotted lines) and cylindrical bore (in solid lines).

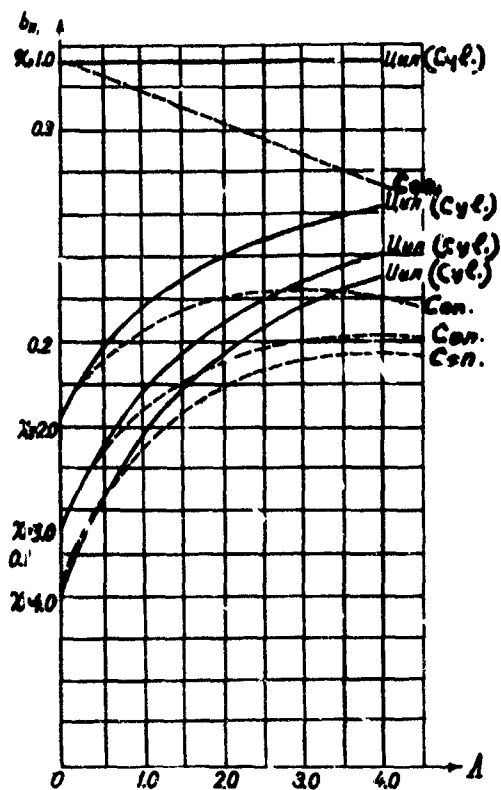


Fig. 178 - The curves $(\beta_{x,1})$ and $(\beta_{\text{max},1})$ at various x are shown on Fig. 178 for conic bore (in dotted lines) and cylindrical bore (in solid lines)

The process of guiding of the projectile with the two bands in the conic bore differs considerably from the guiding in the cylindrical bore of the projectile with one driving copper band. In the latter case the resistance is sharply increased at the very beginning of the engraving of the band into rifling and as soon as the band is engraved at the full depth of the rifling the resistance also very abruptly diminishes. At the whole travel of the projectile only 1% ($K_3 \omega = 0.01$) of the energy is absorbed by the resistance of friction in rifling. During the motion of the projectile with two bands in the conic bore, the engraving and squeezing of both bands and their more massive parts continue during the whole travel and require an ever-increasing amount of work to overcome all these resistances. We will show how all these obstructing factors can be taken into account.

Fig. 179 shows a schematic view of the axial cross-section of the projectile for the German conic guns 28/20 m/m with the two bands - the front leading band and the rear obturating band. The front band has no noticeable cylindrical part. The rear band has a small

cylindrical part ab; conic part bce is gradually converted into the cylindrical surface of the body of the projectile.

Both bands in their axial cross-sections have the shapes of the bodies of the equal resistance to the bending moment - they are wide at the base ef (Fig. 180) and have pointed ends a.

Diameter (Fig. 181) $d'_o > d_o$; diameter of the body of the projectile $d_1 < d_o$.

(to make room for the compressed front band around the body of the projectile). At the beginning of the motion the front band moves through 35 m/m of the smooth cylindrical bore and then begins its engraving into the rifled conic bore. Powder gases act on the inner cavity of the rear band and press its cylindrical part ab to the surface of the bore. The surface of this part ab is: $S_{no} = \pi d'_o l_o$ (Fig. 179). At the gradual engraving into rifling both bands are compressed and stretched back. Fig. 180 shows the rear band after passing the muzzle, the outer surface of band has the engraved marks of the rifling.

In order to evaluate the work required to produce the deformation of the surface of the rear band we will

assume (see Fig. 181 and Fig. 182) that the length of the generatrix (ℓ_n) of the rear band $ecba$ will be preserved when the generatrix after its deformation will be $ecb'a'$ (Fig. 181)

$$\text{i.e. } \ell_n = ecba = ecb'a'$$

The deformation of the rubbing cylindrical surface consists of the transformation of the initial cylindrical surface of diameter d_o' into the cylindrical surface of diameter d . The area of this surface is: $S_n = \pi d(a'b' + b'c)$

$$\text{but } b'c = bc = \frac{d_o' - d}{2 \sin \alpha}$$

$$\text{or } bc = \frac{d_o' - d}{2 \sin \alpha} \quad (\text{See Fig. 181})$$

Remembering that $y = \frac{d}{d_o'}$ and $S_o = \frac{\pi}{4} \cdot d_o'^2$

we will have:

$$\begin{aligned} S_n &= \pi y d_o' \left(b_o + \frac{d_o' - d}{2 \sin \alpha} \right) = \frac{\pi}{4} d_o'^2 y \left[\frac{4b_o}{d_o'} + \frac{2(1-y)}{\sin \alpha} \right] = \frac{\pi d_o'^2 y}{4} \left[\left(\frac{4b_o}{d_o'} + \frac{2}{\sin \alpha} \right) \frac{y}{y} - \frac{2y}{\sin \alpha} \right] = \\ &= S_o y^2 \left[\left(\frac{4b_o}{d_o'} + \frac{2}{\sin \alpha} \right) \frac{1}{y} - \frac{2}{\sin \alpha} \right] = S \left[\left(\frac{4b_o}{d_o'} + \frac{2}{\sin \alpha} \right) \frac{1}{y} - \frac{2}{\sin \alpha} \right] \end{aligned}$$

here: $S = S_o y^2$ is a current cross-section.

$$\text{Thus: } \frac{S_n}{S} = \left[\left(\frac{4b_o}{d_o'} + \frac{2}{\sin \alpha} \right) \frac{1}{y} - \frac{2}{\sin \alpha} \right]$$

is the ratio of the surface S_n of the engraved rear band to the cross-section of the conic bore. Since y is

continually decreased this ratio is continually increased.

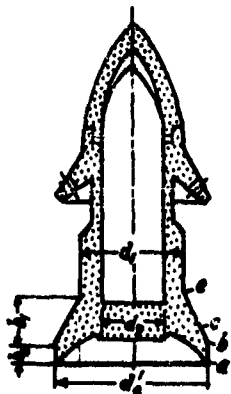


Fig. 179
Cross-sectional view of the armor-piercing shell of the 28/20 mm conic gun.

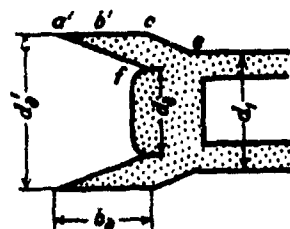


Fig. 180
The rear band after its passing through the conic bore.

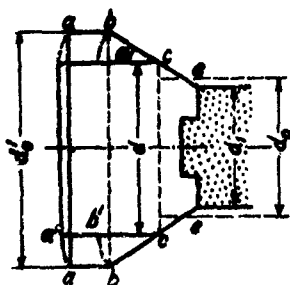


Fig. 181
Schematic view of the pressing of the rear band in the conic bore.

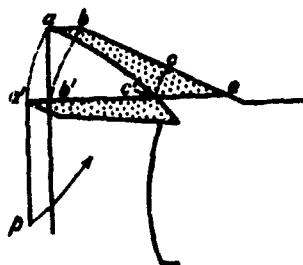


Fig. 182
Schematic view of the deformation of the rear band during the pressing into the conic bore.

The force of friction R_r between the band and the conic surface of bore will be: $R_r = \xi \gamma S_n p$

Here the factor $\xi < 1$ signifies that the pressure p does not act over the frictional surface at its full value and besides this as we can see in Fig. 182 the pressure p does not act on the part ec' which means that the whole surface S_n is not involved in the value of the force of friction R_r .

The work against this force will be: $\int R_r d\ell = \xi \gamma \int S_n p d\ell$

$$\text{or: } \int R_r d\ell = \xi \gamma \int \left[\left(4 \frac{e_0}{d_0} + \frac{2}{\sin \alpha} \right)^{\frac{1}{2}} - \frac{2}{\sin \alpha} \right] p s d\ell$$

Having $\frac{1}{y}$ at its constant average value out of the integration, we will have:

$$\int R_r d\ell = \xi \gamma \left[\left(4 \frac{e_0}{d_0} + \frac{2}{\sin \alpha} \right) \left(\frac{1}{y} \right)_{av} - \frac{2}{\sin \alpha} \right] \int p dw$$

and since $\int p dw = \frac{mv^2}{2}$

We finally will have:

$$\int R_r d\ell = \xi \gamma \left[\left(4 \frac{e_0}{d_0} + \frac{2}{\sin \alpha} \right) \left(\frac{1}{y} \right)_{av} - \frac{2}{\sin \alpha} \right] \frac{mv^2}{2}$$

Thus the relative work spent against the resistance of the friction will be: $K_3'' = \xi \gamma \left[\left(4 \frac{e_0}{d_0} + \frac{2}{\sin \alpha} \right) \left(\frac{1}{y} \right)_{av} - \frac{2}{\sin \alpha} \right]$

Remembering that $y = \sqrt[3]{1 - \frac{\lambda}{\lambda_k}}$, we will have:

$$\left(\frac{1}{y} \right)_{av} = \left(\frac{\lambda}{\lambda_k} \right) \int \left(1 - \frac{\lambda}{\lambda_k} \right)^{\frac{1}{3}} d\left(\frac{\lambda}{\lambda_k} \right)$$

570

After the integration (with the auxiliary variable

$\epsilon = 1 - \frac{A}{\lambda_K}$ we will have:

$$\left(\frac{1}{y}\right)_{av} = \frac{3}{2} \cdot \frac{(1-y^2)}{\left(\frac{A}{\lambda_K}\right)}$$

We may have the following Table 5 for $\left(\frac{1}{y}\right)_{av}$ and K_3

Table 5

$\frac{A}{\lambda_K}$	0.0	0.10	0.20	0.30	0.40	0.50	0.60	0.70
$\left(\frac{1}{y}\right)_{av}$	1.0	1.017	1.037	1.059	1.082	1.110	1.143	1.183
K_3	0.0400	0.0445	0.0563	0.0658	0.0762	0.0884	0.1028	0.1204

From the table we find that the coefficient K_3'' which for the cylindrical guns is constant and about 0.010 is markedly larger for the conic guns and varies from 0.040 to 0.120.

But it should be remembered that in our evaluation of K_3'' we did not take into account the work spent on the deformation of the bands and on overcoming the resistances of the rifled walls of the conic bore in their contacts with the bands.

Special experiments 1943-1945 have been made with the projectiles for 28/20 m/m conic guns. These projectiles have been pulled through special conic dies (matrices) having different angles β of their conicities. The tested projectiles were divided into 3 groups: 1) with both bands on; 2) with the front band alone and 3) with the rear band alone. The results - diagrams of the pulling forces as functions of ℓ are shown on Fig. 183 and Fig. 184.

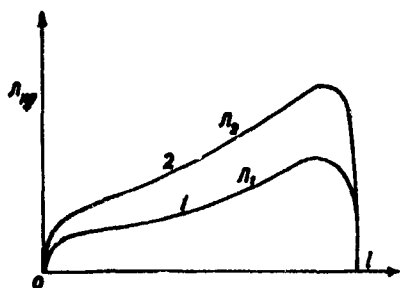


Fig. 183

π_1 - Rifling force for the Front band alone

π_2 - Pulling force for the Rear band alone

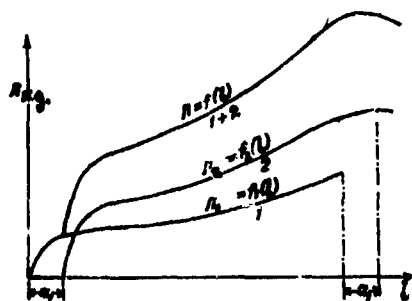


Fig. 184

A summary action of π_1 and π_2 ; (1+2) curve represents a sum of ordinates of curve 1 and curve 2. Distance is measured between the bands.

The value of angle β (varied from $20^\circ-21^\circ$ to $11^\circ-12^\circ$) does not affect much the pulling force π (not more than 11-12% of π).

The projectiles were pulled through the dies (matrices) by means of Ansler's press. The following regularities were observed on the (π , ℓ) curves obtained.

1. Since the rear band is more massive than the front band its curve π_2 (Fig. 183) is higher than the curve π_1 (front band). $(\pi_2)_{max.}$ is almost twice as large as $(\pi_1)_{max.}$

2. When the projectile has both bands (Fig. 184) and the distance between bands is a , then the curve for the rear band (curve 2) is displaced at the distance a , from the beginning of the curve 1 (front band).

3. The curve (1 + 2) of the total pulling force for the projectile with both bands starts from the point on the curve 1 at the distance a , from the Π -axis.

4. The total work of the pulling force $\int \Pi dl$ is largely affected by the total length of travel of the projectile pulled through the matrix.

Thus obtained curves (Π_n, l) in matrices must be converted into the curves (Π_c, l) of the force Π_c acting in the conic bore of a gun.

Table of Experimental Results with the Projectiles Statically Pulled Through the Matrices.

of Matrix	$\tan \beta$	Length of the conic part m/m	$\Pi_{max.}$ for two bands Kg.	$\Pi_{max.}$ for the rear band Kg.	$\Pi_{max.}$ for the front band Kg.
1	0.040	100	3500	2620	1550
2	0.025	160	3250	2350	1180
3	0.020	200	3100	2250	1100

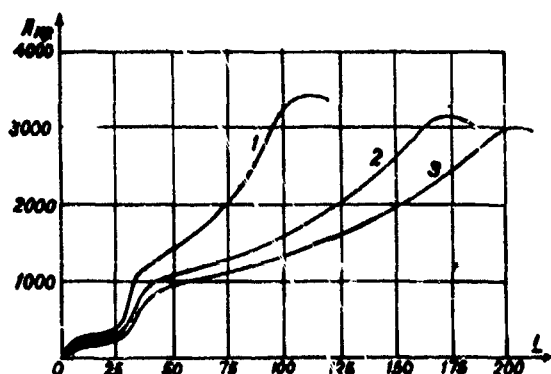


Fig.185 - Diagrams for Π : 1 - for $\text{tag } \beta = 0.040$;
2 - for $\text{tag } \beta = 0.025$; 3 - for $\text{tag } \beta = 0.020$.

1.5. A Formula for Conversion of the Force Π_M (acting in the Matrix) into the Force Π_c (acting in the Conic Gun).

Fig. 186 shows the acting forces during the travel of the projectile having two bands along the conic canal (angle β)

The following forces are at work:

1. Force Π acting along the axis of the projectile.

2. Force of reaction N' which is uniformly distributed over the surface of the front band and is normal to this surface.

3. Force of reaction N'' of the same nature acting on the rear band.

4. Force of friction ν, N'

5. Force of friction ν, N''

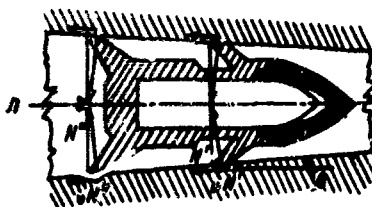


Fig. 186 - Schematic view of forces acting on the projectile in the conic gun.

Projecting all forces on the axis of the projectile and on the perpendicular axis we will have:

Along the projectile-axis: $\Pi = N(\sin\beta + \nu\cos\beta)$

here $N = N' + N''$

Radial forces: over the front band: $Q^1 = N'(\cos\beta - \nu\sin\beta)$

over the rear band: $Q'' = N''(\cos\beta - \nu\sin\beta)$

Radial forces produce the plastic deformation of the bands.

We assume that in the conic bore of a gun and in the conic matrix at their equal cross-sections of equal

diameters the radial forces are equal.

Let us denote forces related to the conic bore with the subscripts C and forces related to the matrix by the subscript M .

Then the equality of the radial forces is expressed as

$$N_M (\cos \beta_M - \gamma_{1M} \sin \beta_M) = N_C (\cos \beta_C - \gamma_{1C} \sin \beta_C) \dots (54)$$

$$\text{axial force in matrix: } \Pi_M = N_M (\sin \beta_M + \gamma_{1M} \cos \beta_M)$$

$$\text{axial force in conic gun: } \Pi_C = N_C (\sin \beta_C + \gamma_{1C} \cos \beta_C)$$

$$\text{Hence: } \frac{\Pi_C}{\Pi_M} = \frac{N_C}{N_M} \cdot \frac{\sin \beta_C + \gamma_{1C} \cos \beta_C}{\sin \beta_M + \gamma_{1M} \cos \beta_M}$$

putting $\frac{N_C}{N_M}$ in here (from (54) we will have:

$$\Pi_C = \Pi_M \cdot \frac{(\cos \beta_M - \gamma_{1M} \sin \beta_M)(\sin \beta_C + \gamma_{1C} \cos \beta_C)}{(\cos \beta_C - \gamma_{1C} \sin \beta_C)(\sin \beta_M + \gamma_{1M} \cos \beta_M)}$$

or:

$$\Pi_C = \Pi_M \cdot \frac{\tan \beta_M}{\tan \beta_C} \cdot \frac{\cot \beta_M - \gamma_{1M}}{\cot \beta_C - \gamma_{1C}} \cdot \frac{\tan \beta_C + \gamma_{1C}}{\tan \beta_M + \gamma_{1M}} \dots (55)$$

Since $\frac{\tan \beta_M}{\tan \beta_C} \cdot \frac{\cot \beta_M - \gamma_{1M}}{\cot \beta_C - \gamma_{1C}} \approx 1$, is very close to 1.

We may write:

$$\Pi_C = \Pi_M \cdot \frac{\tan \beta_C + \gamma_{1C}}{\tan \beta_M + \gamma_{1M}} \dots (56)$$

This formula has been verified by the experiment of pulling two projectiles through the matrices with different angles β . From the values of the pulling forces

π_1 and π_2 ., the value of the coefficient of friction γ_N has been calculated and found to be 0.16, which is exactly the practical value for this coefficient.

The coefficient of friction is affected by the velocity of motion and its value is varied as it is given by the formula: $\gamma = \gamma_0 \frac{1+a_1\gamma}{1+a_2\gamma}$ here $a_1 < a_2$

From the experiments of M. Shlaposhnikov we have:

$$\gamma_0 = 0.27; \quad a_1 = 0.0213; \quad a_2 = 0.133$$

Robinson (Thermodynamics of Firearms, 1943) gives

$\gamma = 0.05$ at $v > 200$ m/s. As the average practical value of γ we may take 0.10.

Fig. 187 shows the diagram of $\pi_c = f(l)$ for the conic gun 28/20 m/m at $\gamma = 0.10$

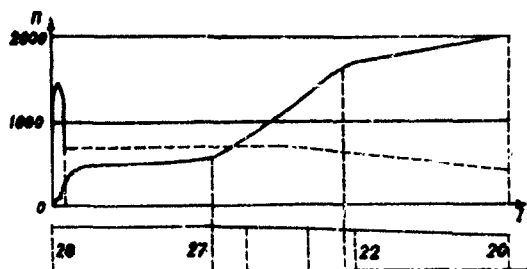


Fig. 187 A diagram showing the force $\pi_c = f(l)$ pulling the projectile through the conic bore of a gun 28/20 m/m. A lower part shows the axial cross-section of the bore with its varying diameters from 28 m/m to 20 m/m.

The calculated work of the static pulling through the matrix for this gun is about $1320 \frac{\text{Kg}}{\text{dm}}$ which is nearly 10% of the muzzle kinetic energy of the projectile. The total work $\int \pi d l$ largely depends on the value of ν but not on $\tan \beta$.

Thus the coefficient φ_c for the conic gun has the form: $\varphi_c = a_c + b_c \frac{\omega}{q}$
and $a_c = 1 + K_2 + K_2' + K_2'' + K_2^{(K)} + K_5$

Here $K_2 \sim 0.01$ is the relative work spent on the rotation of the projectile:

$K_2' \sim 0.02$ is the relative work spent on overcoming the friction of the two bands in the rifling;

$K_2^{(K)} \sim 0.10$ is the relative work spent on overcoming the resistance of the deformation and friction over the surface of the bore $K_2^{(K)} = \frac{\int \pi d l}{(\frac{\pi d^2}{4})}$

$K_2'' \sim 0.04-0.08$ is the relative work on overcoming the additional friction of the rear band pressed against the surface of the bore by gases.

$K_5 \sim 0.01$ is the relative work moving the recoiling system

Thus the total $\Sigma K \sim 0.18-0.22$

And finally we have that $a_c = 1.20$, and $b_c = \frac{1}{3} \gamma \frac{1-\frac{\gamma}{2}}{1+\gamma} \sim 0$

For the cylindrical bore:

for $\frac{\omega}{2} = 1$ we have $\varphi = 1.03 + \frac{1}{3} \cdot (1) = 1.363$

For the conic bore, at $\frac{\omega}{2} = 1$

$$\varphi_c = 1.20 + 0.222 = 1.422$$

For $\frac{\omega}{2} = 1.5$

For the cylindrical bore: $\varphi = 1.03 + \frac{1}{3} \cdot \frac{3}{2} = 1.53$

For the conic bore: $\varphi_c = 1.20 + 0.333 = 1.533$

For $\frac{\omega}{2} = 2.0$

For the cylindrical bore: $\varphi = 1.03 + \frac{2}{3} = 1.70$

For the conic bore: $\varphi_c = 1.20 + 0.444 = 1.644$

For $\frac{\omega}{2} = 1.5$ both coefficients φ and φ_c are equal.

At the higher $\frac{\omega}{2} > 1.5$ for the muzzle velocities $v_s > 1500 \text{ m/s}$, φ_c decrease (in ℓ_c), and the conic gun becomes a more efficient gun than the cylindrical one. Thus at high muzzle velocities, the conic gun has the advantage over the cylindrical gun not only because its length can be shorter, but also because the work required for the movement of gases within the conic bore is considerably less.

We have the following equations:

The equation of motion:

$$S p - \frac{4}{3} \gamma S_n p - \Pi = \varphi m \frac{dv}{dt} \dots (a)$$

here p - gas pressure on the projectile.

The equation of work:

$$p(W_p + W) = f\omega\psi - \frac{1}{2}\varphi_2 m v^2 - \theta \int_0^l \pi dl - \xi \int_0^l \gamma S_n p dl \quad (b)$$

The equation of the rate of burning:

$$u = u_0 p \quad (c)$$

The equation for gas formation:

$$\psi = \kappa_0 z + \kappa_1 \lambda z^2 \quad (d)$$

The relationship between p and p_{av} (average):

$$p_{av} = p \left[1 + \frac{1}{3} \cdot \frac{2}{\varphi_1} \cdot \frac{1 + \frac{\kappa_0}{\lambda}}{\lambda + 1} \right] \quad (e)$$

The coefficient φ_1 accounts for the work against the resistance of the rifling and for the rotational motion of the projectile ($\varphi_1 = 1.02$). The coefficient

φ_2 accounts for the various secondary work except the two: $\int \pi dl$ and $\xi \int \gamma S_n p dl$ which are accounted for separately.

$$\varphi_2 = 1 + \kappa_2 + \kappa'_3 + \kappa_4 + \kappa_5 \sim 1.03 + \epsilon_c \frac{\omega}{z}$$

here: $\epsilon_c = \frac{1}{3} \gamma \cdot \frac{1 + \frac{\kappa_0}{\lambda}}{\lambda + 1}$; $\gamma = \frac{d}{d_0}$; $\kappa = \frac{L}{L_0}$

It is advisable to apply the above system of equations to a simple case with a small ω and a fine powder with a very fast rate of burning. Then the equations (c) and (d) can be omitted, because we have a case of instantaneous burning; the coefficient φ_2 is very close to the constant value and the obstructing forces

$R = \frac{1}{2} \gamma S_n \rho_0$ and Π can be easily evaluated as they have in this simplified case a prevailing importance. Thus we will be able to see how close all the above shown calculations will be to the experimental results.

The equation (a) can be rewritten:

$$S \rho_0 \left[1 - \frac{1}{2} \gamma \frac{S_n}{S} - \frac{\Pi}{S \rho_0} \right] = \varphi m \frac{dv}{dt}$$

and we may select such a combination of Δ and ρ_0 at which the results in the left part will be even negative i.e. the projectile will not be propelled out of the gun and will stop within the bore.

Chapter 2 - Solution of the Problem of Interior Ballistics for the Conic Bore.

The principal assumptions remain the same as for the cylindrical bore: instantaneous ignition, the geometric law of the burning; the law of the rate of burning: $u = u_0 \rho$;

the instantaneous engraving of the band at the initial pressure ρ_0 , an unchangeable chemical composition of gases during their expansion. The principal distinction is: the variable cross-section of the bore.

The principal relationships:

$$\varphi m \frac{dv}{dt} = S p - \text{the equation of motion} \quad (57)$$

$$u = \frac{ds}{dt} = u_0 \rho - \text{the law of the rate of burning.} \quad (58)$$

$$\varphi m v dv = p s dl = p dW - \text{the equation of the elementary work.} \quad (59)$$

$$p(W_\psi + W) = f\omega\psi - \frac{\rho}{2}\psi m v^2, \quad \text{where:}$$

$$W_\psi = W_0 \left[1 - \frac{\alpha}{f} - \Delta(\alpha - \frac{1}{f})\psi \right] \quad - \text{the equation of the trans-formation of the energy} \quad (60)$$

W_ψ is the free volume of the chamber at the moment when part ψ of the charge has been burned.

From (57) and (58) we have: $S dx = u \rho m dv$

$$dv = \frac{S}{\rho m} \cdot \frac{\rho}{u} dx = \frac{S}{\psi m} \cdot I_x dx \quad (61)$$

here: $x = z - z_0 = \frac{z}{\lambda} - \frac{z_0}{\lambda}$

λ - is the relative thickness of the powder burned out from the beginning of the motion of the projectile:

z_0 - the thickness of powder burned out at the moment of the beginning of motion.

λ_0 - the relative thickness of powder; ψ_0 - part of the charge burned at the moment of the beginning of motion of the projectile,

Rewriting (61): $dv = \frac{S_0}{\psi m} \cdot \frac{I_x S}{S_0} dx \quad (62)$

The principal difficulty in solving these equations for the conic bore is that we have not yet found the relationship between the variable $(\frac{S}{S_0})$ and v or x , which fact precludes the possibility of integration of the equation (62). From the solution of our problem for the cylindrical bore, however, we may find the relationship between v and W or $A = \frac{W}{W_0}$.

We have already seen that at the same loading conditions for the conic and cylindrical bores we may assume that the curves (ν, Λ) for both of these bores are identical; hence we have means to establish the relationship between $(\frac{S}{S_0})$ and W or Λ . For doing this we take Λ as our independent variable.

Thus from (62) we have: $\nu = \frac{S_0 I_N}{\varphi m} \int \frac{S}{S_0} dx$

The function $\frac{S}{S_0}$ can be taken out of the integral at its average value $(\frac{S_{av}}{S_0})$ and then we have:

$$\nu = \frac{S_0 I_N}{\varphi m} \cdot \frac{S_{av}}{S_0} x \dots (63)$$

But since $\nu_{con} = \nu_{cyl}$.

We will have: $\frac{S_0}{\varphi m} \cdot \frac{S_{av}}{S_0} x_{con} = \frac{S_0 I_N}{\varphi m} \cdot x_{cyl}$

$$\text{and } x_{con} = \frac{x_{cyl} \cdot S_0}{S_{av}} \quad \text{i.e. } x_{con} > x_{cyl} \dots (64)$$

From (59) and (60) we have:

$$\frac{dW}{W\psi+W} = \frac{d\Lambda}{\Lambda\psi+\Lambda} = \frac{1}{f\omega} \cdot \frac{\varphi m \nu d\nu}{\psi - \frac{\nu^2}{2\omega}} \dots (65)$$

Here: $\psi = \omega_2 + \omega_3 \lambda^2 = \psi_0 + \omega_3 x + \omega_3 \lambda x^2$

Taking $d\nu$ from (64) and ν from (63) and denoting $B_0 = \frac{S_0^2 I_N^2}{f\omega \varphi m}$

We will have (65) in the following form

$$\frac{d\Lambda}{\Lambda\psi+\Lambda} = \frac{B_0 \frac{S_{av}}{S_0} \cdot \frac{S}{S_0} x dx}{\psi_0 + \omega_3 x - [B_0 (\frac{S_{av}}{S_0})^2 \frac{x^2}{2} - \omega_3 \lambda] x^2} = \frac{B_0 \frac{S_{av}}{S_0} \cdot \frac{S}{S_0} x dx}{\psi_0 + \kappa_1 x - B_3 x^2} \quad (66)$$

Here: $B_3 = B_0 \theta \left(\frac{S_{av}}{S_0} \right)^2 - \omega_3 \lambda$

An analogous equation for the cylindrical bore of caliber d_0 is :

$$\frac{d\Lambda}{\Lambda_0 + \Lambda} = \frac{B_0 (x dx)_{cyl.}}{\psi_0 + K_1 x_{cyl.} - B_1 x_{cyl.}^2} \dots (67)$$

$$\text{here: } B_1 = B_2^0 - \kappa \lambda$$

$$\text{and } B_0 = \frac{S_0^2 I_{\lambda}^2}{f \omega \psi m}.$$

From (66) and (67) we can see that the parameters

B_0 and B_1 are constant for the cylindrical bore, and the analogous parameters for the conic bore become variables depending on the value of the cross-section of the bore.

In the numerator of (66) the product $\frac{S_{av}}{S_0} \cdot \frac{S}{S_0}$ is a function of Λ and should be transferred into the left part of the equation, for integration and $\left(\frac{S_{av}}{S_0}\right)^2$ can be taken either at its average value or as a constant along the whole range of x according to the value of range for x .

Here we will take: $\frac{S}{S_0} = y^2$; $\frac{S_{av}}{S_0} \sim y$; $\frac{S}{S_0} \cdot \frac{S_{av}}{S_0} = y^3 = 1 - \frac{\Lambda}{\Lambda_c}$.

Then (66) will be rewritten:

$$\frac{d\Lambda}{(\Lambda_0 + \Lambda) \left(1 - \frac{\Lambda}{\Lambda_c}\right)} = \frac{B_0 x dx}{\psi_0 + K_1 x - B_1 x^2} = \frac{-B_0}{B_1} \cdot \frac{x dx}{x^2 - \frac{K_1}{B_1} x - \frac{\psi_0}{B_1}} \dots (68)$$

Here the right part of the equation is the same as in the equation for the cylindrical bore and represents the differential of Drosdov's function (for integration

B_s should be taken at its average value along the range of the integration from 0 to x .)

Thus the right part of (68) is:

$$-\frac{B_s}{B_s} \int_0^x \frac{x dx}{x^2 - \frac{K_s}{B_s} x - \frac{\psi_0}{B_s}} = \log_e Z \frac{B_s}{B_s}$$

and can be evaluated from Tables by entries: $\gamma = \frac{B_s \psi_0}{K_s^2}$

and $\beta = \frac{B_s}{K_s} x$; the left part of (68) also can be integrated, and here Λ_ψ can be taken as an average

$(\Lambda_\psi)_{av}$ being constant for all values of ψ , or we can take a value Λ_ψ for each $\psi = \psi_0 + K_s x + \alpha \lambda x^2$ (in the same way as shown for the integration with the value of $C_{\psi av}$).

The left part of (68) can be rewritten:

$$\frac{d\Lambda}{(\Lambda_{\psi_{av}} + \Lambda)(1 - \frac{\Lambda}{\Lambda_c})} = \frac{\Lambda_c d\Lambda}{(\Lambda_{\psi_{av}} + \Lambda)(\Lambda_c - \Lambda)} = \frac{\Lambda_c}{\Lambda_c + \Lambda_{\psi_{av}}} \left[\frac{d\Lambda}{\Lambda_{\psi_{av}} + \Lambda} - \frac{-d\Lambda}{\Lambda_c - \Lambda} \right]$$

and then:

$$\frac{d\Lambda}{(\Lambda_{\psi_{av}} + \Lambda)(1 - \frac{\Lambda}{\Lambda_c})} = \frac{\Lambda_c}{\Lambda_c + \Lambda_{\psi_{av}}} d \left[\log_e \frac{\Lambda_{\psi_{av}} + \Lambda}{\Lambda_c - \Lambda} \right]$$

After the integration (from 0 to x and from 0 to Λ) we have:

$$\left(\frac{1 + \frac{\Lambda}{\Lambda_{\text{cvr}}}}{1 - \frac{\Lambda}{\Lambda_c}} \right)^{\frac{\Lambda_c}{\Lambda_c \Lambda_{\text{cvr}}}} = Z_x^{-\frac{B_0}{B_s}} \dots (69)$$

Denoting: $\frac{B_0}{B_s} \left(1 + \frac{\Lambda_{\text{cvr}}}{\Lambda_c} \right) = A_K$

$$\text{We have: } \frac{1 + \frac{\Lambda}{\Lambda_{\text{cvr}}}}{1 - \frac{\Lambda}{\Lambda_c}} = Z^{-A_K} \dots (70)$$

Solving (69) with respect to Λ we will have:

$$\Lambda = \Lambda_{\text{cvr}} \frac{Z_x^{-A_K} - 1}{1 + \frac{\Lambda_{\text{cvr}}}{\Lambda_c} Z_x^{-A_K}} \dots (71)$$

For the cylindrical bore we had:

$$\Lambda_{\text{cvr}} = \Lambda_{\text{cvr}} \left(Z_x^{-\frac{B_0}{B_s}} - 1 \right) \dots (72)$$

$$\text{here } B_s = \frac{B_0}{2} - \kappa \lambda$$

The numerator of (71) is of the same structure as (72) but instead of the constant exponent $-\frac{B_0}{B_s}$ we have in (71): $A_K = \frac{B_0}{B_s} \left(1 + \frac{\Lambda_{\text{cvr}}}{\Lambda_c} \right)$ and $B_s = \frac{B_0}{2} \cdot \left(\frac{S_{\text{cvr}}}{S_0} \right)^2 - \kappa \lambda$

In (71) we have denominator which is > 1 and is constantly increasing during the burning of powder and motion of projectile along the conic bore.

Thus we may say that (70) expresses clearly the specific significance of the variability of the cross-

section of the bore and its effect on the elements of the firing from the conic bore.

For the gas pressure we will have:

$$p = f \Delta \cdot \frac{\psi - \left(\frac{x}{x_m}\right)^2}{\lambda_p + 1} = f \Delta \cdot \frac{\psi + \kappa_1 x - \beta_2 x^2}{\lambda_p + 1} \quad (73)$$

Since for the given x and $v_{con} > v_{cyl}$ and $\lambda_{con} < \lambda_{cyl}$.

$p_{con} > p_{cyl}$ the pressure in the conic bore will be higher than in the cylindrical bore.

Formula (73) can be rewritten:

$$p = f \Delta \cdot \frac{\psi - \frac{\beta_2}{2} \left(\frac{x}{x_m}\right)^2 x^2}{\lambda_p + 1} \quad (74)$$

Having differentiated (74) with respect to x and making $\frac{dp}{dx} = 0$ we will find x_m at which the pressure will be the maximum pressure p_m . We give here the value of x_m without the algebraical details of its derivation:

$$x_m = \frac{\kappa_1}{\frac{\beta_2 \left(\frac{x}{x_m}\right)_m^2 \left[\left(\frac{x}{x_m}\right)_m + \theta\right]}{1 + \frac{\beta_2}{f} \left(\alpha - \frac{1}{f}\right)} - 2\kappa_1 \lambda}$$

If S is constant this formula becomes our previous formula for x_m in the cylindrical bore.

The Fig. 188 shows the curve (p, λ) and (v, λ) for the cylindrical bore: 1 - for p and 1' for v

and for the conic bore: 2 - for p and 2' for v

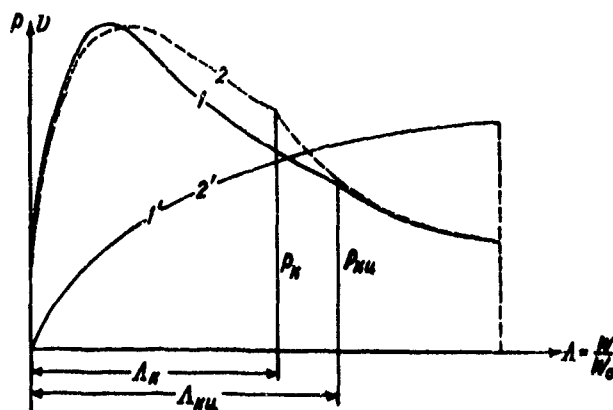


Fig. 188 Curves (p, λ) and (v, λ) for cylindrical and conic bores. p_n at the end of burning has $(\lambda_n)_{\text{con.}} < (\lambda_n)_{\text{cyl.}}$

Chapter 3 - The Ballistic Design of the Conic Gun

Since the very purpose of the conic gun is to shorten the length of a very high muzzle velocity gun, the design of this gun is directed to finding a conic bore corresponding to the cylindrical one with a minimum bore volume.

Suppose we are given the following initial data: a muzzle caliber d_2 , weight of projectile q and its muzzle velocity v_2 ; it is required to design a conic bore for these conditions.

We find the additional data: $C_5 = \frac{q}{d_2^3}$; $\frac{v_2^3}{x_2^3}$; $C_6 = C_5 \cdot \frac{2d_2^2}{x_2^2}$

the ratio $\beta = \frac{d_2}{d_0} = \sqrt[3]{\frac{C_{g2}}{C_{g0}}} = \sqrt[3]{\frac{16}{7}} \dots \sqrt[3]{\frac{18}{6}} \approx 1.32 - 1.44$

Now, from practice (armor piercing projectiles) we know that C_{g2} (at the muzzle) varies from 16 to 18, and the limits for the minimum C_{g0} (at the initial caliber d_0) are from 6 to 7, then we find that the range of possible variation for β will be: $\sqrt[3]{\frac{16}{7}} - \sqrt[3]{\frac{18}{6}}$

i. e. from 1.32 to 1.44

In German guns 28 20 m/m and 75/45 m/m is respectively 1.4 and 1.363. We will take $\beta = \sqrt[3]{\frac{16}{6}} = 1.385$.

For $C_{g0} = 6$ we will have $d_0 = 1.895 d_2$ and we find the characteristics of the cylindrical gun with this d_0 as caliber and with v_0 and ρ_m having the minimum volume.

$$h_{w0} = 85.82 \frac{t \cdot m}{K^2} ; \frac{w}{q} ; \varphi = a_c + b_c \frac{w}{q} ; a_c = 1.20$$

$$b_c = 0.222 ; (v_0 c_h) = \frac{v_0^2}{n} ; n = \sqrt{\frac{w}{q \cdot q}}$$

Next we find from Tables (C.A.B.): $B ; \Lambda_K ; \Lambda_2 ; h_K = \frac{\Lambda_K}{\Lambda_2}$
 $W_0 ; \frac{L}{d_0} = \frac{L_2}{d_0} (\Lambda_2 + 1) ; \frac{L_2}{d_0} = \frac{L_0}{d_0} \Lambda_2 ; d = d_0$

from this data we find:

Volume of chamber $W_0 = S_0 \ell$, where $S_0 = \pi d_0^2$

The working volume of bore: $W_2 = S_0 \ell$, which is equal to the volume of the conic bore. Thus from the

volume W_2 and from the ratio $\frac{d_2^2}{d_0^2}$ and from the formula

$W_2 = W_{con}(1 - \gamma_2^3)$ we calculate W_{con} , which is the volume of the whole cone: $W_{con} = \frac{W_2}{1 - \gamma_2^3}$

For the truncated cone: $W_2 = S_{av} \cdot \ell_2 = S_0 \frac{1 + \gamma_2 + \gamma_2^2}{3} \ell_2$.

$$\text{hence: } \ell_2 = \frac{3W_2}{S_0(1 + \gamma_2 + \gamma_2^2)} \quad \text{and} \quad \tan \beta = \frac{d_0 - d_2}{2\ell_2}$$

Taking $\gamma = \frac{\ell_2}{\ell_c}$, we will find $\frac{\ell_2}{\ell_c} = \ell_c$ and $L_c = \ell_c + \ell_2$ and the full length of the barrel: $L_2 = L_c + 2d_0$.

($2d_0$ for the breech part)

Taking $\Lambda_m = 0.6$ and $W_m = 0.6 W_0$ we calculate

$$\gamma_m = \sqrt[3]{1 - \frac{W_m}{W_{con}}} \quad \text{and} \quad \frac{(S_{av})_m}{S_0} = \frac{1 + \gamma_m}{2}$$

Calculate $\frac{I_m}{d_0} = \frac{(I_m)_{av} S_0}{d_0 (S_{av})_m}$; $I_m = (I_m)_{av} \cdot \frac{S_0}{(S_{av})_m}$ i.e. the impulse giving the desired β_m . From the theory we know that the end of burning will be closer to the beginning of motion than it is in the cylindrical bore and $(\beta_m)_{con} = \frac{W_{con}}{W_2}$ is smaller than $(\beta_m)_{cyl} = \frac{W_m}{W_2} = \left(\frac{\ell_m}{\ell_2}\right)_{cyl}$.

For the calculation of the curves of pressures and velocities for the conic bore we first calculate the curves (v, w) and (v, Λ) for the cylindrical bore (Using Tables C.A.B., 1942). Having the values of v we will find $x_{cyl} = \frac{v}{v_0}$, here $v_0 = \frac{S_0 I_m}{\ell_m}$ is the velocity at the end of burning of powder, when there is no initial pressure of engraving.

Taking W corresponding to v from the curve (v, W) we calculate the values of $y = \sqrt[3]{1 - \frac{W^2}{W_0^2}}$; $W_c = \frac{W_0^2}{1 - y^2}$; $\frac{S_{av}}{S_0} = \frac{1 + y + y^2}{3}$

Dividing x_{avr} by $\frac{S_{av}}{S_0}$ we will find $x_{con} = \frac{x_{avr}}{(\frac{S_{av}}{S_0})}$; the value $x_N = (p - 2_0)$ will determine $(W_N)_{con}$ and the velocity $(v_N)_{con}$ at the end of burning.

Using the values of x we will calculate

$$\psi = \psi_0 + \kappa \delta_0 x + \kappa \lambda x^2$$

and the pressure $p = f \omega \cdot \frac{\psi - (\frac{v_N}{v_0})^2}{W_\psi + W} = f \omega \cdot \frac{\psi - (\frac{v_N}{v_0})^2}{\Lambda_\psi + \Lambda}$

here $W_\psi = W_0(1 - \frac{x}{\delta_0}) - \omega(\alpha - \frac{x}{\delta_0})\psi$; $\Lambda_\psi = 1 - \frac{x}{\delta_0} - \Delta(\alpha - \frac{x}{\delta_0})\psi$

and v_0 and W the same as for the cylindrical bore.

For the end of the first period $\psi_N = 1$ and $p_N = f \Delta \cdot \frac{1 - (\frac{v_N}{v_0})^2}{1 - \alpha \Delta + \Lambda_N}$

muzzle velocity v_2 and p_2 are

found from the formulas:

$$v_2^2 = v_{avr}^2 \left[1 - \left(1 - \frac{v_N^2}{v_{avr}^2} \right) \left(\frac{1 - \alpha \Delta + \Lambda_N}{1 - \alpha \Delta + \Lambda_2} \right)^{\theta} \right]$$

$$p_2 = p_N \left(\frac{1 - \alpha \Delta + \Lambda_N}{1 - \alpha \Delta + \Lambda_2} \right)^{1+\theta}; \quad v_{avr}^2 = \frac{2g}{\varphi} \cdot \frac{f}{\theta} \cdot \frac{\omega}{\gamma}$$

The coefficient of the utilization of the unit weight of charge:
$$\zeta_{\omega} = \frac{m \psi_2^2}{2\omega} = \frac{(\frac{\psi_2^2}{2})}{(\frac{\omega}{m})}$$

The $(\psi_2)_{con}$ obtained is very close to the $(\psi_2)_{exp.}$ at the same values of W_2 and W_0 at the same loading conditions except the value of I_x .

Using the results obtained we may, if necessary, introduce certain corrections in order to have with a better accuracy both required ψ_2^2 and ρ_m .

B I B L I O G R A P H Y

The First Part

1. F. Engels The Artillery. Selected military works.
Vol. I. Moscow 1940. p. 214
2. Granz Lehrbuch der Ballistik (1920-1926)
3. Charbonnier - Ballistique Interieure (1908)
4. M. E. Serebryakov - The introduction to the study
of the physical law of the burning of
the smokeless powders (Dissertation).
Military Technical Academy. 1929.
5. M. E. Serebryakov - The physical law of burning in
the Interior Ballistics (Dissertation
for the Doctor's degree) 1940.
6. Muraour Les lois de combustion des poudres
colloïdaux. Bulletin de la Societe
Chymique de France (1926-1927) and
Comptes Rendus de l'Academie de
Sciences.
7. P. N. Shaposhnikov - On the motion of the powder
gases behind the moving projectile. The
Reports of the Artillery Academy,
vol. 44. 1945.
8. D. A. Frank-Kamenetzky - The Theory of the uniform-
ly spreading flame. Journal of the
Physical Chemistry, 1938, No. 12
9. I. B. Zeldovich - The Theory of the propagation of
the detonation in gases. Journal of the
experimental and Physical Chemistry.
1942, vol. XII, No. 11-No. 12.
10. A. F. Brink, Prof. of the Artillery Academy -
The Interior Ballistics. 1901, p. I.

11. I. P. Grave, prof. of the Artillery Academy, - Pyrostatics (Edited by the Artillery Academy) 1938.
12. I. P. Grave - The expressions for the relative burned amounts of the american powders at their fragmentation. Reports of the Artillery Academy, vol. I, 1932.
13. G. V. Oppokov - The Interior Ballistics, 1933.
14. I. P. Grave - An essay on the Theoretical Study of the law of development of the powder pressure in a closed vessel. Edited by the Artillery Academy, 1904.
15. N. F. Drosdov, prof. of the Artillery Academy. - Solutions of the problems of the Interior Ballistics, 1910.
16. N. F. Drosdov - Tables for the solutions of the problems of Interior Ballistics. 1933
17. M. E. Serebryakov - The physico-chemical basis for the evaluation of the variations of temperature of the powder gases in guns and a selection of the exponent. Reports of the Artillery Academy, vol. XIX, p. 105.
18. I. P. Grave - Pyrodynamics, p. II, 1934.

In The Second Part

1. N. F. Drosdov - The Solution of the basic equation of the Interior Ballistics. Reports of the Artillery Academy, 1936, vol. XIX - XX.
2. G. V. Oppokov - On the accuracy of certain analytical methods of solution of the basic problem of the Interior Ballistics for the first period. Bulletin of the Scient. Techn. Commission of the Chief Artillery Board, No. 2, 1932.

3. E. L. Bravin - On the methods of the evaluation of the time interval at the beginning of the motion of a projectile. Reports of the Artillery Academy, vol. XIV, 1939.
4. A. N. Krylov - Lectures on the Calculus of approximations. 1933.
5. G. V. Oppokov - The numerical analysis in its applications to the Artillery Technics, 1939.
6. M. E. Serebryakov, G. V. Oppokov, K. K. Greten - The Interior Ballistics. 1939.
7. N. A. Zabudsky, Prof. of the Artillery Academy - On the gas pressure of the smokeless powders in the bore of the gun. 1894.
8. N. A. Zabudsky - On the powder gas pressure in the bore of the 3 inch gun and the velocities of its projectile. 1914
9. V. E. Sloukhotsky - Corrective formulas in the Interior Ballistics - 1941.
10. D. A. Ventzel - Interior Ballistics - Edition of the Military Aviation Academy, 1939.
11. E. L. Bravin - On the error in the calculation of time in the Tables for Solutions of the problems of Interior Ballistics. Reports of the Artillery Academy, vol. XIV, 1935.
12. Tables of the Interior Ballistics, parts I, II, III, IV. 1942-1943.
13. B. N. Okunev - Collected information for the solutions of the problems of Interior Ballistics, No. 5. 1940 (Edited by the Military Navy Academy).
14. M. S. Gorokhov and A. I. Sviridov - The principal problems of Interior Ballistics, 1940.

15. G. V. Oppokov - The principal problems of the Interior Ballistics. 1940
16. N. F. Drosdov - Solution of the problems of Interior Ballistics for the smokeless powder of the tubular form. Reports of the Artillery Academy, vol. XXX, 1940
17. M. S. Gorokhov - Interior Ballistics, p. I, p. II, p. III, 1943.
18. I. P. Grave - Pyrodynamics, p. II, Edited by the Artillery Academy, 1934.
19. B. N. Okunev - A general Theory of the similarity of the Artillery Systems, 1938 - Edited by the Artillery and Navy Academies.
20. V. E. Sloukhotzky - The productivity of the powder charges. Reports of the Artillery Academy vol. XVIII, 1934.
21. M. E. Serebryakov - On the question of the ballistic design of the gun barrel. Reports of the Artillery Academy vol. XXX, 1940.
22. M. E. Serebryakov - The influence of the variations of the Chemical composition of powders on the constructional data of the gun with the minimum volume. Works of the Scientific Researches Institutes. No. 8, 1946.

In The Third Part

1. I. P. Grave - Pyrodynamics - Edited by the Artillery Academy 1927.
2. N. F. Drosdov - Solution of the basic equation of Interior Ballistics - Reports of the Artillery Academy, vols. XIX-XX, 1936.
3. Robinson - Thermodynamics of firearms - 1943.

4. V. E. Sloukhetzky - Method of the calculations of the combined powder charges - 1944.
5. M. E. Serebryakov - The physical law of burning in Interior Ballistics. 1940.
6. G. V. Oppokov - Solution of the problem of the Interior Ballistics for the combined charges. Reports of the Artillery Academy, 1942.
7. G. V. Oppokov - Numerical analysis in its application to the Artillery Techniques, 1939.
8. G. V. Oppokov - The principal problems of Interior Ballistics. 1940.

TABLE OF CONTENTS

(Complete translation of the course in
Interior Ballistics of Prof. M. E. Serebryakov)

Foreword

Introduction

The subject and problems of Interior Ballistics
Various branches of Interior Ballistics
The importance of Interior Ballistics in the ballistic
design of the artillery system
The history of the development of Interior Ballistics
List of terms, notations and definitions

Part One

Physical Fundamentals of Interior Ballistics

Section I

Powder as the Source of Energy

Chapter 1 - General Information
Chapter 2 - The Principal Characteristics of Powder

Section II

General Pyrostatics

The principal relationships and laws of gas formation
at the burning of powder in a closed vessel.
Chapter 1 - The Burning of Powder
Chapter 2 - The Characteristic Equation of Powder Gases
Chapter 3 - Evolution of the Amount of Heat Transmitted
through the Walls of the Closed Volume
Chapter 4 - The Law of Gas Formation
Chapter 5 - The Law of the Variation of the Pressure, as
a Function of Time.

Section III

The Ballistic Analysis of Powders Based on the Physical
Law of Burning
Chapter 1 - A Development of Methods of Ballistic Analysis
of Powders

Section III (Continued)

- Chapter 2 - Ballistic Analysis of the Actual Burning of Powder
- Chapter 3 - Special Features of Burning of Powders with the Narrow Channels
- Chapter 4 - The Application of the Integral Diagrams

Section IV

Physical Fundamentals of Pyrodynamics

- Chapter 1 - The Phenomenon of Firing and Its Principal Relationships
- Chapter 2 - Balance of Energy during the Firing
- Chapter 3 - The Study of the Principal Relationships
- Chapter 4 - Acting Forces during the Travel of the Projectile
- Chapter 5 - Formulas for the Evaluation of the Secondary Works performed by Powder Gases
- Chapter 6 - Additional Questions

Section V

The Outflowing Gases from the Gun

General Remarks

- Chapter 1 - General Information on Gas Dynamics
- Chapter 2 - Application of the Principal Formulas
- Chapter 3 - Burning of Powder in A Partially Closed Volume
- Chapter 4 - A Brief Theory of the Muzzle Brakes

Part Two

Theory and Practice of the Solution of Problems of Interior Ballistics

(Theoretical and Applied Pyrodynamics)

Introduction

Section VI

Analytical Methods of Solution of the Direct Problem of Interior Ballistics

Principal Assumptions

Section VI (Continued)

- Chapter 1 - Solution of the Basic Problem in Case of the Initial Pressure of Engraving and the Geometric Law of Burning
- Chapter 2 - The Exact Method of Prof. N. Drosdov
- Chapter 3 - Solution of Problems of Interior Ballistics for Simplest Cases
- Chapter 4 - Principal Relationships for the Simplest Case ($\lambda=1$; $\psi=0$; $\alpha=\frac{1}{2}$)
- Chapter 5 - Some other Methods of Solution of the Problems of Interior Ballistics (written by Prof. G. Oppokov)

Section VII

Numerical Methods of Solution

The Use of Numerical Analysis in Interior Ballistics

- Chapter 1 - Numerical Integration by the Finite Differences
- Chapter 2 - Solution by Means of the Taylor's Series

Section VIII

Empirical Methods of Solution

- Chapter 1 - Monomial and Differential Formulas
- Chapter 2 - Empirical Formulas and Tables

Section IX

Tabular Methods of Solutions of Problems of Interior Ballistics

- Chapter 1 - The Importance of the Tabular Methods for Artillery Practice
- Chapter 2 - Tables for the Principal Elements of the Firing (P ; c_m ; c_n ; v)
- Chapter 3 - Detailed Tables for the Curves of Pressures and Velocities
- Chapter 4 - Tables Based on the Generalized Formulas with a Reduced Number of Parameters and with Relative Variables
- Chapter 5 - General Information on the Theory of Similarity.

Section X

The Ballistic Design of Guns

General Remarks

Chapter 1 - Initial Data

Chapter 2 - Theoretical Fundamentals of Ballistic Design

Chapter 3 - Application of the Basic Relationships to
the Practical Design of Guns

Chapter 4 - Additional Information

Part ThreeSolutions of More Involved Problems of Interior
BallisticsSection XI

More Complicated Cases

Chapter 1 - Solutions for Composite Charges

Chapter 2 - Solution Taking into Account the Gradual
Engraving of the Driving Band

Chapter 3 - Solution in the Case of Minethrowers

Section XII

Guns with Conic Bore (Tapered Guns)

IntroductionChapter 1 - Specific Features and Ballistic Properties
of Conic BoresChapter 2 - Method of Solution of the Problem of Interior
Ballistics for a Gun with a Conic Bore

Chapter 3 - The Ballistic Design of the Conic Gun

Appendices1 - Tables for the Burned Fraction in the Constant
Volume of the Manometric Bomb

2 - Tables of Prof. Brosdov

3 - Tables of Prof. Gorokhov

4 - Tables of the Function: $\int_0^{\beta} Z \cdot \Delta \beta$

5 - Bibliography